



מכון ויצמן למדע
WEIZMANN INSTITUTE OF SCIENCE

Thesis for the degree
Doctor of Philosophy

Submitted to the Scientific Council of the
Weizmann Institute of Science
Rehovot, Israel

By
Omri Golan

עבודת גמר (תזה) לתואר
דוקטור לפילוסופיה

מוגשת למועצה המדעית של
מכון ויצמן למדע
רחובות, ישראל

מאת
עמרי גולן

היבטים גאומטריים וחישוביים
של חומר קוונטי טופולוגי כיראלי

**Geometric and computational aspects
of chiral topological quantum matter**

Advisor: Prof. Ady Stern

מנחה: פרופ' עדי שטרן

January 2021

טבת תשפ"א

Abstract

In this thesis, we study chiral topological phases of 2+1 dimensional quantum matter. Such phases are abstractly characterized by their non-vanishing chiral central charge c , a topological invariant which appears as the coefficient of a gravitational Chern-Simons (gCS) action in bulk, and of corresponding gravitational anomalies at boundaries. The chiral central charge is of particular importance in chiral superfluids and superconductors (CSF/Cs), where $U(1)$ particle-number symmetry is broken, and c is, in some cases, the only topological invariant characterizing the system. However, as opposed to invariants which can be probed by gauge fields in place of gravity, the concrete physical implications of c in the context of condensed matter physics is quite subtle, and has been the subject of ongoing research and controversy. The first two parts of this thesis are devoted to the physical interpretation of the gCS action and gravitational anomalies in the context of CSF/Cs, where they are of particular importance, but have nevertheless remained poorly understood.

As a first approach, we demonstrate that, at low energy, fermionic excitations in p -wave CSF/Cs experience an *emergent* relativistic Riemann-Cartan geometry, described by the superconducting order parameter and background $U(1)$ gauge field. This description is then used to infer gCS energy-momentum responses to a space-time dependent order parameter, and relate these to an order parameter induced gravitational anomaly. The presence of torsion in the emergent geometry, as well as the multiplicity of low energy spinors in the case of lattice systems, lead to additional effects which are not of topological origin, but nevertheless mimic closely the above gCS physics. We show how these different phenomena can be disentangled.

We then take on a fully non-relativistic analysis of CSFs, obtaining a low energy effective field theory that consistently captures both their chiral Goldstone mode and their non-relativistic gCS action. Using the theory we find that c cannot be extracted from a measurement of the odd viscosity tensor alone, despite naive expectation based on previous work. Nevertheless, a related observable, termed ‘improved odd viscosity’, does allow for the bulk measurement of c . Additional results of the same spirit are found in Galilean invariant CSFs.

Finally, we turn to a seemingly unrelated aspect of chiral topological phases - their computational complexity. The infamous *sign problem* leads to an exponential complexity in Monte Carlo simulations of generic many-body quantum systems. Nevertheless, many phases of matter are known to admit a sign-problem-free representative, allowing an efficient classical simulation. Motivated by long standing open problems in many-body physics, as well as fundamental questions in quantum complexity, the possibility of *intrinsic* sign problems, where a phase of matter admits no sign-problem-free representative, was recently raised but remains largely unexplored. Here, we establish the existence of an intrinsic sign problem in a broad class of chiral topological phases, defined by the requirement that $e^{2\pi ic/24}$ is *not* the topological spin of an anyon. Within this class, we exclude the possibility of ‘stoquastic’ Hamiltonians for bosons, and of sign-problem-free determinantal Monte Carlo algorithms for fermions. We obtain analogous results for phases that are *spontaneously* chiral, and present evidence for an extension of our results that applies to both chiral and non-chiral topological matter.

Table of Contents

Acknowledgments	5
Publications	6
1 Introduction and summary	1
1.1 Overview	1
1.2 Chiral topological matter	2
1.3 Geometric physics in chiral topological matter	3
1.4 Chiral superfluids and superconductors	6
1.5 Odd viscosity	9
1.6 Quantum Monte Carlo sign problems in chiral topological matter	10
2 Probing topological superconductors with emergent relativistic gravity	14
2.1 Approach and main results	14
2.2 Lattice model	19
2.3 Emergent Riemann-Cartan geometry	26
2.4 Symmetries, currents, and conservation laws	29
2.5 Bulk response	37
2.6 Discussion	51
3 Boundary central charge from bulk odd viscosity: chiral superfluids	55
3.1 Building blocks for the effective field theory	55
3.2 Effective field theory	57
3.3 Benchmarking the effective theory against a microscopic model	58
3.4 Induced action and linear response	60
3.5 Discussion	62
4 Intrinsic sign problem in chiral topological matter	64
4.1 Signs from geometric manipulations	64
4.2 Excluding stoquastic Hamiltonians for chiral topological matter	67
4.3 Spontaneous chirality	70
4.4 DQMC: locality, homogeneity, and geometric manipulations	73

4.5	Excluding sign-free DQMC for chiral topological matter	81
4.6	Conjectures: beyond chiral matter	82
4.7	Discussion	84
5	Outlook	88
	Appendix	89

Acknowledgments

Adding a grain of sand to one of the very many and ever growing summits of the mountain range known as ‘human knowledge’ is truly a great privilege. The climb, however, is usually no easy task, and the one that produced this thesis was no exception. Here, I would like to pause and thank those who supported me en route.

First, I am grateful to my advisor Ady Stern, who suggested an unorthodox but tailor made research direction, and collaborated with me on the first and most challenging part of the work. Ady is a formidable physicist as well as a generous advisor, and provided a rare combination of support and freedom in my research. It was also wonderful to work under someone who views laughter as a way of life.

Subsequent work was performed in mostly long distance but close collaborations with Sergej Moroz, Carlos Hoyos, Félix Rose, Zohar Ringel and Adam Smith. In particular, Sergej, Carlos and Zohar served as additional mentors, each with his own unique style of doing research. I also benefited greatly from extensive discussions with Paul Wiegmann, Andrey Gromov, Ryan Thorngren, Weihan Hsiao, Semyon Klevtsov, Barry Bradlyn and Thomas Kvorning.

The members of my PhD advisory committee, Micha Berkooz and David Mross, as well as my senior group members, Yuval Baum, Ion Cosma Fulga, Jinhong Park, Raquel Queiroz and Tobias Holder, provided much needed physical and meta-physical advice along the way. Our administrative staff, Hava Shapira, Merav Laniado, Einav Yaish, Inna Dombrovsky, Yuval Toledo and Yuri Magidov, sustained an incredibly efficient and warm work environment. I also thank my fellow graduate students Eyal Leviatan, Ori Katz, Dan Klein, Avraham Moriel, Shaked Rozen, Asaf Miron, Yotam Shpira, Adar Sharon, Dan Dviri and, of course, Yuval Rosenberg, who dragged me to the Weizmann institute when we were kids, and got me hooked on physics.

Zooming out, I am grateful to my parents Sharona and Gabi, for their continued support in whatever I choose to do, and to my wife and best friend Adi, for making my life happy and balanced. Since we became parents, my work would not have been possible without Adi’s backing, in particular since the spreading of Coronavirus, which eliminated some of our support systems, as well as the distinction between work and home. Finally, I thank our boys Adam and Shlomi for their smiles, laughter, and curiosity - a reminder of why I was drawn to science in the first place.

Publications

This thesis is based on the following publications:

- Reference [1]: Omri Golan and Ady Stern. Probing topological superconductors with emergent gravity. [Phys. Rev. B](#), **98**:064503, 2018.
- Reference [2]: Omri Golan, Carlos Hoyos, and Sergej Moroz. Boundary central charge from bulk odd viscosity: Chiral superfluids. [Phys. Rev. B](#), **100**:104512, 2019.
- Reference [3]: Omri Golan, Adam Smith, and Zohar Ringel. Intrinsic sign problem in fermionic and bosonic chiral topological matter. [Phys. Rev. Research](#), **2**:043032, 2020.

Complementary results are obtained in:

- Reference [4]: Félix Rose, Omri Golan, and Sergej Moroz. Hall viscosity and conductivity of two-dimensional chiral superconductors. [SciPost Phys.](#), **9**:6, 2020.
- Reference [5]: Adam Smith, Omri Golan, and Zohar Ringel. Intrinsic sign problems in topological quantum field theories. [Phys. Rev. Research](#), **2**:033515, 2020.

1 Introduction and summary

1.1 Overview

The study of *topological phases of matter* began in 1980, when the Hall conductivity in a two-dimensional electron gas was measured to be an integer multiple of e^2/h , to within a relative error of 10^{-7} [6], subsequently reduced below 10^{-10} [7]. Following this discovery, it was theoretically understood that in many-body quantum systems, certain physical observables must be *precisely* quantized, under the right circumstances [8, 9]. Around the same time, quantum field theorists extensively studied the phenomena of *anomalies* [10–12], where classical symmetries and conservation laws are quantum mechanically violated, and discovered the seemingly exotic *anomaly inflow mechanism* [13, 14], which physically interprets anomalies in terms of *topological effective actions* in higher space-time dimensions. It was only later understood that topological effective actions and anomalies actually capture the essential physics of topological phases of matter, and even classify them [15–20].

In particular, 2+1D gapped chiral topological phases are characterized by a gravitational Chern-Simons (gCS) action [21–25] and corresponding 1+1D gravitational anomalies [10, 12, 26], having the chiral central charge c as a precisely quantized coefficient, or topological invariant. The chiral central charge is of particular importance in chiral superfluids and superconductors [15, 27], where $U(1)$ particle-number symmetry is broken spontaneously or explicitly, and c is, in some cases, the only topological invariant characterizing the system at low energy. However, as opposed to topological invariants related to gauge fields for internal symmetries in place of gravity, the concrete physical implications of c (and even its very definition) in the context of condensed matter physics is quite subtle, and has been the subject of ongoing research and controversy [28, 15, 29–32, 17, 33–55]. The first goal of this thesis is to physically interpret the chiral central charge in the context of chiral superfluids and superconductors, where it is of particular importance, but has nevertheless remained poorly understood. This goal is pursued in Sec.2-3.

A seemingly unrelated aspect of chiral topological phases is the complexity of simulating them on classical (as opposed to quantum) computers. It is generally believed that chiral topological matter is ‘hard’ to simulate efficiently with classical resources. Concretely, it is known that chiral topological phases do not admit local commuting projector Hamiltonians [56–59, 54], nor do they admit local Hamiltonians with a PEPS state as an exact ground state [60–63]. We will be interested in quantum Monte Carlo (QMC) simulations, arguably the most important tools in computational many-body quantum physics [64–71], and in the infamous *sign problem*, which is the generic obstruction to an efficient QMC simulation [72–74].

The accumulated experience of QMC practitioners suggests that the sign problem was never solved in chiral topological matter. Since these phases are abstractly defined by their non-vanishing chiral central charge, one may suspect that the chiral central charge and related gravitational phenomena pose an obstruction to sign-problem-free QMC. Such an obstruction is termed *intrinsic sign problem* [75, 76], and is of interest beyond the context of chiral topological matter, as it is widely accepted that long-standing open problems in many-body quantum physics, such as the nature of high-temperature

superconductivity [77–80], dense nuclear matter [81–83], and the fractional quantum Hall state at filling $5/2$ [84–88, 55], remain open because no solution to the sign problem in a relevant model has thus far been found. Since the aforementioned open problems are all fermionic, we are particularly motivated to study the possibility of intrinsic sign problems in fermionic matter. The second goal of this thesis, pursued in Sec. 4, is to establish the existence of an intrinsic sign problem in chiral topological phases of matter, based on their non-vanishing chiral central charge, and with an emphasis on fermionic systems.

The following Sec. 1.2–1.6 introduce the central concepts described above in more detail, pose the main questions we address in this thesis, and summarize the answers we find.

1.2 Chiral topological matter

A gapped local many-body quantum Hamiltonian is said to be in a topological phase of matter if it cannot be deformed to a trivial reference Hamiltonian, without closing the energy gap or violating locality. If a symmetry is enforced, only symmetric deformations are considered, and it is additionally required that the symmetry is not spontaneously broken [89, 90]. For Hamiltonians defined on a lattice, a natural trivial Hamiltonian is given by the atomic limit of decoupled lattice sites, where the symmetry acts independently on each site. In this thesis we consider both lattice and continuum models.

Topological phases with a unique ground state on the 2-dimensional torus exist only with a prescribed symmetry group¹ and are termed symmetry protected topological phases (SPTs) [91–93]. When such phases are placed on the cylinder, they support anomalous boundary degrees of freedom which cannot be realized on isolated 1-dimensional spatial manifolds, as well as corresponding quantized bulk response coefficients. Notable examples are the integer quantum Hall states, topological insulators, and topological superconductors [94]. Topological superconductivity and superfluidity will be discussed in detail in Sec. 1.4.

Topological phases with a degenerate ground state subspace on the torus are termed topologically ordered, or symmetry enriched if a symmetry is enforced [95, 96]. Beyond the phenomena exhibited by SPTs, these support localized quasiparticle excitations with anyonic statistics and fractional charge under the symmetry group. Notable examples are fractional quantum Hall states [97, 98], quantum spin liquids [99], and fractional topological insulators [100, 101].

In this thesis, we consider *chiral* topological phases, where the boundary degrees of freedom that appear on the cylinder propagate unidirectionally. At energies small compared with the bulk gap, the boundary can be described by a chiral conformal field theory (CFT) [102, 103], while the bulk reduces to a chiral topological field theory (TFT) [104, 19], see Fig. 1(a). Such phases may be bosonic and fermionic, and may be protected or enriched by an on-site symmetry, but we will not make use of this symmetry in our analysis - only the chirality of the phase will be used.

A notable example for chiral topological phases is given by Chern insulators [105–107]: SPTs protected by the $U(1)$ fermion number symmetry, which admit free-fermion Hamiltonians. The single

¹A subtle point is that the minimal symmetry group for fermionic systems is fermion parity - the \mathbb{Z}_2 group generated by $(-1)^N$, where N is the fermion number. This should be contrasted with bosonic systems, which may have no symmetries.

particle spectrum of a Chern insulator on the cylinder is depicted in Fig.1(b). Another notable example are the topologically ordered Kitaev spin liquids [104, 108], which can be described by Majorana fermions with a single particle spectrum similar to Fig.1(b), coupled to a \mathbb{Z}_2 (fermion-parity) gauge field. Note that the velocity v of the boundary CFT is a non-universal parameter which generically changes as the microscopic Hamiltonian is deformed. More generally, different chiral branches may have different velocities.

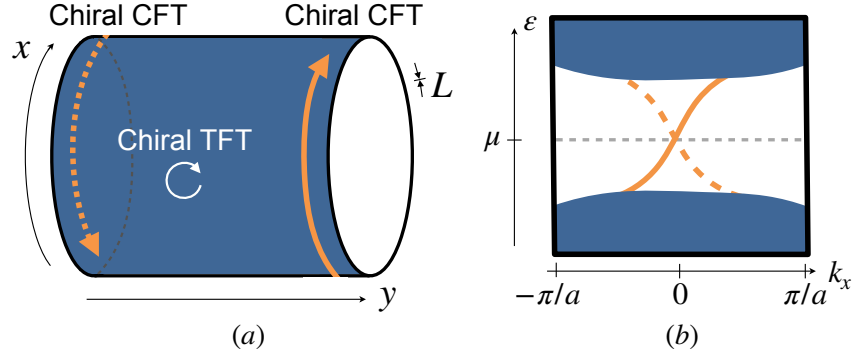


Figure 1: Chiral topological phases of matter on the cylinder. (a) The low energy description of a chiral topological phase is comprised of two, counter propagating, chiral conformal field theories (CFTs) on the boundary, and a chiral topological field theory (TFT) in the bulk. (b) Examples: schematic single-particle spectrum of a Chern insulator and of the Majorana fermions describing a Kitaev spin liquid. Assuming discrete translational symmetry with spacing a in the x direction, one can plot the single-particle eigen-energies ε on the cylinder as a function of (quasi) momentum k_x . This reveals an integer number of chiral dispersion branches whose eigen-states are supported on one of the two boundary components. In the Chern insulator (Kitaev spin liquid) these correspond to the Weyl (Majorana-Weyl) fermion CFT, with $c = \pm 1$ ($c = \pm 1/2$) per branch. The velocity, $v = |\partial\varepsilon/\partial k_x|$ at the chemical potential μ , is a non-universal parameter.

The chirality of the boundary CFT and bulk TFT is manifested by their non-vanishing chiral central charge c , which is rational and *universal* - it is a topological invariant with respect to continuous deformations of the Hamiltonian which preserve locality and the bulk energy gap, and therefore constant throughout a topological phase [109, 104, 39, 42]. On the boundary c is defined with respect to an orientation of the cylinder, so the two boundary components have opposite chiral central charges. Since, as described below, c is much better understood from the boundary perspective, we sometimes refer to it as the *boundary* chiral central charge. A main theme of this thesis is the study of c from the *bulk* perspective, and the relation between the two perspectives implied by the anomaly inflow mechanism.

1.3 Geometric physics in chiral topological matter

The non-vanishing of c implies a number of geometric, or 'gravitational', physical phenomena [102, 103, 34, 43, 42, 44]. In particular, the boundary supports a non-vanishing energy current J_E , which receives

a correction

$$J_E(T) = J_E(0) + 2\pi T^2 \frac{c}{24}, \quad (1.1)$$

at a temperature $T > 0$, and in the thermodynamic limit $L = \infty$, where L is the circumference of the cylinder. Note that we set $K_B = 1$ and $\hbar = 1$ throughout. Within CFT, this correction is universal since it is independent of v . Taking the two counter propagating boundary components of the cylinder into account, and placing these at slightly different temperatures, leads to a thermal Hall conductance $K_H = c\pi T/6$ [110, 15, 111], a prediction that recently led to the first measurements of c [112, 113, 84, 114].

In analogy with Eq.(1.1), the boundary of a chiral topological phase also supports a non-vanishing ground state (or $T = 0$) momentum density $p(L)$, which receives a universal correction on a cylinder with finite circumference $L < \infty$. The details of this finite-size correction will be described in Sec.4, where it is used to relate the chiral central charge (as well as the topological spins of anyon excitations) to the complexity of simulating chiral topological matter on classical computers.

Abstractly, both $T > 0$ and $L < \infty$ corrections described above follow directly from the (chiral) Virasoro anomaly, or Virasoro central extension, which defines c in 2D CFT. Equivalently, these corrections can be understood in terms of the 'global' gravitational anomaly - the complex phase accumulated by a CFT partition function on the torus under a Dehn twist [102, 103]. This anomaly is termed 'global' since the Dehn twist is a large coordinate transformation, or more accurately, an element of the diffeomorphism group of the torus, which lies outside of the connected component of the identity. The Dehn twist is therefore the geometric analog of the large $U(1)$ gauge transformation used in the celebrated Laughlin argument, and an attempt has been made to follow this analogy and produce a 'thermal Laughlin argument' [50].

The chiral central charge also implies a 'local', or 'perturbative' gravitational anomaly, which, at least in the context of relativistic QFT in curved space-time, physically corresponds to the non-conservation of energy-momentum in the presence of curvature gradients [10, 12, 26]. Through the anomaly inflow mechanism, or in more physical terms, through bulk+boundary energy-momentum conservation, this boundary anomaly implies a gravitational Chern-Simons (gCS) term in the effective action describing the 2+1D bulk of a chiral topological phase [21–25]². In turn, the gCS term implies a quantized energy-momentum-stress response to curvature gradients, in the bulk³.

Though the gCS term is relatively well understood in the context of relativistic QFT, its concrete physical content in the non-relativistic setting of condensed matter physics is quite subtle, due to the following reasons:

1. Physically, the actual gravitational field of the earth is usually negligible in condensed matter experiments. It is therefore clear that the adjective 'gravitational' used above cannot be taken

²Whether the gCS term matches the boundary *global* gravitational anomaly as well is, to the best of my knowledge, an open problem.

³In fact, the gCS contribution to the energy-momentum-stress tensor is proportional to the mathematically important Cotton tensor of the metric [115].

literally, and requires further interpretation. Namely, one must find a physical probe relevant in condensed matter experiments, which will somehow mimic the effects of a strong gravitational field. This scenario is often referred to as 'analog gravity' or 'emergent gravity' [27]. Mathematically, this corresponds to a physically accessible geometric structure on the space-time occupied by the system of interest, in the spirit of general relativity⁴. The most straight forward example is given by strain - a physical deformation of the sample on which the system resides [116]. An additional set of examples is given by spin-2 inhomogeneities [117] and collective excitations [28, 27, 29, 30, 33, 45]. Finally, Luttinger's trick relates temperature gradients to an applied gravitational field [118, 119, 37, 40, 41, 120, 50].

2. Fundamentally, the coupling of a system to gravity generally depends on its global space-time symmetries in the absence of gravity. For example, relativistic systems will couple differently from Galilean invariant systems. Even when the spatial symmetries are fixed, the gravitational background may vary, e.g Riemannian vs. Riemann-Cartan geometry, which are both relativistic. Moreover, for systems defined on a lattice, there is no definite, or universal, prescription for a coupling to gravity at all, as opposed to lattice gauge fields which are very well understood. The coupling of a system to gravity therefore relies on more refined information than that used to classify topological phases of matter. In particular, known results in relativistic QFT do not directly apply to the non-relativistic condensed matter systems we are interested in.
3. Technically, when describing gravity in terms of a metric, the gCS term is third order in derivatives, so obtaining effective actions that contain it *consistently*, i.e account for *all* possible terms up to the same order, is nontrivial.

Naturally, the pioneering approaches to the above difficulties were based on an adaptation of known results in relativistic QFT [28, 15, 17] (see also [31, 121]), an approach that we carefully and critically follow in Sec.2. A much more advanced treatment developed over the past decade, primarily in the context of quantum Hall states [29, 30, 33–35, 38–49, 51–55]. In particular, a *non-relativistic* gCS term arises in quantum Hall states, and produces corrections to the odd viscosity (introduced below) at finite wave-vector, and in curved background [34, 42, 43, 39, 49]. We follow this observation in Sec.3. We note a couple of additional central results from the literature:

1. In quantum Hall states, the chiral central charge contributes to the braiding statistics and angular momentum of conical defects [122, 123], the latter was recently observed in an optical realization of integer quantum Hall states [124, 53].
2. The gCS term is not directly related to $K_H = c\pi T/6$ through Luttinger's trick, simply because it is too high in derivatives of the background metric [25]. Moreover, careful analysis in quantum Hall states shows that K_H receives no bulk contribution at all [40, 41], and is therefore purely a boundary phenomenon, as explained below Eq.(1.1). Nevertheless, derivatives of K_H can be

⁴We use the words geometry and gravity interchangeably from here on.

computed from the bulk Hamiltonian a la Luttinger [119, 32, 41], resulting in a relative topological invariant for gapped lattice systems [54]. The latter gives a rigorous 2+1D lattice definition for the chiral central charge.

1.4 Chiral superfluids and superconductors

An important class of 2+1D chiral topological phases appears in chiral superfluids and superconductors (CSFs and CSCs, or CSF/Cs), where the ground state is a condensate of Cooper pairs of fermions, which are spinning around their centre of mass with a non-vanishing angular momentum $\ell \in \mathbb{Z}$ [15, 27], see Fig.2. As reviewed below, CSF/Cs appear in a wide range of physical systems, all of which have been the subject of extensive and continued research effort, going back to the classic body of work on superfluid ^3He [125]. The interest in CSF/Cs comes from two fronts, a fermionic/topological front, and a bosonic/symmetry-breaking front, both resulting directly from the ℓ -wave condensate. A central theme of this thesis is the intricate interplay between these two facets of CSF/Cs.

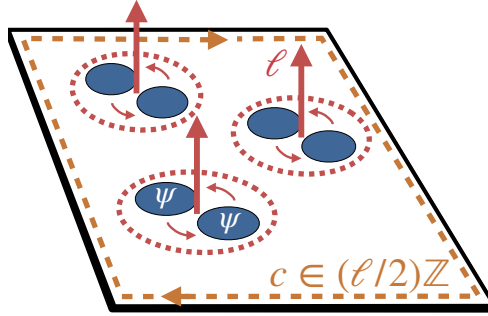


Figure 2: Chiral superfluids and superconductors (CSF/Cs) are comprised of fermions ψ , which form Cooper pairs with non-vanishing relative angular momentum $\ell \in \mathbb{Z}$ (red arrows), in units of \hbar . As a result, CSF/Cs support boundary degrees of freedom (dashed orange) with a chiral central charge $c \in (\ell/2)\mathbb{Z}$.

On the fermionic/topological front, the ℓ -wave condensate leads to an energy gap for single fermion excitations, which form a chiral SPT phase of matter: a topological superconductor [126, 127]. Topological superconductors are of interest since their chiral central charge $c \in (\ell/2)\mathbb{Z}$ can be half-integer, indicating the presence of chiral Majorana spinors on boundaries, each contributing an additive $\pm 1/2$ to c , where the sign depends on their chirality. In turn, this implies the presence of Majorana bound states, or zero modes, in the cores of vortices [15]. The observation of Majorana fermions, which are their own anti-particles, and may not exist in nature as elementary particles, is of fundamental interest. Moreover, Majorana bound states are closely related to non-abelian Ising anyons [128], which have been proposed as building blocks for topological quantum computers [129, 97].

On the bosonic/symmetry-breaking front, the ℓ -wave condensate implies an exotic symmetry breaking pattern, which leads to an unusual spectrum of bosonic excitations, and as a result, an unusual hydrodynamic description. In more detail, the condensation of ℓ -wave Cooper pairs corresponds to a non-vanishing ground-state expectation value for the operator $\psi^\dagger (\partial_x \pm i\partial_y)^{|\ell|} \psi^\dagger$, where ψ^\dagger is a fermion

creation operator⁵ and $\pm = \text{sgn}(\ell)$. An ℓ -wave condensate implies the breaking of time reversal symmetry T and parity (spatial reflection) P down to PT , and of the symmetry groups generated by particle number N and angular momentum L down to a diagonal subgroup

$$U(1)_N \times SO(2)_L \rightarrow U(1)_{L-(\ell/2)N}. \quad (1.2)$$

In CSFs, this symmetry breaking occurs spontaneously, due to a symmetric two-body attractive interaction between fermions. This phenomenon is generic, at least from the perspective of perturbative Fermi-surface renormalization group [130]. Thin films of $^3\text{He-A}$ are experimentally accessible p -wave CSFs [131–134], and there are many proposals for the realization of various ℓ -wave CSFs in cold atoms [135–141]. The spontaneous symmetry breaking (1.2) implies a single Goldstone field, charged under the broken generator $N + (\ell/2)L$, as well as massive Higgs fields, which are $U(1)_N$ -neutral, and carry angular momentum 0 and $\pm 2\ell$ [142–144, 1, 145]. In particular, p -wave ($\ell = \pm 1$) superfluids support Higgs fields of angular momentum 0 and ± 2 , which form a spatial metric, including a non-relativistic analog of the graviton [28, 15, 27]. This observation will play a central role in Sec.2. The angular momentum $\ell/2$ carried by the Goldstone field leads to a P, T -odd hydrodynamic description, including an odd (or Hall) viscosity, which is introduced below, and studied in Sec.3.

An *intrinsic* CSC is obtained if the $U(1)_N$ symmetry is gauged, by coupling to a dynamical gauge field. This gauge field physically corresponds to the 3+1D electromagnetic interaction between electrons, which are themselves confined to a 2+1D lattice of ions. Experimental evidence for chiral superconductivity was recently reported in Ref.[146]. One may also consider an emergent 2+1D gauge field, with a Chern-Simons and/or Maxwell dynamics. In particular, this leads to CSFs of ‘composite fermions’ [15, 147, 148], including field theoretic descriptions of the non-abelian candidates for the fractional quantum Hall state observed at filling $5/2$ [84], a subject of ongoing debate [85–87, 149, 88]. The symmetry breaking pattern (1.2) may also occur explicitly, due the proximity of a conventional s -wave superconductor (SC) to 2+1D spin-orbit coupled metal, in which case we speak of a *proximity induced* CSC, an observation of which was reported in Refs.[150, 151]. Note that in this case the Goldstone and Higgs fields can be viewed as non-dynamical.

Despite the large body of work on boundary Majorana fermions in CSFs and CSCs (CSF/Cs), the bulk geometric physics corresponding to these through anomaly inflow, and presumably captured by a gCS action, remains poorly understood, due to the difficulties mentioned in Sec.1.3. In fact, most existing statements, though made in truly pioneering and seminal work [28, 15, 17], are speculative, and are primarily based on an inaccurate adaptation of known results in relativistic QFT to p -wave CSF/Cs. An understanding of the bulk geometric physics is of particular importance since, in the simplest case of spin-less fermions with no additional internal symmetry, the only charge carried by the boundary Majorana fermions is energy-momentum, and the only boundary anomalies and bulk

⁵Due to Fermi statistics, ℓ must be odd if ψ is spin-less. An even ℓ requires spin-full fermions forming spin-less (singlet) Cooper pairs, $\psi_\uparrow^\dagger (\partial_x \pm i\partial_y)^{|\ell|} \psi_\downarrow^\dagger$. Spin-full fermions can also form spin-1 (triplet) Cooper pairs with odd ℓ , as is the case in $^3\text{He-A}$. Since the geometric physics we are interested in is independent of the spin of the Cooper pair, we restrict attention to spin-less fermions for odd ℓ , and write our expressions per spin component for even ℓ .

topological effective actions are therefore gravitational⁶. In particular, the boundary Majorana fermions are always $U(1)_N$ -neutral, and it follows that no $U(1)_N$ boundary anomaly or bulk topological effective action occurs⁷. Motivated by this state of affairs, the goal of Sec.2-3 is to turn the insightful ideas of Refs.[28, 15, 17] into concrete physical predictions.

As a first approach to the problem, in Sec.2 we follow Refs.[28, 15, 17] and utilize the low energy relativistic description of p -wave CSF/Cs, which exists because the p -wave condensate $\psi^\dagger (\partial_x \pm i\partial_y) \psi^\dagger$ is first order in derivatives. The main questions we ask are:

What type of space-time geometry emerges in the low energy relativistic description of p -wave superfluids and superconductors? What are the physical implications of the emergent relativistic geometry to these non-relativistic systems?

Our answer to the first question is that the fermionic excitations in p -wave CSF/Cs correspond at low energy to a massive relativistic Majorana spinor, which is minimally coupled to an emergent Riemann-Cartan geometry. This geometry is described by the p -wave order parameter $\Delta^i \sim \delta^{ij} \psi^\dagger \partial_j \psi^\dagger$, made up of the Goldstone and Higgs fields, as well as a $U(1)_N$ gauge field. As opposed to the Riemannian geometry previously believed to emerge [28, 15, 17], Riemann-Cartan space-times are characterized by a non-vanishing torsion tensor, in addition to the curvature tensor [154]. In condensed matter physics (or elasticity theory), torsion is well known to describe the density of lattice dislocations [155–158]⁸, and our results provide a new mechanism by which torsion can emerge - due to the symmetry breaking pattern (1.2) at $\ell = \pm 1$. The above statements are relevant if one aims at studying relativistic fermions in nontrivial space-times using table-top experiments [159], or if one hopes that emergent relativistic geometry in condensed matter can answer fundamental questions about the seemingly relativistic geometry of our universe [27]. Here, however, we are interested in answering the second question posed above.

As expected, a gCS term appears in the low energy effective action of p -wave CSF/Cs, and we find that it produces a precisely quantized bulk energy-momentum-stress response to the p -wave Higgs fields. Accordingly, a (perturbative) gravitational anomaly that depends on the Higgs fields appears on the boundary, implying a c -dependent transfer of energy-momentum between bulk and boundary. The emergence of torsion leads to additional interesting terms in the bulk effective action. In particular, a non-topological 'gravitational *pseudo* Chern-Simons' term produces an energy-momentum-stress response closely mimicking that of the gCS term, and we show how to disentangle the two responses in order to extract c from bulk measurements. In lattice models, the low energy description consists of an even number of relativistic Majorana spinors - a fermion doubling phenomena. Surprisingly, we

⁶For spin-full p -wave CSFs, one can exploit $SU(2)$ spin rotation symmetry, and does not have to resort to gravitational probes [152, 15, 153].

⁷An exception to this rule occurs in Galilean invariant systems, where momentum and $U(1)_N$ -current are identified, as we will see in Sec.3.

⁸Similarly, curvature traditionally describes the density of lattice disclinations, as well as the curving of a two-dimensional material in three dimensional space. It is also known that temperature gradients correspond to time-like torsion via Luttinger's trick [37, 41].

find that these spinors experience slightly different emergent geometries. As a result, additional 'gravitational Chern-Simons difference' terms are possible, which are again not of topological origin, but nevertheless imply responses which must be carefully distinguished from those of the gCS term. All other terms in the bulk effective action are either higher in derivatives, or are lower in derivatives but naively diverge within the relativistic description. The latter 'UV-sensitive' terms cannot be reliably interpreted based on the relativistic description, and require a non-relativistic treatment. In particular, the relativistic, UV-sensitive, and somewhat controversial 'torsional Hall viscosity' [155–158, 160, 41], is found in Sec.3 to correspond to the non-relativistic and well understood odd (or Hall) viscosity of CSF/Cs [161–163, 36, 164], which is introduced below.

Before continuing, we note that there has been considerable recent interest in torsional physics in condensed matter, in systems described at low energy by 3+1D Weyl (or Majorana-Weyl) spinors, namely Weyl semi-metals and $^3\text{He-A}$ [165–170], and in Kitaev's honeycomb model [171, 172].

1.5 Odd viscosity

The odd (or Hall) viscosity η_o is a non-dissipative, time reversal odd, stress response to strain-rate [173–175, 160, 176], which can appear even in superfluids (SFs) and incompressible (or gapped) fluids, where the more familiar and intuitive dissipative viscosity vanishes. The observable signatures of η_o are actively studied in a variety of systems [177–186], and recently led to its measurement in a colloidal chiral fluid [187] and in graphene's electron fluid under a magnetic field [188].

In isotropic 2+1 dimensional fluids, the odd viscosity tensor at zero wave-vector ($\mathbf{q} = 0$) reduces to a single component. In analogy with the celebrated quantization of the odd (or Hall) conductivity in the quantum Hall (QH) effect [9, 8, 189, 106, 190, 191], this component obeys a quantization condition

$$\eta_o^{(1)} = -(\hbar/2) s \cdot n_0, \quad s \in \mathbb{Q}, \quad (1.3)$$

in incompressible quantum fluids, such as integer and fractional QH states [173, 161, 162]. Here n_0 is the ground state density, and s is a rational-valued topological invariant⁹, labeling the many-body ground state, which can be interpreted as the average angular momentum per particle (in units of \hbar , which is henceforth set to 1).

Remarkably, Eq.(1.3) also holds in CSFs, though they are compressible. Computing $\eta_o^{(1)}$ in an ℓ -wave CSF, one finds Eq.(1.3) with the intuitive angular momentum per fermion, $s = \ell/2$ [161–163, 36, 164]. Thus, a measurement of $\eta_o^{(1)}$ at $\mathbf{q} = \mathbf{0}$ can be used to obtain the angular momentum ℓ of the Cooper pair, but carries no additional information. It is therefore clear that the symmetry breaking pattern (1.2) which defines ℓ , rather than ground-state topology, is the origin of the quantization $s = \ell/2$ in CSFs¹⁰.

⁹In fact, an $SO(2)_L$ -symmetry-protected topological invariant.

¹⁰Accordingly, the quantization of s is broken in a mixture of CSFs with different ℓ s, where $U(1)_N \times SO(2)_L$ is completely broken. In the mixture $s \equiv -2\eta_o^{(1)}/n = \sum_i n_i (\ell_i/2) / \sum_i n_i$ retains its meaning as an average angular momentum per particle, but is no longer quantized. This should be contrasted with multicomponent QH states [42], where all n_i s are proportional to the same applied magnetic field through the filling factors $\nu_i \in \mathbb{Q}$, and s remains quantized.

Nevertheless, the gapped fermions in a CSF do carry non-trivial ground-state topology labeled by the central charge $c \in (\ell/2)\mathbb{Z}$, and, based on results in quantum Hall states [34, 43, 42], a c -dependent correction to $\eta_o^{(1)}$ of Eq.(1.3) is therefore expected to appear at small non-zero wave-vector,

$$\delta\eta_o^{(1)}(\mathbf{q}) = -\frac{c}{24} \frac{1}{4\pi} q^2. \quad (1.4)$$

This raises the questions:

In chiral superfluids, can the boundary chiral central charge be extracted from a measurement of the bulk odd viscosity? Can it be extracted from any bulk measurement?

Providing a definite answer to these questions is the main goal of Sec.3, and requires a fully non-relativistic treatment of CSFs. The main reason for this is that the relativistic low energy description misses most of the physics of the Goldstone field. Analysis of Goldstone physics in CSFs was undertaken in Refs.[192–195, 153, 196–198], most of which revolving around the non-vanishing, yet non-quantized, Hall (or odd) conductivity in CSFs. More recently, Refs.[163, 164] considered CSFs in curved (or strained) space, following the pioneering work [199] on s -wave ($\ell = 0$) SFs. These works demonstrated that the Goldstone field, owing to its charge $L + (\ell/2)N$, produces the $\mathbf{q} = \mathbf{0}$ odd viscosity (1.3), and it is therefore natural to expect that a q^2 correction similar to (1.4) will also be produced. Nevertheless, Refs.[163, 164] did not consider the derivative expansion to the high order at which q^2 corrections to η_o would appear, nor did they detect any bulk signature of c at lower orders. In Sec.3 we obtain a low energy effective field theory that consistently captures both the chiral Goldstone mode and the gCS term, thus unifying and extending the seemingly unrelated analysis of Refs.[199, 163, 164] and Sec.2. Using the theory we show that c cannot be extracted for a measurement of the odd viscosity alone, as suggested by Eq.(1.4). Nevertheless, a related observable, termed ‘improved odd viscosity’, does allow for the bulk measurement of c . Additional results of the same spirit are found in Galilean invariant CSFs.

1.6 Quantum Monte Carlo sign problems in chiral topological matter

Utilizing a random sampling of phase-space according to the Boltzmann probability distribution, Monte Carlo simulations are arguably the most powerful tools for numerically evaluating thermal averages in classical many-body physics [200]. Though the phase-space of an N -body system scales exponentially with N , a Monte-Carlo approximation with a fixed desired error is usually obtained in polynomial time [72, 201]. In *Quantum* Monte Carlo (QMC), one attempts to perform Monte-Carlo computations of thermal averages in quantum many-body systems, by following the heuristic idea that quantum systems in d dimensions are equivalent to classical systems in $d + 1$ dimensions [65, 71].

The difficulty with any such quantum to classical mapping, henceforth referred to as a *method*, is the infamous *sign problem*, where the mapping can produce complex, rather than non-negative, Boltzmann weights p , which do not correspond to a probability distribution. Faced with a sign problem, one can try to change the method used and obtain $p \geq 0$, thus *curing the sign problem* [73, 74]. Alternatively,

one can perform QMC using the weights $|p|$, which is often done but generically leads to an exponential computational complexity in evaluating physical observables, limiting ones ability to simulate large systems at low temperatures [72].

Conceptually, the sign problem can be understood as an obstruction to mapping quantum systems to classical systems, and accordingly, from a number of complexity theoretic perspectives, a generic curing algorithm in polynomial time is not believed to exist [72, 202, 75, 73, 203, 74]. In many-body physics, however, one is mostly interested in universal phenomena, i.e phases of matter and the transitions between them, and therefore representative Hamiltonians which are free of the sing problem (henceforth 'sign-free') often suffice [68]. In fact, QMC simulations continue to produce unparalleled results, in all branches of many-body quantum physics, precisely because new sign-free models are constantly being discovered [64, 204, 66–71]. Designing sign-free models requires *design principles* (or “de-sign” principles) [68, 205] - easily verifiable properties that, if satisfied by a Hamiltonian and method, lead to a sign-free representation of the corresponding partition function. An important example is the condition $\langle i | H | j \rangle \leq 0$ where $i \neq j$ label a local basis, which implies non-negative weights p in a wide range of methods [68, 203]. Hamiltonians satisfying this condition in a given basis are known as *stoquastic* [202], and have proven very useful in both application and theory of QMC in bosonic (or spin, or 'qudit') systems [68, 72, 202, 75, 73, 203, 74].

Fermionic Hamiltonians are not expected to be stoquastic in any local basis [72, 71], and alternative methods, collectively known as determinantal quantum Monte-Carlo (DQMC), are therefore used [206, 65, 77, 71, 70]. The search for design principles that apply to DQMC, and applications thereof, has naturally played the dominant role in tackling the sign problem in fermionic systems, and has seen a lot of progress in recent years [207, 205, 208–210, 70, 71]. Nevertheless, long standing open problems in quantum many-body physics continue to defy solution, and remain inaccessible for QMC. These include the nature of high temperature superconductivity and the associated repulsive Hubbard model [77–80], dense nuclear matter and the associated lattice QCD at finite baryon density [81–83], and the enigmatic fractional quantum Hall state at filling 5/2 and its associated Coulomb Hamiltonian [84–88, 55], all of which are fermionic.

One may wonder if there is a fundamental reason that no design principle applying to the above open problems has so far been found, despite intense research efforts. More generally,

Are there phases of matter that do not admit a sign-free representative? Are there physical properties that cannot be exhibited by sign-free models?

We refer to such phases of matter, where the sign problem simply cannot be cured, as having an *intrinsic sign problem* [75]. From a practical perspective, intrinsic sign problems may prove useful in directing research efforts and computational resources. From a fundamental perspective, intrinsic sign problems identify certain phases of matter as inherently quantum - their physical properties cannot be reproduced by a partition function with positive Boltzmann weights.

To the best of our knowledge, the first intrinsic sign problem was discovered by Hastings [75], who proved that no stoquastic, commuting projector, Hamiltonians exist for the 'doubled semion' phase [211],

which is bosonic and topologically ordered. In Ref.[5], we generalize this result considerably - excluding the possibility of stoquastic Hamiltonians in a broad class of bosonic non-chiral topological phases of matter. Additionally, Ref.[76] demonstrated, based on the algebraic structure of edge excitations, that no translationally invariant stoquastic Hamiltonians exist for bosonic chiral topological phases.

In Sec.4, we will establish a new criterion for intrinsic sign problems in chiral topological matter, and take the first step in analyzing intrinsic sign problems in fermionic systems. First, based on the well established 'momentum polarization' method for characterizing chiral topological matter [212, 213, 38, 214], we obtain a variant of the result of Ref.[76] - excluding the possibility of stoquastic Hamiltonians in a broad class of bosonic chiral topological phases. We then develop a formalism with which we obtain analogous results for systems comprised of both bosons *and* fermions - excluding the possibility of sign-free DQMC simulations.

Phase of matter	Parameterization	c	$\{h_a\}$	Intrinsic sign problem?
Laughlin (B) [55]	Filling $1/q$, ($q \in 2\mathbb{N}$)	1	$\{a^2/2q\}_{a=0}^{q-1}$	In 98.5% of first 10^3
Laughlin (F) [55]	Filling $1/q$, ($q \in 2\mathbb{N} - 1$)	1	$\{(a + 1/2)^2 / 2q\}_{a=0}^{q-1}$	In 96.7% of first 10^3
Chern insulator (F) [3]	Chern number $\nu \in \mathbb{Z}$	ν	$\{\nu/8\}$	For $\nu \notin 12\mathbb{Z}$
ℓ -wave superconductor (F) [2]	Pairing channel $\ell \in 2\mathbb{Z} - 1$	$-\ell/2$	$\{-\ell/16\}$	Yes
Kitaev spin liquid (B) [104]	Chern number $\nu \in 2\mathbb{Z} - 1$	$\nu/2$	$\{0, 1/2, \nu/16\}$	Yes
$SU(2)_k$ Chern-Simons (B) [215]	Level $k \in \mathbb{N}$	$3k/(k+2)$	$\{a(a+2)/4(k+2)\}_{a=0}^k$	In 91.6% of first 10^3
E_8 K -matrix (B) [216]	Stack of $n \in \mathbb{N}$ copies	$8n$	$\{0\}$	For $n \notin 3\mathbb{N}$
Fibonacci anyon model (B) [215]		$14/5 \pmod{8}$	$\{0, 2/5\}$	Yes
Pfaffian (F) [217]		$3/2$	$\{0, 1/2, 1/4, 3/4, 1/8, 5/8\}$	Yes
PH-Pfaffian (F) [217]		$1/2$	$\{0, 0, 1/2, 1/2, 1/4, 3/4\}$	Yes
Anti-Pfaffian (F) [217]		$-1/2$	$\{0, 1/2, 1/4, 3/4, 3/8, 7/8\}$	Yes

Table 1: Examples of intrinsic sign problems based on the criterion $e^{2\pi ic/24} \notin \{\theta_a\}$, in terms of the chiral central charge c and the topological spins $\theta_a = e^{2\pi i h_a}$. The number of spins h_a is equal to the dimension of the ground state subspace on the torus. We mark bosonic/fermionic phases by (B/F). The quantum Hall Laughlin phases correspond to $U(1)_q$ Chern-Simons theories. The ℓ -wave superconductor is chiral, e.g $p + ip$ for $\ell = 1$, and comprised of a single flavour of spinless fermions. The data shown refers only to the SPT phase formed by gapped fermionic excitations, see Sec.1.4. Data for the spinfull case is identical to that of the Chern insulator, with $-\ell$ odd (even) in place of ν , for triplet (singlet) pairing. The modulo 8 ambiguity in the central charge of the Fibonacci anyon model corresponds to the stacking of a given realization with copies of the E_8 K -matrix phase. Data for the three quantum Hall Pfaffian phases is given at the minimal filling $1/2$. The physical filling $5/2$ is obtained by stacking with a $\nu = 2$ Chern insulator, and an intrinsic sign problem appears in this case as well.

All of the above mentioned topological phases are gapped, 2+1 dimensional, and described at low energy by a topological field theory [218, 104, 19]. The class of such phases in which we find an intrinsic sign problem is defined in terms of robust data characterizing them: the chiral central charge c , a rational number, as well as the set $\{\theta_a\}$ of topological spins of anyons, a subset of roots of unity. Namely, we find that

$$\text{An intrinsic sign problem exists if } e^{2\pi ic/24} \text{ is not the topological spin of some anyon, i.e } e^{2\pi ic/24} \notin \{\theta_a\}.$$

The above criterion applies to most chiral topological phases, see Table 1 for examples. In particular, we identify an intrinsic sign problem in 96.7% of the first one-thousand fermionic Laughlin phases, and in all non-abelian Kitaev spin liquids. We also find intrinsic sign problems in 91.6% of the first one-thousand $SU(2)_k$ Chern-Simons theories. Since, for $k \neq 1, 2, 4$, these allow for universal quantum computation by manipulation of anyons [219, 97], our results support the strong belief that quantum computation cannot be simulated with classical resources, in polynomial time [220]. This conclusion is strengthened by examining the Fibonacci anyon model, which is known to be universal for quantum computation [97], and is found to be intrinsically sign-problematic.

We stress that both c and $\{\theta_a\}$ have clear observable signatures in both the bulk and boundary of chiral topological matter, some of which have been experimentally observed. The chiral central charge was extensively discussed in previous section, including its observation in Refs.[112, 113, 84, 114, 53]. The topological spins determine the exchange statistics of anyons, predicted to appear in interferometry experiments [97]. Experimental observation remained elusive [221] until it was recently reported in the Laughlin 1/3 quantum Hall state [222]. Additionally, a measurement of anyonic statistics via current correlations [223] was recently reported in the Laughlin 1/3 state [224].

2 Probing topological superconductors with emergent relativistic gravity

In this section, we restrict our attention to spin-less p -wave chiral superfluids and superconductors (CSF/Cs), and analyze the relativistic geometry, or gravity, that emerges at low energy. We seek answers to the questions posed in Sec.1.4.

2.1 Approach and main results

2.1.1 Model and approach

As a starting point, we consider a simple model for spin-less p -wave CSF/Cs [225]. The action is given by

$$S[\psi; \Delta] = \int d^{2+1}x \left[\psi^\dagger \left(i\partial_t + \frac{\delta^{ij}\partial_i\partial_j}{2m^*} - m \right) \psi + \left(\frac{1}{2}\psi^\dagger \Delta^j \partial_j \psi + h.c \right) \right], \quad (2.1)$$

and describes the coupling of a spin-less fermion ψ , with effective mass m^* and chemical potential $-m$, to a p -wave order parameter $\Delta = (\Delta^x, \Delta^y) \in \mathbb{C}^2$. The order parameter corresponds to the condensate of Cooper pairs described in Sec.1.4. In a proximity induced CSC, the order parameter can be thought of as a non-dynamical background field, as it appears in Eq.(2.1). In intrinsic CSCs, and in CSFs, the order parameter is a quantum field which mediates an attractive interaction between fermions, and a treatment of the dynamics of Δ is deferred to Sec.2.6 and 3. The ground-state, or unperturbed, configuration of Δ is the $p_x \pm ip_y$ configuration $\Delta = \Delta_0 e^{i\theta} (1, \pm i)$, where $\Delta_0 > 0$ and θ are constants. The phase θ corresponds to the Goldstone field implied by Eq.(1.2), while the orientation (or chirality) $o = \pm$ corresponds to the breaking of reflection and time reversal symmetries to their product, $P \times T \rightarrow PT$.

One may view the model (2.1) as 'microscopic', as will be done in Sec.3, but here we will think of it as the low energy description of a lattice model, introduced and analyzed in Sec.2.2. In the 'relativistic regime' where the order parameter is much larger than the single particle scales, the lattice model is essentially a lattice regularization of four, generically massive, relativistic Majorana spinors, centered at the particle-hole invariant points $k = -k$ in the Brillouin zone. Around each of these four points, the low energy description is given by an action of the form (2.1). In the relativistic regime the effective mass m^* is large, and in the limit $m^* \rightarrow \infty$ Eq.(2.1) reduces to a relativistic action, with mass m and speed of light $c_{\text{light}} = \Delta_0/\hbar$, for the Nambu spinor $\Psi^\dagger = (\psi^\dagger, \psi)$, which is a Majorana spinor. The different Majorana spinors, associated with the four particle-hole invariant points, have different orientations o_n and masses m_n , where $1 \leq n \leq 4$.

The chiral central charge of the lattice model can be deduced from its Chern number [15, 104, 27, 107]. The n th Majorana spinor contributes $c_n = o_n \text{sgn}(m_n)/4$, and summing over n one obtains the central charge of the lattice model $c = \sum_{n=1}^4 c_n = \sum_{n=1}^4 o_n \text{sgn}(m_n)/4$, which gives the topological phase diagram purely in terms of the low energy relativistic data o_n, m_n , see Sec.2.2. This formula motivates a study of the geometric physics associated with c , purely within the low energy relativistic description,

which we now pursue.

In order to access the physics associated with c , we perturb the order parameter out of the $p_x \pm ip_y$ configuration, and treat $\Delta = (\Delta^x, \Delta^y) \in \mathbb{C}^2$ as a general space-time dependent field. This is analogous to applying an electromagnetic field in order to measure a quantized Hall conductivity in the quantum Hall effect. Following the observations of Refs.[27, 15], we show in Sec.2.3 that, in the relativistic limit, the Majorana spinor Ψ experiences such a general order parameter (along with a general $U(1)_N$ gauge field) as a non trivial gravitational background, namely Riemann-Cartan geometry. See also Sec.2.2.2 for the basics of this statement. Some of the emergent geometry is described by the (inverse) spatial metric

$$g^{ij} = -\Delta^{(i} \Delta^{j)*}, \quad (2.2)$$

where brackets denote the symmetrization, and the sign is a matter of convention. The metric g^{ij} corresponds to the Higgs field included in the order parameter. Parameterizing $\Delta = e^{i\theta} (|\Delta^x|, e^{i\phi} |\Delta^y|)$ with the overall phase θ and relative phase $\phi \in (-\pi, \pi]$, the metric is independent of θ and of the orientation $o = \text{sgn}\phi = \pm$, which splits order parameters into $p_x + ip_y$ -like and $p_x - ip_y$ -like. Note that in the $p_x \pm ip_y$ configuration the metric is euclidian, $g^{ij} = -\Delta_0^2 \delta^{ij}$. For our purposes it is important that the metric be perturbed out of this form, and in particular it is not enough to take the $p_x \pm ip_y$ configuration with a space-time dependent Goldstone field θ .

2.1.2 Topological bulk responses from a gravitational Chern-Simons term

Using the mapping of p -wave CSF/Cs to relativistic Majorana fermions in Riemann-Cartan space-time, we compute and analyze in Sec.2.5 the effective action obtained by integrating over the bulk fermions in the presence of a general order parameter Δ , and $U(1)_N$ gauge field. Here we discuss the main physical implications of this effective action. As already explained in Sec.1.4, we only describe UV-insensitive physics, which can be reliably understood within the low energy relativistic description. This physics is controlled by dimensionless coefficients, including the chiral central charge c in which we are primarily interested.

As expected, the effective action contains a gCS term [21–24, 115, 25]

$$S_{\text{gCS}} = \alpha \int \text{tr} \left(\tilde{\Gamma} \wedge d\tilde{\Gamma} + \frac{2}{3} \tilde{\Gamma} \wedge \tilde{\Gamma} \wedge \tilde{\Gamma} \right), \quad (2.3)$$

with coefficient $\alpha = \frac{c}{96\pi} \in \frac{1}{192\pi} \mathbb{Z}$, and where $\tilde{\Gamma}$ is the Christoffel symbol of the space-time metric obtained from Eq.(2.2), see Sec.2.5.2.2. Although we obtain this result in the limit $m^* \rightarrow \infty$, we expect it to hold throughout the phase diagram. This is based on known arguments for the quantization of the coefficient α due to symmetry, and on the relation with the boundary gravitational anomaly described below.

The gCS term implies a topological bulk response, where energy-momentum currents and densities appear due to a space-time dependent order parameter. To see this in the simplest setting, assume that

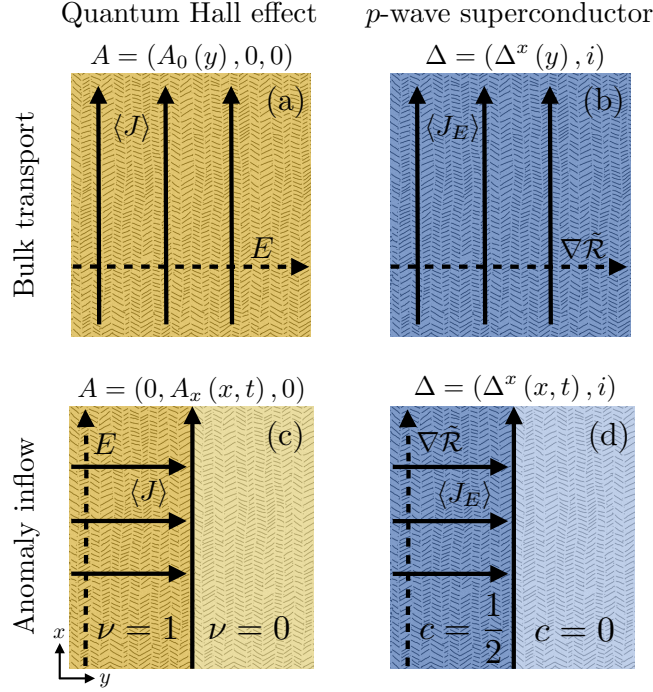


Figure 3: A comparison of the integer quantum Hall effect (IQHE) and its energy-momentum analog in p -wave CSF/Cs. (a) In the IQHE there is a perpendicular electric current $\langle J \rangle$ in response to an applied electric field E , with a quantized Hall conductivity, proportional to the Chern number $\nu \in \mathbb{Z}$, as encoded in a $U(1)_N$ Chern-Simons term. (b) In p -wave CSF/Cs, an energy current $\langle J_E \rangle$ flows in response to a space dependent order parameter Δ , as encoded in a gravitational Chern-Simons term. Derivatives of the curvature $\tilde{\mathcal{R}}$ associated with Δ play the role of the electric field in the IQHE, and $\langle J_E \rangle$ is perpendicular to the curvature gradient $\nabla \tilde{\mathcal{R}}$. The ratio between the magnitudes of $\langle J_E \rangle$ and $\nabla \tilde{\mathcal{R}}$ is quantized, and proportional to the chiral central charge $c \in (1/2)\mathbb{Z}$. As described in the text, the spontaneous breaking of $U(1)_N$ symmetry in p -wave CSF/Cs allows for a gravitational *pseudo* Chern-Simons term, encoding closely related bulk responses, which are not topological in nature. (c) The quantized Hall conductivity implies the existence of a chiral boundary fermion with a $U(1)_N$ anomaly, which can be described as a Weyl fermion at low energy. (d) The analogous response in p -wave CSF/Cs implies the existence of a boundary chiral Majorana fermion with a gravitational anomaly, which can be described as a Majorana-Weyl fermion at low energy.

the order parameter is time independent, and that the relative phase is $\phi = \pm \frac{\pi}{2}$, as in the $p_x \pm ip_y$ configuration, so that $\Delta = e^{i\theta} (|\Delta^x|, \pm i |\Delta^y|)$, $o = \pm$. Then the metric is time independent, and takes the simple form

$$g^{ij} = - \begin{pmatrix} |\Delta^x|^2 & 0 \\ 0 & |\Delta^y|^2 \end{pmatrix}. \quad (2.4)$$

On this background, we find the following contributions to the expectation values of the fermionic energy

current J_E^i , and momentum density P_i ¹¹,

$$\begin{aligned}\langle J_E^i \rangle_{\text{gCS}} &= -\frac{c}{96\pi} \frac{1}{\hbar} \varepsilon^{ij} \partial_j \tilde{\mathcal{R}}, \\ \langle P_i \rangle_{\text{gCS}} &= -\frac{c}{96\pi} \hbar g_{ik} \varepsilon^{kj} \partial_j \tilde{\mathcal{R}}.\end{aligned}\tag{2.5}$$

Here $\tilde{\mathcal{R}}$ is the curvature, or Ricci scalar, of the metric g_{ij} , which is the inverse of g^{ij} , and $\varepsilon^{xy} = -\varepsilon^{yx} = 1$. The curvature for the above metric is given explicitly by

$$\tilde{\mathcal{R}} = -2 |\Delta^x| |\Delta^y| \left(\partial_y \left(\frac{|\Delta^y| \partial_y |\Delta^x|}{|\Delta^x|^2} \right) + \partial_x \left(\frac{|\Delta^x| \partial_x |\Delta^y|}{|\Delta^y|^2} \right) \right).\tag{2.6}$$

It is a nonlinear expression in the order parameter, which is second order in derivatives. Thus the responses (2.5) are third order in derivatives, and start at linear order but include nonlinear contributions as well. The first equation in (2.5) is analogous to the response $\langle J^i \rangle = \frac{\nu}{2\pi} \varepsilon^{ij} E_j$ of the IQHE, see Fig 3(a),(b). The second equation is analogous to the dual response $\langle \rho \rangle = \frac{\nu}{2\pi} B$.

2.1.3 Additional bulk responses from a gravitational pseudo Chern-Simons term

Apart from the gCS term, the effective action obtained by integrating over the bulk fermions also contains an additional term of interest, which we refer to as a gravitational *pseudo* Chern-Simons term (gpCS). To the best of our knowledge, the gpCS term has not appeared previously in the context of p -wave CSF/Cs. It is possible because $U(1)_N$ symmetry is spontaneously broken in p -wave CSF/Cs. In the geometric point of view, this translates to the emergent geometry in p -wave CSF/Cs being not only curved but also torsion-full. The gpCS term produces bulk responses which are closely related to those of gCS, despite it being fully gauge invariant. This gauge invariance implies that it is not associated with a boundary anomaly, nor does its coefficient β need to be quantized. Hence, gpCS does not encode *topological* bulk responses. Remarkably, we find that β is quantized and identical to the coefficient $\alpha = \frac{c}{96\pi}$ of the gCS term in the limit of $m^* \rightarrow \infty$, but we do not expect this value to hold outside of this limit. Let us now describe the bulk responses from gpCS, setting $\beta = \frac{c}{96\pi}$. First, we find the following contributions to the fermionic energy current and momentum density,

$$\begin{aligned}\langle J_E^i \rangle_{\text{gpCS}} &= \frac{c}{96\pi} \varepsilon^{ij} \partial_j \tilde{\mathcal{R}}, \\ \langle P_i \rangle_{\text{gpCS}} &= -\frac{c}{96\pi} g_{ik} \varepsilon^{kj} \partial_j \tilde{\mathcal{R}}.\end{aligned}\tag{2.7}$$

Up to the sign difference in the first equation, these responses are the same as those from gCS (2.5). As opposed to gCS, the gpCS term also contributes to the fermionic charge density $\rho = -\psi^\dagger \psi$. For the bulk responses we have written thus far, every Majorana spinor contributed $c_n = \frac{q_n}{4} \text{sgn}(m_n)$, and summing over n produced the central charge c . For the density response this is not the case. Here, the

¹¹ P_x (P_y) is the density of the x (y) component of momentum.

n th Majorana spinor contributes

$$\langle \rho \rangle_{\text{gpCS}} = \frac{o_n c_n}{24\pi} \sqrt{g} \tilde{\mathcal{R}}, \quad (2.8)$$

where $\sqrt{g} = \sqrt{\det g_{ij}}$ is the emergent volume element. The orientation o_n in Eq. (2.8) makes the sum over the four Majorana spinors different from the central charge, $\sum_{n=1}^4 o_n c_n = \sum_{n=1}^4 \frac{1}{2} \text{sgn}(m_n) \neq c$. The appearance of o_n can be understood by considering the effect of time reversal, since both the density and curvature are time reversal even. The response (2.8) also holds when the order parameter is time dependent, in which case $\tilde{\mathcal{R}}$ will also contain time derivatives. One then finds a time dependent density, but there is no corresponding current response, which is due to the breaking of $U(1)_{\text{Nsymmetry}}$.

To gain some insight into the expressions we have written thus far, we write the operators P, J_E more explicitly. For each Majorana spinor (suppressing the index n),

$$\begin{aligned} P_j &= \frac{i}{2} \psi^\dagger \overleftrightarrow{D}_j \psi, \\ J_E^j &= g^{jk} P_k + \frac{o}{2} \partial_k \left(\frac{1}{\sqrt{g}} \varepsilon^{jk} \rho \right) + O\left(\frac{1}{m^*}\right). \end{aligned} \quad (2.9)$$

The momentum density is the familiar expression for free fermions, but in the energy current we have only written explicitly contributions that survive the limit $m^* \rightarrow \infty$. These contributions are only possible due to the p -wave pairing, and are of order Δ^2 . From the relation (2.9) between J_E, P and ρ we can understand that the equality $\langle J_E^j \rangle_{\text{gCS}} = g^{jk} \langle P_k \rangle_{\text{gCS}}$ expressed in equation (2.5) is a result of the vanishing contribution of gCS to the density ρ . We can also understand the sign difference between the first and second line of (2.7) as a result of (2.8). The important point is that a measurement of the charge density ρ can be used to fix the value of the coefficient β , which is generically unquantized, and thus separate the contributions of gpCS to P, J_E , from those of gCS. In this manner, one can overcome the obscuring of gCS by gpCS.

2.1.4 Bulk-boundary correspondence from gravitational anomaly

Among the two terms in the bulk effective action which we described in Sec.2.1.2-2.1.3, only gCS is related to the boundary gravitational anomaly. This relation can be explicitly analyzed in the case where $\Delta = \Delta_0 e^{i\theta(t,x)} (1 + f(x,t), i)$ is a perturbation of the $p_x + ip_y$ configuration with small f , and there is a domain wall (or boundary) at $y = 0$ where the value of c jumps. For simplicity, assume $c = 1/2$ for $y < 0$ and $c = 0$ for $y > 0$. This situation is illustrated in Fig.3(d). In Appendix A we derive the action for the boundary, or edge mode,

$$S_e = \frac{i}{2} \int dt dx \tilde{\xi} (\partial_t - |\Delta^x(t, x)| \partial_x) \tilde{\xi}, \quad (2.10)$$

which describes a chiral $D = 1 + 1$ Majorana fermion $\tilde{\xi}$ localized on the boundary, with a space-time dependent velocity $|\Delta^x(x, t)| = \Delta_0 |1 + f(x, t)|$. Classically, the edge fermion $\tilde{\xi}$ conserves energy-

momentum in the following sense,

$$\partial_\beta t_{\text{e}}^\beta{}_\alpha + \partial_\alpha \mathcal{L}_{\text{e}} = 0. \quad (2.11)$$

Here t_{e} is the canonical energy-momentum tensor for $\tilde{\xi}$, with indices $\alpha, \beta = t, x$, and \mathcal{L}_{e} is the edge Lagrangian, $S_{\text{e}} = \int dt \mathcal{L}_{\text{e}}$, see Sec.2.4.1.2. For $\alpha = t$ ($\alpha = x$), Eq.(2.11) describes the sense in which the edge fermion conserves energy (momentum) classically. The source term $\partial_\alpha \mathcal{L}_{\text{e}}$ follows from the space-time dependence of \mathcal{L}_{e} through Δ^x . Quantum mechanically, the action S_{e} is known to have a gravitational anomaly, which means that energy-momentum is not conserved at the quantum level [12]. In the context of emergent gravity, this implies that Eq.(2.11) is violated for the expectation values,

$$\partial_\beta \langle t_{\text{e}}^\beta{}_\alpha \rangle + \partial_\alpha \langle \mathcal{L}_{\text{e}} \rangle = -\frac{c}{96\pi} g_{\alpha\gamma} \varepsilon^{\gamma\beta y} \partial_\beta \tilde{\mathcal{R}}. \quad (2.12)$$

This equation is written with $\hbar = 1$ and $c_{\text{light}} = \Delta_0/\hbar = 1$ for simplicity. Since Δ^x depends on time, $\tilde{\mathcal{R}}$ is not the curvature of the spatial metric g_{ij} , but of a corresponding space-time metric $g_{\mu\nu}$ (2.28), and is given by $\tilde{\mathcal{R}} = \ddot{f} - 2\dot{f}^2 + O(f\ddot{f}, f\dot{f}^2)$ in this case. Note that time dependence in this example is crucial. From gCS we find for $\Delta = \Delta_0 e^{i\theta(t,x)} (1 + f(x, t), i)$ the bulk energy-momentum tensor

$$\langle t_\alpha^y \rangle_{\text{gCS}} = -\frac{c}{96\pi} g_{\alpha\gamma} \varepsilon^{\gamma\beta y} \partial_\beta \tilde{\mathcal{R}}, \quad (2.13)$$

which explains the anomaly as the inflow of energy-momentum from the bulk to the boundary,

$$\partial_\beta \langle t_{\text{e}}^\beta{}_\alpha \rangle + \partial_\alpha \langle \mathcal{L}_{\text{e}} \rangle = \langle t_\alpha^y \rangle_{\text{gCS}}. \quad (2.14)$$

Since c jumps from $1/2$ to 0 at $y = 0$ the energy-momentum current (2.13) stops at the boundary and does not extend to the $y > 0$ region. The gravitationally anomalous boundary mode is then essential for the conservation of total energy-momentum to hold. As this example shows, bulk-boundary correspondence follows from bulk+boundary conservation of energy-momentum in the presence of a space-time dependent order parameter.

2.2 Lattice model

In this section we review and slightly generalize a simple lattice model for a p -wave SC [226], which will serve as our microscopic starting point. We describe its band structure and its symmetry protected topological phases, and also explain some of the basics of the emergent geometry which can be seen in this setting.

The hamiltonian is given in real space by

$$H = -\frac{1}{2} \sum_{\mathbf{l}} \left[t\psi_{\mathbf{l}}^\dagger \psi_{\mathbf{l}+x} + t\psi_{\mathbf{l}}^\dagger \psi_{\mathbf{l}+y} + \mu\psi_{\mathbf{l}}^\dagger \psi_{\mathbf{l}} + \delta^x \psi_{\mathbf{l}}^\dagger \psi_{\mathbf{l}+x}^\dagger + \delta^y \psi_{\mathbf{l}}^\dagger \psi_{\mathbf{l}+y}^\dagger + h.c. \right]. \quad (2.15)$$

Here the sum is over all lattice sites $\mathbf{l} \in L$ of a 2 dimensional square lattice $L = a\mathbb{Z} \times a\mathbb{Z}$, with a lattice spacing a . $\psi_{\mathbf{l}}^\dagger, \psi_{\mathbf{l}}$ are creation and annihilation operators for spin-less fermions on the lattice, with the canonical anti commutators $\{\psi_{\mathbf{l}}^\dagger, \psi_{\mathbf{l}'}\} = \delta_{\mathbf{l}\mathbf{l}'}$. $\mathbf{l} + x$ denotes the nearest neighboring site to \mathbf{l} in the x direction. The hopping amplitude t is real and μ is the chemical potential. Apart from the single particle terms $t\psi_{\mathbf{l}}^\dagger\psi_{\mathbf{l}+x} + t\psi_{\mathbf{l}}^\dagger\psi_{\mathbf{l}+y} + \mu$, there is also the pairing term $\delta^x\psi_{\mathbf{l}}^\dagger\psi_{\mathbf{l}+x}^\dagger + \delta^y\psi_{\mathbf{l}}^\dagger\psi_{\mathbf{l}+y}^\dagger$, with the order parameter $\delta = (\delta^x, \delta^y) \in \mathbb{C}^2$. We think of δ as resulting from a Hubbard-Stratonovich decoupling of interactions, in which case we refer to it as intrinsic, or as being induced by proximity to an s -wave SC. In both cases we treat δ as a bosonic background field that couples to the fermions.

The generic order parameter is charged under a few symmetries of the single particle terms. The order parameter has charge 2 under the global $U(1)$ group generated by $Q = -\sum_{\mathbf{l}} \psi_{\mathbf{l}}^\dagger\psi_{\mathbf{l}}$, in the sense that $e^{-i\alpha Q} H(e^{2i\alpha}\delta) e^{i\alpha Q} = H(\delta)$, which physically represents the electromagnetic charge -2 of Cooper pairs¹². The order parameter is also charged under time reversal T , which is an anti unitary transformation satisfying $T^2 = 1$, that acts as the complex conjugation of coefficients in the Fock basis corresponding to $\psi_{\mathbf{l}}, \psi_{\mathbf{l}}^\dagger$. The equation $T^{-1}H(\delta^*)T = H(\delta)$ shows $\delta \mapsto \delta^*$ under time reversal. Finally, δ is also charged under the point group symmetry of the lattice, which for the square lattice is the Dihedral group D_4 . The continuum analog of this is that the order parameter is charged under spatial rotations and reflections, and more generally, under space-time transformations (diffeomorphisms), which is due to the orbital angular momentum 1 of Cooper pairs in a p -wave SC. This observation will be important for our analysis, and will be discussed further below.

In an intrinsic $p_x \pm ip_y$ SC, the configuration of δ which minimizes the ground state energy is given by $\delta = \delta_0 e^{i\theta} (1, \pm i)$, where $\delta_0 > 0$ is determined by the minimization, but the sign $o = \pm 1$ and the phase θ (which dynamically corresponds to a goldstone mode) are left undetermined. See [27] for a pedagogical discussion of a closely related model within mean field theory. A choice of θ and o corresponds to a spontaneous symmetry breaking of the group $U(1) \times \{1, T\}$ including both the $U(1)$ and time reversal transformations. More accurately, in the $p_x \pm ip_y$ SC, the group $(U(1) \times \{1, T\}) \times D_4$ is spontaneously broken down to a certain diagonal subgroup. We discuss the continuum analog of this and its implications in section 2.4.1.2.

Crucially, we do not restrict δ to the $p_x \pm ip_y$ configuration, and treat it as a general two component complex vector $\delta = (\delta^x, \delta^y) \in \mathbb{C}^2$. In the following we will take δ to be space time dependent, $\delta \mapsto \delta_{\mathbf{l}}(t)$, and show that this space time dependence can be thought of as a perturbation to which there is a topological response, but for now we assume δ is constant.

¹²Since δ has charge 2, H commutes with the fermion parity $(-1)^Q$. The Ground state of H will therefore be labelled by a fermion parity eigenvalue ± 1 , in addition to the topological label which is the Chern number [15, 227]. Fermion parity is a subtle quantity in the thermodynamic limit, and will not be important in the following.

2.2.1 Band structure and phase diagram

Writing the Hamiltonian (2.15) in Fourier space, and in the BdG form in terms of the Nambu spinor $\Psi_{\mathbf{q}} = (\psi_{\mathbf{q}}, \psi_{-\mathbf{q}}^\dagger)^T$ we find

$$\begin{aligned} H &= \frac{1}{2} \int_{BZ} \frac{d^2 \mathbf{q}}{(2\pi)^2} \Psi_{\mathbf{q}}^\dagger \begin{pmatrix} h_{\mathbf{q}} & \delta_{\mathbf{q}} \\ \delta_{\mathbf{q}}^* & -h_{\mathbf{q}} \end{pmatrix} \Psi_{\mathbf{q}} + \text{const} \\ &= \frac{1}{2} \int_{BZ} \frac{d^2 \mathbf{q}}{(2\pi)^2} \Psi_{\mathbf{q}}^\dagger (\mathbf{d}_{\mathbf{q}} \cdot \boldsymbol{\sigma}) \Psi_{\mathbf{q}} + \text{const}, \end{aligned} \quad (2.16)$$

with $h_{\mathbf{q}} = -t \cos(aq_x) - t \cos(aq_y) - \mu$ real and symmetric, and $\delta_{\mathbf{q}} = -i\delta^x \sin(aq_x) - i\delta^y \sin(aq_y)$ complex and anti-symmetric. Here $\boldsymbol{\sigma} = (\sigma^x, \sigma^y, \sigma^z)$ is the vector of Pauli matrices and BZ is the Brillouin zone $BZ = (\mathbb{R}/\frac{2\pi}{a}\mathbb{Z})^2$. By definition, the Nambu spinor obeys the reality condition $\Psi_{\mathbf{q}}^\dagger = (\sigma^x \Psi_{-\mathbf{q}})^T$, and is therefore a Majorana spinor, see appendix B.5.1. Accordingly, the BdG Hamiltonian is particle-hole (or charge conjugation) symmetric, $\sigma^x H(\mathbf{q})^* \sigma^x = -H(-\mathbf{q})$, and therefore belongs to symmetry class D of the Altland-Zirnbauer classification of free fermion Hamiltonians [107]. The constant in (2.16) is $\frac{1}{2} \text{tr} h = \frac{V}{2} \int \frac{d^2 \mathbf{q}}{(2\pi)^2} h_{\mathbf{q}}$ where V is the infinite volume. This operator ordering correction is important as it contributes to physical quantities such as the energy density and charge density, but we will mostly keep it implicit in the following. The BdG band structure is given by $E_{\mathbf{q}, \pm} = \pm \frac{1}{2} E_{\mathbf{q}}$ where

$$E_{\mathbf{q}} = |\mathbf{d}_{\mathbf{q}}| = \sqrt{h_{\mathbf{q}}^2 + |\delta_{\mathbf{q}}|^2}. \quad (2.17)$$

For the $p_x \pm ip_y$ configuration $|\delta_{\mathbf{q}}|^2 = \delta_0^2 (\sin^2 aq_x + \sin^2 aq_y)$, and therefore $E_{\mathbf{q}}$ can only vanish at the particle-hole invariant points $a\mathbf{K}^{(1)} = (0, 0)$, $a\mathbf{K}^{(2)} = (0, \pi)$, $a\mathbf{K}^{(3)} = (\pi, \pi)$, $a\mathbf{K}^{(4)} = (\pi, 0)$, which happens when $\mu = -2t, 0, 2t, 0$. Representative band structures are plotted in Fig. 4. For $\delta_0 \ll t$ the spectrum takes the form of a gapped single particle Fermi surface with gap $\sim \delta_0$, while for $\delta_0 \gg t$ one obtains Four regulated relativistic fermions centered at the points $\mathbf{K}^{(n)}$, $1 \leq n \leq 4$ with masses $m_n = -2t - \mu, -\mu, 2t - \mu, -\mu$, speed of light $c_{\text{light}} = a\delta_0/\hbar$, bandwidth $\sim \delta_0$ and momentum cutoff $\sim a^{-1}$.

With generic μ, δ_0 the spectrum is gapped, and the Chern number ν labeling the different topological phases is well defined. It can be calculated by $\nu = \int_{BZ} \frac{d^2 k}{2\pi} \text{tr}(\mathcal{F})$ where \mathcal{F} is the Berry curvature on the Brillouin zone BZ [107]. A more general definition is $\nu = \frac{1}{24\pi^2} \int_{\mathbb{R} \times BZ} \text{tr}(G dG^{-1})^3$ ¹³, where $G(k_0, k_x, k_y)$ is the single particle propagator [27], which remains valid in the presence of weak interactions, as long as the gap does not close. For two band Hamiltonians such as (2.16), ν reduces to the homotopy type of the map $\hat{\mathbf{d}}_{\mathbf{q}} = \mathbf{d}_{\mathbf{q}}/|\mathbf{d}_{\mathbf{q}}|$ from BZ (which is a flat torus) to the sphere,

$$\nu = \frac{1}{(2\pi)^2} \int_{BZ} d^2 \mathbf{q} \hat{\mathbf{d}}_{\mathbf{q}} \cdot \left(\partial_{q_y} \hat{\mathbf{d}}_{\mathbf{q}} \times \partial_{q_x} \hat{\mathbf{d}}_{\mathbf{q}} \right) \in \mathbb{Z}. \quad (2.18)$$

¹³More explicitly, $\nu = \frac{1}{24\pi^2} \text{tr} \int_{\mathbb{R} \times BZ} d^3 k \varepsilon^{\alpha\beta\gamma} (G \partial_\alpha G^{-1}) (G \partial_\beta G^{-1}) (G \partial_\gamma G^{-1})$.

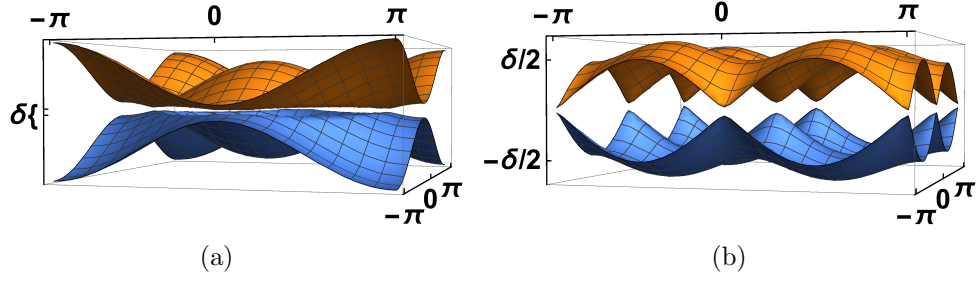


Figure 4: Generic band structure of the lattice model. (a) When the order parameter is much smaller than the single particle bandwidth $\delta \ll t$, the spectrum takes the form of a gapped single particle Fermi surface with gap $\sim \delta$. This regime describes the onset of superconductivity, and it is appropriate to refer to δ as the “gap function”. (b) When the order parameter is much larger than the single particle scales $\delta \gg t, \mu$, the spectrum takes the form of four regulated relativistic fermions centered at the particle-hole invariant points $(0, 0), (0, \pi), (\pi, 0), (\pi, \pi)$, in units of the inverse lattice spacing a^{-1} . We will be working in this regime.

One obtains $\nu = 0$ for $|\mu| > 2t$, $\nu = \pm 1$ for $\mu \in (0, 2t)$ and $\nu = \mp 1$ for $\mu \in (-2t, 0)$. The topological phase diagram is plotted in Fig.5(a).

Away from the $p_x \pm ip_y$ configuration, the topological phase diagram is essentially unchanged. For $\text{Im}(\delta^{x*}\delta^y) \neq 0$, gap closings happen at the same points $\mathbf{K}^{(n)}$ and the same values of μ described above. ν takes the same values, with the orientation $o = \text{sgn}(\text{Im}(\delta^{x*}\delta^y))$, described below, generalizing the sign ± 1 that characterizes the $p_x \pm ip_y$ configuration. For $\text{Im}(\delta^{x*}\delta^y) = 0$ the spectrum is always gapless. The topological phase diagram is most easily understood from the formula $\nu = \frac{1}{2} \sum_{n=1}^4 o_n \text{sgn}(m_n)$ where $o_n = \pm 1$ are orientations associated with the relativistic fermions which we describe below [228].

It will also be useful consider a slight generalization of the single particle part of the lattice model, with un-isotropic hopping $t^x \psi_{\mathbf{l}}^\dagger \psi_{\mathbf{l}+x} + t^y \psi_{\mathbf{l}}^\dagger \psi_{\mathbf{l}+y}$. This changes the masses to $m_1 = -(t_1 + t_2) - \mu, m_2 = t_1 - t_2 - \mu, m_3 = t_1 + t_2 - \mu, m_4 = -(t_1 - t_2) - \mu$. In particular, the degeneracy between the masses m_2, m_4 breaks, and additional trivial phases appear around $\mu = 0$. See Fig.5(b).

2.2.2 Basics of the emergent geometry

A key insight which we will extensively use, originally due to Volovik, is that the order parameter is in fact a *vielbein*. In the present space-time independent situation, this vielbein is just a 2×2 matrix which generically will be invertible

$$e_A^j = \begin{pmatrix} \text{Re}(\delta^x) & \text{Re}(\delta^y) \\ \text{Im}(\delta^x) & \text{Im}(\delta^y) \end{pmatrix} \in GL(2), \quad (2.19)$$

where $A = 1, 2, j = x, y$. More accurately, e_A^j is invertible if $\det(e_A^i) = \text{Im}(\delta^{x*}\delta^y) \neq 0$. We refer to an order parameter as singular if $\text{Im}(\delta^{x*}\delta^y) = 0$. From the vielbein one can calculate a metric, which in

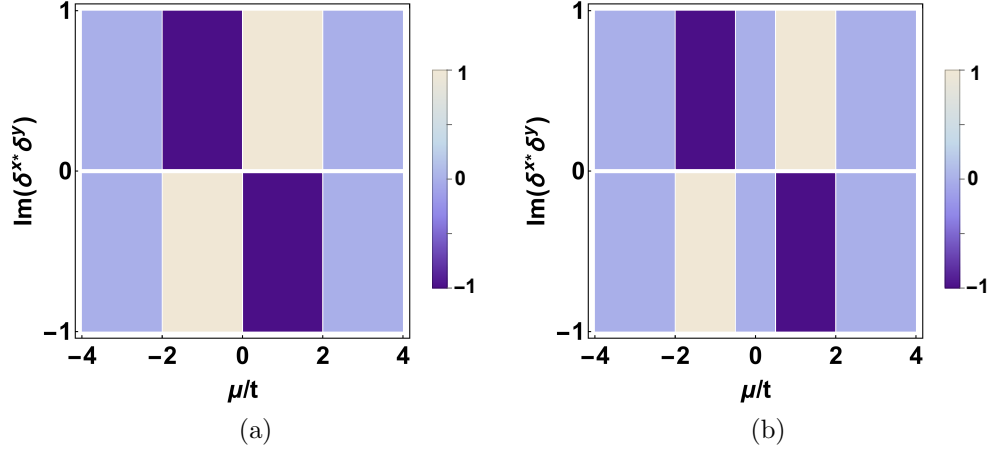


Figure 5: The topological phase diagram of the lattice model is simplest to understand from the formula $\nu = \frac{1}{2} \sum_{n=1}^4 o_n \text{sgn}(m_n)$ for the Chern number in terms of the masses and orientations of low energy relativistic fermions. (a) Topological phase diagram for isotropic hopping t . Units on the vertical axis are arbitrary, the topological phase diagram only depends on the orientation $o = \text{sgn}(\text{Im}(\delta^{x*} \delta^y))$. (b) Topological phase diagram for anisotropic hopping $t^x \neq t^y$, additional trivial phases exist around $\mu = 0$. Here $t = \frac{t^x + t^y}{2}$.

the present situation is a general symmetric positive semidefinite matrix

$$g^{ij} = e_A^i \delta^{AB} e_B^j = \delta^{(i} \delta^{j)*} = \begin{pmatrix} |\delta^x|^2 \text{Re}(\delta^x \delta^{y*}) & \\ \text{Re}(\delta^x \delta^{y*}) & |\delta^y|^2 \end{pmatrix}.$$

Every vielbein determines a metric uniquely, but the converse is not true. Vielbeins e, \tilde{e} that are related by an internal reflection and rotation $e_A^j = \tilde{e}_B^j L_A^B$ with $L \in O(2)$ give rise to the same metric. By diagonalization, it is also clear that any metric can be written in terms of a vielbein. Therefore the set of (constant) metrics can be parameterized by the coset $GL(2)/O(2)$. To see this explicitly we parameterize $\delta = e^{i\theta} (|\delta^x|, e^{i\phi} |\delta^y|)$ with the overall phase θ and relative phase $\phi \in (-\pi, \pi]$. Then

$$g^{ij} = \begin{pmatrix} |\delta^x|^2 & |\delta^x| |\delta^y| \cos \phi \\ |\delta^x| |\delta^y| \cos \phi & |\delta^y|^2 \end{pmatrix} \quad (2.20)$$

is independent of θ which parametrizes $SO(2)$ and $\text{sgn} \phi$ which parametrizes $O(2)/SO(2)$. Note that the group $O(2)$ of internal rotations and reflections is just $U(1) \rtimes \{1, T\}$ acting on e_A^j . In more detail, $\delta \mapsto e^{2i\alpha} \delta$ (or $\delta \mapsto \delta^*$) corresponds to $e_A^i \mapsto L_A^B e_B^i$ with

$$L = \begin{pmatrix} \cos 2\alpha & \sin 2\alpha \\ -\sin 2\alpha & \cos 2\alpha \end{pmatrix} \left(\text{or } L = \begin{pmatrix} 1 & 0 \\ 0 & -1 \end{pmatrix} \right). \quad (2.21)$$

The internal reflections, corresponding to a reversal of time, flip the *orientation* of the vielbein

$o = \text{sgn}(\det(e_A^i)) = \text{sgn}(\text{Im}(\delta^{x*}\delta^y))$, and therefore every quantity that depends on o is time reversal odd. We will also refer to o as the orientation of the order parameter. An order parameter with a positive (negative) orientation can be thought of as $p_x + ip_y$ -like ($p_x - ip_y$ -like).

For the $p_x \pm ip_y$ configuration, $\delta = e^{i\theta}\delta_0(1, \pm i)$, one obtains a scalar metric $g^{ij} = \delta_0\delta^{ij}$, independent of the phase θ and the orientation $o = \pm$. We see that θ, o correspond precisely to the $O(2) = U(1) \ltimes \{1, T\}$ degrees of freedom of the vielbein to which the metric is blind to. Thus the metric g^{ij} corresponds to the Higgs part of the order parameter, by which we mean the part of the order parameter on which the ground state energy depends, in the intrinsic case.

The fact that $U(1)$ transformations map to internal rotations also appears naturally in the BdG formalism which we will use in the following. Consider the Nambu spinor $\Psi = (\psi, \psi^\dagger)^T$. It follows from the $U(1)$ action $\psi \mapsto e^{i\alpha}\psi$ that $\Psi \mapsto e^{i\alpha\sigma^z}\Psi$ where σ^z is the Pauli matrix. We see that $U(1)$ acts on Ψ as a spin rotation. Moreover, the fact that δ has charge 2 while ψ has charge 1 implies e is an $SO(2)$ vector while Ψ is a spinor.

2.2.3 Non-relativistic continuum limit

Consider the lattice model (2.15), with a general space time dependent order parameter $\delta_{\mathbf{l}} = (\delta_{\mathbf{l}}^x(t), \delta_{\mathbf{l}}^y(t))$, and minimally coupled to electromagnetism,

$$H = -\frac{1}{2} \sum_{\mathbf{l}} \left[t\psi_{\mathbf{l}}^\dagger e^{iA_{\mathbf{l},\mathbf{l}+x}} \psi_{\mathbf{l}+x} + (\mu_{\mathbf{l}} + A_{\mathbf{l},\mathbf{l}}) \psi_{\mathbf{l}}^\dagger \psi_{\mathbf{l}} + \delta_{\mathbf{l}}^x \psi_{\mathbf{l}}^\dagger e^{iA_{\mathbf{l},\mathbf{l}+x}} \psi_{\mathbf{l}+x}^\dagger + (x \leftrightarrow y) + h.c. \right]. \quad (2.22)$$

Here $A_{\mathbf{l},\mathbf{l}'}$, $A_{\mathbf{l},\mathbf{l}}$ are the components of a $U(1)$ gauge field describing background electromagnetism, on the discrete space and continuous time. We will work in the relativistic regime $\delta_0 \gg t, \mu$ where δ_0 is a characteristic scale for δ . To obtain a continuum description, we split BZ into four quadrants $BZ = \cup_{n=1}^4 BZ^{(n)}$ centered around the four points $\mathbf{K}^{(n)}$, and decompose the fermion operator $\psi_{\mathbf{l}}$ as a sum $\psi_{\mathbf{l}} = \sum_{n=1}^4 \psi_{\mathbf{l}}^{(n)} e^{i\mathbf{K}^{(n)} \cdot \mathbf{l}}$, where $\psi_{\mathbf{l}}^{(n)} e^{i\mathbf{K}^{(n)} \cdot \mathbf{l}}$ has non zero Fourier modes only in $BZ^{(n)}$. Thus the fermions $\psi^{(n)}$ all have non zero Fourier modes only in $BZ^{(n)} - \mathbf{K}^{(n)} = [-\frac{\pi}{2a}, \frac{\pi}{2a}]^2$. This restriction of the quasi momenta provides the fermions $\psi^{(n)}$ with a *physical* cutoff $\sim a^{-1}$, which will be important when we compare results from the continuum description to the lattice model. Assuming μ, δ, A have small derivatives relative to a^{-1} , the inter fermion terms in H can be neglected and H splits into a sum $H \approx \sum_{n=1}^4 H^{(n)}$, with $H^{(n)}$ a Hamiltonian for $\psi^{(n)}$. We then expand the Hamiltonians $H^{(n)}$ in small $\psi^{(n)}$ derivatives relative to a^{-1} . The resulting Hamiltonian, focusing on the point $\mathbf{K}^{(1)} = (0, 0)$, is the p -wave superfluid (SF) Hamiltonian

$$H_{\text{SF}} = \int d^2x \left[\psi^\dagger \left(-\frac{D^2}{2m^*} + m - A_t \right) \psi - \left(\frac{1}{2} \psi^\dagger \Delta^j \partial_j \psi^\dagger + h.c. \right) \right], \quad (2.23)$$

where the fermion field has been redefined such that $\{\psi^\dagger(x), \psi(x')\} = \delta^{(2)}(x - x')$. Here $D_\mu = \partial_\mu - iA_\mu$ is the $U(1)$ -covariant derivative, with the connection $A = A_j dx^j$ related to $A_{\mathbf{l},\mathbf{l}'}$ by $A_{\mathbf{l},\mathbf{l}'} = \int_{\mathbf{l}}^{\mathbf{l}'} A$, and $D^2 = \delta^{ij} D_i D_j$ with $i, j = x, y$. Note the appearance of the flat background spatial metric δ^{ij} . The

effective mass is related to the hopping amplitude $1/m^* = a^2 t$, and the order parameter is $\Delta = a\delta$, so it is essentially the lattice order parameter. The chemical potential for the p -wave SF is $-m$. The coupling to A in the pairing term is lost, since $\psi^\dagger \psi^\dagger = 0$. For this reason it is a derivative and not a covariant derivative that appears in $\psi^\dagger \Delta^j \partial_j \psi^\dagger$, and one can verify that this term is gauge invariant. Moreover, due to the anti-commutator $\{\psi^\dagger(x), \psi^\dagger(y)\} = 0$ any operator put between two ψ^\dagger s is anti-symmetrized, and in particular $\psi^\dagger \Delta^j \partial_j \psi^\dagger = \psi^\dagger \frac{1}{2} \{\Delta^j, \partial_j\} \psi^\dagger$ where $\{\Delta^j, \partial_j\}$ is the anti-commutator of differential operators. This Hamiltonian is essentially the one considered in [15] for the p -wave SF. The corresponding action is the p -wave SF action

$$S_{\text{SF}}[\psi, \Delta, A] = \int d^{2+1}x \left[\psi^\dagger \left(iD_t + \frac{D^2}{2m^*} - m \right) \psi + \left(\frac{1}{2} \psi^\dagger \Delta^j \partial_j \psi^\dagger + h.c \right) \right], \quad (2.24)$$

in which ψ, ψ^\dagger are no longer fermion operators, but independent Grassmann valued fields, $\{\psi(x), \psi^\dagger(x')\} = 0$. This action comes equipped with a momentum cutoff $\Lambda_{UV} \sim a^{-1}$ inherited from the lattice model.

For the other points $\mathbf{K}^{(2)}, \mathbf{K}^{(3)}, \mathbf{K}^{(4)}$ the SF action obtained is slightly different. The chemical potential for the n th fermion is $-m_n$. The order parameter for the n th fermion is $\Delta_{(n)}^x = a\delta^x e^{iK_x^{(n)}}$, $\Delta_{(n)}^y = a\delta^y e^{iK_y^{(n)}}$, and we note that $e^{iK_j^{(n)}} = \pm 1$. The order parameters for $\mathbf{K}^{(1)} = (0, 0)$, $\mathbf{K}^{(3)} = (\pi, \pi)$ are related by an overall sign, which is a $U(1)$ transformation, and so are the order parameters for $\mathbf{K}^{(2)} = (0, \pi)$, $\mathbf{K}^{(4)} = (\pi, 0)$. Thus the order parameters for $n = 1, 3$ are physically indistinguishable, and so are order parameters for $n = 2, 4$. The order parameters for $n = 1$ and $n = 2$ are however physically distinct. First, the orientations $o_n = \text{sgn}(\text{Im}(\Delta_{(n)}^{x*} \Delta_{(n)}^y))$ are different, with $o_1 = -o_2$. Second, the metrics $g_{(n)}^{ij} = \Delta_{(n)}^{(i} \Delta_{(n)}^{j)*}$ are generically different, with the same diagonal components, but $g_{(1)}^{xy} = -g_{(2)}^{xy}$. We note that if the relative phase between δ^x and δ^y is $\pm\pi/2$, as in the $p_x \pm ip_y$ configuration, then all metrics $g_{(n)}^{ij}$ are diagonal and therefore equal. These differences between the orientations and metrics of the different lattice fermions will be important later on.

Similarly, the effective mass tensor which in (2.23), for $n = 1$, is $(M^{-1})^{ij} = \frac{\delta^{ij}}{m^*}$, has different signatures for different n , but this will not be important for our analysis. For now we continue working with the action (2.24) for the $n = 1$ fermion, keeping the other lattice fermions implicit until section 2.5.2.3.

2.2.4 Relativistic continuum limit

Since we work in the relativistic regime $\delta \gg t, \mu$ we can treat the term $\psi^\dagger \frac{D^2}{2m^*} \psi$ as a perturbation and compute quantities to zeroth order in $1/m^*$. Then S_{SF} reduces to what we refer to as the relativistic limit of the p -wave SF action, given in BdG form by

$$S_{\text{rSF}}[\psi, \Delta, A] = \frac{1}{2} \int d^{2+1}x \Psi^\dagger \begin{pmatrix} i\partial_t + A_t - m \frac{1}{2} \{\Delta^j, \partial_j\} \\ -\frac{1}{2} \{\Delta^{*j}, \partial_j\} i\partial_t - A_t + m \end{pmatrix} \Psi. \quad (2.25)$$

It is well known that when Δ takes the $p_x \pm ip_y$ configuration $\Delta = \Delta_0 e^{i\theta} (1, \pm i)$ and $A = 0$ this action is that of a relativistic Majorana spinor in Minkowski space-time, with mass m and speed of light

$c_{\text{light}} = \frac{\Delta_0}{\hbar}$. In the following, we will see that for general Δ and A , (2.25) is the action of a relativistic Majorana spinor in curved and torsion-full space-time. We will sometimes refer to the relativistic limit as $m^* \rightarrow \infty$, though this is somewhat loose, because in the relativistic regime both m^* is large and m is small.

Before we go on to analyze the p -wave SF in the relativistic limit, it is worth considering what of the physics of the p -wave SF is captured by the relativistic limit, and what is not. First, the coupling to A_x, A_y is lost, so the relativistic limit is blind to the magnetic field. Since superconductors are usually defined by their interaction with the magnetic field, the relativistic limit is actually insufficient to describe the properties of the p -wave SF as a superconductor. Of course, a treatment of superconductivity also requires the dynamics of Δ . Likewise, the term $\frac{1}{2m^*}\psi^\dagger D^2\psi = \frac{1}{2m^*}\psi^\dagger \delta^{ij} D_i D_j \psi$ seems to be the only term in S_{SF} that includes the flat background metric δ^{ij} , describing the real geometry of space. It appears that the relativistic limit is insufficient to describe the response of the system to a change in the real geometry of space¹⁴. Nevertheless, as is well known, the relativistic limit does suffice to determine the topological phases of the p -wave SC as a free (and weakly interacting) fermion system. Indeed, the Chern number labeling the different topological phases can be calculated by the formula $\nu = \frac{1}{2} \sum_{n=1}^4 o_n \text{sgn}(m_n)$, which only uses data from the relativistic limit. Here the sum is over the four particle-hole invariant points of the lattice model, with orientations o_n and masses m_n . This suggests that at least some physical properties characterizing the different free fermion topological phases can be obtained from the relativistic limit. Indeed, in the following we will see how a topological bulk response and a corresponding boundary anomaly can be obtained within the relativistic limit.

2.3 Emergent Riemann-Cartan geometry

We argue that (2.25) is precisely the action which describes a relativistic massive Majorana spinor in a curved and torsion-full background known as Riemann-Cartan (RC) geometry, with a particular form of background fields. We refer the reader to [154] parts I.1 and I.4.4, for a review of RC geometry and the coupling of fermions to it, and provide only the necessary details here, focusing on the implications for the p -wave SF. For simplicity we work locally and in coordinates, and we defer the treatment of global aspects to appendix B.6.

The action describing the dynamics of a Majorana spinor on RC background in 2+1 dimensional space-time can be written as

$$S_{\text{RC}}[\chi, e, \omega] = \frac{1}{2} \int d^{2+1}x |e| \bar{\chi} \left[\frac{i}{2} e_a^\mu \left(\gamma^a D_\mu - \overleftarrow{D}_\mu \gamma^a \right) - m \right] \chi. \quad (2.26)$$

Here χ is a Majorana spinor with mass m obeying, as a field operator, the canonical anti-commutation relation $\{\chi(x), \chi(y)\} = \frac{\delta^{(2)}(x-y)}{|e(x)|}$, where we suppressed spinor indices. As a Grassmann field $\{\chi(x), \chi(y)\} = 0$. The field e_a^μ is an inverse vielbein which is an invertible matrix at each point in space-time. The indices $a, b, \dots \in \{0, 1, 2\}$ are $SO(1, 2)$ (Lorentz) indices which we refer to as internal indices, while

¹⁴In fact, some of the response to the real geometry can be obtained, see our discussion, section 2.6.

$\mu, \nu, \dots \in \{t, x, y\}$ are coordinate indices.

We will also use $A, B, \dots \in \{1, 2\}$ for spatial internal indices and $i, j, \dots \in \{x, y\}$ for spatial coordinate indices

The vielbein e^a_μ , is the inverse of e^μ_a , such that $e^a_\mu e^\mu_b = \delta^a_b$, $e^a_\mu e^\mu_b = \delta^a_b$. It is often useful to view the vielbein as a set of linearly independent (local) one-forms $e^a = e^a_\mu dx^\mu$. The metric corresponding to the vielbein is $g_{\mu\nu} = e^a_\mu \eta_{ab} e^b_\nu$ and the inverse metric is $g^{\mu\nu} = e^\mu_a \eta^{ab} e^\nu_b$, where $\eta_{ab} = \eta^{ab} = \text{diag}[1, -1, -1]$ is the flat Minkowski metric. Internal indices are raised and lowered using η , while coordinate indices are raised and lowered using g and its inverse. Using e one can replace internal indices with coordinate indices and vice versa, e.g. $v^a = e^a_\mu v^\mu$. The volume element is defined by $|e| = |\det e^a_\mu| = \sqrt{g}$. $\{\gamma^a\}_{a=0}^2$ are gamma matrices obeying $\{\gamma^a, \gamma^b\} = 2\eta^{ab}$, and we will work with $\gamma^0 = \sigma^z$, $\gamma^1 = -i\sigma^x$, $\gamma^2 = i\sigma^y$ ¹⁵. The covariant derivative $D_\mu = \partial_\mu + \omega_\mu$ ¹⁶ contains the spin connection $\omega_\mu = \frac{1}{2}\omega_{ab\mu}\Sigma^{ab}$, where $\Sigma^{ab} = \frac{1}{4}[\gamma^a, \gamma^b]$ generate the spin group $Spin(1, 2)$ which is the double cover of the Lorentz group $SO(1, 2)$. Note that $\omega_{ab\mu} = -\omega_{ba\mu}$ and therefore $\omega^a_{b\mu}$ is an $SO(1, 2)$ connection. It follows that ω is metric compatible, $D_\mu \eta_{ab} = 0$. It is often useful to work (locally) with a connection one-form $\omega = \omega_\mu dx^\mu$. $\bar{\chi}$ is the Dirac conjugate defined as in Minkowski space-time $\bar{\chi} = \chi^\dagger \gamma^0$. The derivative \overleftarrow{D}_μ acts only on $\bar{\chi}$ and is explicitly given by $\chi \overleftarrow{D}_\mu = \partial_\mu \bar{\chi} - \bar{\chi} \omega_\mu$.

Our statement is that $S_{\text{RC}}[\chi, e, \omega]$ evaluated on the fields

$$\chi = |e|^{-1/2} \Psi, \quad e^\mu_a = \begin{pmatrix} 1 & 0 & 0 \\ 0 & \text{Re}(\Delta^x) & \text{Re}(\Delta^y) \\ 0 & \text{Im}(\Delta^x) & \text{Im}(\Delta^y) \end{pmatrix}, \quad \omega_\mu = -2A_\mu \Sigma^{12}, \quad (2.27)$$

reduces precisely to $S_{\text{rSF}}[\psi, \Delta, A]$ of equation (2.25), where one must keep in mind that S_{RC} is written in relativistic units where $\hbar = 1$ and $c_{\text{light}} = \Delta_0/\hbar = 1$, which we will use in the following. Moreover, the functional integral over χ is equal to the functional integral over Ψ . This refines the original statement by Volovik and subsequent work by Read and Green [15]. We defer the proof to appendices B.1 and B.3, where we also address certain subtleties that arise. Here we describe the particular RC geometry that follows from (2.27), and attempt to provide some intuition for this geometric description of the p -wave SF. Starting with the vielbein, note that the only nontrivial part of e^μ_a is the spatial part e^j_A , which is just the order parameter Δ , as in (2.19). The inverse metric we obtain from our vielbein is

$$g^{\mu\nu} = e^\mu_a \eta^{ab} e^\nu_b = \begin{pmatrix} 1 & 0 & 0 \\ 0 & -|\Delta^x|^2 & -\text{Re}(\Delta^x \Delta^{*y}) \\ 0 & -\text{Re}(\Delta^x \Delta^{*y}) & -|\Delta^y|^2 \end{pmatrix}, \quad (2.28)$$

where the spatial part $g^{ij} = -\Delta^{(i} \Delta^{j)*}$ is the Higgs part of the order parameter, as in (2.20). For the $p_x \pm ip_y$ configuration the metric reduces to the Minkowski metric. If Δ is time independent $g^{\mu\nu}$ describes

¹⁵The gamma matrices form a basis for the Clifford algebra associated with η . The above choice of basis is a matter of convention.

¹⁶We use the notation D for spin, Lorentz, and $U(1)$ covariant derivatives in any representation, and the exact meaning should be clear from the field D acts on.

a Riemannian geometry which is trivial in the time direction, but we allow for a time dependent Δ . A metric of the form (2.28) is said to be in gaussian normal coordinates with respect to space [229].

The $U(1)$ connection A_μ maps to a $Spin(2)$ connection $\omega_\mu = -2A_\mu \Sigma^{12} = -iA_\mu \sigma^z$ which corresponds to spatial spin rotations. This is a special case of the general $Spin(1,2)$ connection which appears in RC geometry. The fact that $U(1)$ transformations map to spin rotations when acting on the Nambu spinor Ψ is a general feature of the BdG formalism as was already discussed in section 2.2.2. From the spin connection ω it is natural to construct a curvature, which is a matrix valued two-form defined by $R_b^a = d\omega_b^a + \omega_c^a \wedge \omega_b^c$. In local coordinates x^μ it can be written as $R_b^a = \frac{1}{2} R_{b\mu\nu}^a dx^\mu \wedge dx^\nu$, where the components are given explicitly by $R_{b\mu\nu}^a = \partial_\mu \omega_{b\nu}^a - \partial_\nu \omega_{b\mu}^a + \omega_{c\mu}^a \omega_{b\nu}^c - \omega_{c\nu}^a \omega_{b\mu}^c$. It follows from (2.27) that in our case the only non zero components are

$$R_{12} = -R_{21} = -2F, \quad (2.29)$$

where the two form $F = dA$ is the $U(1)$ field strength, or curvature, comprised of the electric and magnetic fields.

2.3.1 Torsion and additional geometric quantities

Since we treat A and Δ as independent background fields, so are the spin connection ω and vielbein e . This situation is referred to as the first order vielbein formalism for gravity [154]. Apart from the metric g and the curvature R which we already described, there are a few more geometric quantities which can be constructed from e, ω , and that will be used in the following. These additional quantities revolve around the notion of torsion.

The torsion tensor T is an important geometrical quantity, but a pragmatic way to view it is as a useful parameterization for the set of all spin connections ω , for a fixed vielbein e . Thus one can work with the variables e, T instead of e, ω . We will see later on that the bulk responses in the p -wave SC are easier to describe using e, T . This is analogous to, and as we will see, generalizes, the situation in s -wave SC, where the independent degrees of freedom are A and $\Delta = |\Delta| e^{i\theta}$, but it is natural to change variables and work with Δ and $D_\mu \theta = \partial_\mu \theta - 2A_\mu$ instead. We now provide the details.

The torsion tensor, or two-form, is defined in terms of e, ω as $T^a = De^a$, or in coordinates $T_{\mu\nu}^a = 2D_{[\mu} e_{\nu]}^a$. Since our temporal vielbein $e^0 = dt$ is trivial and the connection ω is only an $SO(2)$ connection, $T^0 = 0$ for all A and Δ . All other components of the torsion are in general non trivial, and are given by $T_{ij}^A = D_i e_j^A - D_j e_i^A$, $T_{ti}^A = -T_{it}^A = D_t e_i^A$. This describes the simple change of variables from ω to T .

Going from T back to ω is slightly more complicated, and is done as follows. One starts by finding the ω that corresponds to $T = 0$. The solution is the unique torsion free spin connection $\tilde{\omega} = \tilde{\omega}(e)$ which we refer to as the Levi Civita (LC) spin connection¹⁷. This connection is given explicitly by $\tilde{\omega}_{abc} = \frac{1}{2} (\xi_{abc} + \xi_{bca} - \xi_{cab})$ where $\xi_{bc}^a = 2e_b^\mu e_c^\nu \partial_{[\mu} e_{\nu]}^a$. Now, for a general ω the difference $C_{b\mu}^a = \omega_{b\mu}^a - \tilde{\omega}_{b\mu}^a$ is referred to as the contorsion tensor, or one-form. It carries the same information as T and the two are related by $T^a = C_b^a \wedge e^b$ ($T_{\mu\nu}^a = 2C_{b[\mu}^a e_{\nu]}^b$) and $C_{\mu\alpha\nu} = \frac{1}{2} (T_{\alpha\mu\nu} + T_{\mu\nu\alpha} - T_{\nu\alpha\mu})$. One can then reconstruct

¹⁷The unique torsion free spin connection $\tilde{\omega}$ is also referred to as the Cartan connection in the literature.

ω from e, T as $\omega = \tilde{\omega}(e) + C(e, T)$. Note that $\omega, \tilde{\omega}$ are both connections, but C, T are tensors.

For the $p_x \pm ip_y$ configuration $\Delta = \Delta_0 e^{i\theta} (1, \pm i)$ one finds $\tilde{\omega}_{12\mu} = -\tilde{\omega}_{21\mu} = -\partial_\mu \theta$ (with all other components vanishing), and it follows that $C_{12\mu} = D_\mu \theta$. These are familiar quantities in the theory of superconductivity, and one can view $\tilde{\omega}$ and C as generalizations of these. General formulas are given in appendix B.4.

Using $\tilde{\omega}$ one can define a covariant derivative \tilde{D} and curvature \tilde{R} just as D and R are constructed from ω . The quantity $\tilde{R}^\mu_{\nu\rho\sigma}$ is the usual Riemann tensor of Riemannian geometry and general relativity. Note that $\tilde{R}^\mu_{\nu\rho\sigma}$ depends solely on g which is the Higgs part of the order parameter Δ . Since g is flat in the $p_x \pm ip_y$ configuration, we conclude that a non vanishing Riemann tensor requires a deviation of the Higgs part of Δ from the $p_x \pm ip_y$ configuration. As in Riemannian geometry we can define the Ricci tensor $\tilde{\mathcal{R}}_{\nu\sigma} = \tilde{R}^\mu_{\nu\mu\sigma}$ and Ricci scalar $\tilde{\mathcal{R}} = \tilde{\mathcal{R}}^\nu_\nu$. Examples for the calculation of $\tilde{\mathcal{R}}$ in terms of Δ were given in section 2.1.2.

Another important quantity which can be constructed from e, ω is the affine connection $\Gamma^\alpha_{\beta\mu} = e_a^\alpha (\partial_\mu e^\alpha_\beta + \omega^a_{b\mu} e^b_\beta) = e_a^\alpha D_\mu e^\alpha_\beta$, or affine connection (local) one-form $\Gamma^\alpha_\beta = \Gamma^\alpha_{\beta\mu} dx^\mu$. It is not difficult to see that T is the anti symmetric part of Γ , $T^\rho_{\mu\nu} = \Gamma^\rho_{\mu\nu} - \Gamma^\rho_{\nu\mu}$, and it follows that the LC affine connection $\tilde{\Gamma}^\alpha_{\beta\mu} = e_a^\alpha \tilde{D}_\mu e^a_\beta$, for which $T = 0$, is symmetric in its the two lower indices. This is the usual metric compatible and torsion free connection of Riemannian geometry, given by the Christoffel symbol $\tilde{\Gamma}_{\alpha\beta\mu} = \frac{1}{2} (\partial_\mu g_{\beta\alpha} + \partial_\beta g_{\alpha\mu} - \partial_\alpha g_{\mu\beta})$. Γ appears in covariant derivatives of tensors with coordinate indices, for example $\nabla_\mu v^\alpha = \partial_\mu v^\alpha + \Gamma^\alpha_{\beta\mu} v^\beta$, $\nabla_\mu v_\alpha = \partial_\mu v_\alpha - v_\beta \Gamma^\beta_{\alpha\mu}$, and so on. We also denote by ∇ the total covariant derivative of tensors with both coordinate and internal indices, which includes both ω and Γ . Thus, for example, $\nabla_\mu v^a_\nu = \partial_\mu v^a_\nu + \omega^a_{b\mu} v^b_\nu - v^a_\nu \Gamma^\nu_{\mu\alpha} = D_\mu v^a_\nu - v^a_\nu \Gamma^\nu_{\mu\alpha}$. The most important occurrence of ∇ is in the identity $\nabla_\nu e^a_\mu = 0$, which follows from the definition of Γ in this formalism, and is sometimes called the first vielbein postulate. It means that the covariant derivative ∇ commutes with index manipulation preformed using e, η and g . To obtain more intuition for what Γ is from the p -wave SC point of view, we can write it as $\Gamma^\alpha_{a\mu} = -D_\mu e^\alpha_a$. Then it is clear that the non vanishing components of $\Gamma^\alpha_{a\mu}$ are given by $\Gamma^j_{1\mu} + i\Gamma^j_{2\mu} = -D_\mu \Delta^j$

2.4 Symmetries, currents, and conservation laws

In order to map fermionic observables in the p -wave SF to those of a Majorana fermion in RC space-time, it is usefull is to map the symmetries and the corresponding conservation laws between the two. We start with S_{SF} , and then review the analysis of S_{RC} and show how it maps to that of S_{SF} , in the relativistic limit. The bottom line is that there is a sense in which electric charge and energy-momentum are conserved in a p -wave SC, and this maps to the sense in which spin and energy-momentum are conserved for a Majorana spinor in RC space-time.

2.4.1 Symmetries, currents, and conservation laws of the p -wave superfluid action

2.4.1.1 Electric charge $U(1)$ gauge transformations act on ψ, Δ, A by

$$\psi \mapsto e^{i\alpha}\psi, \quad \Delta \mapsto e^{2i\alpha}\Delta, \quad A_\mu \mapsto A_\mu + \partial_\mu\alpha. \quad (2.30)$$

This symmetry of $S_{\text{SF}}[\psi, \Delta, A]$ implies a conservation law for electric charge,

$$\partial_\mu J^\mu = -i\psi^\dagger \Delta^j \partial_j \psi^\dagger + h.c., \quad (2.31)$$

where $J^\mu = -\frac{\delta S}{\delta A_\mu}$ is the fermion electric current. Since A_μ does not enter the pairing term, J^μ is the same as in the normal state where $\Delta = 0$,

$$J^t = -\psi^\dagger \psi, \quad J^j = -\frac{\delta^{jk}}{m^*} \frac{i}{2} \psi^\dagger \overleftrightarrow{D}_k \psi. \quad (2.32)$$

Here $\psi^\dagger \overleftrightarrow{D}_k \psi = \psi^\dagger D_k \psi - (D_k \psi^\dagger) \psi$. The conservation law (2.31) shows that the fermionic charge alone is not conserved due to the exchange of charge between the fermions ψ and Cooper pairs Δ . If one adds a ($U(1)$ gauge invariant) term $S'[\Delta, A]$ to the action and considers Δ as a dynamical field, then it is possible to use the equation of motion $\frac{\delta(S'+S)}{\delta \Delta} = 0$ for Δ and the definition $J_\Delta^\mu = -\frac{\delta S'}{\delta A_\mu}$ of the Cooper pair current in order to rewrite (2.31) as $\partial_\mu (J^\mu + J_\Delta^\mu) = 0$. This expresses the conservation of total charge in the p -wave SC.

2.4.1.2 Energy-momentum Energy and momentum are at the heart of our analysis, and obtaining the correct expressions for these quantities, as well as interpreting correctly the conservation laws they satisfy, will be crucial.

In flat space, one usually starts with the canonical energy-momentum tensor. For a Lagrangian $\mathcal{L}(\phi, \partial\phi, x)$, where ϕ is any fermionic or bosonic field, it is given by

$$t^\mu_\nu = \frac{\partial \mathcal{L}}{\partial \partial_\mu \phi} \partial_\nu \phi - \delta^\mu_\nu \mathcal{L}, \quad (2.33)$$

and satisfies, on the equation of motion for ϕ ,

$$\partial_\mu t^\mu_\nu = -\partial_\nu \mathcal{L}, \quad (2.34)$$

which can be obtained from Noether's first theorem for space-time translations. Thus t^μ_ν is conserved if and only if the Lagrangian is independent of the coordinate x^ν . This motivates the identification of t^μ_t as the energy current, and of t^μ_j as the current of the j th component of momentum (j -momentum). t^t_t is just the Hamiltonian density, or energy density, and t^t_j is the j -momentum density.

It is well known however, that the canonical energy-momentum tensor may fail to be gauge invariant, symmetric in its indices, or traceless, in situations where these properties are physically required, and

it is also sensitive to the addition of total derivatives to the Lagrangian. To obtain the physical energy-momentum tensor one can either “improve“ t^μ_ν or appeal to a geometric (gravitational) definition which directly provides the physical energy-momentum tensor [154, 230].

We will comment on the coupling of the p -wave SF to a real background geometry our discussion, section 2.6, but here we fix the background geometry to be flat, and instead continue by introducing the $U(1)$ -covariant canonical energy-momentum tensor. It can be shown to coincide with the physical energy-momentum tensor obtained by coupling the p -wave SF to a real background geometry. Since we work with a fixed flat background geometry in this section, we will only consider space-time transformations which are symmetries of this background, and it will suffice to consider space-time translations and spatial rotations.

The $U(1)$ -covariant canonical energy-momentum tensor is relevant in the following situation. Assume that the x dependence in \mathcal{L} is only through a $U(1)$ gauge field to which ϕ is minimally coupled, $\mathcal{L}(\phi, \partial\phi, x) = \mathcal{L}(\phi, D\phi)$. Then, t^μ_ν is not gauge invariant, and therefore physically ambiguous. This is reflected in the conservation law (2.34) which takes the non covariant form

$$\partial_\mu t^\mu_\nu = J^\mu \partial_\nu A_\mu, \quad (2.35)$$

where $J^\mu = -\frac{\partial \mathcal{L}}{\partial A_\mu}$ is the $U(1)$ current. This lack of gauge invariance is to be expected, as this conservation law follows from translational symmetry, and translations do not commute with gauge transformations. Instead, one should use $U(1)$ -covariant space-time translations, which are translations from x to $x + a$ followed by a $U(1)$ parallel transport from $x + a$ back to x , $\phi(x) \mapsto e^{iq \int_{x-a}^x A} \phi(x - a)$ where $\phi \mapsto e^{iq\alpha} \phi$ under $U(1)$ and the integral is over the straight line from $x - a$ to a . This is still a symmetry because the additional $e^{iq \int_{x-a}^x A}$ is just a gauge transformation. The conservation law that follows from this modified action of translations is

$$\partial_\mu t^\mu_{\text{cov } \nu} = F_{\nu\mu} J^\mu, \quad (2.36)$$

where $F_{\mu\nu} = \partial_\mu A_\nu - \partial_\nu A_\mu$ is the electromagnetic field strength, and

$$t^\mu_{\text{cov } \nu} = \frac{\partial \mathcal{L}}{\partial D_\mu \phi} D_\nu \phi - \delta^\mu_\nu \mathcal{L} = t^\mu_\nu - J^\mu A_\nu \quad (2.37)$$

is the $U(1)$ -covariant version of t^μ_ν , which we refer to as the $U(1)$ -covariant canonical energy-momentum tensor. The right hand side of (2.36) is just the usual Lorentz force, which acts as a source of $U(1)$ -covariant energy-momentum. We stress that the covariant and non covariant conservation laws are equivalent, as can be verified by using the fact that $\partial_\mu J^\mu = 0$ in this case. Both hold in any gauge, but in (2.36) all quantities are gauge invariant.

For the p -wave SF one obtains the $U(1)$ -covariant energy-momentum tensor

$$\begin{aligned}
t_{\text{cov } t}^t &= \frac{i}{2} \psi^\dagger \overleftrightarrow{D}_t \psi - \mathcal{L} \\
&= \frac{\delta^{ij} D_i \psi^\dagger D_j \psi}{2m^*} + m \psi^\dagger \psi - \left(\frac{1}{2} \psi^\dagger \Delta^j \partial_j \psi^\dagger + h.c. \right), \\
t_{\text{cov } j}^t &= \frac{i}{2} \psi^\dagger \overleftrightarrow{D}_j \psi, \\
t_{\text{cov } t}^i &= -\frac{\delta^{ik} (D_k \psi)^\dagger D_t \psi}{2m^*} + \frac{1}{2} \psi^\dagger \Delta^i \partial_t \psi^\dagger + h.c., \\
t_{\text{cov } j}^i &= -\frac{\delta^{ik} (D_k \psi)^\dagger D_j \psi}{2m^*} + \frac{1}{2} \psi^\dagger \Delta^i \partial_j \psi^\dagger + h.c. - \delta_j^i \mathcal{L}.
\end{aligned} \tag{2.38}$$

The $U(1)$ -covariant conservation law is slightly more complicated than (2.36) due the additional background field Δ ,

$$\partial_\mu t_{\text{cov } \nu}^\mu = \frac{1}{2} \psi^\dagger \partial_j \psi^\dagger D_\nu \Delta^j + h.c. + F_{\nu\mu} J^\mu, \tag{2.39}$$

where we have used the $U(1)$ conservation law (2.31), and $D_\mu \Delta^j = (\partial_\mu - 2iA_\mu) \Delta^j$. This conservation law shows that ($U(1)$ -covariant) fermionic energy-momentum is not conserved due to the exchange of energy-momentum with the background fields A, Δ . Apart from the Lorentz force there is an additional source term due to the space-time dependence of Δ .

As in the case of the electric charge, if one considers Δ as a dynamical field and uses its equation of motion, (2.39) can be written as¹⁸

$$\partial_\mu (t_{\text{cov } \nu}^\mu + t_{\Delta \text{ cov } \nu}^\mu) = F_{\nu\mu} (J^\mu + J_\Delta^\mu), \tag{2.40}$$

which is of the general form (2.36).

Note that the spatial part $t_{\text{cov } j}^i$ is not symmetric,

$$t_{\text{cov } y}^x - t_{\text{cov } x}^y = \frac{1}{2} \psi^\dagger (\Delta^x \partial_y - \Delta^y \partial_x) \psi^\dagger + h.c., \tag{2.41}$$

which physically represents an exchange of angular momentum between Δ and ψ , possible because of the intrinsic angular momentum of Cooper pairs in a p -wave SC. Explicitly, the ($U(1)$ -covariant) angular momentum current is given by $J_\varphi^\mu = t_{\text{cov } \varphi}^\mu = t_{\text{cov } \nu}^\mu \zeta^\nu$ where $\zeta = x\partial_y - y\partial_x = \partial_\varphi$ is the generator of spatial rotations around $x = y = 0$, and φ is the polar angle. From (2.39) and (2.41) we find its conservation

¹⁸ $t_{\Delta \text{ cov } \nu}^\mu$ is the $U(1)$ -covariant energy-momentum tensor of Cooper pairs. It is defined by (2.37) with $\phi = \Delta$ and $\mathcal{L} = \mathcal{L}'(\Delta, \Delta^*, D\Delta, D\Delta^*)$ being the (gauge invariant) term added to the p -wave SF Lagrangian. Here it is important that the coupling of Δ to ψ in (2.24) can be written without derivatives of Δ .

law

$$\begin{aligned}\partial_\mu J_\varphi^\mu &= \left(\frac{1}{2} \psi^\dagger \partial_j \psi^\dagger D_\varphi \Delta^j + h.c + F_{\varphi\mu} J^\mu \right) \\ &\quad + \frac{1}{2} \psi^\dagger (\Delta^x \partial_y - \Delta^y \partial_x) \psi^\dagger + h.c,\end{aligned}\tag{2.42}$$

which shows that even when the Lorentz force in the φ direction vanishes and Δ is ($U(1)$ -covariantly) constant in the φ direction, Δ still acts a source for fermionic angular momentum, due to the last term.

Even though fermionic angular momentum is never strictly conserved in a p -wave SF, it is well known that a certain combination of fermionic charge and fermionic angular momentum can be strictly conserved [36, 231–233]. Indeed, using (2.42) and (2.31),

$$\begin{aligned}\partial_\mu \left(J_\varphi^\mu \mp \frac{1}{2} J^\mu \right) &= \left(\frac{1}{2} \psi^\dagger \partial_j \psi^\dagger D_\varphi \Delta^j + h.c + F_{\varphi\mu} J^\mu \right) \\ &\quad \pm \frac{i}{2} \psi^\dagger (\Delta^x \pm i \Delta^y) (\partial_x \mp i \partial_y) \psi^\dagger + h.c.\end{aligned}\tag{2.43}$$

We see that when $F_{\varphi\mu} = 0$, $D_\varphi \Delta = 0$ and $\Delta^y = \pm i \Delta^x$, the above current is strictly conserved

$$\partial_\mu \left(J_\varphi^\mu \mp \frac{1}{2} J^\mu \right) = 0,\tag{2.44}$$

which occurs in the generalized $p_x \pm ip_y$ configuration $\Delta = e^{i\theta(r,t)} \Delta_0(r,t) (1, \pm i)$, written in the gauge $A_\varphi = 0$, and where $r = \sqrt{x^2 + y^2}$. This conservation law follows from the symmetry of the generalized $p_x \pm ip_y$ configuration under the combination of a spatial rotation by an angle α and a $U(1)$ transformation by a phase $\mp \alpha/2$.

2.4.2 Symmetries, currents, and conservation laws in the geometric description

The symmetries and conservation laws for Dirac fermions have been described recently in [156]. Here we review the essential details (for Majorana fermions) and focus on the mapping to the symmetries and conservation laws of the p -wave SF action (2.25), which were described in section 2.4.1.

2.4.2.1 Currents in the geometric description The natural currents in the geometric description are defined by the functional derivatives of the action S_{RC} with respect to the background fields e, ω ,

$$J_a^\mu = \frac{1}{|e|} \frac{\delta S_{\text{RC}}}{\delta e_\mu^a}, \quad J^{ab\mu} = \frac{1}{|e|} \frac{\delta S_{\text{RC}}}{\delta \omega_{ab\mu}}.\tag{2.45}$$

J_a^μ is the energy momentum (energy-momentum) tensor and $J^{ab\mu}$ is the spin current. Note that we use J as opposed to J to distinguish the geometric currents from the p -wave SF currents described in the previous section, though the two are related as shown below.

Calculating the geometric currents for the action (2.26) one obtains

$$\begin{aligned} 2J_a^\mu &= \mathcal{L}_{\text{RC}} e_a^\mu - \frac{i}{2} \bar{\chi} \left(\gamma^\mu D_a - \overleftarrow{D}_a \gamma^\mu \right) \chi, \\ 2J^{ab\mu} &= -\frac{1}{4} \bar{\chi} \chi e_c^\mu \varepsilon^{abc}, \end{aligned} \quad (2.46)$$

where $\mathcal{L}_{\text{RC}} = \bar{\chi} \left[\frac{i}{2} e_a^\mu \left(\gamma^\mu D_\mu - \overleftarrow{D}_\mu \gamma^\mu \right) - m \right] \chi$ is (twice) the Lagrangian, which vanishes on the χ equation of motion. We see that J_a^μ is essentially the $SO(1,2)$ -covariant version of the canonical energy-momentum tensor of the spinor χ . We also see that the spin current $J^{ab\mu}$ has a particularly simple form in $D = 2 + 1$, it is just the spin density $\frac{1}{2} \bar{\chi} \chi$ times a tensor $-\frac{1}{2} e_c^\mu \varepsilon^{abc}$ that only depends on the background field e . Using the expressions (2.27) for the geometric fields we find that J_a^μ , $J^{ab\mu}$ are related simply to the electric current and the ($U(1)$ -covariant) canonical energy-momentum tensor described in section 2.4.1, in the limit $m^* \rightarrow \infty$,

$$\begin{aligned} J^\mu &= 4 |e| J^{12\mu} = -\psi^\dagger \psi \delta_t^\mu, \\ t_{\text{cov } \nu}^\mu &= -|e| J_\nu^\mu = \begin{cases} \frac{i}{2} \psi^\dagger \overrightarrow{D}_\nu \psi & \mu = t \\ \frac{1}{2} \psi^\dagger \Delta^j \partial_\nu \psi^\dagger + h.c & \mu = j \end{cases}. \end{aligned} \quad (2.47)$$

Here we have simplified t_{cov} using the equation of motion for ψ , and one can also use the equation of motion to remove time derivatives and obtain Schrodinger picture operators. For example, $t_{\text{cov } t}^t = \frac{i}{2} \psi^\dagger \overrightarrow{D}_t \psi = m \psi^\dagger \psi - (\frac{1}{2} \psi^\dagger \Delta^j \partial_j \psi^\dagger + h.c)$ is just the ($U(1)$ -covariant) Hamiltonian density in the relativistic limit. The expression for the energy current $t_{\text{cov } t}^i$ is more complicated, and it is convenient to write it using some of the geometric quantities introduced above

$$\begin{aligned} t_{\text{cov } t}^j &= g^{jk} \frac{i}{2} \psi^\dagger \overrightarrow{D}_k \psi - \frac{o}{2} \partial_k \left(\frac{1}{|e|} \varepsilon^{jk} \psi^\dagger \psi \right) \\ &\quad - (\psi^\dagger \psi) g^{jk} C_{12k}. \end{aligned} \quad (2.48)$$

This is an expression for the energy current in terms of the momentum and charge densities, and it will be obtained below as a consequence of Lorentz symmetry in the relativistic limit. We now describe the symmetries of the action (2.26) and the conservation laws they imply for these currents. As expected, these conservation laws turn out to be essentially the ones derived in section (2.4.1), in the relativistic limit.

2.4.2.2 Spin The Lorentz Lie algebra $so(1,2)$ is comprised of matrices $\theta \in \mathbb{R}^{3 \times 3}$ with entries θ_b^a such that $\theta_{ab} = -\theta_{ba}$. These can be spanned as $\theta = \frac{1}{2} \theta_{ab} L^{ab}$ where the generators $L^{ab} = -L^{ba}$ are defined such that ηL^{ab} is the antisymmetric matrix with 1 (-1) at position a, b (b, a) and zero elsewhere. The spinor representation of θ is

$$\hat{\theta} = \frac{1}{2} \theta_{ab} \Sigma^{ab}, \quad \Sigma^{ab} = \frac{1}{4} [\gamma^a, \gamma^b]. \quad (2.49)$$

Local Lorentz transformations act on χ, e, ω by

$$\begin{aligned}\chi &\mapsto e^{-\hat{\theta}} \chi, \quad e_a^\mu \mapsto e_b^\mu (e^\theta)_a^b, \\ \omega_\mu &\mapsto e^{-\hat{\theta}} (\partial_\mu + \omega_\mu) e^{\hat{\theta}}.\end{aligned}\tag{2.50}$$

The subgroup of $SO(1, 2)$ that is physical in the p -wave SC is $SO(2)$ generated by L^{12} . Using the relations (2.27) between the p -wave SC fields and the geometric fields, and choosing $\theta = \theta_{12} L^{12} = -2\alpha L^{12}$, the transformation law (2.50) reduces to the $U(1)$ transformation (2.30),

$$\psi \mapsto e^{i\alpha} \psi, \quad \Delta \mapsto e^{2i\alpha} \Delta, \quad A_\mu \mapsto A_\mu + \partial_\mu \alpha.\tag{2.51}$$

The factor of 2 in $\theta_{12} = -2\alpha$ shows that $U(1)$ actually maps to $Spin(2)$, the double cover of $SO(2)$. Moreover, the fact that Δ has $U(1)$ charge 2 while ψ has $U(1)$ charge 1 corresponds to e_a^μ being an $SO(1, 2)$ vector while χ is an $SO(1, 2)$ spinor. The Lie algebra version of (2.50) is

$$\delta\chi = -\frac{1}{2}\theta_{ab}\Sigma^{ab}\chi, \quad \delta e_\mu^a = -\theta_b^a e_\mu^b, \quad \delta\omega_{b\mu}^a = D_\mu\theta_b^a.\tag{2.52}$$

Invariance of S_{RC} under this variation implies the conservation law

$$\nabla_\mu J^{ab\mu} - J^{ab\rho} T_{\mu\rho}^\mu = J^{[ab]},\tag{2.53}$$

valid on the equations of motion for χ [156, 41]. This conservation law relates the anti symmetric part of the energy-momentum tensor to the divergence of spin current. Essentially, the energy-momentum tensor isn't symmetric due to the presence of the background field ω which transforms under $SO(1, 2)$. From a different point of view, the vielbein e acts as a source for the fermionic spin current since it is charged under $SO(1, 2)$. Inserting the expressions (2.27) into the $(a, b) = (1, 2)$ component of (2.53) we obtain (2.31),

$$\partial_\mu J^\mu = -i\psi^\dagger \Delta^j \partial_j \psi^\dagger + h.c.\tag{2.54}$$

The other components of (2.53) follow from the symmetry under local boosts, which is only a symmetry of S_{SF} when $m^* \rightarrow \infty$. These can be used to obtain the formula (2.48) for the energy current of the p -wave SF, in the limit $m^* \rightarrow \infty$, in terms of the momentum and charge densities.

2.4.2.3 Energy-momentum A diffeomorphism is a smooth invertible map between manifolds. We consider only diffeomorphisms from space-time to itself and denote the group of such maps by $Diff$. Since the flat background metric δ^{ij} decouples in the relativistic limit, it makes sense to consider all diffeomorphisms, and not restrict to symmetries of δ^{ij} as we did in section 2.4.1.2.

Locally, diffeomorphisms can be described by coordinate transformations $x \mapsto x' = f(x)$. The lie algebra is that of vector fields $\zeta^\nu(x)$, which means diffeomorphisms in the connected component of the

identity $Diff_0$ can be written as $f(x) = f_1(x)$ where $f_\varepsilon(x) = \exp_x(\varepsilon\zeta) = x + \varepsilon\zeta(x) + O(\varepsilon^2)$ is the flow of ζ [234]. $Diff$ acts on the geometric fields by the pullback

$$\begin{aligned}\chi(x) &\mapsto \chi(f(x)), \quad e_\mu^a(x) \mapsto \partial_\mu f^\nu e_\nu^a(f(x)), \\ \omega_\mu(x) &\mapsto \partial_\mu f^\nu \omega_\nu(f(x)).\end{aligned}\tag{2.55}$$

The action of $Diff$ on the p -wave SF fields is similar, and follows from (2.55) supplemented by the dictionary (2.27). For $f \in Diff_0$ generated by ζ , the Lie algebra version of (2.55) is given by the Lie derivative,

$$\begin{aligned}\delta\chi &= \mathcal{L}_\zeta\chi = \zeta^\mu\partial_\mu\chi, \\ \delta e_\mu^a &= \mathcal{L}_\zeta e_\mu^a = \partial_\mu\zeta^\nu e_\nu^a + \zeta^\nu\partial_\nu e_\mu^a, \\ \delta\omega_\mu &= \mathcal{L}_\zeta\omega_\mu = \partial_\mu\zeta^\nu\omega_\nu + \zeta^\nu\partial_\nu\omega_\mu.\end{aligned}\tag{2.56}$$

Since these variations are not Lorentz covariant, they will give rise to a conservation law which is not Lorentz covariant. This follows from the fact that the naive $Diff$ action (2.55) does not commute with Lorentz gauge transformations, as was described for the simpler case of translations and $U(1)$ gauge transformations in section 2.4.1.2. Instead, one should use the Lorentz-covariant $Diff$ action, which is the pull back from $f(x)$ to x followed by a Lorentz parallel transport from $f(x)$ to x along the integral curve $\gamma_{x,\zeta}(\varepsilon) = \exp_x(\varepsilon\zeta) = f_\varepsilon(x)$,

$$\begin{aligned}\chi(x) &\mapsto P\chi(f(x)), \\ e_\mu^a(x) &\mapsto P_b^a\partial_\mu f^\nu e_\nu^b(f(x)), \\ \omega_\mu(x) &\mapsto P[\partial_\mu f^\nu\omega_\nu(f(x)) + \partial_\mu]P^{-1},\end{aligned}\tag{2.57}$$

where $P = \frac{1}{2}P_{ab}\Sigma^{ab}$ and $P = \mathcal{P}\exp\left(-\int_{\gamma_{x,\zeta}}\omega\right)$ is the spin parallel transport given by the path ordered exponential. At the Lie algebra level, this modification of (2.55) amounts to an infinitesimal Lorentz gauge transformation generated by $\theta_{ab} = -\zeta^\rho\omega_{ab\rho}$, which modifies (2.56) to the covariant expressions

$$\begin{aligned}\delta\chi &= \zeta^\mu\nabla_\mu\chi, \\ \delta e_\mu^a &= \nabla_\mu\zeta^a - T_{\mu\nu}^a\zeta^\nu, \\ \delta\omega_\mu &= \zeta^\nu R_{ab\nu\mu}.\end{aligned}\tag{2.58}$$

Since the usual $Diff$ and Lorentz actions on the fields are both symmetries of S_{RC} , so is the Lorentz-covariant $Diff$ action. This leads directly to the conservation law

$$\nabla_\mu J_\nu^\mu - J_\nu^\rho T_{\mu\rho}^\mu = T_{\nu\mu}^b J_b^\mu + R_{bc\nu\mu} J^{bc\mu},\tag{2.59}$$

valid on the equations of motion for χ [41, 156]. We find it useful to rewrite (2.59) in a way which

isolates the effect of torsion,

$$\tilde{\nabla}_\mu J^\mu_\nu = C_{ab\nu} J^{[ab]} + R_{ab\nu\mu} J^{ab\mu}, \quad (2.60)$$

where we note that the curvature also depends on the torsion, $R = \tilde{R} + \tilde{D}C + C \wedge C$. Equation (2.59) can also be massaged to the non-covariant form

$$\partial_\mu (|e| J^\mu_\nu) = (e^\rho_a D_\nu e^a_\mu) |e| J^\mu_\rho + R_{\nu\mu ab} |e| J^{ab\mu}. \quad (2.61)$$

Using the dictionary (2.27) and the subsequent paragraph, and (2.47), this reduces to

$$\partial_\mu t^\mu_{\text{cov } \nu} = (D_\nu \Delta^j) \frac{1}{2} \psi^\dagger \partial_j \psi^\dagger + h.c + F_{\nu\mu} J^\mu, \quad (2.62)$$

which is just the energy-momentum conservation law (2.39) for the p -wave SF (with $m^* \rightarrow \infty$).

Writing the conservation law in the form (2.61) may not seem natural from the geometric point of view because it uses the partial derivative as opposed to a covariant derivative. It is however natural from the p -wave SC point of view, where space-time is actually flat and e is viewed as a bosonic field with no geometric role, which is the order parameter Δ . This point is important in the context of the gravitational anomaly in the p -wave SC, see Appendix A.2.

Similar statements hold for other mechanisms for emergent/analogue gravity, see section I.6 of [27] and [235], and were also made in the gravitational context without reference to emergent phenomena [236].

2.5 Bulk response

2.5.1 Currents from effective action

The effective action for the background fields is obtained by integrating over the spin-less fermion ψ ,

$$e^{iW_{\text{SF}}[\Delta, A]} = \int D\psi^\dagger D\psi e^{iS_{\text{SF}}[\psi, \psi^\dagger, \Delta, A]}. \quad (2.63)$$

The integral is a fermionic coherent state functional integral, over the Grassmann valued fields ψ, ψ^\dagger , and the action S_{SF} is given in (2.24).

As described in section 2.3, in the relativistic limit W_{SF} is equal to the effective action obtained by integrating over a Majorana fermion coupled to RC geometry,

$$\begin{aligned} e^{iW_{\text{SF}}[\Delta, A]} &= e^{iW_{\text{RC}}[e, \omega]} \\ &= \int D(|e|^{1/2} \chi) e^{iS_{\text{RC}}[\chi, e, \omega]}, \end{aligned} \quad (2.64)$$

where e, ω are given in terms of Δ, A by (2.27).

It follows from the definition (2.45) of the spin current $J^{ab\mu}$ and the energy-momentum tensor J^μ_a as

functional derivatives of S_{RC} that their ground state expectation values are given by

$$\langle J_a^\mu \rangle = \frac{1}{|e|} \frac{\delta W_{\text{RC}}}{\delta e_\mu^a}, \quad \langle J^{ab\mu} \rangle = \frac{1}{|e|} \frac{\delta W_{\text{RC}}}{\delta \omega_{ab\mu}}. \quad (2.65)$$

Using the mapping (2.47) between J_a^μ , $J^{ab\mu}$ and $t_{\text{cov } \nu}^\mu$, J^μ we see that

$$\begin{aligned} \langle J^\mu \rangle &= 4|e| \langle J^{12\mu} \rangle = 4 \frac{\delta W_{\text{RC}}[e, \omega]}{\delta \omega_{12\mu}}, \\ \langle t_{\text{cov } \nu}^\mu \rangle &= -|e| e_\nu^a \langle J_a^\mu \rangle = -e_\nu^a \frac{\delta W_{\text{RC}}[e, \omega]}{\delta e_\mu^a}. \end{aligned} \quad (2.66)$$

This is the recipe we will use to obtain the expectation values $\langle J^\mu \rangle, \langle t_{\text{cov } \nu}^\mu \rangle$ from the effective action W_{RC} for a Majorana spinor in RC space-time.

Note that in (2.66) there are derivatives with respect to all components of the vielbein, not just the spatial ones which we can physically obtain from Δ . For this reason, to get all components of $\langle t_{\text{cov } \nu}^\mu \rangle$, we should obtain W_{RC} for general e , take the functional derivative in (2.66), and only then set e to the configuration obtained from Δ according to (2.27). From the p -wave SF point of view, this corresponds to the introduction of a fictitious background field e_0^μ which enters S_{SF} by generalizing $\psi^\dagger i D_t \psi$ to $\psi^\dagger \frac{i}{2} e_0^\mu \overleftrightarrow{D}_\mu \psi$, and setting $e_0^\mu = \delta_t^\mu$ at the end of the calculation, as in [41].

Before we move on, we offer some intuition for the expressions (2.66). The first equation in (2.66) follows from the definition $J^\mu = -\frac{\delta S_{\text{SF}}}{\delta A_\mu}$ of the electric current and the simple relation $\omega_{12\mu} = -\omega_{21\mu} = -2A_\mu$ between the spin connection and the $U(1)$ connection. The second equation in (2.66) is slightly trickier. It implies that the (relativistic part of the) energy-momentum tensor $t_{\text{cov } \nu}^\mu$ is given by a functional derivative with respect to the order parameter Δ , because Δ is essentially the vielbein e . This may seem strange, and it is certainly not the case in an s -wave SC, where $\frac{\delta H}{\delta \Delta} \sim \psi_\uparrow^\dagger \psi_\downarrow^\dagger$ has nothing to do with energy-momentum. In a p -wave SC, the operator $\frac{\delta H}{\delta \Delta^j} \sim \psi^\dagger \partial_j \psi^\dagger$ contains a spatial derivative which hints that it is related to fermionic momentum. More accurately, we see from (2.38) that the operator $\psi^\dagger \partial_j \psi^\dagger$ enters the energy-momentum tensor in a p -wave SC.

2.5.2 Effective action from perturbation theory

2.5.2.1 Setup and generalities We consider the effective action for a p -wave SF on the plane \mathbb{R}^2 , with the corresponding space-time manifold $M_3 = \mathbb{R}_t \times \mathbb{R}^2$, by using perturbation theory around the $p_x \pm i p_y$ configuration $\Delta = \Delta_0 e^{i\theta} (1, \pm i)$ with no electromagnetic fields $\partial_\mu \theta - 2A_\mu = 0$. After $U(1)$ gauge fixing $\theta = 0$ ¹⁹, we obtain $\Delta = \Delta_0 (1, \pm i)$, $A = 0$. Let us start with the $p_x + i p_y$ configuration, which has a positive orientation, in which case the corresponding (gauge fixed) vielbein and spin connection are just $e_a^\mu = \delta_a^\mu$ and $\omega_{ab\mu} = 0$. A perturbation of the $p_x + i p_y$ configuration corresponds to $e_a^\mu = \delta_a^\mu + h_a^\mu$ with a small h and to a small spin connection $\omega_{ab\mu}$. In other words, a perturbation of the $p_x + i p_y$ configuration without electromagnetic fields corresponds to a perturbation of flat and torsion-less space-time.

¹⁹In doing so we are ignoring the possibility of vortices, see [198].

The effective action for a Dirac spinor in a background RC geometry was recently calculated perturbatively around flat and torsionless space-time, with a positive orientation, in the context of geometric responses of Chern insulators [156, 157]. This is equal to $2W_{\text{RC}}$ where W_{RC} is the effective action for a Majorana spinor in RC geometry.

At this point it seems that we can apply these results in order to obtain the effective action for the p -wave SC, in the relativistic limit. There is however, an additional ingredient in the perturbative calculation of the effective action which we did not yet discuss, which is the renormalization scheme used to handle diverging integrals. We refer to terms in the effective action that involve diverging integrals as *UV sensitive*. The values one obtains for such terms depend on the details of the renormalization scheme, or in other words, on microscopic details that are not included in the continuum action.

For us, the continuum description is simply an approximation to the lattice model, where space is a lattice but time is continuous. This implies a physical cutoff Λ_{UV} for wave-vectors, but not for frequencies. In particular, such a scheme is not Lorentz invariant, even though the action in the relativistic limit is. Lorentz symmetry is in any case broken down to spatial $SO(2)$ for finite m^* . For these reasons, UV sensitive terms in the effective action W_{RC} for the p -wave SC will be assigned different values than those obtained before, using a fully relativistic scheme.

The perturbative calculation within the renormalization scheme outlined above is described in appendix E, where we also demonstrate that it produces physical quantities that approximate those of the lattice model, and compare to the fully relativistic schemes used in previous works. In the following we will focus on the UV *insensitive* part of the effective action, and in doing so we will obtain results which are essentially²⁰ independent of microscopic details that do not appear in the continuum action. We start by quoting the fully relativistic results of [156, 157], and then restrict our attention to the UV insensitive part of the effective action, and describe the physics of the p -wave SC it encodes.

2.5.2.2 Effective action for a single Majorana spinor The results of [156, 157] can be written as

$$\begin{aligned} 2W_{\text{RC}}[e, \omega] &= \frac{\kappa_H}{2} \int_{M_3} Q_3(\tilde{\omega}) \\ &+ \frac{\zeta_H}{2} \int_{M_3} e^a D e_a - \frac{\kappa_H}{2} \int_{M_3} \tilde{\mathcal{R}} e^a D e_a \\ &+ \frac{1}{2\kappa_N} \int_{M_3} \left(\tilde{\mathcal{R}} - 2\Lambda + \frac{3}{2}c^2 \right) |e| d^3x + \dots \end{aligned} \quad (2.67)$$

where

$$Q_3(\tilde{\omega}) = \text{tr} \left(\tilde{\omega} d\tilde{\omega} + \frac{2}{3} \tilde{\omega}^3 \right) \quad (2.68)$$

²⁰See the discussion of $O\left(\frac{m}{\Lambda_{UV}}\right)$ corrections below.

is the Chern-Simons (local) 3-form, $c = C_{abc}\varepsilon^{abc}$ is the totally antisymmetric piece of the contorsion tensor, and $\kappa_H, \zeta_H, 1/\kappa_N, \Lambda/\kappa_N$ are coefficients that will be discussed further below. The first two lines of (2.67) are written in terms of differential forms, and the third line is written in terms of scalars. By scalars we mean *Diff* invariant objects. In the differential forms the wedge product is implicit, as it will be from now on, so $\tilde{\omega} \wedge d\tilde{\omega}$ is written as $\tilde{\omega}d\tilde{\omega}$ and so on. The integrals over differential forms can be written as integrals over pseudo-scalars,

$$\begin{aligned} e^a D e_a &= \left(e^a_\alpha D_\beta e^b_\gamma \frac{1}{|e|} \varepsilon^{\alpha\beta\gamma} \right) |e| d^3x = -o c |e| d^3x, \\ Q_3(\tilde{\omega}) &= \left(\tilde{\omega}^a_{b\alpha} \partial_\beta \tilde{\omega}^b_{a\gamma} + \frac{2}{3} \tilde{\omega}^a_{b\gamma} \tilde{\omega}^b_{c\beta} \tilde{\omega}^c_{a\gamma} \right) \frac{1}{|e|} \varepsilon^{\alpha\beta\gamma} |e| d^3x, \end{aligned} \quad (2.69)$$

which are only invariant under the orientation preserving subgroup of *Diff* which we denote *Diff*₊. Here $o = \text{sgn}(\det(e))$ is the orientation of e . These expressions are odd under orientation reversing diffeomorphisms because so are o and the pseudo-tensor $\frac{1}{|e|} \varepsilon^{\alpha\beta\gamma}$ ²¹.

Equation (2.67) can be expanded in the perturbations h_a^μ and $\omega_{ab\mu}$ to reveal the order in perturbation theory at which the different terms arise, see appendix E. Additionally, at every order in the perturbations the effective action can be expanded in powers of derivatives of the perturbations over the mass m . The terms written explicitly above show up at first and second order in h, ω and at up to third order in their derivatives. They also include higher order corrections that make them *Diff*₊ and Lorentz gauge invariant, or invariant up to total derivatives.

All other contributions denoted by $+\dots$ are at least third order in the perturbations or fourth order in derivatives. Such a splitting is not unique [156], but the form (2.67) has been chosen because it is well suited for the study of the bulk responses.

Let us now describe the different terms in (2.67). The first term is the gravitational Chern-Simons (gCS) term. It has a similar structure to the more familiar $U(1)$ CS term $\int \text{Ad}A$, and is in fact an $SO(1,2)$ CS term, but note that the LC spin connection $\tilde{\omega}$ is a functional of the vielbein e . It is important that the spin connection in gCS is not ω , since through $\omega_\mu = -2A_\mu \Sigma^{12}$ this would imply a quantized Hall conductivity in a p -wave SC, which does not exist [15, 153]. As it is written in (2.67), gCS is invariant under *Diff*₊, but not under $SO(1,2)$ if M_3 has a boundary. This is the boundary $SO(1,2)$ anomaly, which is discussed further in section 2.5.3. Using the relation $\tilde{\Gamma}^\alpha_{\beta\mu} = e^\alpha_a (\delta^a_b \partial_\mu + \tilde{\omega}^a_{b\mu}) e^b_\beta$ between $\tilde{\Gamma}$ and $\tilde{\omega}$, one can derive an important formula,

$$Q_3(\tilde{\Gamma}) - Q_3(\tilde{\omega}) = \text{tr} \left[\frac{1}{3} (ede^{-1})^3 + d \left(de^{-1} e \tilde{\Gamma} \right) \right], \quad (2.70)$$

where unusually, $e = (e^a_\mu)$ is treated in this expression as a matrix valued function [23, 25]. The variation

²¹In this section ε always stands for the usual totally anti symmetric symbol, normalized to 1. Thus $\varepsilon^{123} = \varepsilon^{xyt} = \varepsilon_{xyt} = 1$. Note that ε^{abc} is an $SO(1,2)$ tensor, and an $O(1,2)$ pseudo-tensor, while $\varepsilon^{\mu\nu\rho} = \det(e) e^\mu_a e^\nu_b e^\rho_c \varepsilon^{abc}$ is a (coordinate) tensor density, $\frac{1}{\det(e)} \varepsilon^{\mu\nu\rho}$ is a tensor and $\frac{1}{|e|} \varepsilon^{\mu\nu\rho} = \frac{1}{|\det(e)|} \varepsilon^{\mu\nu\rho}$ is a pseudo-tensor.

with respect to e of the two terms on the right hand side is a total derivative, which means that they are irrelevant for the purpose of calculating bulk responses. One can therefore use $Q_3(\tilde{\Gamma})$, which only depends on the metric $g_{\mu\nu}$, instead of $Q_3(\tilde{\omega})$. The form $\int_{M_3} Q_3(\tilde{\Gamma})$ of gCS is invariant under $SO(1,2)$ but not under $Diff_+$, as opposed to $\int_{M_3} Q_3(\tilde{\omega})$. Thus the right hand side of (2.70) has the effect of shifting the boundary anomaly from $SO(1,2)$ to $Diff$.

The second term in (2.67) has a structure similar to a CS term with e^a playing the role of a connection, and indeed some authors refer to it as such [237]. Nevertheless, it is $SO(1,2)$ and $Diff_+$ invariant, as can be seen from (2.69). This term was related to the torsional Hall viscosity in [156], where it was discussed extensively. The third term in (2.67) is also $SO(1,2)$ and $Diff_+$ invariant. We refer to this term as *gravitational pseudo Chern-Simons* (gpCS), to indicate its similarity to gCS, and the fact that it is not a Chern-Simons term. The similarity between gCS and gpCS is demonstrated and put in a broader context in the discussion, section 2.6. In section 2.5.4 we will see that gCS and gpCS produce similar contributions to bulk responses. For now, we simply note that both terms are second order in \hbar and third order in derivatives of h .

The third line in (2.67) contains the Einstein-Hilbert action with a cosmological constant Λ familiar from general relativity, and an additional torsional contribution $\propto c^2$. The coefficient $1/\kappa_N$ of the Einstein-Hilbert term is usually related to a Newton's constant $G_N = \kappa_N/8\pi$. Note that in Riemannian geometry, where torsion vanishes and $\omega = \tilde{\omega}$, only the gCS term, the Einstein-Hilbert term, and the cosmological constant survive.

The coefficients $\kappa_H, \zeta_H, 1/\kappa_N, \Lambda/\kappa_N$ are given by frequency and wave-vector integrals that arise within the perturbative calculation, and are described in appendix E. In particular $\zeta_H, 1/\kappa_N, \Lambda/\kappa_N$ are dimension-full, with mass dimensions 2, 1, 3, and naively diverge. In other words, they are UV sensitive. On the other hand, κ_H is dimensionless and UV insensitive. With no regularization, one finds

$$\kappa_H = \frac{1}{48\pi} \frac{\text{sgn}(m) o}{2}. \quad (2.71)$$

Thus, the effective action for a single Majorana spinor can be written as

$$W_{\text{RC}}[e, \omega] = \frac{1/2 \text{sgn}(m) o}{96\pi} W[e, \omega] + \dots \quad (2.72)$$

where

$$W[e, \omega] = \int_{M_3} Q_3(\tilde{\omega}) - \int_{M_3} \tilde{\mathcal{R}} e^a D e_a \quad (2.73)$$

is the sum of gCS and gpCS, and the dots include UV sensitive terms, or terms of a higher order in derivatives or perturbations, as described above.

Since the lattice model implies a finite physical cutoff Λ_{UV} for wave-vectors, (2.72) is exact only for $m/\Lambda_{UV} \rightarrow 0$. For non-zero m there are small $O(m/\Lambda_{UV})$ corrections²² to (2.72). We will keep these

²²All expressions here are with $\hbar = c_{\text{light}} = 1$. Restoring units one finds $\frac{m}{\Lambda_{UV}} \sim \frac{\max(t, \mu)}{\delta}$ and so $\frac{m}{\Lambda_{UV}} \ll 1$ in the

corrections implicit for now, and come back to them in section 2.5.3.

2.5.2.3 Summing over Majorana spinors As discussed in Appendix 2.2, the continuum description of the p -wave SC includes four Majorana spinors labeled by $1 \leq n \leq 4$, with masses m_n , which are coupled to vielbeins $e_{(n)}$. Let us repeat the necessary details. The vielbein $e_{(1)}$ is associated with the order parameter δ of the underlying lattice model, as in (2.27), up to an unimportant rescaling by the lattice spacing a . For this reason we treat it as a fundamental vielbein and write $e = e_{(1)}$ in some expressions. The other vielbeins $(e_{(n)})_a^\mu$ are obtained from e by multiplying one of the columns $\mu = x, y$ or both by -1 . This implies that $o = o_1 = o_3 = -o_2 = -o_4$, and that the metrics $g_{(n)}^{\mu\nu}$ are identical apart from $g^{xy} = g_{(1)}^{xy} = g_{(3)}^{xy} = -g_{(2)}^{xy} = -g_{(4)}^{xy}$. With this in mind, we can sum over the four Majorana spinors and obtain an effective action for the p -wave SC,

$$\begin{aligned} W_{\text{SC}}[e, \omega] &= \sum_{n=1}^4 W_{\text{RC}}[e_{(n)}, \omega] \\ &= \frac{1/2}{96\pi} \sum_{n=1}^4 \frac{\text{sgn}(m_n) o_n}{2} W[e_{(n)}, \omega] + \dots \end{aligned} \quad (2.74)$$

Note that the Chern number of the lattice model is given by $\nu = \sum_{n=1}^4 \text{sgn}(m_n) o_n/2$, but since W also depends on the different vielbeins $e_{(n)}$, (2.74) does not only depend on ν in the general case.

Some simplification is possible however. Since $e_{(1)} = e_{(3)}$ and $e_{(2)} = e_{(4)}$ up to a space-time independent $SO(2) (U(1))$ transformation,

$$\begin{aligned} W_{\text{SC}}[e, \omega] &= \sum_{l=1}^2 \frac{\nu_l/2}{96\pi} W[e_{(l)}, \omega] + \dots \\ &= \sum_{l=1}^2 \frac{\nu_l/2}{96\pi} \int_{M_3} Q_3(\tilde{\omega}_{(l)}) + \dots \end{aligned} \quad (2.75)$$

where in the second line, we have only written explicitly gCS terms. Here we defined

$$\begin{aligned} \nu_1 &= \frac{o_1}{2} (\text{sgn}(m_1) + \text{sgn}(m_3)), \\ \nu_2 &= \frac{o_2}{2} (\text{sgn}(m_2) + \text{sgn}(m_4)), \end{aligned} \quad (2.76)$$

which are both integers, $\nu_1, \nu_2 \in \mathbb{Z}$. The Chern number of the lattice model is given by the sum $\nu = \nu_1 + \nu_2$. Thus the lattice model seems to behave like a bi-layer, with layer index $l = 1, 2$. In the relativistic regime.

topological phases of the model $\nu_1 = 0$, $\nu = \nu_2 = \pm 1$, and so

$$\begin{aligned} W_{\text{SC}}[e, \omega] &= \frac{\nu/2}{96\pi} W[e_{(2)}, \omega] + \dots \\ &= \frac{\nu/2}{96\pi} \int_{M_3} Q_3(\tilde{\omega}_{(2)}) + \dots \end{aligned} \quad (2.77)$$

where again, in the second line we have only written explicitly the gCS term. This result is close to what one may have guessed. In the topological phases with Chern number $\nu \neq 0$, the effective action contains a single gCS term, with coefficient $\frac{\nu/2}{96\pi}$. A result of this form has been anticipated in [28, 15, 31, 17, 121], but there are a few details which are important to note. First, apart from gCS, W also contains the a gpCS term of the form $\int_{M_3} \tilde{\mathcal{R}} e^a D e_a$, which is possible due to the emergent torsion. Second, the connection that appears in the CS form Q_3 is a LC connection, and not the torsion-full connection ω . Moreover, this LC connection is not $\tilde{\omega}$, but a modification of it $\tilde{\omega}_{(2)}$, where the subscript (2) indicates the effect of the multiple Majorana spinors in the continuum description of the lattice model. Third, the geometric fields e, ω are given by Δ, A .

In the trivial phases $\nu_1 = -\nu_2 \in \{-1, 0, 1\}$, $\nu = 0$, and we find

$$\begin{aligned} W_{\text{SC}}[e, \omega] &= \frac{\nu_1/2}{96\pi} [W[e_{(1)}, \omega] - W[e_{(2)}, \omega]] + \dots \\ &= \frac{\nu_1/2}{96\pi} \left[\int_{M_3} Q_3(\tilde{\omega}_{(1)}) - \int_{M_3} Q_3(\tilde{\omega}_{(2)}) \right] + \dots \end{aligned} \quad (2.78)$$

This result is quite surprising. Instead of containing no gCS terms, some trivial phases contain the difference of two such terms, with slightly different spin connections. One may wonder if these trivial phases are really trivial after all. This is part of a larger issue which we now address.

2.5.3 Symmetries of the effective action

By considering the gauge symmetry of the effective action we can reconstruct the topological phase diagram appearing in Fig.5 from (2.75). This will also help us understand which of our results are special to the relativistic limit, and which should hold throughout the phase diagram. By gauge symmetry we refer in this section to the $SO(2)$ subgroup of $SO(1, 2)$, which corresponds to the physical $U(1)$ symmetry of the p -wave SC. Equation (2.70) shows that we can equivalently consider $Diff$ symmetry. The physical reason for this equivalence is that the p -wave order parameter is charged under both symmetries, and therefore maps them to one another.

The effective action was calculated within perturbation theory on the space-time manifold $M_3 = \mathbb{R}_t \times \mathbb{R}^2$, but for this discussion, we use its locality to assume it remains locally valid on more general M_3 , which may be closed (compact and without a boundary) or have a boundary. A closed space-time is most simply obtained by working on $M_3 = \mathbb{R}_t \times M_2$ with M_2 closed, and with background fields Δ, A which are periodic in time, such that \mathbb{R}_t can be compactified to a circle.

As described in appendix B.6, a non singular order parameter endows M_3 with an orientation and

a spin structure, and in particular requires that M_2 be orientable [238], which we assume. Thus, for example, we exclude the possibility of M_2 being the Mobius strip. Moreover, a non singular order parameter on a closed M_2 requires that M_2 contain $(g - 1) o$ magnetic monopoles [15], where g is the genus of M_2 , and we assume that this condition is satisfied. For example, if M_2 is the sphere then it must contain a single monopole or anti-monopole depending on the orientation o [239, 240].

2.5.3.1 Quantization of coefficients The first fact about the gCS term that we will need, is that gauge symmetry of $\alpha \int_{M_3} Q_3(\tilde{\omega})$ for all closed M_3 requires that α be quantized such that $\alpha \in \frac{1}{192\pi}\mathbb{Z}$, see equation (2.27) of [24]. In order to understand how generic is our result (2.75), we will check what quantization condition on α_1, α_2 is required for gauge symmetry of $\alpha_1 \int_{M_3} Q_3(\tilde{\omega}_{(1)}) + \alpha_2 \int_{M_3} Q_3(\tilde{\omega}_{(2)})$ on all closed M_3 . Following the arguments of [24] we find that $\alpha_1 + \alpha_2 \in \frac{1}{192\pi}\mathbb{Z}$, but $\alpha_1, \alpha_2 \in \mathbb{R}$ are not separately restricted, see appendix C. It is therefore natural to define $\alpha = \alpha_1 + \alpha_2$ and rewrite

$$\begin{aligned} & \alpha_1 \int_{M_3} Q_3(\tilde{\omega}_{(1)}) + \alpha_2 \int_{M_3} Q_3(\tilde{\omega}_{(2)}) \\ &= \alpha \int_{M_3} Q_3(\tilde{\omega}_{(2)}) + \alpha_1 \int_{M_3} [Q_3(\tilde{\omega}_{(1)}) - Q_3(\tilde{\omega}_{(2)})], \end{aligned} \quad (2.79)$$

where $\alpha \in \frac{1}{192\pi}\mathbb{Z}$ but $\alpha_1 \in \mathbb{R}$. Comparing with the result (2.75), we identify $\alpha = \frac{\nu/2}{96\pi}$, $\alpha_1 = \frac{\nu_1/2}{96\pi}$, and we conclude that ν must be precisely an integer and equal to the Chern number, while ν_1 need not be quantized. We therefore interpret the $O(m/\Lambda_{\text{UV}})$ corrections to $\alpha = \frac{\nu/2}{96\pi}$ produced in our computation as artifacts of our approximations²³, which must vanish due to gauge invariance. On the other hand, we interpret the quantization $\alpha_1 = \frac{\nu_1/2}{96\pi}$ as a special property of the relativistic limit with both $m^* \rightarrow \infty$ and $m \rightarrow 0$, which should not hold throughout the phase diagram.

So far we have only considered gCS terms. As already explained, the gpCS term is gauge invariant on any M_3 , and we therefore see no reason for the quantization of its coefficient. Explicitly, $-\beta \int_{M_3} \tilde{\mathcal{R}} e^a D e_a$ is gauge invariant for all $\beta \in \mathbb{R}$. Thus we interpret the approximate quantization of the coefficients of gpCS terms as a special property of the relativistic limit, which should not hold throughout the phase diagram. We note that even for a relativistic spinor any $\beta \in \mathbb{R}$ can be obtained, by adding a non minimal coupling to torsion [156].

²³Specifically, in obtaining the relativistic continuum approximation we split the Brillouin zone BZ into four quadrants and linearized the lattice Hamiltonian (2.16) in every quadrant. Applying any integral formula for the Chern number to the approximate Hamiltonian will give a result $\nu_{\text{apprx}} = \frac{1}{2} \sum_{n=1}^4 o_n \text{sgn}(m_n) + O(m/\Lambda_{\text{UV}})$ which is only approximately quantized in the relativistic regime, simply because the approximate Hamiltonian is discontinuous on BZ . Nevertheless, the known quantization $\nu \in \mathbb{Z}$ and the fact that $\nu_{\text{apprx}} \approx \nu$ are enough to obtain the exact result $\nu = \frac{1}{2} \sum_{n=1}^4 o_n \text{sgn}(m_n)$.

In light of the above, it is natural to interpret (2.75) as a special case of

$$\begin{aligned} W_{\text{SC}}[e, \omega] &= \frac{\nu/2}{96\pi} \int_{M_3} Q_3(\tilde{\omega}_{(2)}) \\ &+ \alpha_1 \int_{M_3} [Q_3(\tilde{\omega}_{(1)}) - Q_3(\tilde{\omega}_{(2)})] \\ &- \beta_1 \int_{M_3} \tilde{\mathcal{R}}_{(1)} e_{(1)}^a D e_{(1)a} - \beta_2 \int_{M_3} \tilde{\mathcal{R}}_{(2)} e_{(2)}^a D e_{(2)a} + \cdots \end{aligned} \quad (2.80)$$

where $\nu \in \mathbb{Z}$ is the Chern number and $\alpha_1, \beta_1, \beta_2$ are additional, non quantized, yet dimensionless, response coefficients. In the relativistic limit $\alpha_1, \beta_1, \beta_2$ happen to be quantized, but this is not generic. Only the first gCS term encodes topological bulk responses, proportional to the Chern number ν , and below we will see that only this term is related to an edge anomaly. We can also write (2.80) more symmetrically,

$$\begin{aligned} W_{\text{SC}}[e, \omega] &= \sum_{l=1}^2 \left[\alpha_l \int_{M_3} Q_3(\tilde{\omega}_{(l)}) - \beta_l \int_{M_3} \tilde{\mathcal{R}}_{(l)} e_{(l)}^a D e_{(l)a} \right] + \cdots \end{aligned} \quad (2.81)$$

but here we must keep in mind the quantization condition $\alpha_1 + \alpha_2 = \frac{\nu/2}{96\pi} \in \frac{1}{192\pi} \mathbb{Z}$.

This equation should be compared with the result in the relativistic limit (2.75), where α_l, β_l are all quantized, and $\alpha_l = \beta_l$. We note that the quantization of α_l, β_l in the relativistic limit can be understood on dimensional grounds: in this limit there are simply not enough dimension-full quantities which can be used to construct dimensionless quantities, beyond $\text{sgn}(m_n)$ and o_n . Of course, this does not explain why $\alpha_l = \beta_l$ in the relativistic limit.

2.5.3.2 Boundary anomalies We can strengthen the above conclusions by considering space-times M_3 with a boundary. The second fact about the gCS term that we will need is that it is not gauge invariant when M_3 has a boundary, even with a properly quantized coefficient. In more detail, the $SO(2)$ variation of gCS is given by

$$\delta_\theta \int_{M_3} Q_3(\tilde{\omega}) = -\text{tr} \int_{\partial M_3} d\theta \tilde{\omega}. \quad (2.82)$$

Up to normalization, the boundary term above is called the consistent Lorentz anomaly, which is one of the forms in which the gravitational anomaly manifests itself [12]²⁴. The anomaly $\text{tr} \int_{\partial M_3} d\theta \tilde{\omega}$ is a local functional that can either be written as the gauge variation of a local bulk functional, as it is written above, or as the gauge variation of a *nonlocal* boundary functional $F[\tilde{\omega}]$, such that $\delta_\theta F[\tilde{\omega}] = \int_{\partial M_3} d\theta \tilde{\omega}$, but cannot be written as the gauge variation of a local boundary functional [241]. The difference of two

²⁴Generally speaking, *consistent* anomalies are given by symmetry variations of functionals. We will also discuss below the more physical *covariant* anomalies, which correspond to the actual inflow of some charge from bulk to boundary

gCS terms is also not gauge invariant,

$$\begin{aligned} & \delta_\theta \left[\int_{M_3} Q_3(\tilde{\omega}_{(1)}) - \int_{M_3} Q_3(\tilde{\omega}_{(2)}) \right] \\ &= -\text{tr} \int_{\partial M_3} d\theta (\tilde{\omega}_{(1)} - \tilde{\omega}_{(2)}), \end{aligned} \quad (2.83)$$

but here there is a local boundary term that can produce the same variation, given by $\text{tr}(\tilde{\omega}_{(1)}\tilde{\omega}_{(2)})$.

The physical interpretation is as follows. Since $F[\tilde{\omega}]$ is non local it can be interpreted as the effective action obtained by integrating over a gapless, or massless, boundary field coupled to e . These are the boundary chiral Majorana fermions of the p -wave SC. The statement that F cannot be local implies that this boundary field cannot be gapped. In this manner the existence of the gCS term in the bulk effective action, with a coefficient that is fixed within a topological phase, implies the existence of gapless degrees of freedom that cannot be gapped within a topological phase. We study this bulk-boundary correspondence in more detail in Appendix A. Naively, the difference of two gCS terms implies the existence of two boundary fermions with opposite chiralities, one of which is coupled to $e_{(1)}$ and the other coupled to $e_{(2)}$. The boundary term $\int_{\partial M_3} \text{tr}(\tilde{\omega}_{(1)}\tilde{\omega}_{(2)})$ can only be generated if the two counter propagating fermions are coupled, and its locality indicates that this coupling can open a gap. Thus the term $\int_{\partial M_3} \text{tr}(\tilde{\omega}_{(1)}\tilde{\omega}_{(2)})$ represents the effect of a generic interaction between two counter propagating chiral Majorana fermions.

Again, as opposed to the gCS term, the gpCS term is gauge invariant on any M_3 , and is therefore unrelated to edge anomalies. Thus, in the effective action (2.80), only the first gCS term is related to an edge anomaly.

2.5.3.3 Time reversal and reflection symmetry of the effective action Time reversal T and reflection R are discussed in appendices B.5.2 and B.5.3. The orientation o of the order parameter is odd under both T, R , and it follows that so are the coefficients ν_l . Therefore ν_l are T, R -odd response coefficients. More generally, α_l, β_l in (2.81) are T, R -odd response coefficients. As described in section 2.5.2.2, integrals over differential forms are also odd under the orientation reversing diffeomorphisms T, R , and therefore W_{SC} is invariant under T, R .

2.5.4 Calculation of currents

To derive the currents we start with the expression

$$\alpha_1 \int_{M_3} Q_3(\tilde{\omega}) - \beta_1 \int_{M_3} \tilde{\mathcal{R}} e^a D e_a + \dots \quad (2.84)$$

which is the effective action for the layer $l = 1$. We then sum the results over $l = 1, 2$, as in (2.81), to get the full low energy response of the lattice model, keeping in mind that $\alpha_1 + \alpha_2 = \frac{\nu/2}{96\pi} \in \frac{1}{192\pi}\mathbb{Z}$.

2.5.4.1 Bulk response from gravitational Chern-Simons terms For the purpose of calculating the contribution of gCS to the bulk energy-momentum tensor it is easier to use $Q_3(\tilde{\Gamma})$ instead of $Q_3(\tilde{\omega})$. The result is [22, 115, 25]

$$\langle J_a^\mu \rangle_{\text{gCS}} = \frac{1}{|e|} \frac{\delta}{\delta e_\mu^a} \left[\alpha_1 \int_{M_3} Q_3(\tilde{\Gamma}) \right] = 4\alpha_1 \tilde{C}_a^\mu, \quad (2.85)$$

where \tilde{C} is the Cotton tensor, which can be written as

$$\tilde{C}^{\mu\nu} = -\frac{1}{\sqrt{g}} \varepsilon^{\rho\sigma(\mu} \tilde{\nabla}_\rho \tilde{\mathcal{R}}_{\sigma}^{\nu)}. \quad (2.86)$$

Relevant properties of the Cotton tensor are $\tilde{\nabla}_\mu \tilde{C}^{\mu\nu} = 0$, $\tilde{C}_\mu^\mu = 0$, and $C^{[\mu\nu]} = 0$. It follows from (2.85) that

$$\langle t_{\text{cov } \nu}^\mu \rangle_{\text{gCS}} = -|e| \langle J_\nu^\mu \rangle_{\text{gCS}} = -4\alpha_1 |e| \tilde{C}_\nu^\mu. \quad (2.87)$$

For order parameters of the form

$$\Delta = e^{i\theta} (|\Delta^x|, \pm i |\Delta^y|) \quad (2.88)$$

the metrics for both layers $l = 1, 2$ are identical. Since \tilde{C} only depends on the metric it follows that for such order parameters the summation over $l = 1, 2$ gives

$$\langle t_{\text{cov } \nu}^\mu \rangle_{\text{gCS}} = -|e| \langle J_\nu^\mu \rangle_{\text{gCS}} = -\frac{\nu/2}{96\pi} 4 |e| \tilde{C}_\nu^\mu. \quad (2.89)$$

Put differently, the difference of gCS terms in (2.81), with coefficient α_1 , does not produce a bulk response for such order parameters. This provides a simple way to separate the topological invariant ν from the non quantized α_1 .

The Cotton tensor takes a simpler form if the geometry is a product geometry, where the metric is of the form $ds^2 = g_{\alpha\beta}(x^\alpha) dx^\alpha dx^\beta + \sigma dz^2$. Here $\sigma = \pm 1$ depends on whether z is a space-like or time-like coordinate, and we will use both in the following. The two coordinates x^α are space-like if z is time-like and mixed if z is space-like. In this case the curvature is determined by the curvature scalar, which corresponds to the curvature scalar of the two dimensional metric $g_{\alpha\beta}$. In particular $\mathcal{R}_\beta^\alpha = \frac{1}{2} \mathcal{R} \delta_\beta^\alpha$ and the other components of \mathcal{R}_ν^μ vanish. Then

$$\langle J^{\alpha z} \rangle_{\text{gCS}} = \langle J^{z\alpha} \rangle_{\text{gCS}} = \alpha_1 \frac{1}{|e|} \varepsilon^{z\alpha\beta} \partial_\beta \tilde{\mathcal{R}}, \quad (2.90)$$

and the other components vanish. In terms of $t_{\text{cov } \nu}^\mu$,

$$\begin{aligned}\langle t_{\text{cov } z}^\alpha \rangle_{\text{gCS}} &= -\alpha_1 \sigma \varepsilon^{z\alpha\beta} \partial_\beta \tilde{\mathcal{R}}, \\ \langle t_{\text{cov } \alpha}^z \rangle_{\text{gCS}} &= -\alpha_1 g_{\alpha\beta} \varepsilon^{z\beta\gamma} \partial_\gamma \tilde{\mathcal{R}}.\end{aligned}\tag{2.91}$$

Taking $z = t$ is natural in the context of the p -wave SC, since the emergent metric (2.28) is always a product metric if Δ is time independent. Then, with a general time independent order parameter,

$$\begin{aligned}\langle J_E^i \rangle_{\text{gCS}} &= \langle t_{\text{cov } t}^i \rangle_{\text{gCS}} = -\alpha_1 \varepsilon^{ij} \partial_j \tilde{\mathcal{R}}, \\ \langle P_i \rangle_{\text{gCS}} &= \langle t_{\text{cov } i}^t \rangle_{\text{gCS}} = -\alpha_1 g_{ik} \varepsilon^{kj} \partial_j \tilde{\mathcal{R}},\end{aligned}\tag{2.92}$$

where $\tilde{\mathcal{R}}$ is the curvature associated with the spatial metric $g^{ij} = -\Delta^{(i} \Delta^{j)*}$. Again, for order parameters of the form (2.88) the metrics for both layers $l = 1, 2$ are identical, and the summation over $l = 1, 2$ produces

$$\begin{aligned}\langle J_E^i \rangle_{\text{gCS}} &= -\frac{\nu/2}{96\pi} \varepsilon^{ij} \partial_j \tilde{\mathcal{R}}, \\ \langle P_i \rangle_{\text{gCS}} &= -\frac{\nu/2}{96\pi} g_{ik} \varepsilon^{kj} \partial_j \tilde{\mathcal{R}}.\end{aligned}\tag{2.93}$$

These are the topological bulk responses described in section 2.1.2. It is also usefull to consider order parameters of the form

$$\Delta = \Delta_0 e^{i\theta} (1, e^{i\phi}),\tag{2.94}$$

where ϕ is space dependent. Here the metrics satisfy $g^{xy} = g_{(1)}^{xy} = -g_{(2)}^{xy} = \Delta_0^2 \cos \phi$, with the other components constant, and therefore the Ricci scalars satisfy $\mathcal{R} = \mathcal{R}_{(1)} = -\mathcal{R}_{(2)}$. The summation over $l = 1, 2$ for such order parameters then gives

$$\langle J_E^i \rangle_{\text{gCS}} = -(\alpha_1 - \alpha_2) \varepsilon^{ij} \partial_j \tilde{\mathcal{R}}.\tag{2.95}$$

Unlike the sum $\alpha_1 + \alpha_2 = \frac{\nu/2}{96\pi}$, the difference $\alpha_1 - \alpha_2 = 2\alpha_1 - \frac{\nu/2}{96\pi}$ is not quantized. The response (2.95) is therefore not a topological bulk response. Measuring $\langle J_E \rangle$ for an order parameter such that $\mathcal{R} = \mathcal{R}_{(1)} = \mathcal{R}_{(2)}$, and then for an order parameter such that $\mathcal{R} = \mathcal{R}_{(1)} = -\mathcal{R}_{(2)}$, allows one to fix both α_1, α_2 , or both ν and α_1 .

To demonstrate how closely (2.95) can resemble a topological bulk response, we go back to the lattice model. In the relativistic limit we found that some trivial phases, where $\nu = 0$, have $\alpha_1 = \frac{\nu_1/2}{192\pi} \neq 0$. It follows that these trivial phases have *in the relativistic limit* a quantized response

$$\langle J_E^i \rangle_{\text{gCS}} = -2\alpha_1 \varepsilon^{ij} \partial_j \tilde{\mathcal{R}} = -\frac{\nu_1}{96\pi} \varepsilon^{ij} \partial_j \tilde{\mathcal{R}},\tag{2.96}$$

for order parameters $\Delta = \Delta_0 e^{i\theta} (1, e^{i\phi})$.

Another case of interest is when z is a spatial coordinate. As an example, we take $z = y$. This decomposition is less natural in the p -wave SC, as can be seen from (2.28). It allows for time dependence, but restricts the configuration the order parameter can take at any given time. A simple example for an order parameter that gives rise to a product metric with respect to y is $\Delta = \Delta_0 e^{i\theta(t,x)} (1 + f(t,x), \pm i)$, which is a perturbation of the $p_x \pm ip_y$ configuration with a small real function f . Then

$$\langle t_{\text{cov } \alpha}^y \rangle_{\text{gCS}} = -\frac{\nu/2}{96\pi} g_{\alpha\beta} \varepsilon^{\beta\gamma y} \partial_\gamma \tilde{\mathcal{R}}, \quad (2.97)$$

where we have summed over $l = 1, 2$. This is an interesting contribution to the x -momentum current and energy current in the y direction. If we consider, as in Fig. 3, a boundary or domain wall at $y = 0$, between a topological phase and a trivial phase where $\nu = 0$, we see that there is an inflow of energy and x -momentum into the boundary from the topological phase. This shows that energy and x -momentum are accumulated on the boundary, at least locally, which corresponds to the boundary gravitational anomaly. We complete the analysis of this situation from the boundary point of view in Appendix A.3.

2.5.4.2 Bulk response from the gravitational pseudo Chern-Simons term The gpCS term $-\beta_1 \int_{M_3} \tilde{\mathcal{R}} e^a D e_a$ contributes to the energy-momentum tensor, and also provides a contribution to the spin density,

$$\begin{aligned} \langle J^{\mu\nu} \rangle_{\text{gpCS}} &= \beta_1 \left\{ \frac{1}{|e|} \varepsilon^{\mu\nu\rho} \partial_\rho \tilde{\mathcal{R}} - \frac{1}{|e|} \varepsilon^{\mu\rho\sigma} \tilde{\mathcal{R}} T_{\rho\sigma}^\nu + 2o \left[\left(\tilde{\nabla}^\mu \tilde{\nabla}^\nu - g^{\mu\nu} \tilde{\nabla}^2 \right) - \tilde{\mathcal{R}}^{\mu\nu} \right] c \right\}. \\ \langle J^{ab\mu} \rangle_{\text{gpCS}} &= \beta_1 o \tilde{\mathcal{R}} \varepsilon^{abc} e_c^\mu \end{aligned} \quad (2.98)$$

These are calculated in appendix D.

Using (2.66), the above contribution to the spin density corresponds to a contribution to the charge density,

$$\langle J^t \rangle_{\text{gpCS}} = 4\beta_1 o |e| \tilde{\mathcal{R}}. \quad (2.99)$$

The most notable feature of this density is that it is not accompanied by a current, even for time dependent background fields, where $\partial_\mu \langle J^\mu \rangle = \partial_t \langle J^t \rangle \neq 0$. This represents the non conservation of fermionic charge in a p -wave SC (2.31). The appearance of o can be understood from (2.69). One can also understand the appearance of o based on time reversal symmetry. Since both J^t and $\tilde{\mathcal{R}}$ are time reversal even, the coefficient of the above response cannot be β_1 , which is time reversal odd.

We now discuss the energy-momentum contributions $\langle J^{\mu\nu} \rangle_{\text{gpCS}}$ in (2.98), with the purpose of comparing them to the gCS contributions $\langle J^{\mu\nu} \rangle_{\text{gCS}}$. To do this in the simplest setting, we restrict to a product geometry with respect to the coordinate z as described in the previous section. We will also assume for simplicity that torsion vanishes, and generalize to non-zero torsion in appendix D. For a torsion-less

product geometry $\langle J^{\mu\nu} \rangle_{\text{gpCS}}$ reduces to

$$-\langle J^{\alpha z} \rangle_{\text{gpCS}} = \langle J^{z\alpha} \rangle_{\text{gpCS}} = \beta_1 \frac{1}{|e|} \varepsilon^{z\alpha\beta} \partial_\beta \tilde{\mathcal{R}}. \quad (2.100)$$

Note that while the gpCS term vanishes in a torsion-less geometry, the currents it produces, given by its functional derivatives, do not. Comparing with (2.90), we see that $\langle J^{z\alpha} \rangle_{\text{gpCS}} \propto \langle J^{z\alpha} \rangle_{\text{gCS}}$, while $\langle J^{\alpha z} \rangle_{\text{gpCS}} \propto -\langle J^{\alpha z} \rangle_{\text{gCS}}$, with the proportionality constant α_1/β_1 , that goes to 1 in the relativistic limit. This demonstrates the similarity between the gpCS and gCS terms.

In particular, we find in a time independent situation the following contributions to the energy current and momentum density,

$$\begin{aligned} \langle J_E^i \rangle_{\text{gpCS}} &= \langle t_{\text{cov } t}^i \rangle_{\text{gpCS}} = \beta_1 \varepsilon^{ij} \partial_j \tilde{\mathcal{R}}, \\ \langle P_i \rangle_{\text{gpCS}} &= \langle t_{\text{cov } i}^t \rangle_{\text{gpCS}} = -\beta_1 g_{ik} \varepsilon^{kj} \partial_j \tilde{\mathcal{R}}. \end{aligned} \quad (2.101)$$

Comparing with (2.92), we see that $\langle P_i \rangle_{\text{gpCS}} \propto \langle P_i \rangle_{\text{gCS}}$, while $\langle J_E^i \rangle_{\text{gpCS}} \propto -\langle J_E^i \rangle_{\text{gCS}}$. This sign difference can be understood from the density response (2.99), and the relation (2.48) between the operators J_E and P , in the relativistic limit. With vanishing torsion it reduces to

$$J_E^j - g^{jk} P_k = \frac{o}{2} \varepsilon^{jk} \partial_k \left(\frac{1}{|e|} J^t \right). \quad (2.102)$$

Thus the gCS contributions (2.92) satisfy $\langle J_E^j \rangle_{\text{gCS}} - g^{jk} \langle P_k \rangle_{\text{gCS}} = 0$ because gCS does not contribute to the density. On the other hand, the gpCS does contribute to the density, which is why $\langle J_E^j \rangle_{\text{gpCS}} - g^{jk} \langle P_k \rangle_{\text{gpCS}} \neq 0$. This conclusion holds regardless of the value of the coefficient β_1 of gpCS. One can therefore fix the value of β_1 by a measurement of the density, and thus separate the topological bulk responses (gCS) from the non-topological bulk responses (gpCS).

More accurately, we have seen that the lattice model behaves as a bi-layer with layer index $l = 1, 2$, and there are actually two coefficients β_1, β_2 . As in the previous section, one can extract both β_1, β_2 by first considering an order parameter (2.88) such that $\mathcal{R} = \mathcal{R}_{(1)} = \mathcal{R}_{(2)}$, and then considering an order parameter (2.94) such that $\mathcal{R} = \mathcal{R}_{(1)} = -\mathcal{R}_{(2)}$.

Another case of interest is when z is a spatial coordinate, and as in the previous section we take $z = y$, $\Delta = \Delta_0 e^{i\theta(t,x)} (1 + f(t, x), \pm i)$. We then find from (2.100), $\langle J^{y\alpha} \rangle_{\text{gpCS}} = \beta_1 \frac{1}{|e|} \varepsilon^{z\alpha\beta} \partial_\beta \tilde{\mathcal{R}}$, or

$$\langle t_{\text{cov } \alpha}^y \rangle_{\text{gpCS}} = -\beta_1 g_{\alpha\beta} \varepsilon^{\beta\gamma y} \partial_\gamma \tilde{\mathcal{R}}. \quad (2.103)$$

In the presence of a boundary (or domain wall) at $y = 0$, this describes an inflow of energy and x -momentum from the bulk to the boundary, such that $\langle t_{\text{cov } \alpha}^y \rangle_{\text{gpCS}} \propto \langle t_{\text{cov } \alpha}^y \rangle_{\text{gCS}}$. After summing over $l = 1, 2$ one finds the proportionality constant $\frac{\alpha_1 + \alpha_2}{\beta_1 + \beta_2}$, that goes to 1 in the relativistic limit. Nevertheless, we argue that $\langle t_{\text{cov } \alpha}^y \rangle_{\text{gCS}}$ corresponds to a boundary gravitational anomaly while $\langle t_{\text{cov } \alpha}^y \rangle_{\text{gpCS}}$ does not, in accordance with section 2.5.3.2. The relation between gCS and the boundary gravitational anomaly

is well known within the gravitational description, and is described from the p -wave SC point of view in Appendix A.3. The fact that $\langle t_{\text{cov } \alpha}^y \rangle_{\text{gpCS}}$ is unrelated to any boundary anomaly follows from the fact that it is $SO(1,2)$ and $Diff$ invariant. Due to this invariance the bulk gpCS term produces not only the bulk currents (2.98), but also boundary currents, such that bulk+boundary energy-momentum is conserved. In a product geometry with $z = y$ we find the boundary currents

$$\begin{aligned}\langle j^{\alpha\beta} \rangle_{\text{gpCS}} &= -\beta_1 \frac{1}{|e|} \varepsilon^{\alpha\beta y} \tilde{\mathcal{R}}, \\ \langle j^{ab\mu} \rangle_{\text{gpCS}} &= 0,\end{aligned}\tag{2.104}$$

which are calculated in appendix D. We see that

$$\tilde{\nabla}_\alpha \langle j^{\alpha\beta} \rangle_{\text{gpCS}} = \langle J^{y\beta} \rangle_{\text{gpCS}}.\tag{2.105}$$

This conservation law is the statement of bulk+boundary conservation of energy-momentum within the gravitational description. It can be understood from (2.60), by noting that the source terms in (2.60) vanish because $\langle j^{ab\mu} \rangle_{\text{gpCS}} = 0$, and because we assumed torsion vanishes. The additional source term $\langle J^{y\beta} \rangle_{\text{gpCS}}$, absent in (2.60), represents the inflow from the bulk. In Appendix A.3 we translate (2.105) to the language of the p -wave SC.

2.6 Discussion

Beyond the relativistic limit In this section we have shown that there is a topological bulk response of p -wave CSF/Cs to a perturbation of their order parameter, which follows from a gCS term, and we described a corresponding gravitational anomaly of the edge states. The coefficient of gCS was found to be $\alpha = \frac{c}{96\pi}$ where c is the chiral central charge, as anticipated. We provided arguments, based on symmetry and topology, for the validity of these results beyond the relativistic limit in which they were computed. The appearance of torsion in the emergent geometry brought about a surprise: an additional term, closely related but distinct from gCS, which we referred to as gravitational pseudo Chern-Simons (gpCS), with a dimensionless coefficient $\beta = \frac{c}{96\pi} = \alpha$. The gpCS term is completely invariant under the symmetries we considered, and is therefore unrelated to edge anomalies. Therefore, the quantization of β seems to be a property of the relativistic limit²⁵, which will not hold throughout the phase diagram.

The above results are based on a careful mapping of p -wave CSF/Cs, in the regime where the order parameter is large, to relativistic Majorana spinors in a curved and torsion-full space-time. Though the relativistic limit captures a rich geometric physics in CSF/Cs, it is in fact very limited in its ability to describe the full non-relativistic system, as discussed in Appendix 2.2.4. This raises the question of whether the results obtained in this section truly characterize p -wave CSF/Cs, especially in the physically important weak coupling limit where Δ is small, which is opposite to the relativistic limit.

²⁵The quantization of β can be understood on dimensional grounds - in the relativistic limit there are simply not enough dimension-full quantities which can be used to construct dimensionless quantities, beyond $\text{sgn}(m)$ and o . Of course, this does not explain why $\beta = \alpha$ in the relativistic limit.

Moreover, it is natural to ask whether the results obtained here apply to ℓ -wave CSF/Cs with $|\ell| > 1$, which do not admit a relativistic low energy description. These questions will be answered, in part, in Sec.3, where we perform a general non-relativistic analysis of continuum models for ℓ -wave CSF/Cs. In order to address these questions in the context of lattice models, numerical studies seem to be required. Recently, such studies were initiated in the context of emergent gravity in Kitaev's honeycomb model [171, 172], which is closely related to the p -wave CSF/Cs discussed in this section. For non-topological physical properties, the results show that the lattice model is well described by relativistic predictions, but only in the relativistic regime, where the masses of low energy relativistic fermions are small and the correlation length is large, as might be expected. An interesting question is whether the topological physics associated with the gCS term is more robustly captured by the relativistic predictions made in this section.

Real background geometry and manipulation of the order parameter In this section we considered p -wave CSF/Cs in flat space, and focused on the emergent geometry described by a general p -wave order parameter. It is also natural to consider the effect of a real background geometry, obtained by deforming, or straining, the 2-dimensional sample in 3-dimensional space, possibly in a time dependent manner. Treating this at the level of the lattice model is beyond the scope of this thesis, but we can take the non-relativistic action (2.1) as a starting point. On a general deformed sample it generalizes to

$$S[\psi; \Delta, A, G] = \int d^{2+1}x \sqrt{G} \left[\psi^\dagger \frac{i}{2} \overleftrightarrow{D}_t \psi - \frac{1}{2m^*} G^{ij} D_i \psi^\dagger D_j \psi + \left(\frac{1}{2} \Delta^j \psi^\dagger \partial_j \psi + h.c \right) \right], \quad (2.106)$$

which now depends on three background fields: the order parameter Δ^j , the $U(1)$ connection A_μ , which enters $D_\mu = \partial_\mu - iA_\mu$, and includes a chemical potential, and the real background metric G , coming from the embedding of the 2-dimensional sample in 3-dimensional space, which corresponds to the strain tensor $u^{ij} = (G^{ij} - \delta^{ij})/2$. This action is written for the fermion ψ , which satisfies $\{\psi^\dagger(x), \psi(y)\} = \delta^{(2)}(x-y)/\sqrt{G(x)}$ as an operator. In this problem there are two (inverse) metrics, the real G^{ij} and emergent $g^{ij} = \Delta^{(i} \Delta^{j)*}$, and it is interesting to study their interplay. In our analysis we focused on the relativistic limit, where $m^* \rightarrow \infty$. In this limit the metric G completely decouples from the action, when written in terms of the fundamental fermion density $\tilde{\psi} = G^{1/4} \psi$ [242, 243, 34]. Thus, results obtained within the relativistic limit, are essentially unaffected by the background metric G . This conclusion is appropriate as long as the order parameter is treated as an independent background field, which is always suitable for the purpose of integrating out the gapped fermion density ψ . One then obtains the bulk currents and densities that we have described, which depend on the configuration of Δ , and the question that remains is what this configuration physically is. Two scenarios are of importance.

The first scenario is that of a proximity induced CSC, where the order parameter is induced by proximity to a conventional s -wave SC. In this case both G and g are background metrics, a scenario similar to a bi-metric description of anisotropic quantum Hall states [46]. In this case the magnitude of the order parameter depends on the distance between the sample and the s -wave SC, so if the position of the s -wave SC is fixed but the sample is deformed, a space-time dependent order parameter is obtained.

One can also obtain the same effect by considering a flat sample, where G is euclidian, and an s -wave SC with a curved surface, leading to non-Euclidian g . This provides one route to a manipulation of the order parameter that will result in the bulk effects we have described.

The second scenario is that of intrinsic CSCs, and CSFs, where the order parameter is dynamical. The order parameter splits into a massive Higgs field, which is the emergent metric g^{ij} , and a massless Goldstone field which is the overall phase θ . The quantum theory of the emergent metric g^{ij} is on its own an interesting problem, which will be discussed in Sec.5. Nevertheless, as long as the probes A, G are slow compared to the Higgs mass, g^{ij} can be treated as fixed to its instantaneous ground state configuration, which in general will depend on the details of the attractive fermionic interaction. For an interaction that depends only on the geodesic distance, the ground state configuration is expected to be the curved space $p_x \pm ip_y$ configuration, where the pairing term is $\Delta_0 e^{i\theta} \psi^\dagger (E_1^j \partial_j \pm i E_2^j \partial_j) \psi^\dagger$, see Appendix J and Refs.[15, 163, 164, 238, 240]. Here Δ_0 is a constant, θ is the Goldstone phase, and E is a vielbein for the real metric G , such that $G^{ij} = E_A^i \delta^{AB} E_B^j$, which is a fixed background field²⁶. What this means, in the language of this section, is that the emergent metric is proportional to the real metric, $g^{ij} = \Delta_0^2 G^{ij}$. It follows that the responses to the emergent metric g that we have described are, in this case, responses to the real metric G . This suggests a second route to the manipulation of the order parameter that will result in the bulk effects we have described.

Of course, in the intrinsic case one cannot ignore the dynamics of the Goldstone phase θ , which will be gapless as long as A is treated as a background field, as appropriate in CSFs. It is then interesting to see how the results obtained in this section are modified by the dynamics of θ . The interplay between the topological gCS term and the θ -dependent gpCS term suggests a non-trivial modification, which will be explored in Sec.3.

Towards experimental observation There are a few basic questions that arise when trying to make contact between the phenomena described in this section and a possible experimental observation. Here we take as granted that one has at one's disposal either a p -wave CSF/C, or a candidate material. The first question is how to manipulate the Higgs part of the order parameter, which is the emergent metric, and was discussed above.

The second natural question is how to measure energy currents and momentum densities. Also relevant, though not accentuated in this section, is a measurement of the stress tensor, comprised of the spatial components of the energy-momentum tensor. One possible approach, which provides both a means to manipulate the order parameter, and a measurement of energy-momentum-stress is a measurement of the phonon spectrum à la [244–246]. For the gpCS term, apart from energy-momentum-stress, there is also the density response (2.8), which is a simpler quantity for measurement, though not a *topological* bulk response. A possible way to avoid the need to measure energy-momentum-stress may be possible in a Galilean invariant system, where electric current and momentum density are closely related. The simplest scenario is that of a p -wave CSF on a curved sample (2.106), where one assumes that the emergent metric follows the real metric, $g^{ij} = \Delta_0^2 G^{ij}$. Here the electric current is related to the

²⁶The $SO(2)_L$ ambiguity in choosing E can be incorporated into θ , which has $SO(2)_L$ charge 1

momentum density by

$$J^i = -\frac{G^{ij}}{m^*} P_j. \quad (2.107)$$

Our result (2.5) then implies that the expectation value $\langle J^i \rangle$ has a contribution related to the gCS term,

$$\langle J^i \rangle_{\text{gCS}} = -\frac{G^{ij}}{m^*} \langle P_j \rangle_{\text{gCS}} = \frac{1}{m^*} \frac{c}{96\pi} \hbar \varepsilon^{ij} \partial_j \tilde{\mathcal{R}}.$$

This is not a topological response per se, due to the appearance of m^* . But, if m^* is known, then the central charge c can be extracted from a measurement of the electric current, which may be simpler to measure than energy-momentum-stress. This motivates the study of Galilean invariant CSFs, which will be pursued in Sec.3.

Hall viscosity and torsional Hall viscosity In the effective action (2.67) for a Majorana spinor in Riemann-Cartan space-time, there is a term $(\zeta_H/2) \int e_a D e^a$, which describes an energy-momentum-stress response termed *torsional Hall viscosity* [155–157], due to its similarities with the odd (or Hall) viscosity η_o that occurs in quantum Hall states and CSF/Cs [116, 247, 34, 163, 164]. As opposed to the well understood η_o , the torsional Hall viscosity ζ_H remains somewhat controversial [158, 160, 41], because it only appears if a non-symmetric stress tensor is used, and because it is UV-sensitive. The latter is also the reason that, in this section, we avoided from interpreting ζ_H in the context of p -wave CSF/Cs. However, the mapping between p -wave CSF/Cs and relativistic Majorana spinors in Riemann-Cartan space-time developed in this section, along with the existence of a Hall viscosity on one side of the mapping, and of a torsional Hall viscosity on the other, strongly suggests that the two types of Hall viscosity should map to one another, in this context. Moreover, it is known that the gCS term implies universal corrections to η_o at non-zero wave-vector or in curved background [34, 42, 43], and that the gpCS term implies curvature corrections to ζ_H [156], which we expect to be non-universal. These observations provide us with a strong motivation to study the interplay between torsional Hall viscosity, Hall viscosity, and chiral central charge in CSFs, which we do in Sec.3.

3 Boundary central charge from bulk odd viscosity: chiral superfluids

As discussed in Sec.2.6, our analysis of CSF/Cs within the relativistic limit raises many questions which require a fully non-relativistic treatment. These questions revolve around the quantization of coefficients, application of strain (or a background metric), odd viscosity, dynamics of the Goldstone mode, and Galilean symmetry, and will be addressed in this section. In particular, we will answer the questions posed in Sec.1.5, by deriving a low energy effective field theory that consistently captures both the chiral Goldstone mode implied the symmetry breaking pattern (1.2), and the gCS term discussed in Sec.2. This theory unifies and extends the seemingly unrelated analysis of Refs.[199, 163, 164] and Sec.2.

3.1 Building blocks for the effective field theory

In order to probe a CSF, we minimally couple it to two background fields - a time-dependent spatial metric G_{ij} , which we use to apply strain $u_{ij} = (G_{ij} - \delta_{ij})/2$ and strain-rate $\partial_t u_{ij}$, and a $U(1)_N$ -gauge field $A_\mu = (A_t, A_i)$, where we absorb a chemical potential $A_t = -\mu + \dots$. The microscopic action S is then invariant under $U(1)_N$ gauge transformations, implying the number conservation $\partial_\mu(\sqrt{G}J^\mu) = 0$, where $\sqrt{G}J^\mu = -\delta S/\delta A_\mu$. It is also clear that S is invariant under *spatial* diffeomorphisms generated by $\delta x^i = \xi^i(\mathbf{x})$, if G_{ij} transforms as a tensor and A_μ as a 1-form. Less obvious is the fact that a Galilean invariant fluid is additionally symmetric under $\delta x^i = \xi^i(t, \mathbf{x})$, provided one adds to the transformation rule of A_i a non-standard piece that depends on the non-relativistic mass m [199, 248, 163, 35, 249–252],

$$\delta A_i = -\xi^k \partial_k A_i - A_k \partial_i \xi^k + m G_{ij} \partial_t \xi^j. \quad (3.1)$$

We refer to $\delta x^i = \xi^i(\mathbf{x}, t)$ as *local Galilean symmetry* (LGS), as it can be viewed as a local version of the Galilean transformation $\delta x^i = v^i t$. The LGS implies the momentum conservation law²⁷

$$\frac{1}{\sqrt{G}} \partial_t (\sqrt{G} m J^i) + \nabla_j T^{ji} = n E_i + \varepsilon^{ij} J_j B, \quad (3.2)$$

where $\sqrt{G} T^{ij} = 2\delta S/\delta G^{ij}$ is the stress tensor and the right hand side is the Lorentz force. This identifies the momentum density $P^i = m J^i$ - a familiar Galilean relation.

Since CSFs spontaneously break the rotation symmetry in flat space, in order to describe them in curved, or strained, space, it is necessary to introduce a background vielbein. This is a field E_j^A valued in $GL(2)$, such that $G_{ij} = E_i^A \delta_{AB} E_j^B$, where $A, B \in \{1, 2\}$. For a given metric G the vielbein E is not unique - there is an internal $O(2)_{P,L} = \mathbb{Z}_{2,P} \ltimes SO(2)_L$ ambiguity, or symmetry, acting by $E_j^A \mapsto O_B^A E_j^B$,

²⁷We use the notation $\varepsilon^{\mu\nu\rho}$ for the totally anti-symmetric (pseudo) tensor, normalized such that $\varepsilon^{xyt} = 1/\sqrt{G}$, as well as $\varepsilon^{ij} = \varepsilon^{ij t}$.

$O \in O(2)_{P,L}$. The generators L, P correspond to *internal* spatial rotations and reflections, and are analogs of angular momentum and spatial reflection (parity), acting on the tangent space rather than on space itself. The inverse vielbein E_B^j is defined by $E_j^A E_B^j = \delta_B^A$.

The charge $N + (\ell/2)L$ of the Goldstone field θ implies the covariant derivative

$$\nabla_\mu \theta = \partial_\mu \theta - A_\mu - s_\theta \omega_\mu, \quad (3.3)$$

with a *geometric spin* $s_\theta = \ell/2$. Here ω_μ is the non-relativistic spin connection, an $SO(2)_L$ -gauge field which is E_j^A -compatible, see Appendix F. So far we assumed that the microscopic fermion ψ does not carry a geometric spin, $s_\psi = 0$, which defines the physical system of interest, see Fig.6(a). It will be useful, however, to generalize to $s_\psi \in (1/2)\mathbb{Z}$. A non-zero s_ψ changes the SSB pattern (1.2), by modifying the geometric spin of the Goldstone field to $s_\theta = s_\psi + \ell/2$ and the unbroken generator to $L - s_\theta N$. In the special case $s_\psi = -\ell/2$ the Cooper pair is geometrically spin-less and L is unbroken, as in an s -wave SF, see Fig.6(b). This $s_\theta = 0$ CSF is, however, distinct from a conventional s -wave SF, because P and T are still broken down to PT , and we therefore refer to it as a *geometric s -wave* (gs-wave) CSF, to distinguish the two. In particular, a central charge $c \neq 0$, which is P, T -odd, is not forbidden by symmetry, and is in fact independent of s_ψ . This makes the gs-wave CSF particularly useful for our purposes.

We note that ω_μ transforms as a 1-form under LGS only if $B/2m$ is added to ω_t [163, 164], which we do implicitly throughout. For ψ , this is equivalent to adding a g-factor $g_\psi = 2s_\psi$ [250].

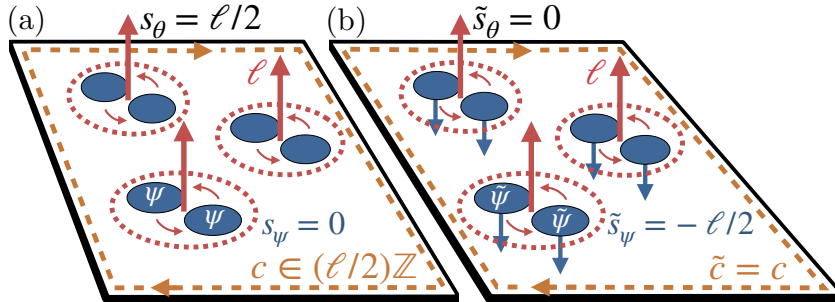


Figure 6: (a) A CSF is comprised of fermions ψ which carry no *geometric spin*, $s_\psi = 0$, which form Cooper pairs with relative angular momentum $\ell \in \mathbb{Z}$ (red arrows). The geometric spin $s_\theta = \ell/2$ of the Cooper pair gives rise to the $\mathbf{q} = \mathbf{0}$ odd viscosity (1.3), with $s = s_\theta$. The CSF supports boundary degrees of freedom (dashed orange) with a chiral central charge $c \in (\ell/2)\mathbb{Z}$, which cannot be extracted from the odd viscosity $\eta_o(\mathbf{q})$ alone (3.13). (b) In an auxiliary CSF the fermion $\tilde{\psi}$ is assigned a geometric spin $\tilde{s}_\psi = -\ell/2$ (blue arrows). The geometric spin of the Cooper pair therefore vanishes, $\tilde{s}_\theta = \ell/2 + \tilde{s}_\psi = 0$, as in an s -wave superfluid, but the central charge is unchanged, $\tilde{c} = c$. As a result, the small \mathbf{q} behavior of the odd viscosity $\tilde{\eta}_o(\mathbf{q})$ depends only on c (3.14). The improved odd viscosity of the CSF is defined as the odd viscosity of the auxiliary CSF, and is given explicitly by (3.17).

3.2 Effective field theory

Based on the above characterization of CSFs, the low energy, long wave-length, behavior of the system can be captured by an effective action $S_{\text{eff}}[\theta; A, G; \ell, c]$, formally obtained by integrating out all massive degrees of freedom - the single fermion excitations and the Higgs fields. In this Section we describe a general expression for S_{eff} , compatible with the symmetries, SSB pattern, and ground state topology of CSFs.

The effective action can be written order by order in a derivative expansion, with the power counting scheme $\partial_\mu = O(p)$, $A_\mu, G_{ij} = O(1)$, $\theta = O(p^{-1})$ [199, 163]. The spin connection is a functional of G_{ij} that involves a single derivative (see Appendix F), so $\omega_\mu = O(p)$. Denoting by \mathcal{L}_n the term in the Lagrangian which is $O(p^n)$ and invariant under all symmetries, we have $S_{\text{eff}} = \sum_{n=0}^{\infty} \int d^2x dt \sqrt{G} \mathcal{L}_n$. The desired q^2 corrections to η_0 are $O(p^3)$, which poses the main technical difficulty.

The leading order Lagrangian

$$\mathcal{L}_0 = P(X), \quad X = \nabla_t \theta - \frac{1}{2m} G^{ij} \nabla_i \theta \nabla_j \theta, \quad (3.4)$$

was studied in detail in [163], and contains the earlier results of [192–195, 153, 196, 197]. Here X is the unique $O(1)$ scalar, which reduces to the chemical potential μ in the ground state(s) $\partial_\mu \theta = 0$, and P is an arbitrary function of X that physically corresponds to the ground state pressure $P_0 = P(\mu)$. The function P also determines the ground state density $n_0 = P'(\mu)$, and the leading dispersion of the Goldstone mode $\omega^2 = c_s^2 q^2$, where $c_s^2 = \partial_{n_0} P_0 / m = P'(\mu) / P''(\mu) m$ is the speed of sound. For $\ell \neq 0$, the spin connection appears in each $\nabla \theta$, see Eq.(3.3), and so \mathcal{L}_0 includes $O(p)$ contributions, which produce the leading odd viscosity and conductivity, discussed below. There are no additional terms at $O(p)$, so that $\mathcal{L}_1 = 0$ [163].

At $O(p^2)$ one has

$$\mathcal{L}_2 = F_1(X) R + F_2(X) [m K_i^i - \nabla^2 \theta]^2 + F_3(X) [2m (\nabla_i K_j^j - \nabla^j K_{ji}) \nabla^i \theta] + \dots, \quad (3.5)$$

where $K_{ij} = \partial_t G_{ij} / 2$ and R are the extrinsic curvature and Ricci scalar of the spatial slice at time t [229], the F s are arbitrary functions of X , and dots indicate additional terms which do not contribute to η_0 up to $O(p^2)$, see Appendix H.2 for the full expression. The Lagrangian \mathcal{L}_2 was obtained in [199] for s -wave SFs. For $\ell \neq 0$ the spin connection in $\nabla \theta$ produces $O(p^3)$ contributions to \mathcal{L}_2 , and, in turn, non-universal q^2 corrections to η_0 .

The term \mathcal{L}_3 is the last ingredient required for reliable results at $O(p^3)$. Most importantly, it includes the non-relativistic gCS term [42, 44], $\mathcal{L}_3 = \mathcal{L}_{\text{gCS}} + \dots$, where

$$\mathcal{L}_{\text{gCS}} = -\frac{c}{48\pi} \omega d\omega. \quad (3.6)$$

Here $\omega d\omega = \varepsilon^{\mu\nu\rho} \omega_\mu \partial_\nu \omega_\rho$, and c is the chiral central charge of the boundary degrees of freedom, as required to match the boundary gravitational anomaly [23, 25, 1]. Unlike the lower order terms, \mathcal{L}_{gCS} is

independent of θ , and encodes only the response of the fermionic topological phase to the background metric. The direct confirmation of (3.6) within a non-relativistic microscopic model has been anticipated for some time [28, 15], and is a main result of Appendix J. In Appendices G.5 and H.4 we argue that additional terms in \mathcal{L}_3 do not produce q^2 corrections to η_o .

There are three symmetry-allowed topological terms that can be added to S_{eff} [253, 254, 34, 35, 39, 255, 43, 42, 256, 47, 52]. These are the $U(1)$ Chern-Simons (CS) and first and second Wen-Zee (WZ1, WZ2) terms, which can be added to \mathcal{L}_1 , \mathcal{L}_2 , \mathcal{L}_3 , respectively ²⁸,

$$\frac{\nu}{4\pi} \left(\text{Ad}A - 2\bar{s}\omega dA + \bar{s}^2\omega d\omega \right). \quad (3.7)$$

As our notation suggests, WZ2 and gCS are identical for the purpose of local bulk responses, of interest here, but the two are globally distinct [42, 44, 52]. Based on symmetry, and ignoring boundary physics, the independent coefficients ν , $\nu\bar{s}$, and $\nu\bar{s}^2$ obey certain quantization conditions [24], but are otherwise unconstrained. The absence of a boundary $U(1)_N$ -anomaly then fixes $\nu = 0$ [1], but leaves $\nu\bar{s}$, $\nu\bar{s}^2$ undetermined [42, 44, 52]. One can argue that a Chern-Simons term can only appear for the unbroken generator $L - s_\theta N$, so that $\nu = 0$ implies $\nu\bar{s} = \nu\bar{s}^2 = 0$. Moreover, in the following section we will see that a perturbative computation within a canonical model for $\ell = \pm 1$ shows that $\nu\bar{s} = \nu\bar{s}^2 = 0$, which applies to any deformation of the model (which preserves the symmetries, SSB pattern, and single fermion gap), due to the quantization of $\nu\bar{s}$, $\nu\bar{s}^2$. Accordingly, we set $\nu\bar{s} = \nu\bar{s}^2 = 0$ in the following.

3.3 Benchmarking the effective theory against a microscopic model

In this section we take a complementary approach and compute S_{eff} perturbatively, starting from a canonical microscopic model for a p -wave CSF. The perturbative computation verifies the general expression in a particular example, and determines the coefficients of topological terms which are not completely fixed by symmetry. It also gives one a sense of the behavior of the coefficients of non-topological terms as a function of microscopic parameters such as the chemical potential μ and mass m . In particular, the results of Sec.2 are reproduced in the relativistic limit $m \rightarrow \infty$.

Here we will outline the computation and describe its results, omitting many technical details which can be found in Appendix J. The microscopic model is given by

$$S_m = \int d^2x dt \sqrt{G} \left[\frac{i}{2} \psi^\dagger \overleftrightarrow{\nabla}_t \psi - \frac{1}{2m} G^{ij} \nabla_i \psi^\dagger \nabla_j \psi + \left(\frac{1}{2} \Delta^j \psi^\dagger \nabla_j \psi + h.c \right) - \frac{1}{2\lambda} G_{ij} \Delta^{i*} \Delta^j \right], \quad (3.8)$$

where the covariant derivative of the spin-less (or single component) fermion ψ is $\nabla_\mu = \partial_\mu + iA_\mu + is_\psi \omega_\mu$. Note that we allow for a *geometric* spin s_ψ , as discussed in Sec.3.1. Apart from the standard non-relativistic kinetic term, the action includes the simplest attractive two-body interaction [225, 238], mediated by the complex vector Δ^i , the order parameter, with coupling constant $\lambda > 0$. A simplified version of this action was already discussed in Sec.2.6.

²⁸These are not LGS invariant, and would need to be modified along the lines of [248, 249, 251].

For a given Δ^j , the fermion ψ is gapped, unless the chemical potential μ or chirality $\ell = \text{sgn}(\text{Im}(\Delta^x \Delta^{y*}))$ are tuned to 0, and forms a fermionic topological phase characterized by the boundary chiral central charge [15, 27, 107]

$$c = -(\ell/2) \Theta(\mu) \in \{0, \pm 1/2\}. \quad (3.9)$$

An effective action $S_{\text{eff,m}}[\Delta; A, G]$ for Δ^j in the background A_μ, G_{ij} is then obtained by integrating over the fermion. The subscript 'm' indicates that this is obtained from the particular microscopic model S_m . Since Eq.(3.8) is quadratic in ψ, ψ^\dagger , obtaining $S_{\text{eff,m}}$ is formally straight forward, and leads to a functional Pfaffian.

To zeroth order in derivatives $S_{\text{eff,m}}[\Delta; A, G] = -V[\Delta; G]$, where the potential V is minimized by the $p_x \pm ip_y$ order parameter. In flat space this is given by the familiar $\Delta^j \partial_j = \Delta_0 e^{-2i\theta} (\partial_x \pm i\partial_y)$. Here Δ_0 is a fixed function of m, μ and λ , determined by the minimization, while the phase θ and chirality $\ell = \pm 1$ are undetermined. In order to write down the $p_x \pm ip_y$ configuration in curved space it is necessary to use the background vielbein [163, 238]

$$\Delta^j = \Delta_0 e^{-2i\theta} (E_1^j \pm iE_2^j). \quad (3.10)$$

Fluctuations of Δ away from these configurations correspond to massive Higgs modes, which should in principle be integrated out to obtain a low energy action $S_{\text{eff,m}}[\theta; A, G]$ that can be compared with the general S_{eff} of the previous section. We will simply ignore these fluctuations, and obtain $S_{\text{eff,m}}[\theta; A, G]$ by plugging Eq.(3.10) into $S_{\text{eff,m}}[\Delta; A, G]$. This will suffice as a derivation of S_{eff} from a microscopic model. A proper treatment of the massive Higgs modes will only further renormalize the coefficients we find, apart from the central charge c .

To practically compare the actions S_{eff} and $S_{\text{eff,m}}$ we expand them in fields, to second order around $\theta = 0, A_\nu = -\mu \delta_\nu^t, G_{ij} = \delta_{ij}$, and in derivatives, to third order, see appendices H and J.5. Equating these two double expansions leads to an overdetermined system of equations for the phenomenological parameters in S_{eff} in terms of the microscopic parameters in S_m , with a unique solution. In particular, we find the dimensionless parameters

$$\begin{aligned} \frac{P''}{m} &= \frac{1}{2\pi} \begin{Bmatrix} 1 \\ \frac{1}{1+2\kappa} \end{Bmatrix}, & F'_1 &= \frac{1}{96\pi} \begin{Bmatrix} 1 \\ \frac{3}{1+2\kappa} \end{Bmatrix}, & mF_2 &= -\frac{1}{128\pi} \begin{Bmatrix} 1+2\kappa \\ \frac{1}{1+2\kappa} \end{Bmatrix}, \\ mF_3 &= \frac{1}{48\pi} \begin{Bmatrix} 1+\kappa \\ \frac{1}{1+2\kappa} \end{Bmatrix}, & c &= \begin{Bmatrix} -\ell/2 \\ 0 \end{Bmatrix}, \end{aligned} \quad (3.11)$$

where $\kappa = |\mu|/m\Delta_0^2 > 0$, primes denote derivatives with respect to μ , and the cases refer to $\mu > 0$ and $\mu < 0$. We note that for $\mu > 0$ there is a single particle Fermi surface, with energy $\varepsilon_F = \mu$ and wave-vector $k_F = \sqrt{2m\mu}$, which for small λ will acquire an energy gap $\varepsilon_\Delta = \Delta_0 k_F \ll \varepsilon_F$. In this weak-coupling regime, it is natural to parametrize the coefficients in (3.11) using the small parameter

$$\varepsilon_\Delta/\varepsilon_F = \sqrt{2/\kappa}.$$

The coefficient P'' determines the leading odd (or Hall) conductivity and has been computed previously in the literature [192–195, 153, 196, 197, 163, 198], while F_1, F_2 and F_3 , to the best of our knowledge, have not been computed previously, even for an s -wave SF. Crucially, Eq.(3.11) shows that the coefficient c of the bulk gCS term matches the known boundary central charge (3.9), which is a main result of the perturbative computation. It follows that there is no WZ2 term in $S_{\text{eff},m}$, so $\nu\bar{s}^2 = 0$, in accordance with the general discussion of the previous section. We additionally confirm that $\nu = \nu\bar{s} = 0$.

A few additional comments regarding Eq.(3.11) are in order:

1. The seeming quantization of P''/m and F'_1 for $\mu > 0$ is a non-generic result, as was shown explicitly for P''/m [198].
2. The free fermion limit $\kappa \rightarrow \infty$, or $\Delta_0 \rightarrow 0$, of certain coefficients in (3.11) diverges for $\mu > 0$ but not for $\mu < 0$. This signals the breakdown of the gradient expansion for a gapless Fermi surface, but not for gapped free fermions.
3. The opposite limit, $\kappa \rightarrow 0$, or $m \rightarrow \infty$, is the relativistic limit studied in Sec.2, in which the fermionic part of the model reduces to a 2+1 dimensional Majorana spinor with mass μ and speed of light Δ_0 , coupled to a Riemann-Cartan geometry described by Δ^i, A_μ . Accordingly, there is a sense in which the limit $\kappa \rightarrow \infty$ of $S_{\text{eff},m}$ reproduces the effective action of a massive Majorana spinor in Riemann-Cartan space-time (see Sec.2.5). In particular, in the limit $\kappa \rightarrow 0$ the dimensionless coefficients (3.11) are all quantized, as expected based on dimensional analysis. Apart from c , only the coefficient F'_1 is discontinuous at $\mu = 0$ within this limit, with a quantized discontinuity $-(\ell/4)[F'_1(0^+) - F'_1(0^-)] = (\ell/2)/96\pi$ that matches the coefficient β of the *gravitational pseudo Chern-Simons* term of Sec.2. As anticipated in Sec.2, the coefficient c remains quantized away from the relativistic limit, while β , or F'_1 , does not. Finally, we note that our perturbative computation of the gCS term generalizes the computations of Refs.[257–261] and Appendix E for relativistic fermions, and reduces to these as $\kappa \rightarrow 0$.

3.4 Induced action and linear response

By expanding S_{eff} to second order in the fields $\theta, A_t - \mu, A_i, u_{ij}$, and performing Gaussian integration over θ , we obtain an induced action $S_{\text{ind}}[A_\mu, u_{ij}]$ that captures the linear response of CSFs to the background fields, see Appendix I for explicit expressions. Taking functional derivatives one obtains the expectation values $J^\mu = G^{-1/2}\delta S_{\text{ind}}/\delta A_\mu$, $T^{ij} = G^{-1/2}\delta S_{\text{ind}}/\delta u_{ij}$ of the current and stress, and from them the conductivity $\sigma^{ij} = \delta J^i/\delta E_j$, the viscosity $\eta^{ij,kl} = \delta T^{ij}/\delta \partial_t u_{kl}$, and the mixed response function $\kappa^{ij,k} = \delta T^{ij}/\delta E_k = \delta J^k/\delta \partial_t u_{ij}$. We will also need the static susceptibilities $\chi_{JJ}^{\mu,\nu}, \chi_{TJ}^{ij,\nu}$, defined by restricting to time independent A_μ, u_{ij} , and computing $\delta J^\mu/\delta A_\nu$ and $\delta J^\nu/\delta u_{ij}$, respectively.

Before we compute η_o , it is useful to restrict its form based on dimensionality and symmetries: space-time translations and spatial rotations, as well as PT . The analysis is performed in Appendices

G.1-G.4, and results in the expression

$$\eta_o(\omega, \mathbf{q}) = \eta_o^{(1)} \sigma^{xz} + \eta_o^{(2)} [(q_x^2 - q_y^2) \sigma^{0x} - 2q_x q_y \sigma^{0z}], \quad (3.12)$$

which is written in a basis of anti-symmetrized tensor products of the symmetric Pauli matrices, $\sigma^{ab} = 2\sigma^{[a} \otimes \sigma^{b]}$ [174]. As components of the strain tensor, the matrices σ^x, σ^z correspond to shears, while the identity matrix σ^0 corresponds to a dilatation. The details of the system are encoded in two independent coefficients $\eta_o^{(1)}, \eta_o^{(2)} \in \mathbb{C}$, which are themselves arbitrary functions of ω, q^2 . In the case of uniform strain ($\mathbf{q} = \mathbf{0}$), the odd viscosity tensor reduces to a single component, $\eta_o(\omega, \mathbf{0}) = \eta_o^{(1)}(\omega) \sigma^{[x} \otimes \sigma^{z]}$, as is well known [173–175, 160, 176]. The additional component $\eta_o^{(2)}$ has not been discussed much in the literature [34, 262], and also appears in the presence of vector, or pseudo-vector, anisotropy [263, 264], in which case \mathbf{q} should be replaced by a background vector \mathbf{b} . The expression (3.12) applies at finite temperature, out of equilibrium, and in the presence of disorder that preserves the symmetries on average. For clean systems at zero temperature, $\eta_o^{(1)}, \eta_o^{(2)}$ are both real, even functions of ω . In gapped systems $\eta_o^{(1)}, \eta_o^{(2)}$ will usually be regular at $\omega = 0 = q^2$, though an exception to this rule was recently found in Ref.[4].

For the CSF, we find the $\omega = 0$ coefficients

$$\begin{aligned} \eta_o^{(1)}(q^2) &= -\frac{1}{2} s_\theta n_0 - \left(\frac{c}{24} \frac{1}{4\pi} + s_\theta C^{(1)} \right) q^2 + O(q^4), \\ \eta_o^{(2)}(q^2) &= \frac{1}{2} s_\theta n_0 q^{-2} + \left(\frac{c}{24} \frac{1}{4\pi} + s_\theta C^{(2)} \right) + O(q^2), \end{aligned} \quad (3.13)$$

where $C^{(1)}, C^{(2)} \in \mathbb{R}$ are generically non-zero, and are given by particular linear combinations of the dimensionless coefficients $F'_1(\mu), mF_2(\mu), mF_3(\mu)$, defined in (3.5), see Appendix I for more details.

The leading term in $\eta_o^{(1)}$ is the familiar (1.3), which also appears in gapped states, while the non-analytic leading term in $\eta_o^{(2)}$ is possible because the superfluid is gapless, and does not contribute to the viscosity tensor when $q \rightarrow 0$ at $\omega \neq 0$ [163]. Both leading terms obey the same quantization condition due to SSB, can be used to extract s_θ , and are independent of c . The sub-leading corrections to both $\eta_o^{(1)}, \eta_o^{(2)}$ contain the quantized gCS contributions proportional to c , but also the non-universal coefficients $C^{(1)}, C^{(2)}$. Thus the central charge cannot be extracted from a measurement of η_o alone.

Noting that the non-universal sub-leading corrections to η_o originate from the geometric spin $s_\theta = \ell/2$ of the Goldstone field, one is naturally led to consider the gs -wave CSF, where $s_\theta = 0$, and the odd viscosity is, to leading order in q , purely due to the gCS term

$$\begin{aligned} \tilde{\eta}_o^{(1)}(q^2) &= -\frac{c}{24} \frac{1}{4\pi} q^2 + O(q^4), \\ \tilde{\eta}_o^{(2)}(q^2) &= \frac{c}{24} \frac{1}{4\pi} + O(q^2). \end{aligned} \quad (3.14)$$

Here and below we use O and \tilde{O} , for the quantity O in the CSF and in the corresponding gs -wave CSF, respectively. Equation (3.14) follows from (3.13) by setting $s_\theta = 0$, but can be understood directly from S_{eff} . Indeed, for the gs -wave CSF, S_{eff} is identical to that of the conventional s -wave SF up to $O(p^2)$, but

contains the additional \mathcal{L}_{gCS} at $O(\omega q^2)$, which is the leading P, T -odd term, and produces the leading odd viscosity (3.14).

Due to the LGS (3.1)-(3.2), the viscosity (3.14) implies also

$$\tilde{\chi}_{TJ,o}^{ij,k} = -\frac{i}{m} \frac{c}{48\pi} q_{\perp}^i q_{\perp}^j q_{\perp}^k + O(q^4), \quad (3.15)$$

where $q_{\perp}^i = \varepsilon^{ij} q_j$, and the subscript “o” (“e”) refers to the P, T -odd (even) part of an object, which is odd (even) in ℓ . In particular, a steady P, T -odd current $\tilde{J}_o^k = -\frac{1}{m} \frac{c}{96\pi} \partial_{\perp}^k R + O(q^4)$ flows perpendicularly to gradients of curvature, which has the linearized form $R = -2\partial_{\perp}^i \partial_{\perp}^j u_{ij}$. We stress that the fundamental relation is the momentum density $\tilde{P}_o^k = -\frac{c}{96\pi} \partial_{\perp}^k R + O(q^4)$, which follows from the odd viscosity (3.14) along with momentum conservation, irrespective of Galilean symmetry. This relation was predicted for p -wave CSFs based on the relativistic limit, see Sec.2.1.2 and 2.6. We conclude that, in the gs -wave CSF, c can be extracted from a measurement of $\tilde{\eta}_o$, and in the Galilean invariant case, also from a measurement of the current \tilde{J} in response to (time-independent) strain.

Though the simple results above do not apply to the physical system of interest, the CSF, there is a relation between the observables of the CSF and the corresponding gs -wave CSF, which we can utilize. At the level of induced actions it is given by the simple relation

$$\tilde{S}_{\text{ind}}[A_{\mu}, u_{ij}] = S_{\text{ind}}[A_{\mu} - (\ell/2) \omega_{\mu}, u_{ij}], \quad (3.16)$$

where ω_{μ} is expressed through u_{ij} as in Appendix F, and by taking functional derivatives one finds relations between response functions [250]. In particular,

$$\tilde{\eta}_o^{ij,kl} = \eta_o^{ij,kl} - \frac{\ell}{4} n_0 (\sigma^{xz})^{ij,kl} + \frac{i\ell}{4} \left(\kappa_e^{ij,(k} q_{\perp}^{l)} - \kappa_e^{kl,(i} q_{\perp}^{j)} \right) + \frac{\ell^2}{16} \sigma_o q_{\perp}^{(i} \varepsilon^{j)(k} q_{\perp}^{l)}, \quad (3.17)$$

where the response functions $\eta_o, \sigma_o, \kappa_e$ depend on ω, \mathbf{q} . In a Galilean invariant system one further has

$$\tilde{\chi}_{TJ,o}^{ij,k} = \chi_{TJ,o}^{ij,k} - \frac{\ell}{4m} \chi_{TJ,e}^{ij,t} i q_{\perp}^k + \frac{\ell}{2} i q_{\perp}^{(i} \chi_{JJ,e}^{j),k} + \frac{\ell^2}{8m} q_{\perp}^{(i} \chi_{JJ,o}^{j),t} q_{\perp}^k, \quad (3.18)$$

and we note the relations $\chi_{TJ,e}^{ij,t} = \kappa_e^{ij,k} i q_k$, $\chi_{JJ,o}^{j,t} = \sigma_o q_{\perp}^j$, $\chi_{JJ,e}^{j,k} = \rho_e q_{\perp}^j q_{\perp}^k$, between the above susceptibilities, the response functions κ_e, σ_o , and the London diamagnetic response ρ_e . Though the above expressions are a mouthful, they correspond to the simple subtraction of an angular momentum $\ell/2$ per fermion, as expressed by Eq.(3.16).

3.5 Discussion

Equations (3.14) and (3.17) are the main results of this Section. They rely on the SSB pattern (1.2), but not on Galilean symmetry. Equation (3.17) expresses $\tilde{\eta}_o$ as a bulk observable of CSFs, which we refer to as the *improved odd viscosity*. According to (3.14), the leading term in the expansion of $\tilde{\eta}_o(0, \mathbf{q})$ around $\mathbf{q} = \mathbf{0}$ is fixed by c . Since this leading term occurs at second order in \mathbf{q} , in order to extract c one needs

to measure σ_o , χ_e , and η_o , at zeroth, first, and second order, respectively. In a Galilean invariant system, (3.14) and (3.17) imply (3.15) and (3.18) respectively, which, in turn, show that c can be extracted in an experiment where $U(1)_N$ fields and strain are applied, and the resulting number current and density are measured. In particular, a measurement of the stress tensor is not required. Since $U(1)_N$ fields can be applied in Galilean invariant fluids by tilting and rotating the sample [265], we believe that a bulk measurement of the boundary central charge, through (3.15) and (3.18), is within reach of existing experimental techniques [132, 131, 133, 134].

The problem of obtaining c from a bulk observable has been previously studied in QH states, described by (3.6)-(3.7) [253, 254, 34, 35, 39, 255, 43, 42, 256, 44, 47, 52]. It was found that c can only be extracted if $\text{vars} = \overline{s^2} - \bar{s}^2 = 0$, as in Laughlin states, or in a single filled Landau level. Under this condition, the response to strain, at fixed $A_\mu - \bar{s}\omega_\mu$, depends purely on c [42, 44] - a useful theoretical characterization, which seems challenging experimentally. However, the improved odd viscosity (3.17), constructed here, applies also to $\text{vars} = 0$ QH states, with ℓ replaced by $-2\bar{s}$, and defines a concrete bulk observable which is precisely quantized, and determined by c .

4 Intrinsic sign problem in chiral topological matter

The question of intrinsic Monte Carlo sign problems was motivated in Sec.1.6, where we also stated and discussed the criterion $e^{2\pi ic/24} \notin \{\theta_a\}$, which we obtain for intrinsic sign problems in chiral topological phases. Here we precisely state and derive the results that hold under this criterion.

In Sec.4.1 we discuss the universal finite-size correction to the boundary momentum density in chiral topological phases, arriving at the 'momentum polarization' Eq.(4.2). Relying on the above, Sec.4.2 then obtains Result 1 - an intrinsic sign problem in bosonic chiral topological matter. In Sec.4.3 we perform a similar analysis for the case where chirality (or time reversal symmetry breaking), appears spontaneously rather than explicitly, arriving at Result 2. We then turn to fermionic systems. In Sec.4.4 we develop a formalism which unifies and generalizes the currently used DQMC algorithms, and the corresponding design principles. In Sec.4.5, we obtain within this formalism Result 1F and Result 2F, the fermionic analogs of Results 1 and 2. Section 4.6 describes a conjectured extension of our results that applies beyond chiral phases, and unifies them with the intrinsic sign problems found in our parallel work [5]. In Sec.5 we discuss our results and provide an outlook for future work.

4.1 Signs from geometric manipulations

4.1.1 Momentum finite-size correction

In analogy with the $T > 0$ correction to the energy current in Eq.(1.1), the boundary of a chiral topological phase, described by a chiral CFT, also supports a non-vanishing ground state (or $T = 0$) momentum density p , which receives a universal correction on a cylinder with finite circumference $L < \infty$,

$$p(L) = p(\infty) + \frac{2\pi}{L^2} \left(h_0 - \frac{c}{24} \right). \quad (4.1)$$

Equation (4.1) is the main property of chiral topological matter that we use below, so we discuss it in detail. The appearance of the chiral central charge is a manifestation of the global gravitational anomaly, as explained in Sec.1.3. The rational number h_0 is a *chiral* conformal weight from the boundary CFT. Like the chiral central charge, the two boundary components of the cylinder have opposite h_0 s, see Fig.1. From the bulk TFT perspective, h_0 corresponds to the topological spin of an anyon quasi-particle, defined by the phase $\theta_0 = e^{2\pi i h_0}$ accumulated as the anyon undergoes a 2π rotation [104]. The set $\{\theta_a\}_{a=1}^N$ of topological spins of anyons is associated with the N -dimensional ground state subspace on the torus, and the unique $\theta_0 = e^{2\pi i h_0}$ defined by (4.1) corresponds to the generically unique ground state on the cylinder, with a finite-size energy separation $\sim 1/L$ from the low lying excited states, see Appendix K.

As the equation $\theta_0 = e^{2\pi i h_0}$ suggests, only $h_0 \bmod 1$ is universal for a topological phase. The integer part of h_0 can change as the Hamiltonian is deformed on the cylinder, while maintaining the bulk gap, and even as a function of L for a fixed Hamiltonian. Additionally, the choice of θ_0 from the set $\{\theta_a\}$

is non-universal, and can change due to bulk gap preserving deformations, or as a function of L . Both types of discontinuous jumps in h_0 may be accompanied by an accidental degeneracy of the ground state on the cylinder. Therefore, the universal and L -independent statement regarding h_0 is that, apart from accidental degeneracies, $e^{2\pi i h_0} = \theta_0 \in \{\theta_a\}$ - a fact that will be important in our analysis.

The non-trivial behavior of h_0 described above appears when the boundary corresponds to a non-conformal deformation of a CFT, by e.g a chemical potential. As demonstrated analytically and numerically in Appendix L, such behavior appears already in the simple context of Chern insulators with non-zero Fermi momenta, as would be the case in Fig.1(b) if the chemical potential μ is either raised or lowered.

4.1.2 Momentum polarization

In this section we describe a procedure for the extraction of $h_0 - c/24$ in Eq.(4.1), given a lattice Hamiltonian on the cylinder. Since the two boundary components carry opposite momentum densities, the ground state on the cylinder does not carry a total momentum, only a 'momentum polarization'. It is therefore clear that some sort of one-sided translation will be required.

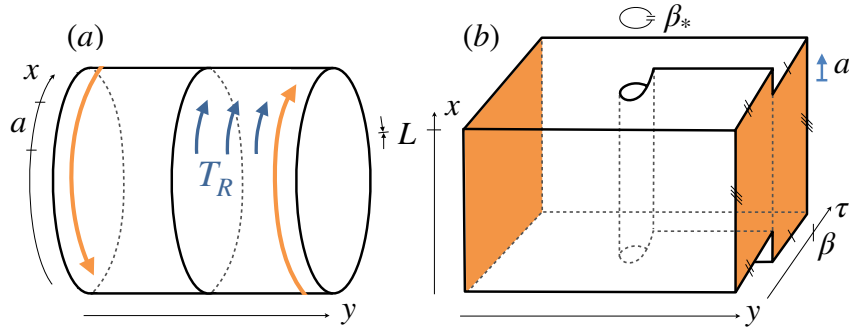


Figure 7: Momentum polarization. (a) Hamiltonian, or spatial, point of view. The operator T_R translates the right half of the cylinder by one unit cell, a distance a , in the x direction. It acts as the identity on the left boundary component, and as a translation on the right boundary component. The object \tilde{Z}/Z is the thermal expectation value of T_R . (b) Field theory, or space-time, point of view. The object \tilde{Z} is the partition function on a space-time carrying a screw dislocation. The space-time region occupied by the boundary components of the spatial cylinder is colored in orange. The screw dislocation can be described as an additional boundary component, on which T_R acts as a translation, with a high effective temperature $1/\beta_*$.

Following Ref.[212], we define $\tilde{Z} := \text{Tr}(T_R e^{-\beta H})$, which is related to the usual partition function $Z = \text{Tr}(e^{-\beta H})$ ($\beta = 1/T$), by the insertion of the operator T_R , which translates the right half of the cylinder by one unit cell in the periodic x direction, see Fig.7(a). The object \tilde{Z} satisfies

$$\tilde{Z} = Z \exp \left[\alpha N_x + \frac{2\pi i}{N_x} \left(h_0 - \frac{c}{24} \right) + o(N_x^{-1}) \right], \quad (4.2)$$

where N_x is the number of sites in the x direction, $\alpha \in \mathbb{C}$ is non-universal and has a negative real part, and $o(N_x^{-1})$ indicates corrections that decay faster than N_x^{-1} as $N_x \rightarrow \infty$. The above expression is valid

at temperatures low compared to the finite-size energy differences on the boundary, $\beta^{-1} = o(N_x^{-1})$, see Appendix K.

Equation (4.2) follows analytically from the low energy description of chiral topological matter in terms of chiral TFT and CFT [212], and was numerically scrutinized in a large number of examples in Refs.[212, 213, 38, 61, 214], as well as in Appendix L. Nevertheless, we are not aware of a rigorous proof of Eq.(4.2) for gapped lattice Hamiltonians. Therefore, in stating our results we will use the assumption ‘the Hamiltonian H is in a chiral topological phase of matter’, the content of which is that H admits a low energy description in terms of a chiral TFT with chiral central charge c and topological spins $\{\theta_a\}$, and in particular, Eq.(4.2) holds for any bulk-gap preserving deformation of H , with $e^{2\pi i h_0} \in \{\theta_a\}$ (apart from accidental degeneracies on the cylinder, as explained below Eq.(4.1)). In the remainder of this section we further discuss the content of Eq.(4.2) and its expected range of validity, in light of the Hamiltonian and space-time interpretations of \tilde{Z} .

From a Hamiltonian perspective, \tilde{Z}/Z is the thermal expectation value of T_R , evaluated at a temperature β^{-1} low enough to isolate the ground state. The exponential decay expressed in Eq.(4.2) appears because T_R is not a symmetry of H , and $-\text{Re}(\alpha)$ can be understood as the energy density of the line defect where T_R is discontinuous, see Fig.7(a). In fact, we expect Eq.(4.2) to hold irrespective of whether the *uniform* translation is a symmetry of H , or of the underlying ‘lattice’ on which H is defined, which may be any polygonalization of the cylinder (see Ref.[266] for a similar scenario). The only expected requirement is that the low energy description of H is homogeneous. Furthermore, if Eq.(4.2) only holds after a disorder averaging of \tilde{Z}/Z , our results and derivations in the following sections remain unchanged.

There is also a simple space-time interpretation of \tilde{Z} , which will be useful in the context of DQMC. The usual partition function $Z = \text{Tr}(e^{-\beta H})$ has a functional integral representation in terms of bosonic fields ϕ (fermionic fields ψ) defined on space, the cylinder C in our case, and the imaginary time circle $S^1_\beta = \mathbb{R}/\beta\mathbb{Z}$, with periodic (anti-periodic) boundary conditions [267]. In $\tilde{Z} = \text{Tr}(T_R e^{-\beta H})$, the insertion of T_R produces a twisting of the boundary conditions of ϕ, ψ in the time direction, such that \tilde{Z} is the partition function on a space-time carrying a screw dislocation, see Fig.7(b).

The above interpretation of \tilde{Z} , supplemented by Eq.(4.1), allows for an intuitive explanation of Eq.(4.2), which loosely follows its analytic derivation [212]. As seen in Fig.7(b), the line where T_R is discontinuous can be interpreted as an additional boundary component at a high effective temperature, $\beta_* \ll L/v$. Since the effective temperature is much larger than the finite size energy-differences $2\pi v/L$ on the boundary CFT, the screw dislocation contributes no finite size corrections to \tilde{Z} . This leaves only the contribution of the boundary component on the right side of the cylinder, where T_R produces the phase $e^{iaLp(L)}$, assuming $\beta_* \ll L/v \ll \beta$. Equation (4.1) then leads to the universal finite size correction $(2\pi i/N_x)(h_0 - c/24)$.

4.2 Excluding stoquastic Hamiltonians for chiral topological matter

In this section we consider bosonic (or 'qudit', or spin) systems, and a single design principle - existence of a local basis in which the many-body Hamiltonian is stoquastic. A sketch of the derivation of Result 1 is that the momentum polarization \tilde{Z} is positive for Hamiltonians H' which are stoquastic in an on-site and homogenous basis, and this implies that $\theta_0 = e^{2\pi ic/24}$ for any Hamiltonian H obtained from H' by conjugation with a local unitary.

4.2.1 Setup

The many body Hilbert space is given by $\mathcal{H} = \otimes_{\mathbf{x} \in X} \mathcal{H}_{\mathbf{x}}$, where the tensor product runs over the sites $\mathbf{x} = (x, y)$ of a 2-dimensional lattice X , and $\mathcal{H}_{\mathbf{x}}$ are on-site 'qudit' Hilbert spaces of finite dimension $d \in \mathbb{N}$. With finite-size QMC simulations in mind, we consider a square lattice with spacing 1, $N_x \times N_y$ sites, and periodic boundary conditions, so that $X = \mathbb{Z}_{N_x} \times \mathbb{Z}_{N_y}$ is a discretization of the flat torus $(\mathbb{R}/N_x\mathbb{Z}) \times (\mathbb{R}/N_y\mathbb{Z})$. Generalization to other 2-dimensional lattices is straight forward. On this Hilbert space a gapped r -local Hamiltonian $H = \sum_{\mathbf{x}} H_{\mathbf{x}}$ is assumed to be given. Here the terms $H_{\mathbf{x}}$ are supported within a range r of \mathbf{x} - they are defined on $\otimes_{|\mathbf{y}-\mathbf{x}| \leq r} \mathcal{H}_{\mathbf{y}}$ and act as the identity on all other qudits.

Fix an tensor product basis $|s\rangle = \otimes_{\mathbf{x} \in X} |s_{\mathbf{x}}\rangle$, labeled by strings $s = (s_{\mathbf{x}})_{\mathbf{x} \in X}$, where $s_{\mathbf{x}} \in \{1, \dots, d\}$ labels a basis $|s_{\mathbf{x}}\rangle$ for $\mathcal{H}_{\mathbf{x}}$. For any vector $\mathbf{d} \in X$, the corresponding translation operator $T^{\mathbf{d}}$ is defined in this basis, $T^{\mathbf{d}}|s\rangle = |t^{\mathbf{d}}s\rangle$, with $(t^{\mathbf{d}}s)_{\mathbf{x}} = s_{\mathbf{x}+\mathbf{d}}$. These statements assert that $|s\rangle$ is both an on-site and a homogeneous basis, or *on-site homogenous* for short. Note that $T^{\mathbf{d}}$ acts as a permutation matrix on the $|s\rangle$ s, and in particular, has non-negative matrix elements in this basis.

In accordance with Sec.4.1.2, we assume that the low energy description of H is invariant under $T^{\mathbf{d}}$, as defined above. In doing so, we exclude the possibility of generic background gauge fields for any on-site symmetry that H may posses, which is beyond the scope of this thesis. Nevertheless, commonly used background gauge fields, such as those corresponding to uniform magnetic fields with rational flux per plaquette, can easily be incorporated into our analysis, by restricting to translation vectors \mathbf{d} in a sub-lattice of X . A restriction to sub-lattice translations can also be used to guarantee that $T^{\mathbf{d}}$ acts purely as a translation in the low energy TQFT description. In particular, a lattice translation may permute the anyon types ²⁹. Since the number of anyons is finite, restricting to large enough translations will eliminate this effect. An example is given by Wen's plaquette model, where different anyons are localized on the even/odd sites of a bipartite lattice [268], and a restriction to translations that maps the even (odd) sites to themselves will be made.

Finally, we assume that H is *locally stoquastic*: it is term-wise stoquastic in a local basis. This means that a local unitary operator U exists, such that the conjugated Hamiltonian $H' = UH U^\dagger$ is a sum of local terms $H'_{\mathbf{x}} = UH_{\mathbf{x}}U^\dagger$, which have non-positive matrix elements in the on-site homogeneous basis, $\langle s|H'_{\mathbf{x}}|\tilde{s}\rangle \leq 0$ for all basis states $|s\rangle, |\tilde{s}\rangle$. Note that we include the diagonal matrix elements in the definition, without loss of generality.

²⁹We thank Michael Levin for pointing out this phenomenon.

The term *local unitary* used above refers to a depth- D quantum circuit, a product $U = U_D \cdots U_1$ where each U_i is itself a product of unitary operators with non-overlapping supports of diameter w . It follows that H' has a range $r' = r + 2r_U$, where $r_U = Dw$ is the range of U . Equivalently, we may take U to be a finite-time evolution with respect to an \tilde{r} -local, smoothly time-dependent, Hamiltonian $\tilde{H}(t)$, given by the time-ordered exponential $U = \text{TO}e^{-i \int_0^1 \tilde{H}(t) dt}$. The two types of locality requirements are equivalent, as finite-time evolutions can be efficiently approximated by finite-depth circuits, while finite-depth circuits can be written as finite-time evolutions over time D with piecewise constant w -local Hamiltonians [269, 90].

4.2.2 Constraining c and $\{\theta_a\}$

In order to discuss the momentum polarization, we need to map the stoquastic Hamiltonian H' from the torus X to a cylinder C . This is done by choosing a translation vector $\mathbf{d} \in X$, and then cutting the torus X along a line l parallel to \mathbf{d} . To simplify the presentation we restrict attention to the case $\mathbf{d} = (1, 0)$, where $T^{\mathbf{d}} = T$ (and in the following $T_R^{\mathbf{d}} = T_R$). All other cases amount to a lattice-spacing redefinition, see Appendix M. The cylinder $C = \mathbb{Z}_{N_x} \times \{1, \dots, N_y\}$ is then obtained from the torus $X = \mathbb{Z}_{N_x} \times \mathbb{Z}_{N_y}$ by cutting along the line $l = \{(i, 1/2) : i \in \mathbb{Z}_{N_x}\}$. A stoquastic Hamiltonian on the cylinder can be obtained from that on the torus by removing all local terms H'_x whose support overlaps l , see Fig.8. Note that this procedure may render H' acting as 0 on certain qudits \mathcal{H}_x with x within a range r' of l , but this does not bother us. Since all terms H'_x are individually stoquastic, this procedure leaves H' , now defined on the cylinder, stoquastic. One can similarly map H and U to the cylinder C such that the relation $H' = UH U^\dagger$ remains valid on C .

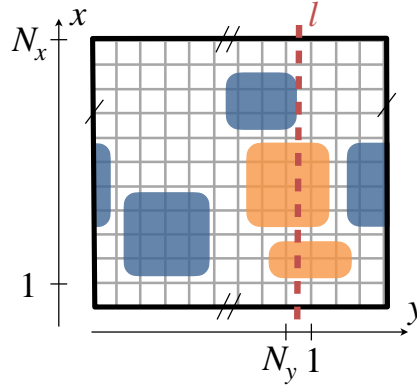


Figure 8: Cutting the torus to a cylinder along the line l . Orange areas mark the supports of Hamiltonian terms H'_x which are removed from H' , while blue areas mark the supports of terms which are kept.

Let us now make contact with the momentum polarization Eq.(4.2). Having mapped H' to the cylinder, we consider the 'partition function'

$$\tilde{Z}' := \text{Tr} \left(e^{-\beta H'} T_R \right), \quad (4.3)$$

where T_R is defined by $T_R |s\rangle = |T_R s\rangle$, $(T_R s)_{x,y} = s_{x+\Theta(y),y}$, and Θ is a heavy side function supported

on the right half of the cylinder. Though \tilde{Z}' is generally different from $\tilde{Z} = \text{Tr}(e^{-\beta H} T_R)$ appearing in Eq.(4.2), it satisfies two useful properties:

1. $\tilde{Z}' > 0$. Both $-H'$ and T_R have non-negative entries in the on-site basis $|s\rangle$, and therefore so does $e^{-\beta H'} T_R$.
2. $H' = U H U^\dagger$ is in the same phase of matter as H , so $c' = c$ and $\{\theta'_a\} = \{\theta_a\}$. Moreover, $h'_0 = h_0$ for all N_x . Treating U as a finite time evolution, we have $H(\lambda) = U(\lambda) H U(\lambda)^\dagger$, where $U(\lambda) := \text{TO} e^{-i \int_0^\lambda \tilde{H}(t) dt}$, as a deformation from H to H' which maintains locality and preserves the bulk-gap. Moreover, the full spectrum on the cylinder is λ -independent, and therefore so is h_0 .

Combining Eq.(4.2), for H' instead of H , with the two above properties leads to

$$\begin{aligned} 1 &= \tilde{Z}' / \left| \tilde{Z}' \right| \\ &= \exp 2\pi i \left[\epsilon' N_x + \frac{1}{N_x} \left(h_0 - \frac{c}{24} \right) + o(N_x^{-1}) \right], \end{aligned} \tag{4.4}$$

where $\epsilon' := \text{Im}(\alpha')$ is generally different from $\epsilon = \text{Im}(\alpha)$ of Eq.(4.2) since $H' \neq H$. The non-universal integer part of h_0 can then be eliminated by raising Eq.(4.4) to the N_x th power,

$$1 = e^{2\pi i \epsilon' N_x^2} \theta_0(N_x) e^{-2\pi i c/24} + o(1), \tag{4.5}$$

where we used $\theta_0 = e^{2\pi i h_0}$, and $o(1) \rightarrow 0$ as $N_x \rightarrow \infty$. We also indicated explicitly the possible N_x -dependence of θ_0 , as described in Sec.4.1.1. We proceed under the assumption that no accidental degeneracies occur on the cylinder, so that $\theta_0(N_x) \in \{\theta_a\}$ for all N_x , deferring the degenerate case to Appendix N. Now, for rational $\epsilon' = n/m$, the series $e^{2\pi i \epsilon' N_x^2}$ ($N_x \in \mathbb{N}$) covers periodically a subset S of the m th roots of unity, including $1 \in S$. On the other hand, for irrational ϵ' the series $e^{2\pi i \epsilon' N_x^2}$ is dense in the unit circle. Combined with the fact that $\theta_0(N_x)$ is valued in the finite set $\{\theta_a\}$, while c is N_x -independent, Equation (4.5) implies that ϵ' must be rational, and that the values attained by $\theta_0(N_x) e^{-2\pi i c/24}$ cover the set S periodically, for large enough N_x . It follows that $1 \in S \subset \{\theta_a e^{-2\pi i c/24}\}$. We therefore have

Result 1 If a local bosonic Hamiltonian H is both locally stoquastic and in a chiral topological phase of matter, then one of the corresponding topological spins satisfies $\theta_a = e^{2\pi i c/24}$. Equivalently, a bosonic chiral topological phase of matter where $e^{2\pi i c/24}$ is not the topological spin of some anyon, i.e $e^{2\pi i c/24} \notin \{\theta_a\}$, admits no local Hamiltonians which are locally stoquastic.

The above result can be stated in terms of the topological **T**-matrix, which is the representation of a Dehn twist on the torus ground state subspace, and has the spectrum $\text{Spec}(\mathbf{T}) = \{\theta_a e^{-2\pi i c/24}\}_a$ [218, 104, 213, 212, 98, 270].

Result 1' If a local bosonic Hamiltonian H is both locally stoquastic and in a chiral topological phase of matter, then the corresponding \mathbf{T} -matrix satisfies $1 \in \text{Spec}(\mathbf{T})$. Equivalently, a bosonic chiral topological phase of matter where $1 \notin \text{Spec}(\mathbf{T})$, admits no local Hamiltonians which are locally stoquastic.

The above result is our main statement for bosonic phases of matter. The logic used in its derivation is extended in Sec.4.3-4.5, where we generalize Result 1 to systems which are fermionic, spontaneously-chiral, or both.

4.3 Spontaneous chirality

The invariants h_0 and c change sign under both time reversal \mathcal{T} and parity (spatial reflection) \mathcal{P} , and therefore require a breaking of \mathcal{T} and \mathcal{P} down to \mathcal{PT} to be non-vanishing. The momentum polarization Eq.(4.2) is valid if this symmetry breaking is explicit, i.e H does not commute with \mathcal{P} and \mathcal{T} separately. Here we consider the case where H is \mathcal{P}, \mathcal{T} -symmetric, but these are broken down to \mathcal{PT} spontaneously, as in e.g intrinsic topological superfluids and superconductors [27, 2, 271]. We first generalize Eq.(4.2) to this setting, and then use this generalization to obtain a spontaneously-chiral analog of Result 1.

Note that the physical time-reversal \mathcal{T} is an *on-site* anti-unitary operator acting *identically* on all qudits, which implies $[\mathcal{T}, T_R] = 0$, while \mathcal{P} is a unitary operator that maps the qudit at \mathbf{x} to that at $P\mathbf{x}$, where P is the nontrivial element in $O(2)/SO(2)$, e.g $(x, y) \mapsto (-x, y)$.

4.3.1 Momentum polarization for spontaneously-chiral Hamiltonians

For simplicity, we begin by assuming that H is 'classically symmetry breaking' - it has two exact ground states on the cylinder, already at finite system sizes. We therefore have two ground states $|\pm\rangle$, such that $|-\rangle$ is obtained from $|+\rangle$ by acting with either \mathcal{T} or \mathcal{P} . In particular, $|\pm\rangle$ have opposite values of h_0 and c . The $\beta \rightarrow \infty$ density matrix is then $e^{-\beta H}/Z = (\rho_+ + \rho_-)/2$, where $\rho_{\pm} = |\pm\rangle\langle\pm|$, and this modifies the right hand side of Eq.(4.2) to its real part,

$$\begin{aligned} \tilde{Z} &:= \text{Tr}(T_R e^{-\beta H}) \\ &= Z e^{-\delta N_x} \cos 2\pi \left[\epsilon N_x + \frac{2\pi}{N_x} \left(h_0 - \frac{c}{24} \right) + o(N_x^{-1}) \right], \end{aligned} \tag{4.6}$$

where $-\delta \pm 2\pi i\epsilon$ are the values of the non-universal α obtained from Eq.(4.2), by replacing $e^{-\beta H}$ by ρ_{\pm} . Indeed, it follows from $[\mathcal{T}, T_R] = 0$ that if two density matrices are related by $\rho_- = \mathcal{T}\rho_+\mathcal{T}^{-1}$, then $\tilde{Z}_{\pm} := Z_{\pm} \text{Tr}(T_R \rho_{\pm})$ are complex conjugates, $\tilde{Z}_- = \tilde{Z}_+^*$.

Now, for a generic symmetry breaking Hamiltonian H , exact ground state degeneracy happens only in the infinite volume limit [272]. At finite size, the two lowest lying eigenvalues of H would be separated by an exponentially small energy difference $\Delta E = O\left(e^{-f N_x^{\lambda}}\right)$, with some $f > 0, \lambda > 0$. The two corresponding eigenstates would be \mathcal{T}, \mathcal{P} -even/odd, of the form $W[|+\rangle \pm |-\rangle]$, where W is a \mathcal{T}, \mathcal{P} -invariant local unitary [90]. One can think of these statements as resulting from the existence

of a bulk-gap preserving and \mathcal{T}, \mathcal{P} -symmetric deformation of H to a 'classically symmetry breaking' Hamiltonian³⁰.

In the generic setting, we have

$$e^{-\beta H}/Z = W(\rho_+ + \rho_-)W^\dagger/2 + O(\beta\Delta E), \quad (4.7)$$

and, following our treatment of the local unitary U in the previous section, Equation (4.6) remains valid, with modified δ, ϵ , but unchanged $h_0 - c/24$. This statement holds for temperatures much higher than ΔE and much smaller than the CFT energy spacing, $\Delta E \ll \beta^{-1} \ll N_x^{-1}$, or more accurately $\beta^{-1} = o(N_x^{-1})$ and $\beta\Delta E = o(N_x^{-1})$ (cf. Sec.4.1.2). Note that the universal content of Eq.(4.6) is the absolute value $|h_0 - c/24|$, since the cosine is even and $\text{sgn}(\epsilon)$ is non-universal.

4.3.2 Constraining c and $\{\theta_a\}$

Let us now assume that a gapped and local Hamiltonian H is \mathcal{T}, \mathcal{P} -symmetric, and is locally stoquastic, due to a unitary U . It follows that $\tilde{Z}' = \text{Tr}(T_R e^{-\beta H'}) > 0$, where $H' = UH U^\dagger$. If U happens to be \mathcal{T}, \mathcal{P} -symmetric, then so is H' , and Eq.(4.6) holds for \tilde{Z}' , with δ', ϵ' in place of δ, ϵ . For a general U , we have

$$e^{-\beta H'}/Z' = UW(\rho_+ + \rho_-)W^\dagger U^\dagger/2 + O(\beta\Delta E), \quad (4.8)$$

where UW need not be \mathcal{T}, \mathcal{P} -symmetric. As result, \tilde{Z}' satisfies a weaker form of Eq.(4.6),

$$0 < \tilde{Z}' = (Z'/2) \sum_{\sigma=\pm} e^{-\delta'_\sigma N_x} e^{2\pi i \sigma [\epsilon'_\sigma N_x + \frac{1}{N_x}(h_0 - \frac{c}{24}) + o(N_x^{-1})]}, \quad (4.9)$$

where δ'_+, ϵ'_+ may differ from δ'_-, ϵ'_- , and we also indicated the positivity of \tilde{Z}' . Now, if $\delta'_+ \neq \delta'_-$, one of the chiral contributions is exponentially suppressed relative to the other as $N_x \rightarrow \infty$, and we can apply the analysis of Sec.4.2. If $\delta'_+ = \delta'_-$, we obtain

$$0 < \sum_{\sigma=\pm} \exp 2\pi i \sigma \left[\epsilon'_\sigma N_x + \frac{1}{N_x} \left(h_0 - \frac{c}{24} \right) + o(N_x^{-1}) \right], \quad (4.10)$$

in analogy with Eq.(3.3). Unlike Eq.(3.3), taking the N_x th power of this equation does not eliminate the mod 1 ambiguity in h_0 . This corresponds to the fact that, as opposed to explicitly chiral systems, stacking copies of a spontaneously chiral system does not increase its net chirality. One can replace T_R in \tilde{Z}' with a larger half-translation T_R^m , which would multiply the argument of the cosine by m . However, since the largest translation on the cylinder is obtained for $m \approx N_x/2$, this does not eliminate the mod 1 ambiguity in h_0 . Moreover, even if it so happens that $\epsilon'_+ = \epsilon'_- = 0$, Equation (4.10) does not imply

³⁰The canonical example is the transverse field Ising model $H(g) = -\sum_{i=1}^{N_x} (Z_i Z_{i+1} + g X_i)$ in 1+1d. Exact ground state degeneracy appears at finite N_x only for $g = 0$, though spontaneous symmetry breaking occurs for all $|g| < 1$, where a splitting $\sim |g|^{N_x}$ appears.

$h_0 - c/24 = 0 \pmod{1}$ since N_x is large.

In order to make progress, we make use of the bagpipes construction illustrated in Fig.9. We attach M identical cylinders, or 'pipes', to the given lattice, and act with T_R on these cylinders. The global topology of the given lattice is unimportant - all that is needed is a large enough disk in which the construction can be applied. The construction does require some form of homogeneity in order to have a unique extension of the Hamiltonian H' to the pipes, and which will be identical for all pipes. We will assume a strict translation symmetry with respect to a sub-lattice, but we believe that this assumption can be relaxed.

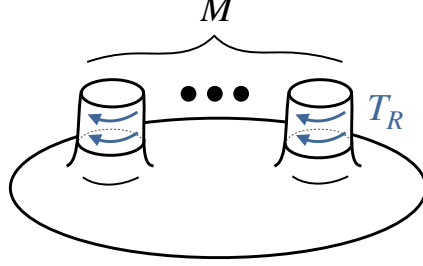


Figure 9: Bagpipes construction. We attach M identical cylinders, or 'pipes', to the given lattice, and define the half translation T_R to act on their top halves, as indicated by blue arrows. The contributions of the pipes to the momentum polarization adds, producing the factor M in Eq.(4.11).

The resulting surface, shown in Fig.9, has negative curvature at the base of each pipe, which requires a finite number of lattice disclinations in this region. In order to avoid any possible ambiguity in the definition of H' at a disclination, one can simply remove any local term H'_x whose support contains a disclination, which amounts to puncturing a hole around each disclination. The resulting boundary components do not contribute to the momentum polarization since T_R acts on these as the identity.

With the construction at hand, the identical contributions of all cylinders to \tilde{Z}' add, which implies

$$0 < \sum_{\sigma=\pm} \exp 2\pi i \sigma M \left[\epsilon'_\sigma N_x + \frac{1}{N_x} \left(h_0 - \frac{c}{24} \right) + o(N_x^{-1}) \right]. \quad (4.11)$$

Setting $M = N_x$ gives

$$0 < e^{2\pi i \epsilon'_+ N_x^2} \theta_0(N_x) e^{-2\pi i c/24} + e^{-2\pi i \epsilon'_- N_x^2} \theta_0^*(N_x) e^{2\pi i c/24} + o(1), \quad (4.12)$$

where we indicate explicitly the possible N_x -dependence of θ_0 . This is the spontaneously chiral analog of Eq.(4.5), and can be analyzed similarly. Since $\theta_0(N_x)$ is valued in the finite set $\{\theta_a\}$, both ϵ'_\pm must be rational, $\epsilon'_\pm = n_\pm/m_\pm$. Restricting then to $N_x = n_x m_+ m_-$, such that $e^{2\pi i \epsilon'_\pm N_x^2} = 1$, and θ_0 attains a constant value θ_a for large enough n_x , we have

$$0 < \text{Re} \left(\theta_a e^{-2\pi i c/24} \right), \quad (4.13)$$

for some anyon a . Repeating the analysis with k times more pipes $M = kN_x$, replaces $\theta_a e^{-2\pi ic/24}$ in Eq.(4.13) with its k th power, for all $k \in \mathbb{N}$. This infinite set of equations then implies $\theta_a e^{-2\pi ic/24} = 1$. To summarize,

Result 2 If a local bosonic Hamiltonian H is both locally stoquastic and in a spontaneously-chiral topological phase of matter, then one of the corresponding topological spins satisfies $\theta_a = e^{2\pi ic/24}$. Equivalently, a bosonic spontaneously-chiral topological phase of matter where $e^{2\pi ic/24}$ is not the topological spin of some anyon, i.e $e^{2\pi ic/24} \notin \{\theta_a\}$, admits no local Hamiltonians which are locally stoquastic.

This extends Result 1 beyond explicitly-chiral Hamiltonians, and clarifies that the essence of the intrinsic sign problem we find is the macroscopic, physically observable, condition $e^{2\pi ic/24} \notin \{\theta_a\}$, as opposed to the microscopic absence (or presence) of time reversal and reflection symmetries.

4.4 DQMC: locality, homogeneity, and geometric manipulations

In order to obtain fermionic analogs of the bosonic results of the previous sections, we first need to establish a framework in which such results can be obtained. In this section we develop a formalism that unifies and generalizes the currently used DQMC algorithms and design principles, and implement within it the geometric manipulations used in previous sections, in a sign-free manner. Since we wish to treat the wide range of currently known DQMC algorithms and design principles on equal footing, the discussion will be more abstract than the simple setting of locally stoquastic Hamiltonians used above. In particular, Sections 4.4.1-4.4.2 lead up to the definition of *locally sign-free DQMC*, which is our fermionic analog of a locally stoquastic Hamiltonian. This definition is used later on in Sec.4.5 to formulate Result 1F and Result 2F, the fermionic analogs of Results 1 and 2. The new tools needed to establish these results are the sign-free geometric manipulations described in Sec.4.4.4.

4.4.1 Local DQMC

In the presence of bosons and fermions, the many-body Hilbert space is given by $\mathcal{H} = \mathcal{H}_F \otimes \mathcal{H}_B$, where \mathcal{H}_F is a fermionic Fock space, equipped with an on-site occupation basis $|\nu\rangle_F = \prod_{\mathbf{x},\alpha} (f_{\mathbf{x},\alpha}^\dagger)^{\nu_{\mathbf{x},\alpha}} |0\rangle_F$, $\nu_{\mathbf{x},\alpha} \in \{0,1\}$, generated by acting with fermionic (anti-commuting) creation operators $f_{\mathbf{x},\alpha}^\dagger$ on the Fock vacuum $|0\rangle_F$. The product is taken with respect to a fixed ordering of fermion species $\alpha \in \{1, \dots, \mathbf{d}_F\}$ and lattice sites $\mathbf{x} \in X$. We will also make use of the single-fermion space $\mathcal{H}_{1F} \cong \mathbb{C}^{|X|} \otimes \mathbb{C}^{\mathbf{d}_F}$, spanned by $|\mathbf{x}, \alpha\rangle_F = f_{\mathbf{x},\alpha}^\dagger |0\rangle_F$, where $|X| = N_x N_y$ is the system size. As in Sec.4.2, \mathcal{H}_B is a many-qudit Hilbert space with local dimension \mathbf{d} . It can also be a bosonic Fock space where $\mathbf{d} = \infty$.

We consider local fermion-boson Hamiltonians H , of the form

$$H = \sum_{\mathbf{x},\mathbf{y}} f_{\mathbf{x}}^\dagger h_0^{\mathbf{x},\mathbf{y}} f_{\mathbf{y}} + H_I, \quad (4.14)$$

where the free-fermion Hermitian matrix $h_0^{\mathbf{x},\mathbf{y}}$ is r_0 -local, it vanishes unless $|\mathbf{x} - \mathbf{y}| \leq r_0$, and we suppress, here and in the following, the fermion species indices. The Hamiltonian H_I describes all possible r_0 -local interactions which preserve the fermion parity $(-1)^{N_f}$, where $N_f = \sum_{\mathbf{x}} f_{\mathbf{x}}^\dagger f_{\mathbf{x}}$, including fermion-independent terms H_B as in Sec.4.2. Thus H_I is of the form

$$H_I = H_B + \sum_{\mathbf{x},\mathbf{y}} f_{\mathbf{x}}^\dagger K_B^{\mathbf{x},\mathbf{y}} f_{\mathbf{y}} + \sum_{\mathbf{x},\mathbf{y},\mathbf{z},\mathbf{w}} f_{\mathbf{x}}^\dagger f_{\mathbf{y}}^\dagger V_B^{\mathbf{x},\mathbf{y},\mathbf{z},\mathbf{w}} f_{\mathbf{z}} f_{\mathbf{w}} + \dots, \quad (4.15)$$

where $K_B^{\mathbf{x},\mathbf{y}}$ (for all $\mathbf{x}, \mathbf{y} \in X$) is a local bosonic operator with range r_0 , and vanishes unless $|\mathbf{x} - \mathbf{y}| \leq r_0$, and similarly for $V_B^{\mathbf{x},\mathbf{y},\mathbf{z},\mathbf{w}}$, which vanishes unless $\mathbf{x}, \mathbf{y}, \mathbf{z}, \mathbf{w}$ are contained in a disk or radius r_0 . In Eq.(4.15) dots represent additional pairing terms of the form ff , $f^\dagger f^\dagger$, or $ffff$, $f^\dagger f^\dagger f^\dagger f^\dagger$, as well as terms with a higher number of fermions, all of which are r_0 -local and preserve the fermion parity.

Since locality is defined in terms of anti-commuting Fermi operators, a local stoquastic basis is not expected to exist, and accordingly, the sign problem appears in any QMC method in which the Boltzmann weights are given in terms of Hamiltonian matrix elements in a local basis [72, 71]. For this reason, the methods used to perform QMC in the presence of fermions are distinct from the ones used in their absence. These are collectively referred to as DQMC [206, 65, 77, 71, 70], and lead to the imaginary time path integral representation of the partition function $Z = \text{Tr}(e^{-\beta H})$,

$$\begin{aligned} Z &= \int D\phi D\psi e^{-S_\phi - S_{\psi,\phi}} \\ &= \int D\phi e^{-S_\phi} \text{Det}(D_\phi) \\ &= \int D\phi e^{-S_\phi} \text{Det}(I + U_\phi), \end{aligned} \quad (4.16)$$

involving a bosonic field ϕ with an action S_ϕ , and a fermionic (grassmann valued) field ψ , with a quadratic action $S_{\psi,\phi} = \sum_{\mathbf{x},\mathbf{x}'} \int d\tau \bar{\psi}_{\mathbf{x},\tau} [D_\phi]_{\mathbf{x},\mathbf{y}} \psi_{\mathbf{y},\tau}$ defined by the ϕ -dependent single-fermion operator D_ϕ . In the third line of Eq.(4.16) we assumed the Hamiltonian form $D_\phi = \partial_\tau + h_{\phi(\tau)}$, and used a standard identity for the determinant in terms of the single-fermion imaginary-time evolution operator $U_\phi = \text{TO} e^{-\int_0^\beta h_{\phi(\tau)} d\tau}$ [206], where TO denotes the time ordering. The field ϕ (ψ) is defined on a continuous imaginary-time circle $\tau \in \mathbb{R}/\beta\mathbb{Z}$, with periodic (anti-periodic) boundary conditions, and on the spatial lattice X . The second and third lines of Eq.(4.16) define the Monte Carlo phase space $\{\phi\}$ and Boltzmann weight

$$\begin{aligned} p(\phi) &= e^{-S_\phi} \text{Det}(D_\phi) \\ &= e^{-S_\phi} \text{Det}(I + U_\phi). \end{aligned} \quad (4.17)$$

In applications, the DQMC representation (4.16) may be obtained from the Hamiltonian H in a number of ways. If a Yukawa type model is assumed as a starting point [70], i.e $H_I = H_B + \sum_{\mathbf{x},\mathbf{y}} f_{\mathbf{x}}^\dagger K_B^{\mathbf{x},\mathbf{y}} f_{\mathbf{y}}$,

then the action S_ϕ is obtained from the Hamiltonian H_B , and $h_{\phi(\tau)} = h_0 + K_B$. Alternatively, the representation (4.16) may be obtained through a Hubbard-Stratonovich decoupling and/or a series expansion of fermionic self-interactions [273, 207, 205]. Such is the case e.g when there are no bosons $\mathcal{H} = \mathcal{H}_F$, and $H_I = \sum_{\mathbf{x}} f_{\mathbf{x}}^\dagger f_{\mathbf{y}}^\dagger V^{\mathbf{x},\mathbf{y},\mathbf{z},\mathbf{w}} f_{\mathbf{z}} f_{\mathbf{w}}$. Note that for a given fermionic self-interaction, there are various possible DQMC representations, obtained e.g via a Hubbard-Stratonovich decoupling in different channels.

To take into account and generalize the above relations between H and the corresponding DQMC representation, we will only assume (i) that the effective single-fermion Hamiltonian $h_{\phi(\tau)}$ reduces to the free fermion matrix $h^{(0)}$ in the absence of ϕ , i.e $h_{\phi(\tau)=0} = h_0$, (ii) that the boson field ϕ is itself an r_0 -local object³¹, and (iii) that the r_0 -locality of h_0 and H_I implies the r -locality of S_ϕ and $h_{\phi(\tau)}$, where r is some function of r_0 , independent of system size. The physical content of these assumptions is that the fields ψ and operators f correspond to the same physical fermion³², and that the boson ϕ mediates *all* fermionic interactions H_I , and therefore corresponds to both the physical bosons in \mathcal{H}_B and to composite objects made of an even number of fermions within a range r_0 (e.g a Cooper pair $\phi \sim ff$).

We can therefore write

$$\begin{aligned} S_\phi &= \sum_{\tau, \mathbf{x}} S_{\phi; \tau, \mathbf{x}}, \\ h_{\phi(\tau)} &= \sum_{\mathbf{x}} h_{\phi(\tau); \mathbf{x}}, \end{aligned} \tag{4.18}$$

where each term $S_{\phi; \tau, \mathbf{x}}$ depends only on the values of ϕ at points (\mathbf{x}', τ') with $|\tau - \tau'|, |\mathbf{x} - \mathbf{x}'| \leq r$, and similarly, each term $h_{\phi(\tau); \mathbf{x}}$ is supported on a disk of radius r around \mathbf{x} , and depends on the values of $\phi(\tau)$ at points \mathbf{x} within this disk.

Note that even though H is Hermitian, we do not assume the same for $h_{\phi(\tau)}$. Non-Hermitian $h_{\phi(\tau)}$ s naturally arise in Hubbard-Stratonovich decouplings, see e.g [274, 205]. Even when $h_{\phi(\tau)}$ is Hermitian for all ϕ , its time-dependence implies that U_ϕ is non-Hermitian, and therefore $\text{Det}(I + U_\phi)$ in Eq.(4.17) is generically complex valued [206]. This is the generic origin of the sign problem in DQMC. Section 4.4.2 below describes the notion of *fermionic design principles*, algebraic conditions on U_ϕ implying $\text{Det}(I + U_\phi) \geq 0$, and defines what it means for such design principles to be local and homogenous.

In the following analysis, we exclude the case of 'classically-interacting fermions', where ϕ is time-independent and h_ϕ is Hermitian. In this case the fermionic weight $\text{Det}(I + e^{-\beta h_\phi})$ is trivially non-negative, and sign-free DQMC is always possible, provided $S_\phi \in \mathbb{R}$. We view such models as 'exactly solvable', on equal footing with free-fermion and commuting projector models. Given a phase of matter, the possible existence of exactly solvable models is independent of the possible existence of sign-free models. Even when an exactly solvable model exists, QMC simulations are of interest for generic questions, such as phase transitions due to deformations of the model [275]. In particular, Ref.[276] utilized

³¹Thus ϕ is a map from sets of lattice sites with diameter less than r_0 , such as links, plaquettes etc., to a fixed vector space \mathbb{C}^k . Additionally, the ϕ integration in (4.16) runs over all such functions. As an example, restricting to constant functions ϕ leads to non-local all to all interactions between fermions.

³²Technically, via the fermionic coherent state construction of the functional integral [267].

a classically-free description of Kitaev’s honeycomb model to obtain the thermal Hall conductance and chiral central charge, which should be contrasted with the intrinsic sign problem we find in the corresponding phase of matter, see Table 1 and Sec.4.5.

4.4.2 Local and homogenous fermionic design principles

The representation (4.16) is sign-free if $p(\phi) = e^{-S_\phi} \text{Det}(I + U_\phi) \geq 0$ for all ϕ . A design principle then amounts to a set of polynomially verifiable properties³³ of S_ϕ and $h_{\phi(\tau)}$ that guarantee that the complex phase of $\text{Det}(I + U_\phi)$ is opposite to that of e^{-S_ϕ} . For the sake of presentation, we restrict attention to the case where S_ϕ is manifestly real valued, and $\text{Det}(I + U_\phi) \geq 0$ due to an algebraic condition on the operator U_ϕ , which we write as $U_\phi \in \mathcal{C}_U$. This is assumed to follow from an algebraic condition on $h_{\phi(\tau)}$, written as $h_{\phi(\tau)} \in \mathcal{C}_h$, manifestly satisfied for all $\phi(\tau)$. The set \mathcal{C}_h is assumed to be closed under addition, while \mathcal{C}_U is closed under multiplication: $h_1 + h_2 \in \mathcal{C}_h$ for all $h_1, h_2 \in \mathcal{C}_h$, and $U_1 U_2 \in \mathcal{C}_U$ for all $U_1, U_2 \in \mathcal{C}_U$.

The simplest example, where $\mathcal{C}_U = \mathcal{C}_h$ is the set of matrices obeying a fixed time reversal symmetry, is discussed in Sec.4.4.3. In Appendix P we review all other design principles known to us, demonstrate that most of them are of the simplified form above, and generalize our arguments to those that are not. Comparing with the bosonic Hamiltonians treated in Sec.4.2, we note that \mathcal{C}_h is analogous to the set of stoquastic Hamiltonians H in a fixed basis, while \mathcal{C}_U is analogous to the resulting set of matrices $e^{-\beta H}$ with non-negative entries.

Design principles, as defined above (and in the literature), are purely algebraic conditions, which carry no information about the underlying geometry of space-time. However, as demonstrated in Sec.4.4.3, in order to allow for local interactions, mediated by an r_0 -local boson ϕ , a design principle must also be local in some sense. We will adopt the following definitions, which are shown to be satisfied by all physical applications of design principles that we are aware of, in Sec.4.4.3 and Appendix P.

Definition (term-wise sign-free): We say that a DQMC representation is term-wise sign-free due to a design principle \mathcal{C}_h , if each of the local terms $S_{\phi;\tau,\mathbf{x}}, h_{\phi(\tau);\mathbf{x}}$ obey the design principle separately, rather than just their sums $S_\phi, h_{\phi(\tau)}$. Thus $S_{\phi;\tau,\mathbf{x}}$ is real valued, and $h_{\phi(\tau);\mathbf{x}} \in \mathcal{C}_h$, for all τ, \mathbf{x} .

This is analogous to the requirement in Sec.4.2.1 that H' be term-wise stoquastic. Note that even when a DQMC representation is term-wise sign-free, the resulting Boltzmann weights $p(\phi)$ are sign-free in a non-local manner: $\text{Det}(I + U_\phi)$ involves the values of ϕ at all space-time points, and splitting the determinant into a product of local terms by the Leibniz formula reintroduces signs, which capture the fermionic statistics. In this respect, the “classical” Boltzmann weights $p(\phi)$ are always non-local in DQMC.

³³That is, properties which can be verified in a polynomial-in- $\beta|X|$ time. As an example, given a local Hamiltonian, deciding whether there exists a local basis in which it is stoquastic is NP-complete [73, 74]. In particular, one does not need to perform the exponential operation of evaluating p on every configuration ϕ to assure that $p(\phi) \geq 0$. Had this been possible, there would be no need for a Monte Carlo sampling of the phase space $\{\phi\}$.

Definition (on-site homogeneous design principle): A design principle is said to be on-site homogeneous if any permutation of the lattice sites $\sigma \in S_X$ obeys it. That is, the operator

$$O_{(\mathbf{x},\alpha),(\mathbf{x}',\alpha')}^{(\sigma)} = \delta_{\mathbf{x},\sigma(\mathbf{x}')}\delta_{\alpha,\alpha'}, \quad (4.19)$$

viewed as a single-fermion imaginary-time evolution operator, obeys the design principle: $O^{(\sigma)} \in \mathcal{C}_U$, for all $\sigma \in S_X$.

This amounts to the statement that the design principle treats all lattice sites on equal footing, since it follows that $U_\phi \in \mathcal{C}_U$ if and only if $O^{(\sigma)}U_\phi O^{(\tilde{\sigma})} \in \mathcal{C}_U$, for all permutations $\sigma, \tilde{\sigma}$. It may be that a design principle is on-site homogeneous only with respect to a sub-lattice $X' \subset X$. In this case we simply treat X' as the spatial lattice, and add the finite set X/X' to the \mathbf{d}_F internal degrees of freedom. Comparing with Sec.4.2.1, on-site homogeneous design principles are analogous to the set of Hamiltonians H' which are stoquastic in an on-site homogeneous basis - any qudit permutation operator has non-negative entries in this basis, like the imaginary time evolution $e^{-\beta H'}$.

With these two notions of locality and homogeneity in design principles, we now define the DQMC analog of locally stoquastic Hamiltonians (see Sec.4.2).

Definition (locally sign-free DQMC): Given a local fermion-boson Hamiltonian H , we say that H allows for a locally sign-free DQMC simulation, if there exists a local unitary U , such that $H' = UHU^\dagger$ has a local DQMC representation (4.16), which is term-wise sign-free due to an on-site homogeneous design principle.

Note that the DQMC representation (4.16) is not of the Hamiltonian but of the partition function, and clearly $Z' = \text{Tr}(e^{-\beta H'}) = \text{Tr}(e^{-\beta H}) = Z$. What the above definition entails, is that it is H' , rather than H , from which the DQMC data $S_\phi, h_{\phi(\tau)}$ is obtained, as described in Sec.4.4.1. This data is then assumed to be term-wise sign-free due to an on-site homogeneous design principle. The local unitary U appearing in the above definition is generally fermionic [277]: it can be written as a finite time evolution $U = \text{TO}e^{-i \int_0^1 \tilde{H}(t)dt}$, where \tilde{H} is a local fermion-boson Hamiltonian, which is either piecewise-constant or smooth as a function of t , c.f Sec.4.2.1.

4.4.3 Example: time reversal design principle

To demonstrate the above definitions in a concrete setting, consider the time-reversal design principle, defined by an anti-unitary operator \mathbb{T} acting on the single-fermion Hilbert space $\mathcal{H}_{1F} \cong \mathbb{C}^{|X|} \otimes \mathbb{C}^{\mathbf{d}_F}$, such that $\mathbb{T}^2 = -I$. The set \mathcal{C}_h contains all \mathbb{T} -invariant matrices, $[\mathbb{T}, h_{\phi(\tau)}] = 0$. It follows that $[\mathbb{T}, U_\phi] = 0$, so that $\mathcal{C}_U = \mathcal{C}_h$ in this case, and this implies $\text{Det}(I + U_\phi) \geq 0$ [81, 274].

A sufficient condition on \mathbb{T} that guarantees that the design principle it defines is on-site homogeneous is that it is of the form $\mathbb{T}_0 = I_{|X|} \otimes \mathbf{t}$, where $I_{|X|}$ is the identity matrix on $\mathbb{C}^{|X|}$, and \mathbf{t} is an anti-unitary on $\mathbb{C}^{\mathbf{d}_F}$ that squares to $-I_{\mathbf{d}_F}$. Equivalently, \mathbb{T} is block diagonal, with identical blocks \mathbf{t} corresponding to the lattice sites $\mathbf{x} \in X$. It is then clear that the permutation matrices $O^{(\sigma)}$ defined in Eq.(4.19) commute

with \mathbb{T} , so $O^{(\sigma)} \in \mathcal{C}_U$ for all $\sigma \in S_X$. Note that the design principle \mathbb{T} may correspond to a *physical* time-reversal \mathcal{T} , discussed in Sec.4.3, only if it is on-site homogenous, which is why we distinguish the two in our notation.

Additionally, if the operator \mathbb{T} is $r_{\mathbb{T}}$ -local with some range $r_{\mathbb{T}} \geq 0$, then any local $h_{\phi(\tau)}$ which is sign-free due to \mathbb{T} can be made term-wise sign-free. Indeed, if $[\mathbb{T}, h_{\phi(\tau)}] = 0$ then

$$\begin{aligned} h_{\phi(\tau)} &= \frac{1}{2} (h_{\phi(\tau)} + \mathbb{T} h_{\phi(\tau)} \mathbb{T}^{-1}) \\ &= \sum_{\mathbf{x}} \frac{1}{2} (h_{\phi(\tau); \mathbf{x}} + \mathbb{T} h_{\phi(\tau); \mathbf{x}} \mathbb{T}^{-1}) \\ &= \sum_{\mathbf{x}} \tilde{h}_{\phi(\tau); \mathbf{x}}, \end{aligned} \tag{4.20}$$

where $\tilde{h}_{\phi(\tau); \mathbf{x}}$ is now supported on a disk of radius $r + 2r_{\mathbb{T}}$ and commutes with \mathbb{T} , for all \mathbf{x} . We see that the specific notion of $r_{\mathbb{T}}$ -locality coincides with the general notion of 'term-wise sign free'. In particular, $\mathbb{T} = \mathbb{T}_0$ has a range $r_{\mathbb{T}} = 0$, and can therefore be applied term-wise.

The above statements imply that if $\mathbb{T} = u \mathbb{T}_0 u^\dagger$, where u is a single-fermion local unitary, and H has a local DQMC representation which is sign-free due to \mathbb{T} , then H allows for a locally sign-free DQMC simulation. Indeed, extending u to a many-body local unitary U , we see that $H' = U H U^\dagger$ admits a local DQMC representation where $[\mathbb{T}_0, h'_{\phi(\tau)}] = 0$. Since \mathbb{T}_0 is on-site homogenous, and $h'_{\phi(\tau)}$ can be assumed term-wise sign-free (see Eq.(4.20)), we have the desired result. As demonstrated in Appendix P, much of the above analysis carries over to other known design principles.

All realizations of \mathbb{T} presented in Ref.[274] in the context of generalized Hubbard models, and in Ref.[70] in the context of quantum critical metals, have the on-site homogeneous form \mathbb{T}_0 , and therefore correspond to locally sign-free DQMC simulations.

We now consider a few specific time-reversal design principles \mathbb{T} . The physical spin-1/2 time reversal $\mathbb{T} = \mathcal{T}^{(1/2)}$, where $\mathcal{T}_{(\mathbf{x}, \alpha), (\mathbf{x}', \alpha')}^{(1/2)} = \delta_{\mathbf{x}, \mathbf{x}'} \varepsilon_{\alpha \alpha'} \mathcal{K}$, and $\alpha, \alpha' \in \{\uparrow, \downarrow\}$ correspond to up and down spin components, is an on-site homogeneous design principle, which accounts for the absence of signs in the attractive Hubbard model [274]. The composition $\mathbb{T} = \mathcal{M} \mathcal{T}^{(1/2)}$ of $\mathcal{T}^{(1/2)}$ with a modulo 2 translation, $\mathcal{M}_{(\mathbf{x}, \alpha), (\mathbf{x}', \alpha')} = \delta_{(-1)^x, (-1)^{x'+1}} \delta_{x_e, x'_e} \delta_{y, y'} \delta_{\alpha, \alpha'}$, where $x_e = 2 \lfloor x/2 \rfloor$ is the even part of x , is an on-site homogeneous design principle with respect to the sub-lattice $X' = \{(2x_1, x_2) : \mathbf{x} \in X\}$, but not with respect to X . On the other hand, the composition $\mathbb{T} = \mathcal{P}^{(0)} \mathcal{T}^{(1/2)}$ of $\mathcal{T}^{(1/2)}$ with a spin-less reflection (or parity) $\mathcal{P}_{(\mathbf{x}, \alpha), (\mathbf{x}', \alpha')}^{(0)} = \delta_{x, -x'} \delta_{y, y'} \delta_{\alpha \alpha'}$, is not on-site homogeneous with respect to any sub-lattice.

The latter example is clearly non-local, and we use it to demonstrate the necessity of locality in design principles. As discussed in Sec.4.3, the breaking of \mathcal{P} and \mathcal{T} down to \mathcal{PT} actually defines the notion of chirality, and therefore \mathcal{PT} is a natural symmetry in chiral topological matter. Accordingly, the design principle $\mathbb{T} = \mathcal{P}^{(0)} \mathcal{T}^{(1/2)}$ applies to a class of models for chiral topological phases, see Appendix O. This seems to allow, from the naive algebraic perspective, for a sign-free DQMC simulation of certain chiral topological phases. However, the weights $p(\phi)$ will only be non-negative for bosonic configurations ϕ which are invariant under $\mathbb{T} = \mathcal{P}^{(0)} \mathcal{T}^{(1/2)}$. Restricting the ϕ integration in Eq.(4.16)

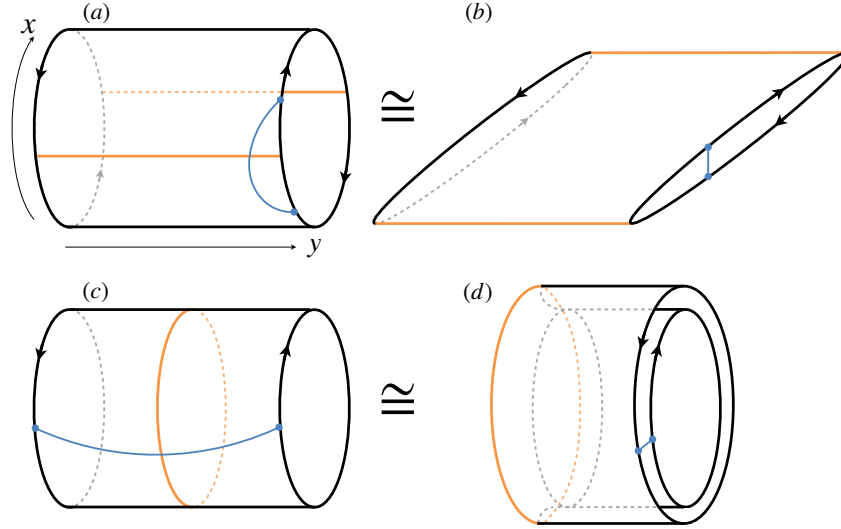


Figure 10: \mathcal{PT} symmetry as a 'non-local design principle' for chiral topological matter. (a), (c): \mathcal{PT} symmetry, where \mathcal{P} is a reflection (with respect to the orange lines) and \mathcal{PT} is an on-site time-reversal, is a natural symmetry in chiral topological phases. If $(\mathcal{PT})^2 = -I$, as is the case when $\mathcal{P} = \mathcal{P}^{(0)}$ is spinless and $\mathcal{T} = \mathcal{T}^{(1/2)}$ is spin-full, it implies the non-negativity of fermionic determinants. Nevertheless, as \mathcal{PT} is non-local, it only allows for QMC simulations with \mathcal{PT} invariant bosonic fields, which mediate non-local interactions (blue lines) between fermions. Arrows indicate the chirality of boundary degrees of freedom. (b), (d): Such non-local interactions effectively fold the system into a non-chiral locally-interacting system supported on half the cylinder, where \mathcal{PT} acts as an on-site time reversal. In particular, the boundary degrees of freedom are now non-chiral. Thus, \mathcal{PT} does not allow for sign-free QMC simulations of chiral topological matter. More generally, fermionic design principles must be local in order to allow for sign-free DQMC simulations of local Hamiltonians.

to such configurations leads to non-local interactions between fermions ψ , coupling the points (x, y) and $(-x, y)$. These interactions effectively fold the non-local chiral system into a local non-chiral system on half of space, see Fig.10. Thus, $\mathbb{T} = \mathcal{P}^{(0)}\mathcal{T}^{(1/2)}$ does *not* allow for sign-free DQMC simulations of chiral topological matter.

4.4.4 Sign-free geometric manipulations in DQMC

Let Z be a partition function in a local DQMC form (4.16), on the discrete torus $X = \mathbb{Z}_{N_x} \times \mathbb{Z}_{N_y}$ and imaginary time circle $S_\beta^1 = \mathbb{R}/\beta\mathbb{Z}$, which is term-wise sign-free due to an on-site homogenous design principle. In this section we show that it is possible to cut X to the cylinder C , and subsequently introduce a screw dislocation in the space-time $C \times S_\beta^1$, which corresponds to the momentum polarization (4.2), while maintaining the DQMC weights $p(\phi)$ non-negative.

Introducing spatial boundaries Given a translation $T^{\mathbf{d}}$ ($\mathbf{d} \in X$), we can cut the torus X along a line l parallel to \mathbf{d} , and obtain a cylinder C where $T^{\mathbf{d}}$ acts as a translation within each boundary component, as in Sec.4.2. Given the DQMC representation (4.16) on X , the corresponding representation on C is obtained by eliminating all local terms $S_{\phi;\tau;\mathbf{x}}, h_{\phi(\tau);\mathbf{x}}$ whose support overlaps l , as in Fig.8. This procedure

may render $S_\phi, h_{\phi(\tau)}$ independent of certain degrees of freedom $\phi(\mathbf{x}, \tau), \psi(\mathbf{x}, \tau)$, with \mathbf{x} within a range r of l , in which case we simply remove such degrees of freedom from the functional integral (4.16)³⁴. Since $S_{\phi;\tau,\mathbf{x}}, h_{\phi(\tau);\mathbf{x}}$ obey the design principle for every \mathbf{x}, τ , the resulting $S_\phi, h_{\phi(\tau)}$ still obey the design principle and the weights $p(\phi)$ remain real and non-negative.

Introducing a screw dislocation in space-time Let us now restrict attention to $\mathbf{d} = (1, 0)$, and make contact with the momentum polarization (4.2). Given a partition function on the space-time $C \times S_\beta^1$, consider twisting the boundary conditions in the time direction,

$$\begin{aligned}\phi_{\tau+\beta,x,y} &= \phi_{\tau,x-\lambda\Theta(y),y}, \\ \psi_{\tau+\beta,x,y} &= -\psi_{\tau,x-\lambda\Theta(y),y}.\end{aligned}\tag{4.21}$$

Note that $\lambda \in \mathbb{Z}_{N_x}$, since $x \in \mathbb{Z}_{N_x}$. In particular, the full twist $\lambda = N_x$ is equivalent to the untwisted case $\lambda = 0$, which is equivalent to the statement that the modular parameter of the torus is defined mod 1 (see e.g example 8.2 of [234]). The case $\lambda = 0$ gives the standard boundary conditions, where the partition function is, in Hamiltonian terms, just $Z = \text{Tr}(e^{-\beta H})$. In this case $Z > 0$ since H is Hermitian, though its QMC representation $Z = \sum_\phi p(\phi)$ will generically involve complex valued weights p . The twisted case $\lambda = 1$ includes the insertion of the half-translation operator

$$\tilde{Z} = \text{Tr}(T_R e^{-\beta H}),\tag{4.22}$$

which appears in the momentum polarization (4.2). Since T_R is unitary rather than hermitian, \tilde{Z} itself will generically be complex. However,

Claim: If Z has a local DQMC representation (4.16), which is term-wise sign-free due to an on-site homogeneous design principle, then \tilde{Z} also has a sign-free QMC representation: $\tilde{Z} = \sum_\phi \tilde{p}(\phi)$, with $\tilde{p}(\phi) \geq 0$. In particular, $\tilde{Z} \geq 0$.

Proof of the claim is provided below. It revolves around two physical points: (i) For the boson ϕ , we only use the fact that all boundary conditions, and those in Eq.(4.21) in particular, are locally invisible. (ii) For the fermion ψ , the local invisibility of boundary conditions does not suffice, and the important point is that translations do not act on internal degrees of freedom, and therefore correspond to permutations of the lattice sites. The same holds for the half translation T_R . This distinguishes translations from internal symmetries, as well as from all other spatial symmetries, which involve point group elements, and generically act non-trivially on internal degrees of freedom. For example, a C_4 rotation will act non-trivially on spin-full fermions.

Proof: We first consider the fermionic part of the Boltzmann weight, $\text{Det}(I + U_\phi)$. The Hamiltonian $h_{\phi(\tau)}$ depends on the values of ϕ at a single time slice τ , and is therefore unaffected by the twist in bosonic

³⁴For r_0 -local ϕ , which is defined on links, plaquettes, etc., we also remove from the functional ϕ integration those links, plaquettes, etc. which overlap l .

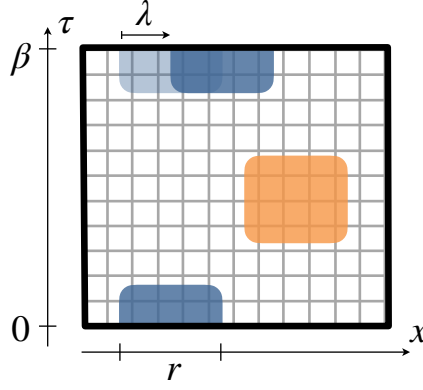


Figure 11: Implementing the bosonic boundary conditions (4.21). The lattice lies in the $x - \tau$ plane, at $y > 0$ where the boundary conditions are non trivial. The orange area marks the support, of diameter r , of a local term $S_{\phi;\tau,\mathbf{x}}$ which is unaffected by the boundary conditions. Blue areas correspond to the support of a local term which is affected by the boundary conditions, with pale blue indicating the un-twisted case $\lambda = 0$.

boundary conditions. It follows that U_ϕ is independent of the twist in bosonic boundary conditions. On the other hand, the fermionic boundary conditions in (4.21) correspond to a change of the time evolution operator $U_\phi \mapsto T_R U_\phi$, in analogy with (4.22). Since the design-principle \mathcal{C}_U is assumed to be on-site homogeneous, and $T_R = O(\sigma)$ is a permutation operator, with $\sigma : (x, y) \mapsto (x + \Theta(y), y)$, we have $T_R U_\phi \in \mathcal{C}_U$, and $\text{Det}(I + T_R U_\phi) \geq 0$.

Let us now consider the bosonic part of the Boltzmann weight e^{-S_ϕ} , where each of the local terms $S_{\phi;\tau,\mathbf{x}}$ is manifestly real valued for all ϕ . We assume that the imaginary time circle S^1_β is discretized, such that the total number of space-time points $(\tau, \mathbf{x}) = u \in U$ is finite. Such a discretization is common in DQMC algorithms [206, 207], and the continuum case can be obtained by taking the appropriate limit. The term $S_{\phi;\tau,\mathbf{x}}$ can then be written as a composition $f \circ g_V$, where f is a real valued function, and $g_V : (\phi_u)_{u \in U} \mapsto (\phi_u)_{u \in V}$ chooses the values of ϕ on which $S_{\phi;\tau,\mathbf{x}}$ depends, where $V \subset U$ is the support of $S_{\phi;\tau,\mathbf{x}}$. The bosonic boundary conditions (4.21) then amount to a modification of the support $V \mapsto V_\lambda$, as depicted in Fig.11, but not of the function f , which remains real valued. In particular, for $\lambda = 1$ we have $S_{\phi;\tau,\mathbf{x}} \mapsto \tilde{S}_{\phi;\tau,\mathbf{x}} = f \circ g_{V_1}$, and $S_\phi \mapsto \tilde{S}_\phi = \sum_{\tau,\mathbf{x}} \tilde{S}_{\phi;\tau,\mathbf{x}} \in \mathbb{R}$.

Combining the above conclusions for the bosonic and fermionic parts of $\tilde{p}(\phi) = e^{-\tilde{S}_\phi} \text{Det}(I + T_R U_\phi)$, we find that $\tilde{p}(\phi) \geq 0$ for all ϕ .

4.5 Excluding sign-free DQMC for chiral topological matter

We are now ready to demonstrate the existence of an intrinsic sign problem in chiral topological matter comprised of bosons *and* fermions, using the machinery of Sections 4.2-4.4.

Let H be a gapped local fermion-boson Hamiltonian on the discrete torus, which allows for a locally sign-free DQMC simulation. Unpacking the definition, this means that $H' = U H U^\dagger$ has a local DQMC representation which is term-wise sign-free due to an on-site homogeneous design principle. As shown in Sec.4.4.4, this implies that $\tilde{Z}' := \text{Tr}(T_R e^{-\beta H'})$, written on the cylinder, also has a local DQMC

representation, obeying a local and on-site design principle, and as a result, $\tilde{Z}' > 0$. Now, as shown in Sec.4.2, the positivity of \tilde{Z}' implies $\theta_a = e^{2\pi ic/24}$ for some anyon a . We therefore have the fermionic version of Result 1,

Result 1F If a local fermion-boson Hamiltonian H , which is in a chiral topological phase of matter, allows for a locally sign-free DQMC simulation, then one of the corresponding topological spins satisfies $\theta_a = e^{2\pi ic/24}$. Equivalently, a chiral topological phase of matter where $e^{2\pi ic/24}$ is not the topological spin of some anyon, i.e $e^{2\pi ic/24} \notin \{\theta_a\}$, admits no local fermion-boson Hamiltonians for which locally sign-free DQMC simulation is possible.

As shown in Sec.4.3, the positivity of \tilde{Z}' implies $\theta_a = e^{2\pi ic/24}$ for some anyon a , even if chirality appears only spontaneously. We therefore obtain the fermionic version of Result 2,

Result 2F If a local fermion-boson Hamiltonian H , which is in a spontaneously-chiral topological phase of matter, allows for a locally sign-free DQMC simulation, then one of the corresponding topological spins satisfies $\theta_a = e^{2\pi ic/24}$. Equivalently, a spontaneously-chiral topological phase of matter where $e^{2\pi ic/24}$ is not the topological spin of some anyon, i.e $e^{2\pi ic/24} \notin \{\theta_a\}$, admits no local fermion-boson Hamiltonians which allow for a locally sign-free DQMC simulation.

In stating these results, we do not restrict to fermionic phases, because bosonic phases may admit a fermionic description, for which DQMC is of interest. When a bosonic phase admits a fermionic description, the bosonic field ϕ in Eq.(4.16) will contain a \mathbb{Z}_2 gauge field that couples to the fermion parity $(-1)^{N_f}$ of ψ . An important series of examples is given by the non-abelian Kitaev spin liquids, which admit a description in terms of gapped Majorana fermions with an odd Chern number ν , coupled to a \mathbb{Z}_2 gauge field [104]. As described in Table 1, the criterion $e^{2\pi ic/24} \notin \{\theta_a\}$ applies to the Kitaev spin liquid, for all $\nu \in 2\mathbb{Z} - 1$. Result 1 then excludes the possibility of locally stoquastic Hamiltonians for the microscopic description in terms of spins, while Result 1F excludes the possibility of locally sign-free DQMC simulations in the emergent fermionic description.

4.6 Conjectures: beyond chiral matter

In Sec.4.2 and Appendices 4.3-4.5 we established a criterion for the existence of intrinsic sign problems in chiral topological matter: if $e^{2\pi ic/24} \notin \{\theta_a\}$, or equivalently $1 \notin \text{Spec}(\mathbf{T})$ (see Result 1'), then an intrinsic sign problem exists. Even if taken at face value, this criterion never applies to non-chiral bosonic topological phases, where $c = 0$, due to the vacuum topological spin $1 \in \{\theta_a\}$. The same statement applies to all bosonic phases with $c \in 24\mathbb{Z}$. In this section we propose a refined criterion for intrinsic sign problems in topological matter, which non-trivially applies to both chiral *and* non-chiral cases, and also unifies the results of this section with those obtained by other means in a parallel work [5].

Reference [266] proposed the 'universal wave-function overlap' method for characterizing topological order from any basis $\{|i\rangle\}$ for the ground state subspace of a local gapped Hamiltonian H on the torus

X. The method is based on the conjecture

$$\langle i | \mathbf{T}_m | j \rangle = e^{-\alpha_{\mathbf{T}} A + o(A^{-1})} \mathbf{T}_{ij}, \quad (4.23)$$

where A is the area of the torus, $\alpha_{\mathbf{T}}$ is a non-universal complex number with non-negative real part, the microscopic Dehn-twist operator \mathbf{T}_m implements the Dehn twist $(x, y) \mapsto (x + y, y)$ on the Hilbert space, and \mathbf{T}_{ij} are the entries of the topological \mathbf{T} -matrix that characterizes the phase of H , in the basis $\{|i\rangle\}$. The same statement applies to any element \mathbf{M} of the mapping class group of the torus, isomorphic to $SL(2, \mathbb{Z})$, with \mathbf{M} in place of \mathbf{T} in Eq.(4.23). The non-universal exponential suppression of the overlap is expected because \mathbf{M}_m will not generically map the ground-state subspace to itself, but if \mathbf{M}_m happens to be a symmetry of H , then $\alpha_{\mathbf{M}} = 0$ [278, 98]. Though we are not aware of a general analytic derivation of Eq.(4.23), it was verified analytically and numerically in a large number of examples in Refs.[266, 270, 279–281], for Hamiltonians in both chiral and non-chiral phases.

Note the close analogy between Eq.(4.23) and the momentum polarization (4.2), where the microscopic Dehn-twist \mathbf{T}_m on the torus and the half translation T_R on the cylinder play a similar role, and non-universal extensive contributions are followed by sub-extensive universal data. To make this analogy clearer, and make contact with the analysis of Sections 4.2 and 4.5, we consider the object $Z_{\mathbf{T}} = \text{Tr}(\mathbf{T}_m e^{-\beta H})$, which satisfies

$$Z_{\mathbf{T}} = Z e^{-\alpha_{\mathbf{T}} A + o(A^{-1})} \text{Tr}(\mathbf{T}), \quad (4.24)$$

and can be interpreted as either the (unnormalized) thermal expectation value of \mathbf{T}_m , or the partition function on a space-time twisted by \mathbf{T} , in analogy with Sec.4.1.2. Equation (4.24) is valid for temperatures $\Delta E \ll 1/\beta \ll E_g$, much lower than the bulk gap E_g and much higher than any finite size splitting in the ground state-subspace, $\Delta E = o(A^{-1})$.

Just like T_R , the operator \mathbf{T}_m acts as a permutation of the lattice sites. Therefore, following Section 4.2 and Appendix 4.5, if H is either locally stoquastic, or admits a locally sign-free DQMC simulation, then $\text{Tr}(\mathbf{T}) \geq 0$. In terms of c and $\{\theta_a\}$, this implies $e^{-2\pi i c/24} \sum_a \theta_a = \text{Tr}(\mathbf{T}) \geq 0$, where the sum runs over all topological spins.

The last statement applies to both bosonic and fermionic Hamiltonians. For bosonic Hamiltonians, it can be strengthened by means of the Frobenius-Perron theorem. If $H' = U H U^\dagger$ is stoquastic in the on-site basis $|s\rangle$, Hermitian, and has a degenerate ground state subspace, then this subspace can be spanned by an orthonormal basis $|i'\rangle$ with positive entries in the on-site basis, $\langle s | i' \rangle \geq 0$, see e.g Ref.[5]. This implies that

$$0 \leq \langle i' | \mathbf{T}_m | j' \rangle = e^{-\alpha'_{\mathbf{T}} A + o(A^{-1})} \mathbf{T}_{i'j'}, \quad (4.25)$$

where $\alpha'_{\mathbf{T}}$ is generally different from $\alpha_{\mathbf{T}}$, but the matrix $\mathbf{T}_{i'j'}$ has the same spectrum as \mathbf{T}_{ij} in Eq.(4.23). This is a stronger form of (J.18), which implies $\mathbf{T}_{i'j'} \geq 0$. Since $\mathbf{T}_{i'j'}$ is also unitary, it is a permutation matrix, $\mathbf{T}_{i'j'} = \delta_{i', \sigma(j')}$ for some $\sigma \in S_N$, where N is the number of ground states. In turn, this implies

that the spectrum of \mathbf{T} is a disjoint union of complete sets of roots of unity,

$$\{\theta_a e^{-2\pi i c/24}\}_{a=1}^N = \text{Spec}(\mathbf{T}) = \bigcup_{k=1}^K R_{n_k}, \quad (4.26)$$

where R_{n_k} is the set of n_k th roots of unity, $n_k, K \in \mathbb{N}$, and $\sum_{k=1}^K n_k = N$. Therefore,

Conjecture 1 A bosonic topological phase of matter where $\{\theta_a e^{-2\pi i c/24}\}$ is not a disjoint union of complete sets of roots of unity, admits no local Hamiltonians which are locally stoquastic.

In particular, this implies an intrinsic sign problem whenever $1 \notin \{\theta_a e^{-2\pi i c/24}\}$, thus generalizing Result 1. Moreover, the above statement applies non-trivially to phases with $c \in 24\mathbb{Z}$. In particular, for non-chiral phases, where $c = 0$, it reduces to the result established in Ref.[5], thus generalizing it as well. The simplest example for a non-chiral phase with an intrinsic sign problem is the doubled semion phase, where $\{\theta_a\} = \{1, i, -i, 1\}$ [211].

Though we are currently unaware of an analog of the Frobenius-Perron theorem that applies to DQMC, we expect that an analogous result can be established for fermionic Hamiltonians.

Conjecture 1F A topological phase of matter where $\{\theta_a e^{-2\pi i c/24}\}$ is not a complete set of roots of unity, admits no local fermion-boson Hamiltonians for which locally sign-free DQMC simulation is possible.

The above conjectures suggest a substantial improvement over the criterion $e^{2\pi i c/24} \notin \{\theta_a\}$. To demonstrate this, we go back to the $1/q$ Laughlin phases and $SU(2)_k$ Chern-Simons theories considered in Table 1. We find a conjectured intrinsic sign problem in *all* of the first one-thousand bosonic Laughlin phases (q even), fermionic Laughlin phases (q odd), and $SU(2)_k$ Chern-Simons theories. In particular, we note that the prototypical $1/3$ Laughlin phase is not captured by the criterion $e^{2\pi i c/24} \notin \{\theta_a\}$, but is conjectured to be intrinsically sign-problematic.

4.7 Discussion

In this section we established the existence of intrinsic sign problems in a broad class of chiral topological phases, namely those where $e^{2\pi i c/24}$ does not happen to be the topological spin of an anyon. Since these intrinsic sign problems persist even when chirality appears spontaneously, they are rooted in the macroscopic and observable data $c, \{\theta_a\}$, rather than the microscopic absence (or presence) of time reversal symmetry. Going beyond the simple setting of stoquastic Hamiltonians, we provided the first treatment of intrinsic sign problems in fermionic systems. In particular, we constructed a general framework which describes all DQMC algorithms and fermionic design principles that we are aware of, including the state of art design principles [205, 209, 208, 210] which are only beginning to be used by practitioners. Owing to its generality, it is likely that our framework will apply to additional design principles which have not yet been discovered, insofar as they are applied locally. We also presented conjectures that strengthen our results, and unify them with those obtained in Refs.[75, 5], under a

single criterion in terms of c and $\{\theta_a\}$. These conjectures also imply intrinsic sign problems in many topological phases not covered by existing results.

Conceptually, our results show that the sign problem is not *only* a statement of computational complexity: it is, in fact, intimately connected with the physically observable properties of quantum matter. Such a connection has long been heuristically appreciated by QMC practitioners, and is placed on a firm and quantitative footing by the discovery of intrinsic sign problems. Despite the progress made here, our understanding of intrinsic sign problems is still in its infancy, and many open questions remain:

Quantum computation and intrinsic sign problems Intrinsic sign-problems relate the physics of topological phases to their computational complexity, in analogy with the classification of topological phases which enable universal quantum computation [219, 97]. As we have seen, many phases of matter that are known to be universal for quantum computation are also intrinsically sign-problematic, supporting the paradigm of 'quantum advantage' or 'quantum supremacy' [220]. Determining whether intrinsic sign-problems appear in *all* phases of matter which are universal for quantum computation is an interesting open problem. Additionally, we identified intrinsic sign problems in many topological phases which are not universal for quantum computation. The intermediate complexity of such phases between classical and quantum computation is another interesting direction for future work.

Unconventional superconductivity and intrinsic sign problems As described in the introduction, a major motivation for the study of intrinsic sign problems comes from long standing open problems in fermionic many-body systems, the nature of high temperature superconductivity in particular. It is currently believed that many high temperature superconductors, and the associated repulsive Hubbard models, are *non-chiral* d -wave superconductors [80, 70], in which we did not identify an intrinsic sign problem. The optimistic possibility that the sign problem can in fact be cured in repulsive Hubbard models is therefore left open, though this has not yet been accomplished in the relevant regime of parameters, away from half filling, despite intense research efforts [79]. Nevertheless, the state of the art DMRG results of Ref.[80] do not exclude the possibility of a *chiral* d -wave superconductor ($\ell = \pm 2$ in Table 1). In this case we do find an intrinsic sign problem, which would account for the notorious sign problems observed in repulsive Hubbard models. More speculatively, it is possible that the mere proximity of repulsive Hubbard models to a chiral d -wave phase stands behind their notorious sign problems. The possible effect of an intrinsic sign problem in a given phase on the larger phase diagram was recently studied in Ref.[282]. There is also evidence for chiral d -wave superconductivity in doped graphene and related materials [283, 284], and our results therefore suggest the impossibility of sign-free QMC simulations of these. We believe that the study of intrinsic sign problems in the context of unconventional superconductivity is a promising direction for future work.

Non-locality as a possible route to sign-free QMC The intrinsic sign problems identified in this thesis add to existing evidence for the complexity of chiral topological phases - these do not admit local

commuting projector Hamiltonians [56–58, 54], nor do they admit local Hamiltonians with a PEPS state as an exact ground state [60–63]. Nevertheless, relaxing the locality requirement does lead to positive results for the simulation of chiral topological matter using commuting projectors or PEPS. First, commuting projector Hamiltonians can be obtained if the local bosonic or fermionic degrees of freedom are replaced by anyonic (and therefore non-local) excitations of an underlying chiral topological phase [59]. Second, chiral topological Hamiltonians can have a PEPS ground state if they include interactions (or hopping amplitudes) that slowly decay as a power-law with distance. One may therefore hope that sign-free QMC simulations of chiral topological matter can also be performed if the locality requirements made in Sec.4.2 are similarly relaxed. Do such ‘weakly-local’ sign-free models exist?

Easing intrinsic sign problems In this section we proved the existence of an intrinsic sign problem in chiral topological phases of matter, but we did not quantify the *severity* of this sign problem, which is an important concept in both practical applications and theory of QMC. The severity of a sign problem is quantified by the smallness of the average sign of the QMC weights p with respect to the distribution $|p|$, i.e $\langle \text{sgn} \rangle := \sum p / \sum |p|$. Since $\langle \text{sgn} \rangle$ can be viewed as the ratio of two partition functions, it obeys the generic scaling $\langle \text{sgn} \rangle \sim e^{-\Delta \beta N}$, with $\Delta \geq 0$, as $\beta N \rightarrow \infty$ [72, 203]. A sign problem exists when $\Delta > 0$, in which case QMC simulations require exponential computational resources, and this is what the intrinsic sign problem we identified implies for ‘most’ chiral topological phases of matter. From the point of view of computational complexity, all that matters is whether $\Delta = 0$ or $\Delta > 0$, but for practical applications the value of Δ is very important, see e.g [283]. One may hope for a possible refinement of our results that provides a lower bound $\Delta_0 > 0$ for Δ , but since we have studied *topological* phases of matter, we view this as unlikely. It may therefore be possible to obtain fine-tuned models and QMC methods that lead to a Δ small enough to be *practically* useful. More generally, it may be possible to search for such models and methods algorithmically, thus *easing* the intrinsic sign problem [203, 285–287]. We also note that the results presented in this thesis do not exclude approaches to the sign-problem based on a modified or constrained Monte Carlo sampling [204, 288, 289], as well as machine-learning aided QMC [290], and infinite-volume diagrammatic QMC [291].

Possible extensions The chiral central charge only appears modulo 24 in our results. Nevertheless, for full value of c is physically meaningful, as reviewed in the introduction. Does an intrinsic sign problem exist in all phases with $c \neq 0$? The results of Ref.[76] strongly suggest this.

The arguments of Appendix 4.6 apply equally well to any element of the modular group, rather than just the topological **T**-matrix, implying that the spectrum of all elements decomposes into full sets of roots of unity. Does this imply a tighter constraint on the TFT data than conjectured in Appendix 4.6? Moreover, the ‘universal wave-function overlap’ conjecture, on which Appendix 4.6 relies, applies also to space-time dimensions $D > 2 + 1$, which suggests intrinsic sign problems in these space-time dimensions, including the beloved $D = 3 + 1$.

Another promising direction involves symmetry protected or enriched topological phases. In particular, the sign problem was cured in a number of bosonic SPT Hamiltonians [292–295], and all SPT ground

states can, by definition, be made non-negative in a local basis. Nevertheless, a ‘symmetry protected’ intrinsic sign problem, where *symmetric* local bases are excluded, was recently discovered [296]. Such constraints may be more useful for designing sign-free models than the stronger intrinsic sign problems discussed in this thesis.

5 Outlook

In this thesis we studied the geometric physics of chiral topological phases, and related this physics to the complexity of simulating such phases using quantum Monte Carlo algorithms. The analysis in Sec.2-3 was focused on chiral superfluids and superconductors, and revealed an intricate interplay of symmetry breaking, topology, and geometry. Though we stressed the Higgs mode as an emergent geometry in the relativistic analysis of Sec.2, the fuller non-relativistic treatment in Sec.3 was carried out at energy scales below the Higgs mass, where the emergent geometry simply follows the background geometry (or strain). We believe that there is beautiful physics to be revealed at higher energy scales, where the dynamics of the Higgs mode will be described by a non-relativistic, parity odd, and in part topological, quantum geometry similar to the Girvin-MacDonald-Platzman (GMP) mode in fractional quantum Hall states [297, 29, 30, 33, 45]. In particular, this physics should be important near a nematic phase transition where the spin-2 Higgs mode becomes light, which can be tuned by attractive Landau interactions [145]. We also believe that, through ‘composite fermions’ [15, 147, 148], this will lead to a new description of the GMP mode in paired quantum Hall states, including the illusive particle-hole invariant Pfaffian, and in analogy with the treatment of the GMP mode in Jain states close to half filling [298–301].

Regarding intrinsic sign problems, we believe that the results obtained in Sec.4, as well as in Refs.[75, 76, 5, 296], represent the tip of an iceberg. Concrete extensions of these results were proposed in Sec.4.7. Beyond these, are there intrinsically sign-problematic phases which are not gapped, not topological, or both? Does the physics of high temperature superconductivity, or of dense nuclear matter, imply an intrinsic sign problem, thus accounting for the persistent sign problems observed by QMC practitioners in relevant models? Taking a broader perspective, intrinsic sign problems form a bridge between the notions of phases of matter and computational complexity. This should be contrasted with most results in quantum complexity [302, 303], which are established for classes of Hamiltonians defined by microscopic conditions such as locality, non-frustration, and stoquasticity, as well as energy gap assumptions, or for specific canonical models, but usually not for phases of matter. In fact, refining statements in quantum complexity to the level of phases was the original motivation for the study of intrinsic sign problems [75]. Additional statements regarding the complexity of phases are given by the classification of topological phases which enable universal quantum computation by anyon braiding [219, 97], and the proof that whenever the area law for entanglement entropy holds for a gapped Hamiltonian, it holds in its entire phase [304]. We find this theme to be promising for both the study of many-body quantum systems, and their use as computational devices.

Appendix

Table of Contents

A	Boundary fermions and gravitational anomaly	91
A.1	Boundary fermions in a product geometry	91
A.2	Boundary gravitational anomaly and anomaly inflow	93
A.3	Implication for the p -wave SC	95
B	Emergent Riemann-Cartan geometry: further details	97
B.1	Equivalent forms of S_{RC} and equality to S_{rSF}	97
B.2	Dirac and BdG equations	99
B.3	Equality of path integrals	100
B.4	Explicit formulas for certain geometric quantities	101
B.5	Discrete symmetries	102
B.6	Global structures and obstructions	106
C	Quantization of coefficients for a sum of gravitational Chern-Simons terms	107
D	Calculation of gravitational pseudo Chern-Simons currents	108
E	Perturbative calculation of the relativistic effective action	110
E.1	Single vertex diagrams	112
E.2	Two vertex diagrams	116
F	Non-relativistic geometric quantities and their perturbative expansion	119
G	Odd viscosity at non-zero wave-vector: generalities	120
G.1	Definition and T symmetry	120
G.2	$SO(2)$ and P symmetries	121
G.3	PT symmetry	123
G.4	Frequency dependence and reality conditions	123
G.5	Odd viscosity from Gaussian integration: a technical result	124
H	Effective action and its perturbative expansion	126

H.1	Zeroth order	126
H.2	Second order	128
H.3	Gravitational Chern-Simons term	129
H.4	Additional terms at third order	129
I	Induced action	130
J	Detailed analysis of the microscopic model Eq.(3.8)	133
J.1	Symmetry	133
J.2	Effective action and fermionic Green's function	133
J.3	Fermionic ground state topology	134
J.4	Symmetry breaking and bosonic ground state in the presence of a background metric .	135
J.5	Perturbative expansion	137
K	Further details regarding Eq.(4.2)	139
K.1	Definition of h_0 and ambiguities in its value	139
K.2	The value of h_0 in fermionic phases of matter	140
L	Momentum polarization with non CFT boundaries	141
L.1	CFT finite-size correction in non CFT boundaries	142
L.2	No finite-size correction at finite temperature	146
M	Cutting the torus along an arbitrary vector	146
N	Dealing with accidental degeneracies on the cylinder	146
O	A 'non-local design principle' for chiral topological matter	148
P	Locality and homogeneity of known design principles	149

A Boundary fermions and gravitational anomaly

It is well known that the p -wave SC has localized degrees of freedom on curves in space where the Chern number ν jumps, due to boundaries, or domain walls in Δ or μ , which at low energies are $D = 1 + 1$ chiral Majorana spinors [15]. In this section we derive the action for the boundary spinor in the presence of a space-time dependent order parameter, and describe its gravitational anomaly and corresponding anomaly inflow.

We start by deriving the boundary action in the geometric description in Appendix A.1, then review the relevant facts regarding the boundary gravitational anomaly within the gravitational description in Appendix A.2, and finally translate the results back to the p -wave SC language in Appendix A.3.

The form of the boundary action in both the geometric description (A.8) and in the p -wave SC language (A.17) is not surprising, and within the geometric description the gravitational anomaly and anomaly inflow are well known. It is the implication of gravitational anomaly and anomaly inflow for the p -wave SC, through the emergent geometry described in sections 2.3 and 2.4, which is the result of this section.

A.1 Boundary fermions in a product geometry

We take the space time manifold to be $\mathbb{R} \times \mathbb{R}^2$, and assume that the vielbein has a product form with respect to the spatial coordinate y ,

$$e^A = e^A_\alpha(x^\alpha) dx^\alpha, \quad e^y = o dy, \quad (\text{A.1})$$

where $\alpha, \beta, \dots \in \{t, x\}$ and $A, B, \dots \in \{0, 1\}$ (unlike the notation of section 2.3 where $A, B, \dots \in \{1, 2\}$). To account for the orientation $o = \text{sgn}(\det e^a_\mu)$ of the vielbein explicitly, we assumed e^A_α has a positive orientation, and wrote $e^y = o dy$. To be concrete we take $o = 1$ for now. It follows that the metric also has the product form $ds^2 = g_{\alpha\beta}(x^\alpha) dx^\alpha dx^\beta - dy^2$ where $g_{\alpha\beta} = e^A_\alpha \eta_{AB} e^B_\beta$. The form of the vielbein implies that the LC spin connection only has the nonzero components $\tilde{\omega}_{AB\alpha}$, which only depend on t, x . We also assume that the spin connection only has nonzero components $\omega_{AB\alpha}$ and depends only on t, x . Under these assumptions $c = C_{abc} \varepsilon^{abc} = 0$, and therefore torsion simply drops out from the action, as can be seen from the form (B.8). This is a result of the low dimensionality of the problem. We further assume that the mass has the form of a flat domain wall in the y direction. By this we mean $m = m(y)$ with boundary conditions $m \rightarrow \pm m_0$ as $y \rightarrow \pm\infty$, and $m_0 \neq 0$, which corresponds to an interface between two distinct phases. To be concrete we take $m_0 > 0$ for now. S_{RC} then takes the form

$$S_{\text{RC}} = \frac{1}{2} \int d^3x |e| \bar{\chi} \left[i e^A_\alpha \gamma^A \tilde{D}_\alpha + i \gamma^2 \partial_y - m(y) \right] \chi. \quad (\text{A.2})$$

This separable form implies the decomposition described in [305, 306], which we now apply to the present situation. Defining $a = \partial_y - m(y)$, $a^\dagger = -\partial_y - m(y)$, $P_\pm = \frac{1}{2}(1 \pm i\gamma^2)$, the action takes the form

$$S_{\text{RC}} = \frac{1}{2} \int d^3x |e| \bar{\chi} \left[i e_A^\alpha \gamma^A \tilde{D}_\alpha + a P_+ + a^\dagger P_- \right] \chi. \quad (\text{A.3})$$

The operators $h_+ = a^\dagger a$ and $h_- = a a^\dagger$ are hermitian and non negative. The positive parts of their spectrum coincide. We denote the positive eigenvalues by $\lambda^2 > 0$, including both the discrete and continuous parts of the spectrum, with the corresponding eigenfunctions $\phi_{\lambda,\pm}$ satisfying $h_\pm \phi_{\lambda,\pm} = \lambda^2 \phi_{\lambda,\pm}$. These eigenfunctions of h_\pm are related by $\phi_{\lambda,+} = \frac{1}{\lambda} a^\dagger \phi_{\lambda,-}$, $\phi_{\lambda,-} = \frac{1}{\lambda} a \phi_{\lambda,+}$, where the sign chosen for λ is arbitrary, and for concreteness we take $\lambda > 0$. Each set of eigenfunctions can be assumed to be orthonormal $\int_{-\infty}^{\infty} dy \phi_{\lambda,\pm}^* \phi_{\lambda',\pm} = \delta_{\lambda\lambda'}$. Apart from the positive part of the spectrum, there can also be a unique eigenfunction with eigenvalue zero, a zero mode, for h_+ or h_- but not both. The only candidates are $\phi_{0,\pm}(y) \propto e^{\pm \int_0^y m(s) ds}$, and a zero mode exists when one of these functions is normalizable. With our choice of boundary conditions for m , only $\phi_{0,-}$ is normalizable. In terms of these eigenfunctions, the natural orthogonal decomposition of the spinor χ is

$$\begin{aligned} \chi(x, y, t) &= P_+ \chi(x, y, t) + P_- \chi(x, y, t) \\ &= \sum_{\lambda > 0} [\chi_{\lambda,+}(x, t) \phi_{\lambda,+}(y) + \chi_{\lambda,-}(x, t) \phi_{\lambda,-}(y)] \\ &\quad + \chi_{0,-}(x, t) \phi_{0,-}(y), \end{aligned} \quad (\text{A.4})$$

where $\chi_{\lambda,\pm}$ are spinors of definite chirality, $P_\pm \chi_{\lambda,\pm} = \chi_{\lambda,\pm}$. Inserting this decomposition into (A.3) we obtain

$$\begin{aligned} S_{\text{RC}} &= \frac{1}{2} \int d^2x |e| \overline{\chi_{0,-}} i e_A^\alpha \gamma^A \tilde{D}_\alpha \chi_{0,-} \\ &\quad + \sum_{\lambda > 0} \frac{1}{2} \int d^2x |e| \overline{\chi_\lambda} \left[i e_A^\alpha \gamma^A \tilde{D}_\alpha + \lambda \right] \chi_\lambda, \end{aligned} \quad (\text{A.5})$$

where $\chi_\lambda = \chi_{\lambda,-} + \chi_{\lambda,+}$. Thus the action splits into an infinite sum of actions for independent $D = 1 + 1$ spinors, coupled to RC geometry, which in the $D = 1 + 1$ case is the same as the coupling to Riemannian geometry. The spinor corresponding to the zero mode is chiral, massless, and exponentially localized on the domain wall as can be seen from the expression $\phi_{0,-}(y) \propto e^{-\int_0^y m(s) ds}$. It represents the robust boundary state that exists between two distinct topological phases. The chiral boundary spinor exhibits a gravitational anomaly, which we describe in the following.

All other spinors are non chiral and massive with masses $\lambda \neq 0$. It is useful to think of the eigenvalue problems $h_\pm \phi_{\lambda,\pm} = (-\partial_y^2 + m^2(y) \pm m'(y)) \phi_{\lambda,\pm}$ as one dimensional time independent Schrodinger problems to understand the eigenvalues λ and eigenfunctions $\phi_{\lambda,\pm}$ [305, 306]. Almost all of the massive spinors correspond to delocalized bulk degrees of freedom, with the functions $\phi_{\lambda,\pm}(y)$ corresponding to “scattering states” of the “Hamiltonians” h_\pm . Additionally, there can be a finite number of “bound states” $\phi_{\lambda,\pm}$, in which case χ_λ corresponds to an additional non-chiral boundary state, which is not

robust, and can always be removed by making the domain wall narrower, or the bulk masses $\pm m_0$ smaller.

Since the action splits into a sum of $D = 1 + 1$ fermionic actions and the decomposition (A.4) is orthogonal, the effective action also splits into a sum

$$W_{\text{RC}}[e, \omega] = W_{\text{R}}^{-}[e] + \sum_{\lambda > 0} W_{\text{R}}[e; \lambda], \quad (\text{A.6})$$

where $W_{\text{R}}[e; \lambda]$ is the effective action obtained by integrating over a $D = 1 + 1$ Majorana spinor with mass $\lambda \neq 0$ coupled to Riemannian geometry, and $W_{\text{R}}^{\pm}[e]$ is the effective action obtained by integrating over a $D = 1 + 1$ massless chiral Majorana spinor coupled to Riemannian geometry, with chirality \pm . Above we assumed $m(\pm\infty) = \pm m_0$ with $m_0 > 0$ and $o = 1$. Generalizing slightly, the net chirality of the boundary spinors is given by

$$C = \frac{o}{2} \text{sgn}(m(\infty)) - \frac{o}{2} \text{sgn}(m(-\infty)). \quad (\text{A.7})$$

The action $S_{\text{R}}^{\pm} = \frac{1}{2} \int d^2x |e| \overline{\chi_{0,\pm}} i e_A^{\alpha} \gamma^A \tilde{D}_{\alpha} \chi_{0,\pm}$ for a single chiral Majorana spinor coupled to Riemannian geometry can be simplified by using a *Majorana representation* for the Clifford algebra, as described in appendix B.5.1. In the Majorana representation $\chi_{0,\pm} = \xi v_{\pm}$ where ξ is a single-component *real* Grassmann field and v_{\pm} are the normalized eigenvectors of $i\gamma^2$, $(i\gamma^2)v_{\pm} = \pm v_{\pm}$. The action S_{R}^{\pm} then reduces to

$$S_{\text{R}}^{\pm} = \frac{i}{2} \int d^2x |e| \xi e_{\mp}^{\alpha} \partial_{\alpha} \xi, \quad (\text{A.8})$$

where $e_{\mp}^{\alpha} = e_0^{\alpha} \mp e_1^{\alpha}$.

A.2 Boundary gravitational anomaly and anomaly inflow

The chiral boundary spinor does not couple to the spin connection ω , and therefore does not distinguish the RC background from a Riemannian background described by the vielbein. This can be seen by examining the $1 + 1$ dimensional version of the conservation laws described in section 2.4.2 for the energy-momentum tensor $j_A^{\alpha} = \frac{1}{|e|} \frac{\delta S_{\text{R}}^{\pm}}{\delta e_A^{\alpha}}$ and spin current $j^{AB\alpha} = \frac{1}{|e|} \frac{\delta S_{\text{R}}^{\pm}}{\delta \omega_{AB\alpha}}$ of the boundary spinor. As in section 2.4.2, these follow from the *Diff* and Lorentz gauge symmetries of the “classical” action S_{R}^{\pm} . Since the boundary fermion does not couple to ω , its spin current vanishes, $j^{AB\alpha} = 0$. Therefore (2.53) takes the form

$$j^{[AB]} = 0, \quad (\text{A.9})$$

expressing the symmetry of the boundary energy-momentum tensor, as in Riemannian geometry. The energy-momentum conservation law (2.59) then takes the form $\nabla_{\alpha} j_{\beta}^{\alpha} - j_{\beta}^{\alpha} T_{\gamma\alpha}^{\gamma} = T_{\beta\alpha}^A j_A^{\alpha}$, which reduces

to

$$\tilde{\nabla}_\alpha j^{\alpha\beta} = C_{AB}^{\beta,[AB]} = 0, \quad (\text{A.10})$$

where $\tilde{\nabla}$ is the LC covariant derivative. This is the energy-momentum conservation law in a background Riemannian geometry. The energy-momentum tensor is given explicitly by

$$j_\beta^\alpha = -\frac{i}{2} e_\mp^\alpha \xi \partial_\beta \xi, \quad (\text{A.11})$$

up to a term that vanishes on the equation of motion for ξ , $i e_\mp^\alpha \partial_\alpha \xi + \frac{i}{2} \xi |e|^{-1} \partial_\alpha (|e| e_\mp^\alpha) = 0$, which can also be written in a manifestly covariant form. One can verify that j_β^α is conserved, symmetric, and traceless on the equation of motion.

Chiral Majorana fermions in $D = 1 + 1$ coupled to Riemannian geometry exhibit a gravitational anomaly, which implies that while the “classical” action S_R^\pm is invariant under both *Diff* and Lorentz gauge transformations, the corresponding effective action W_R^\pm is not ³⁵. A physical manifestation of this phenomena is that the “classical” conservation law $\tilde{\nabla}_\alpha j_\beta^\alpha = 0$ is violated quantum mechanically, $\tilde{\nabla}_\alpha \langle j_\beta^\alpha \rangle \neq 0$. The anomaly can be calculated by various techniques [12, 26], the simplest of which is the calculation of a single Feynman graph, as was originally done in [10] for the two dimensional Weyl spinor, and is reviewed in [26] part 5.1.2 for the case of a Majorana-Weyl spinor relevant here. The gravitational anomaly³⁶ is given by [12]

$$\tilde{\nabla}_\alpha \langle j^{\alpha\beta} \rangle = \frac{\nu/2}{96\pi} \frac{1}{|e|} \varepsilon^{y\beta\alpha} \partial_\alpha \tilde{\mathcal{R}}. \quad (\text{A.12})$$

The physical interpretation of the anomaly, within the gravitational theory, is obtained by identifying the right hand side with the energy-momentum inflow from the bulk, (2.90). Then (A.12) can be written as

$$\tilde{\nabla}_\alpha \langle j^{\alpha\beta} \rangle = \langle J^{y\beta} \rangle, \quad (\text{A.13})$$

which, together with the bulk conservation equation (2.59), is just the statement of energy-momentum conservation for a system with a boundary. This is the anomaly inflow mechanism, recasting what appears to be energy-momentum non-conservation in a $D = 1 + 1$ system, as energy-momentum con-

³⁵ W_R^\pm is an example for the nonlocal boundary functional F discussed in section 2.5.3.

³⁶There are a few ambiguities in describing what the gravitational anomaly is from an intrinsic boundary point of view. First, there is the issue of covariant versus consistent anomalies which also exists in gauge anomalies [12]. See also [25] and part 2 of [307] for a short review. Then, for the consistent gravitational anomaly, there is the issue of Lorentz anomalies versus Einstein (*Diff*) anomalies where one can obtain an effective boundary action that is invariant under local Lorentz transformations but not under *Diff*, or vice versa [12]. It is also useful to discuss linear combinations of the Einstein and Lorentz anomalies, related to the symmetry of the effective action under the Lorentz-covariant *Diff* action (2.57), see part 6.3 of [26]. All of these ambiguities are resolved when calculating the boundary energy-momentum tensor within the anomaly inflow mechanism: the bulk gCS term contributes to the boundary energy-momentum tensor, assuring it is symmetric and covariant, so that the physically relevant gravitational anomaly is the covariant Einstein anomaly [25], which is what we refer to here as “the gravitational anomaly”.

servation in a $D = 2 + 1$ system with a boundary.

A.3 Implication for the p -wave SC

Let us now apply the above to the p -wave SC with a flat domain wall in the chemical potential, $\mu(y)$, which physically represents a fixed chemical potential and an additional y -dependent electric potential. To obtain an emergent geometry which is a product geometry, we take the order parameter to be of the form $\Delta = (\Delta^x, \Delta^y) = \Delta_0 e^{i\theta(t,x)} (1 + f(t, x), \pm i)$ ³⁷ with $\Delta_0 > 0$ and small f . We also assume that $A_y = 0$ and A_t, A_x are functions of t, x . This corresponds to a perturbation of the $p_x \pm ip_y$ configuration. Note that assuming $A_y = 0$ involves a partial $U(1)$ gauge fixing, leaving only y independent gauge transformations $\alpha(t, x)$. These are the $U(1)$ gauge transformations that will be considered in this subsection. After further $U(1)$ gauge fixing such that $\theta \mapsto 0$, using a gauge transformation $\alpha(t, x) = -\theta(t, x)/2$ ³⁸, the inverse vielbein will be of the form

$$e_a^\mu = \begin{pmatrix} 1 & 0 & 0 \\ 0 & 1 + f(t, x) & 0 \\ 0 & 0 & \pm 1 \end{pmatrix}, \quad (\text{A.14})$$

so the vielbein is of the product form (A.1) with $o = \pm 1$. The corresponding inverse metric is given by

$$g^{\mu\nu} = \begin{pmatrix} 1 & 0 & 0 \\ 0 & -(1 + f(t, x))^2 & 0 \\ 0 & 0 & -1 \end{pmatrix}. \quad (\text{A.15})$$

We will also need the Ricci scalar for this metric,

$$\tilde{\mathcal{R}} = \frac{2((1 + f)\partial_t^2 f - 2(\partial_t f)^2)}{(1 + f)^2}. \quad (\text{A.16})$$

Recalling that μ determines the bulk masses m_n , we can use the formula $\nu = \frac{1}{2} \sum_{n=1}^4 o_n \text{sgn}(m_n)$ for the Chern number in terms of the low energy data, and (A.7), to express the net chirality of the boundary spinors as $C = \sum_{n=1}^4 C_n = \Delta\nu$, where $C_n = \frac{o_n}{2} \text{sgn}(m_n(y = \infty)) - \frac{o_n}{2} \text{sgn}(m(y = -\infty))$ and $\Delta\nu = \nu(y = \infty) - \nu(y = -\infty)$. This relation between the boundary net chirality C and the Chern number difference $\Delta\nu$ is the well known bulk-boundary correspondence. It can be derived from index theorems as described in [27], but in the following we will place it on a more physical footing by describing it as a consequence of energy-momentum conservation. Let us now rewrite the action (A.8) in terms of the p -wave SC quantities and in physical units (without setting the emergent speed of light Δ_0 to 1, but

³⁷Assuming that μ depends on y but Δ is independent of y may not be self consistent. Nevertheless, it is a simple ansatz that allows for a description of the boundary fermion and its anomaly, which is fixed within a topological phase [15].

³⁸Here we are explicitly assuming that there are no vortices, such that $\alpha = -\theta/2$ is a gauge transformation.

with $\hbar = 1$),

$$S_e^\pm = \frac{i}{2} \int dt dx \tilde{\xi} (\partial_t \mp |\Delta^x(t, x)| \partial_x) \tilde{\xi}. \quad (\text{A.17})$$

Here $|\Delta^x| = \Delta_0 (1 + f)$ and $\tilde{\xi} = |e|^{1/2} \xi$ is a chiral Majorana spinor *density* from the geometric point of view, but a chiral Majorana spinor from the physical flat space point of view. As an operator $\tilde{\xi}$ satisfies $\{\tilde{\xi}(x_1), \tilde{\xi}(x_2)\} = \delta(x_1 - x_2)$. We see that $|\Delta^x|$ acts as a space-time dependent velocity for the boundary fermions, which reduces to a constant Δ_0 in the $p_x \pm ip_y$ configuration. Note that both fields $|\Delta^x|, \tilde{\xi}$ are uncharged under $U(1)$. This is clear for $|\Delta^x|$, and to see this explicitly for $\tilde{\xi}$ we relate it to the original spin-less fermion ψ and the (phase of the) order parameter Δ ,

$$\psi(t, x, y) \propto \tilde{\xi}(t, x) e^{i\theta(t, x)/2} \phi_{0,\pm}(y) + \dots \quad (\text{A.18})$$

where $\phi_{0,\pm}(y) \propto e^{\pm \int_0^y m(s) ds}$ was defined in Appendix A.1 and the dots represent the massive bulk modes and additional non robust massive boundary modes. From this expression it is clear that $\tilde{\xi}$ is uncharged even though ψ is.

Let us now consider the energy-momentum conservation law for the boundary. The expression $\tilde{\nabla}_\alpha \langle j_\beta^\alpha \rangle = 0$ involves the covariant derivative, and is therefore inappropriate from the p -wave SC point of view, where space-time is flat and e is just the order parameter and has no geometric role. We already described how to interpret covariant energy-momentum conservation laws from the flat space-time point of view in section 2.4.1.2, where we studied the bulk conservation laws. Here we simply repeat the procedure. We first relate the energy-momentum tensor j_β^α to the canonical boundary (or edge) energy-momentum tensor $t_{e\beta}^\alpha$, and write it in terms of $\tilde{\xi}$

$$\begin{aligned} t_{e\beta}^\alpha &= -|e| j_\beta^\alpha = \frac{i}{2} e_\mp^\alpha \tilde{\xi} \partial_\beta \tilde{\xi} \\ &= \begin{cases} \frac{i}{2} \tilde{\xi} \partial_\beta \tilde{\xi} & \alpha = t \\ \mp \frac{i}{2} |\Delta^x(t, x)| \tilde{\xi} \partial_\beta \tilde{\xi} & \alpha = x \end{cases}. \end{aligned} \quad (\text{A.19})$$

This is the correct notion of energy and momentum from the physical flat space-time point of view. Note that the relation between $t_{e\beta}^\alpha$ and j_β^α is the same as for the bulk quantities (2.47), and that since $\tilde{\xi}$ is uncharged the canonical energy-momentum tensor $t_{e\beta}^\alpha$ is automatically $U(1)$ -covariant. We then write the conservation law $\tilde{\nabla}_\alpha \langle j_\beta^\alpha \rangle = 0$ in terms of $t_{e\beta}^\alpha$ and using partial derivatives as $\partial_\alpha t_{e\beta}^\alpha + \frac{i}{2} \tilde{\xi} \partial_\alpha \tilde{\xi} \partial_\beta e_\mp^\alpha = 0$, or more explicitly,

$$\partial_\alpha t_{e\beta}^\alpha \mp \frac{i}{2} \tilde{\xi} \partial_x \tilde{\xi} \partial_\beta |\Delta^x| = 0. \quad (\text{A.20})$$

This is just a special case of the usual conservation law (2.34) for the canonical energy-momentum tensor. As usual, it describes the space-time dependence of the background field $|\Delta^x|$ as a source of energy-momentum for the boundary fermion $\tilde{\xi}$. This is the “classical” analysis of energy momentum-

conservation for the boundary fermion. Quantum mechanically, this equation acquires a correction due to the anomaly and the presence of the bulk. Translating the anomaly equation (A.12) to the flat space-time point of view, we obtain

$$\partial_\alpha \langle t_{e\beta}^\alpha \rangle \mp \frac{i}{2} \langle \tilde{\xi} \partial_x \tilde{\xi} \rangle \partial_\beta |\Delta^x| = -\frac{\nu}{192\pi} g_{\beta\gamma} \varepsilon^{y\gamma\alpha} \partial_\alpha \tilde{\mathcal{R}}. \quad (\text{A.21})$$

As in the gravitational point of view, the right hand side is actually the inflow of energy-momentum from the bulk (2.97),

$$\partial_\alpha \langle t_{e\beta}^\alpha \rangle \mp \frac{i}{2} \langle \tilde{\xi} \partial_x \tilde{\xi} \rangle \partial_\beta |\Delta^x| = \langle t_{\text{cov}\beta}^y \rangle. \quad (\text{A.22})$$

This equation expresses the conservation of energy ($\beta = t$) and x -momentum ($\beta = x$) on the domain wall. Along with the bulk conservation equation (2.39), $\partial_\mu \langle t_{\text{cov}\nu}^\mu \rangle = \frac{1}{2} \langle \psi^\dagger \partial_j \psi^\dagger \rangle D_\nu \Delta^j + h.c + F_{\nu\mu} \langle J^\mu \rangle$ ³⁹, it expresses the sense in which energy-momentum is conserved in a p -wave SC in the presence of a boundary, or domain wall.

We thus obtain the equation $\Delta\nu = C$, usually referred to as bulk boundary correspondence, as a direct consequence of bulk+boundary energy-momentum conservation in the presence of a space-time dependent order parameter.

B Emergent Riemann-Cartan geometry: further details

B.1 Equivalent forms of S_{RC} and equality to S_{rSF}

It is useful to write the action S_{RC} in a few equivalent forms [12, 156]. To pass between these equivalent forms one only needs the identity

$$\partial_\nu (|e| e_a^\nu) = |e| \tilde{\omega}_{ab}^b \quad (\text{B.1})$$

relating e to the LC spin connection, and the following identity, which holds for any spin connection ω but relies on the property $\gamma^a \gamma^b \gamma^c = i\varepsilon^{abc}$ of γ matrices in 2+1 dimensions,

$$\begin{aligned} ie_a^\mu \gamma^a \omega_\mu &= \frac{1}{4} ie_a^\mu \omega_{bc\mu} \{ \gamma^a, \Sigma^{bc} \} + \frac{1}{4} ie_a^\mu \omega_{bc\mu} [\gamma^a, \Sigma^{bc}] \\ &= -\frac{1}{4} \omega_{abc} \varepsilon^{abc} + \frac{1}{2} i \omega_{ab}^b \gamma^a. \end{aligned} \quad (\text{B.2})$$

The most explicit form of the action is

$$S_{\text{RC}} = \frac{1}{2} \int d^{2+1}x |e| \bar{\chi} \left[\frac{1}{2} ie_a^\mu \gamma^a \overleftrightarrow{\partial}_\mu - \frac{1}{4} \omega_{abc} \varepsilon^{abc} - m \right] \chi, \quad (\text{B.3})$$

³⁹We note that the domain wall acts as a source for y -momentum, which is included in the term $F_{\nu\mu} \langle J^\mu \rangle$ since $\mu(y)$ is part of the electric potential A_t .

where the derivatives act only on the spinors. Here we see that in 2+1 dimensions the spin connection only enters through the scalar $\omega_{abc}\varepsilon^{abc}$ as a correction to the mass. It also makes it rather simple to see why S_{RC} is equal to S_{rSF} from (2.25),

$$\begin{aligned}
S_{\text{RC}} &= \frac{1}{2} \int d^{2+1}x |e| \bar{\chi} \left[\frac{1}{2} i e_a^\mu \gamma^a \overleftrightarrow{\partial}_\mu - \frac{1}{4} \omega_{abc} \varepsilon^{abc} - m \right] \chi \\
&= \frac{1}{2} \int d^{2+1}x \Psi^\dagger \gamma^0 \left[\frac{1}{2} i e_a^\mu \gamma^a \overleftrightarrow{\partial}_\mu - \frac{1}{4} \omega_{abc} \varepsilon^{abc} - m \right] \Psi \\
&= \frac{1}{2} \int d^{2+1}x \Psi^\dagger \gamma^0 \left[\frac{i}{2} \gamma^0 \overleftrightarrow{\partial}_t + \frac{1}{2} i e_A^j \gamma^A \overleftrightarrow{\partial}_j + A_t - m \right] \Psi \\
&= \frac{1}{2} \int d^{2+1}x \Psi^\dagger \begin{pmatrix} \frac{i}{2} \overleftrightarrow{\partial}_t + A_t - m & \frac{1}{2} \Delta^j \overleftrightarrow{\partial}_j \\ -\frac{1}{2} \Delta^{j*} \overleftrightarrow{\partial}_j & \frac{i}{2} \overleftrightarrow{\partial}_t - A_t + m \end{pmatrix} \Psi \\
&= \frac{1}{2} \int d^{2+1}x \Psi^\dagger \begin{pmatrix} i\partial_t - m + A_t & \frac{1}{2} \{\Delta^j, \partial_j\} \\ -\frac{1}{2} \{\Delta^{j*}, \partial_j\} & i\partial_t + m - A_t \end{pmatrix} \Psi \\
&= S_{\text{rSF}},
\end{aligned} \tag{B.4}$$

where we have used the dictionary (2.27), and also integrated by parts. In going from the third to the fourth line we have reinstated the emergent speed of light $c_{\text{light}} = \frac{\Delta_0}{\hbar}$, but kept $\hbar = 1$. This completes that proof of the equality $S_{\text{rSF}} = S_{\text{RC}}$, which was stated and explained in section 2.3.

Before we move on, an important comment is in order. Since A_j does not appear in S_{rSF} , it is clear that for the above equality of actions only the identification $\omega_t = -2A_t \Sigma^{12}$ is required, rather than the full $\omega_\mu = -2A_\mu \Sigma^{12}$ of (K.1). Accordingly, ω_j does not appear in S_{RC} when ω, e are both spatial ($\omega_{0A\mu} = 0, e_0^\mu = \delta_t^\mu$), because then

$$\omega_{abc} \varepsilon^{abc} = 2e_0^\mu \omega_{12\mu} = 2\omega_{12t}. \tag{B.5}$$

Thus, for the equality of actions $S_{\text{rSF}} = S_{\text{RC}}$ it is not required that $\omega_j = -2A_j \Sigma^{12}$. Nevertheless, we are actually identifying two QFTs as equal, and there is more to a QFT than its classical action. One must also compare symmetries, observables, and path integral measures (the latter is discussed in appendix B.3). The mapping of symmetries and observables is the subject of section 2.4, and only holds if the full identification $\omega_\mu = -2A_\mu \Sigma^{12}$ is made:

In section 2.4.2.2, we identify the physical $U(1)$ symmetry group with the $Spin(2)$ subgroup of $Spin(1, 2)$ in Riemann-Cartan geometry. For this reason A_μ , which is $U(1)$ connection, really maps to a $Spin(2)$ connection in the geometric point of view, even if certain components of it do not appear in the action S_{rSF} .

In section 2.4.2.1 we discuss the mapping of observables. In particular, even though A_j disappears from the action in the relativistic limit, it does not disappear from the energy-momentum tensor (see (2.47), (2.48), where the derivative D_μ contains A_μ). Moreover, as explained below (2.66), even though the order parameter Δ corresponds to the spatial vielbein in (2.27), in order to obtain the expectation

value of full energy-momentum tensor we must take derivatives of the effective action with respect to all components of the vielbein, not only the spatial ones obtained from Δ . This corresponds to adding to S_{rSF} a fictitious background field e_0^μ which is set to zero after the expectation value is computed. In the presence of e_0^μ the potential A_t generalizes to $e_0^\mu A_\mu$, and so A_j does appear in S_{rSF} . Accordingly, with a general e_0^μ we see from (B.5) that ω_{12j} appears in S_{RC} . The equality $S_{\text{RC}} = S_{\text{rSF}}$ in the presence of e_0^μ is then obtained only if $\omega_j = -2A_j\Sigma^{12}$.

To close this discussion, we note that the identification of Δ^j as a spatial vielbein and A_μ as a $Spin(2)$ connection actually holds beyond the relativistic limit, though this was not discussed in Sec.2. Beyond the relativistic limit A_j will appear in both the action and observables, and identifying the full $\omega_{12\mu}$ with A_μ will be crucial also at the level of the fermionic action.

Going back to equivalent forms of S_{RC} , if we wish to isolate the effect of torsion, we can also write

$$S_{\text{RC}} = \frac{1}{2} \int d^{2+1}x |e| \bar{\chi} \left[\frac{1}{2} i e_a^\mu \gamma^a \overleftrightarrow{\partial}_\mu - \frac{1}{4} \tilde{\omega}_{abc} \varepsilon^{abc} - \frac{1}{4} C_{abc} \varepsilon^{abc} - m \right] \chi, \quad (\text{B.6})$$

or

$$S_{\text{RC}} = \frac{1}{2} \int d^{2+1}x |e| \bar{\chi} \left[\frac{1}{2} i e_a^\mu \left(\gamma^a \tilde{D}_\mu - \overleftarrow{\tilde{D}_\mu} \gamma^a \right) - \left(m + \frac{1}{4} c \right) \right] \chi, \quad (\text{B.7})$$

where we see that in 2+1 dimensions torsion enters only through the scalar $c = C_{abc} \varepsilon^{abc}$ as a correction to the mass. One can also integrate by parts in order to obtain a form from which it is simple to derive the equation of motion,

$$\begin{aligned} S_{\text{RC}} &= \frac{1}{2} \int d^{2+1}x |e| \bar{\chi} \left[i e_a^\mu \gamma^a \tilde{D}_\mu - \frac{1}{4} C_{abc} \varepsilon^{abc} - m \right] \chi \\ &= \frac{1}{2} \int d^{2+1}x |e| \bar{\chi} \left[i e_a^\mu \gamma^a D_\mu - \frac{1}{2} i C_{ab}^b \gamma^a - m \right] \chi. \end{aligned} \quad (\text{B.8})$$

The form in the first equation is special to 2+1 dimensions, but the form in the second equation holds in any dimension.

B.2 Dirac and BdG equations

Since the p -wave SF action is equal to S_{RC} in the relativistic limit, and the fermions χ and Ψ are related simply, the equation of motion for χ , which is the Dirac equation in RC background, maps to the equation of motion for Ψ , which is the BdG equation (in the relativistic limit).

The equation of motion for the Majorana spinor χ needs to be derived carefully, because χ is Grassmann valued and $\bar{\chi} = \chi^T \gamma^0$ cannot be treated as independent of χ . Nevertheless, if the operator between χ^T and χ is particle-hole symmetric, the equations of motion are the same as those of a Dirac

spinor, which are easy to read from (B.8),

$$0 = \left[i e_a^\mu \gamma^a D_\mu - \frac{1}{2} i C_{ab}^b \gamma^a - m \right] \chi. \quad (\text{B.9})$$

This is the Dirac equation in RC background. When inserting $\chi = |e|^{-1/2} \Psi$ and using the identity

$$\partial_\mu |e| = |e| \Gamma_{\mu\rho}^\rho = |e| \tilde{\Gamma}_{\mu\rho}^\rho, \quad (\text{B.10})$$

we obtain

$$0 = \left[i \gamma^\mu \left(D_\mu - \frac{1}{2} \Gamma_{\mu\rho}^\rho \right) - \frac{1}{2} i C_{ab}^b \gamma^a - m \right] \Psi. \quad (\text{B.11})$$

The expression in brackets is the appropriate covariant derivative for a spinor density of weight 1/2 [154], which is what $\Psi = |e|^{1/2} \chi$ is from the geometric point of view. Simplifying this equation using (B.1) and (B.10), we arrive at

$$0 = \left[\frac{1}{2} i \gamma^a \{ e_a^\mu, \partial_\mu \} - \frac{1}{4} \omega_{abc} \varepsilon^{abc} - m \right] \Psi. \quad (\text{B.12})$$

By using the dictionary (2.27) and multiplying by $\gamma^0 = \sigma^z$ this reduces to

$$0 = \begin{pmatrix} i \partial_t + A_t - m & \frac{1}{2} \{ \Delta^j, \partial_j \} \\ -\frac{1}{2} \{ \Delta^{j*}, \partial_j \} & i \partial_t - A_t + m \end{pmatrix} \Psi, \quad (\text{B.13})$$

which is the BdG equation in the relativistic limit. Thus the BdG equation in the relativistic limit is not quite the Dirac equation, because Ψ is a spinor density, though it is the Dirac equation for the spinor χ .

B.3 Equality of path integrals

In appendix B.1 we showed that the action for the p -wave SF in the relativistic limit, is equal to the action for a Majorana fermion coupled to RC geometry. To conclude that the corresponding fermionic path integrals are equal, we also need to verify that the path integral measure for the p -wave SF is equal to that of the Majorana fermion in RC background. For the p -wave SF (2.24), the path integral measure is written formally as $D\psi^\dagger D\psi = \prod_x d\psi^\dagger(x) d\psi(x)$ where x runs over all points in space time. In the BdG formalism we work with the Nambu (or Majorana) spinor $\Psi = (\psi, \psi^\dagger)^T$, in terms of which the measure takes the form $D\psi^\dagger D\psi = D\Psi$. As described in section 2.3 and appendix B.2, from the geometric point of view Ψ is a Majorana spinor density of weight 1/2, and $\chi = |e|^{-1/2} \Psi$ is a Majorana spinor. In terms of the spinor χ , the measure takes the form $D\Psi = D(|e|^{1/2} \chi)$, which is the correct measure for a matter field in curved background [242, 243, 34]. With this measure, the path integral over the Majorana spinor χ formally computes functional pfaffians as in flat space, $e^{iW_M[A]} = \int D(|e|^{1/2} \chi) e^{\frac{i}{2} \int d^d x |e| \chi^T A \chi} = \text{Pf}(iA) = \sqrt{\text{Det} iA}$, where A is an antisymmetric hermitian

operator with respect to the inner product $\langle f, g \rangle = \int d^d x |e| f^\dagger A g$, and the determinant Det is defined by the product of eigenvalues. For a Dirac spinor χ the fermionic path integral formally computes functional determinants, $e^{iW_D[D]} = \int D(|e|^{1/2} \chi^\dagger) D(|e|^{1/2} \chi) e^{i \int d^d x |e| \chi^\dagger D \chi} = \text{Det}(iD)$, where D is hermitian. In particular, the effective action for a Majorana spinor is half that of a Dirac spinor with the same operator, $W_M[A] = \frac{1}{2} W_D[A]$.

B.4 Explicit formulas for certain geometric quantities

Using $\tilde{\omega}_{b\mu}^a = e_\alpha^a \left(\partial_\mu e_b^\alpha + \tilde{\Gamma}_{\beta\mu}^\alpha e_b^\beta \right)$ we can calculate the LC spin connection for a vielbein of the form

$$e_a^\mu = \frac{1}{\Delta_0} \begin{pmatrix} \Delta_0 & 0 & 0 \\ 0 & \text{Re}(\Delta^x) & \text{Re}(\Delta^y) \\ 0 & \text{Im}(\Delta^x) & \text{Im}(\Delta^y) \end{pmatrix} = \begin{pmatrix} 1 & & \\ & e_A^j & \end{pmatrix} \quad (\text{B.14})$$

that occurs in the p -wave SC,

$$\begin{aligned} \tilde{\omega}_{A0t} &= 0, \\ \tilde{\omega}_{A0j} &= e_A^i \frac{1}{2} \partial_t g_{ij}, \\ \tilde{\omega}_{12t} &= \frac{1}{2} \varepsilon^{AB} e_{Ai} \partial_t e_B^i = -\frac{1}{2} \frac{1}{\det(e)} \varepsilon^{ij} e_{Ai} \partial_t e_j^A, \\ \tilde{\omega}_{12j} &= \frac{1}{2} \left(\varepsilon^{AB} e_{Ai} \partial_j e_B^i - \frac{1}{\det(e)} \varepsilon^{kl} \partial_k g_{lj} \right) = -\frac{1}{2} \frac{1}{\det(e)} \varepsilon^{kl} (e_{Ak} \partial_j e_l^A + \partial_k g_{lj}). \end{aligned} \quad (\text{B.15})$$

In terms of the parameterization $\Delta = e^{i\theta} (|\Delta^x|, e^{i\phi} |\Delta^y|)$, as in section 2.2.2, the $SO(2)$ part can be written as

$$\begin{aligned} \tilde{\omega}_{12t} &= o \left[\frac{1}{2} \cot |\phi| \partial_t \log \frac{|\Delta^y|}{|\Delta^x|} - \frac{1}{2} \partial_t |\phi| \right] - \partial_t \theta, \\ \tilde{\omega}_{12x} &= o \left[\frac{|\Delta^y|}{|\Delta^x|} \frac{\cot |\phi|}{\sin |\phi|} \partial_y |\phi| + \left(\frac{1}{\sin^2 |\phi|} - 1 \right) \partial_x |\phi| + \cot |\phi| \partial_x \log |\Delta^y| + \frac{1}{\sin |\phi|} \frac{|\Delta^y|}{|\Delta^x|} \partial_y \log |\Delta^x| \right] - \partial_x \theta, \\ \tilde{\omega}_{12y} &= o \left[-\frac{|\Delta^x|}{|\Delta^y|} \frac{\cot |\phi|}{\sin |\phi|} \partial_x |\phi| - \left(\frac{1}{\sin^2 |\phi|} \right) \partial_y |\phi| - \cot |\phi| \partial_y \log |\Delta^x| - \frac{1}{\sin |\phi|} \frac{|\Delta^x|}{|\Delta^y|} \partial_x \log |\Delta^y| \right] - \partial_y \theta, \end{aligned} \quad (\text{B.16})$$

where $o = \text{sgn} \phi$ is the orientation. Note that the terms in square brackets only depend on the metric degrees of freedom $|\phi|, |\Delta^x|, |\Delta^y|$, and that this reduces to $\tilde{\omega}_{12\mu} = -\partial_\mu \theta$ in the $p_x \pm ip_y$ configuration. We can then obtain explicit formulas for the contorsion using $\omega_{ab\mu} = -2A_\mu (\delta_a^1 \delta_b^2 - \delta_b^1 \delta_a^2)$ and $C_{ab\mu} =$

$$\omega_{ab\mu} - \tilde{\omega}_{ab\mu},$$

$$\begin{aligned} C_{12\mu} &= -2A_\mu - \tilde{\omega}_{12\mu}, \\ C_{A0j} &= -e_A^i \frac{1}{2} \partial_t g_{ij}. \end{aligned} \tag{B.17}$$

We also consider the quantity $c = \varepsilon^{abc} C_{abc}$ which appears in certain forms of the action S_{RC} (2.26), and of the effective action (2.69). Evaluated in terms of Δ and A we find

$$\frac{1}{2}c = C_{12t} = \partial_t \theta - 2A_t - o \left[\frac{1}{2} \cot |\phi| \partial_t \log \frac{|\Delta^y|}{|\Delta^x|} - \frac{1}{2} \partial_t |\phi| \right], \tag{B.18}$$

which reduces to $\frac{1}{2}c = D_t \theta = \partial_t \theta - 2A_t$ in the $p_x \pm ip_y$ configuration.

B.5 Discrete symmetries

B.5.1 Charge conjugation and particle-hole

Our conventions for gamma matrices and spinors follow appendix B of [154]. In three dimensions, if the matrices γ^a define a representation of the Clifford algebra then $-(\gamma^a)^T$ define an equivalent representation. The matrix \mathcal{C} relating the two representations by $-(\gamma^a)^T = \mathcal{C}_b^a \gamma^b = \mathcal{C} \gamma^a \mathcal{C}^{-1}$ is called charge conjugation. In our representation $\gamma^0 = \sigma^z$, $\gamma^1 = -i\sigma^x$, $\gamma^2 = i\sigma^y$, one finds that $\mathcal{C} = \sigma^y$ up to a phase and $\mathcal{C}_b^a = \text{diag}[-1, -1, 1]$, so we see that \mathcal{C} is unitary and $\mathcal{C}^2 = 1$. Likewise, the matrices $(\gamma^a)^\dagger$ also define an equivalent representation, and are therefore related by $(\gamma^a)^\dagger = \mathcal{D}_b^a \gamma^b = \mathcal{D} \gamma^a \mathcal{D}^{-1}$ where \mathcal{D} is the Dirac conjugation. In any unitary representation $\mathcal{D} = i\gamma^0$ up to a phase and $\mathcal{D}_b^a = \text{diag}[1, -1, -1]$. Using \mathcal{D} we define the conjugate spinor $i\bar{\Psi} = \Psi^\dagger \mathcal{D}$. We also note that $-(\gamma^a)^* = \mathcal{B}_b^a \gamma^b = \mathcal{B} \gamma^a \mathcal{B}^{-1}$ with $\mathcal{B} = \mathcal{D} \mathcal{C}$, which will also show up in our discussion of time reversal. In our representation, $\mathcal{B} = \sigma^x$ and $\mathcal{B}_b^a = \text{diag}[-1, 1, -1]$.

A spinor Ψ is called a Majorana spinor if it satisfies the reality condition $i\bar{\Psi} = \Psi^T \mathcal{C}$, which can also be written as $\Psi^\dagger \mathcal{B} = \Psi^T$. In our representation this condition reads $\Psi^\dagger = \Psi^T \sigma^x$, which is the reality condition satisfied by the Nambu spinor $\Psi = (\psi, \psi^\dagger)^T$. We see that the Nambu spinor is a Majorana spinor. The reality condition can also be written as $\Psi = P \Psi$ where $P = \sigma^x K$ and K is the complex conjugation. P is usually referred to as a particle-hole symmetry [107], and it is anti-unitary and $P^2 = 1$. Eventually, the particle-hole symmetry of the p -wave SC maps to the charge conjugation symmetry of the relativistic Majorana fermion, with the differences between the two being a matter of convention.

For any Hamiltonian $H = \frac{1}{2} \int d^2x \Psi^\dagger(x) H_{\text{BdG}} \Psi(x)$, the BdG Hamiltonian H_{BdG} can be assumed to satisfy a reality condition, $\{H_{\text{BdG}}, P\} = 0$. An example is given by (2.25). To make a similar statement for actions, where ψ, ψ^\dagger are Grassmann valued, we need to clarify how the conjugation K acts on the Grassmann algebra generated ψ, ψ^\dagger . This is defined by $K\psi = \psi^\dagger$, $K\psi^\dagger = \psi$, anti-linearity, and a reversal of the ordering of Grassmann numbers. For example, $K(\psi\psi^\dagger) = K\psi^\dagger K\psi = \psi\psi^\dagger$, $K(i\psi) = -i\psi^\dagger$. It is under this complex conjugation that a fermionic action, such as (2.24), is “real”, $K(S_{\text{SF}}[\psi, \psi^\dagger, \Delta, A]) = S_{\text{SF}}[\psi, \psi^\dagger, \Delta, A]$, and it is due to this reality of S_{SF} that we expect to obtain a real effective action after

integrating out the fermions [308]. Then, for any action $S = \frac{1}{2} \int d^{2+1}x \Psi^\dagger(x) S_{\text{BdG}} \Psi(x)$, the operator S_{BdG} can then be assumed to satisfy $\{S_{\text{BdG}}, P\} = 0$, and an example is given by the Dirac operator in (B.8).

When working with Majorana fermions it is useful to use gamma matrices γ^a that form a *Majorana representation* [154], which means that γ^a are all imaginary. In a Majorana representation $\Psi^\dagger \mathcal{B} = \Psi^T$ simplifies to $\Psi^\dagger = \Psi^T$, so a Majorana spinor in a Majorana representation has real components. To obtain a Majorana representation from our representation we change basis in the space of spinors using the unitary matrix $U = \frac{1}{\sqrt{2}} \begin{pmatrix} 1 & 1 \\ -i & i \end{pmatrix}$. Then $\gamma^a \mapsto \tilde{\gamma}^a = U \gamma^a U^\dagger$ and $\Psi \mapsto \tilde{\Psi} = U \Psi$. Explicitly, $\tilde{\gamma}^0 = -\sigma^y$, $\tilde{\gamma}^1 = -i\sigma^z$, $\tilde{\gamma}^2 = -i\sigma^x$, and the Nambu spinor $\Psi = (\psi, \psi^\dagger)^T$ maps to $\tilde{\Psi} = \begin{pmatrix} \tilde{\Psi}_1 \\ \tilde{\Psi}_2 \end{pmatrix} = \frac{1}{\sqrt{2}} \begin{pmatrix} \psi + \psi^\dagger \\ \frac{1}{i}(\psi - \psi^\dagger) \end{pmatrix}$, where $\tilde{\Psi}_1, \tilde{\Psi}_2$ are both real as Grassmann valued fields. As operators $\tilde{\Psi}_1, \tilde{\Psi}_2$ are hermitian and $\{\tilde{\Psi}_i, \tilde{\Psi}_j\} = \delta_{ij}$, so they are *Majorana operators* in the sense of [227]. In the Majorana representation H_{BdG} is imaginary and antisymmetric, and so is S_{BdG} .

B.5.2 Spatial reflection and time reversal in the p -wave superfluid

In section 2.4.1 we discussed the sense in which energy, momentum, and angular momentum are conserved in a p -wave SF, which followed from the symmetry of the p -wave SF action under space-time translations and spatial rotations. There are also discrete (or large) space-time transformations which are of interest. Spatial reflections reverse the orientation of space, and are generated by a single arbitrary reflection, which we take to be $R : y \mapsto -y$, followed by the spatial rotations and translations described previously. R acts naturally on the fields ψ, Δ, A :

$$\begin{aligned} \psi(y) &\mapsto \psi(-y), \\ (\Delta^x, \Delta^y)(y) &\mapsto (\Delta^x, -\Delta^y)(-y), \\ (A_t, A_x, A_y)(y) &\mapsto (A_t, A_x, -A_y)(-y), \end{aligned} \tag{B.19}$$

where we suppressed the dependence on the coordinated t, x which do not transform. One can verify that R is a symmetry of the p -wave SF action (2.24). The best way to understand these transformations is to identify the fields as space-time tensors: ψ is a scalar, $\Delta^j \partial_j$ is a vector field, and $A_\mu dx^\mu$ is a differential 1-form. The above transformation laws are then a special case of how space-time transformations act on space-time tensors, by the pullback/push forward.

Time reversal transformations reverse the orientation of time, and are generated by a single arbitrary time reversal, which we take to be $T : t \mapsto -t$, followed by the time translations described previously. The action of T on the fields includes the transformation laws analogous to (B.19), but additionally involves a complex conjugation, as follows from the Schrodinger equation in the Fock space $i\partial_t |\Omega(t)\rangle = H(t; A, \Delta) |\Omega(t)\rangle$. In our case $H(t; A, \Delta)$ is the p -wave SF Hamiltonian (2.23), in

a notation that stresses the time dependence through the background fields. On the Fock space the complex conjugation is the usual complex conjugation of coefficients in the position basis, defined by $K\psi(x, y)K^{-1} = \psi(x, y)$, $K\psi^\dagger(x, y)K^{-1} = \psi^\dagger(x, y)$, $K|0\rangle = |0\rangle$ and anti-linearity. Acting with it on the p -wave SF Hamiltonian (2.23) we find that the action of T on the background fields Δ, A is

$$\begin{aligned} (\Delta^x, \Delta^y)(t) &\mapsto \Delta^T(t) = (\Delta^x, \Delta^y)^*(-t), \\ (A_t, A_x, A_y)(t) &\mapsto A^T(t) = -(-A_t, A_x, A_y)(-t), \end{aligned} \quad (\text{B.20})$$

where we suppressed the dependence on the coordinates x, y which do not transform. If $|\Omega(t)\rangle$ satisfies the Schrodinger equation with Hamiltonian $H(t; A, \Delta)$ and initial condition $|\Omega\rangle$ then $K|\Omega(-t)\rangle$ satisfies the Schrodinger equation with time reversed Hamiltonian $KH(-t; A, \Delta)K^{-1} = H(t; A^T, \Delta^T)$ and time reversed initial state $K|\Omega\rangle$. As a result one obtains the following relation between expectation values of operators,

$$\langle \Omega | O_{A, \Delta}(-t) | \Omega \rangle = \langle K\Omega | (KOK)_{A^T, \Delta^T}(t) | K\Omega \rangle. \quad (\text{B.21})$$

Here O is a Schrodinger operator considered as an operator at time $t = 0$, and $O_{A, \Delta}(t)$ is its time evolution using $H(t; A, \Delta)$. $|K\Omega\rangle = K|\Omega\rangle$ is the time reversed state, and KOK is the time reversed Schrodinger operator.

To describe how time reversal acts on the action, we need to use the complex conjugation K on the Grassmann algebra, described in B.5.1. We then define the action of time reversal on the Grassmann fields ψ, ψ^\dagger as the analog of (B.19), but with an additional conjugation by K ,

$$\begin{aligned} \psi(t, x, y) &\mapsto \psi^T(t, x, y) = \psi^\dagger(-t, x, y), \\ \psi^\dagger(t, x, y) &\mapsto (\psi^\dagger)^T(t, x, y) = \psi(-t, x, y). \end{aligned} \quad (\text{B.22})$$

Using the transformations (B.20), (B.22) and the “reality” of the action (2.24) one finds

$$\begin{aligned} S_{\text{SF}}[\psi^T, (\psi^\dagger)^T, \Delta^T, A^T] &= -K(S_{\text{SF}}[\psi, \psi^\dagger, \Delta, A]) \\ &= -S_{\text{SF}}[\psi, \psi^\dagger, \Delta, A], \end{aligned} \quad (\text{B.23})$$

so that up to a sign, time reversal is a symmetry of the action. It was shown in [308] that, at least formally, this sign does not effect the value of the fermionic functional integral, and can therefore be ignored. Then time reversal symmetry defined by (B.20), (B.22) can be regraded as a symmetry of the action in the usual sense, and one can use this fact to derive (B.21) using functional integrals.

B.5.3 Spatial reflection and time reversal in the geometric description

In this section we map and slightly generalize R, T , as defined in appendix B.5.2, to the geometric description of the p -wave SC in terms of a Majorana spinor in RC space, given in section 2.3. We

will see that there is a difference between the standard notion of R, T for a spinor in $2 + 1$ dimensions [309] and the notion of R, T for the p -wave SC, described in appendix B.5.2. The reason is that our mapping of the p -wave SC to a Majorana spinor maps charge to spin, and charge is R, T -even, while spin is R, T -odd. This is a general property of the BdG formalism. The main point is that the physical R, T , coming from the p -wave SC, leave the mass m invariant and flip the orientation o , as opposed to the standard R, T for a spinor in $2 + 1$ dimensions, which map $m \mapsto -m$ and leave o invariant. Thus, the contribution $\frac{1}{2}o \cdot \text{sgn}(m)$ of a single Majorana spinor to the Chern number is R, T -odd under both notions of R, T , but for different reasons.

First, by spatial reflection we mean an element of the Diffeomorphism group that reverses the orientation of space but not of time, and not to an internal Lorentz transformation. Since the composition of any spatial reflection with Diff_0 is again a spatial reflection, it suffices to consider a single spatial reflection R . Since spatial reflections are just diffeomorphisms, their action on the fields is already defined by (2.55), which is just the pullback

$$\chi \mapsto R^* \chi, \quad e^a \mapsto R^* e^a, \quad \omega \mapsto R^* \omega, \quad (\text{B.24})$$

and is a symmetry of the action S_{RC} . If space-time is $\mathbb{R}_t \times \mathbb{R}^2$ it suffices to consider $R : y \mapsto -y$, as was done in appendix B.5.2. Then (B.24) takes the explicit form

$$\begin{aligned} \chi(y) &\mapsto \chi(-y), \\ (e_t^a, e_x^a, e_y^a)(y) &\mapsto (e_t^a, e_x^a, -e_y^a)(-y), \\ (\omega_t, \omega_x, \omega_y)(y) &\mapsto (\omega_t, \omega_x, -\omega_y)(-y), \end{aligned} \quad (\text{B.25})$$

which maps to the transformation laws (B.19) of the p -wave SF. The orientation of space-time $o = \text{sgn}(\text{dete})$ is odd under spatial reflections, like the orientation of space. Note that even the flat vielbein $e_\mu^a = \delta_\mu^a$ transforms under R , which corresponds to the mapping of a $p_x + ip_y$ order parameter to a $p_x - ip_y$ order parameter by R .

A time reversal is any diffeomorphism that reverses the orientation of time but not of space. It suffices to consider a single representative, and since we work with space-times of the form $\mathbb{R}_t \times M_2$ we may take $\tau : t \mapsto -t$. Apart from the pullback by τ analogous to (B.25), T also includes additional “external” transformations of the fields, which all trace back to the complex conjugation included in the time reversal operation in quantum mechanics, as in appendix B.5.2. As reviewed in appendix B.5.1, a complex conjugation of the gamma matrices is implemented by $-(\gamma^a)^* = \mathcal{B} \gamma^a \mathcal{B}^{-1} = \mathcal{B}_b^a \gamma^b$ where $\mathcal{B} = \sigma^x$, $\mathcal{B}_b^a = \text{diag}[-1, 1, -1]$ in our representation. We then define the action of T on the fields by

$$\chi \mapsto K(\tau^* \chi), \quad e^a \mapsto \mathcal{B}_b^a \tau^* e^b, \quad \omega \mapsto \mathcal{B}(\tau^* \omega) \mathcal{B}^{-1}, \quad (\text{B.26})$$

where τ^* is the pullback by τ , and K is the complex conjugation of the Grassmann algebra defined in appendix B.5.1. One can check that this is a symmetry of the action S_{RC} up to an irrelevant sign already explained in appendix B.5.2, and that this action of T reduces to the transformation laws (B.20) and

(B.22) of the p -wave SF fields.

The standard time reversal for spinors in 2+1 dimensions is given by $T_s = i\sigma^y K$, where the phase i is a matter of convention. It is anti-unitary and $T_s^2 = -1$. This is related to T through the charge conjugation matrix defined in B.5.1,

$$T_s = iCT \text{ or } T = -iT_s. \quad (\text{B.27})$$

This relates the time reversal T that is natural in the p -wave SC, to the standard time reversal T_s and standard charge conjugation C .

B.6 Global structures and obstructions

We already described the emergent geometry in a p -wave SC locally in section 2.3. Here we complete the description by considering global aspects. We use some elements from the theory of fiber bundles and characteristic classes, which are reviewed in [310, 234] for example.

We work with space-time manifolds of the form $M_3 = \mathbb{R}_t \times M_2$, which represent the world volume of the p -wave SF. M_2 is the sample, the two dimensional spatial surface occupied by the p -wave SF, and \mathbb{R}_t is the real line parameterizing time. Because the order parameter is locally a vector Δ^j with $U(1)$ charge 2, at any time $t \in \mathbb{R}_t$ it is globally a map between vector bundles $\Delta : T^*M_2 \rightarrow E^2$, that acts by $v_j \mapsto \Delta^j v_j$ ⁴⁰. Here T^*M_2 is the co-tangent bundle of the sample M_2 and E^2 is the square of the electromagnetic $U(1)$ vector bundle. E has fibers \mathbb{C} and $U(1)$ -valued transition functions, and its topology is labeled by the monopole number (first Chern number) $\Phi = \frac{1}{2\pi} \int_{M_2} F \in \mathbb{Z}$ if M_2 has no boundary, and it is otherwise trivial. E^2 is obtained from E by replacing every transition function by its square, and therefore the topology of E^2 is labeled by $2\Phi \in 2\mathbb{Z}$. If M_2 has no boundary, the topology of the tangent bundle TM_2 (and that of T^*M_2) is labeled by the Euler characteristic $\chi = 2(1 - g) \in 2\mathbb{Z}$ where g is the genus of M_2 .

As a map $\Delta : T^*M_2 \rightarrow E^2$, if Δ is non singular in the sense of section 2.2.2 ($\det \Delta \neq 0$), it defines three geometric structures on M_2 : a metric, which is g^{ij} , an orientation, $o = \text{sgn}(\det \Delta)$, and a spin structure, which follows from the fact that Δ has charge 2.

To see this, we can think of E^2 as an $SO(2)$ vector bundle, with fibers \mathbb{R}^2 and $SO(2)$ valued transition functions. The map Δ then gives a reduction of the structure group of T^*M_2 from $GL(2)$ to $SO(2)$, thus defining a metric and an orientation. Since the transition functions of E^2 are obtained by squaring the transition functions of E , it is natural to think of E as a $Spin(2)$ vector bundle⁴¹. E^2 therefore naturally carries a spin structure [234], and the mapping $\Delta : T^*M_2 \rightarrow E^2$ then endows M_2 with a spin structure.

The different possible spin structures correspond to an assignment of signs ± 1 to non contractible

⁴⁰Equivalently, Δ is globally a section of $TM_2 \otimes E^2$.

⁴¹Both $Spin(2)$ and $SO(2)$ are isomorphic as Lie groups to $U(1)$, but are related by the double cover $Spin(2) \ni e^{i\alpha} \mapsto e^{2i\alpha} \in SO(2)$.

loops in M_2 , or more precisely to elements of $H^1(M_2, \mathbb{Z}_2)$. Generally, this identification of spin structures with $H^1(M_2, \mathbb{Z}_2)$ is not canonical, which means that there is no natural way to declare one of the spin structures as “trivial”.

In the simple case where TM_2 is trivial as in the case of the torus $M_2 = \mathbb{R}^2/\mathbb{Z}^2$, spin structures correspond canonically to elements of $H^1(M_2, \mathbb{Z}_2)$, which in turn correspond to a choice of periodic or anti-periodic boundary conditions for spinors around the non contractible loops. The boundary condition for the BdG spinor $\Psi = (\psi, \psi^\dagger)^T$ follows from that of the microscopic spin-less fermion ψ , for which it is natural to take fully periodic boundary conditions, which is the “trivial” spin structure. Other boundary conditions have been discussed in [15, 247].

A non singular Δ is not always possible. First, it requires that M_2 be orientable. If M_2 is not orientable Δ would have singularities $\text{sing}(\Delta)$ such that $M_2 - \text{sing}(\Delta)$ is orientable. p -wave SF on non orientable surfaces were considered in [238]. The other obstruction is a mismatch in the topology of E^2 and TM_2 , and is given by $2\Phi + o\chi$, or $\Phi - (g-1)o$ [15]. If the topological invariant $2\Phi + o\chi$ does not vanish then Δ must have singularities. A simple way to obtain this condition is to assume $\tilde{\omega}_{12\mu} = \omega_{12\mu} = -2A_\mu$, which implies $\frac{1}{2}o\sqrt{g}\tilde{R}d^2x = \tilde{R}_{12} = d\tilde{\omega}_{12} = -2dA = -2F$, and use the Gauss-Bonnet formula $\chi = 2(1-g) = \frac{1}{4\pi} \int_{M_2} \tilde{R}\sqrt{g}d^2x$ for the Euler characteristic. The simplest example is $M_2 = S^2$ the sphere, where there must be a monopole $\Phi = o = \pm 1$ for a non singular order parameter with orientation o . Possible singularities of the order parameter on the sphere without a monopole have been studied in [240]. There are no obstructions to the existence of a metric and (in the two dimensional case) of a spin structure.

A simple way to handle singularities of Δ is to exclude them by working with $M_2 - \text{sing}(\Delta)$ instead of M_2 . Then Δ defines on $M_2 - \text{sing}(\Delta)$ and orientation, metric, and spin structure.

The emergent geometry of space-time follows from that of space due to the simple product structure $M_3 = \mathbb{R}_t \times M_2$. Thus the order parameter corresponds to the (inverse) space-time vielbein (2.27), which is globally a map $T^*M_3 \rightarrow E^2$, $v_\mu \mapsto e_a^\mu v_\mu$ where E^2 is now viewed as an $SO(1,2)$ vector bundle. In other words, e is globally a Solder form.

C Quantization of coefficients for a sum of gravitational Chern-Simons terms

As stated in section 2.5.3.1, gauge invariance of

$$K = \alpha_1 \int_{M_3} Q_3(\tilde{\omega}_{(1)}) + \alpha_2 \int_{M_3} Q_3(\tilde{\omega}_{(2)}) \quad (\text{C.1})$$

for all closed M_3 implies $\alpha_1 + \alpha_2 \in \frac{1}{192\pi}\mathbb{Z}$. Here we sketch the derivation, following [24] (section 2.1 and the discussion leading to equation (2.27)). First, only the gauge invariance of e^{iK} is required, because K is a contribution to the effective action, obtained by taking the logarithm of the fermionic path integral, which is a gauge invariant object. Second, the gCS term on a general M_3 is only locally given by

$\alpha \int Q_3(\tilde{\omega})$, not globally. It is convenient to globally define gCS on a given M_3 as $\alpha \int_{M_4} \text{tr}(\tilde{R}^2)$, where M_4 is some four manifold with M_3 as a boundary, $\partial M_4 = M_3$. This is based on the fact that locally on M_4 we have $dQ_3(\tilde{\omega}) = \text{tr}(\tilde{R}^2)$. With this definition, we have

$$e^{iK_{M_4}} = e^{i[\alpha_1 \int_{M_4} \text{tr}(\tilde{R}_{(1)}^2) + \alpha_2 \int_{M_4} \text{tr}(\tilde{R}_{(2)}^2)]}, \quad (\text{C.2})$$

which is clearly gauge invariant, but we must ensure that it is also independent of the arbitrary choice of M_4 . In fact, changing M_4 corresponds precisely to performing a large gauge transformation on M_3 , see [311] for a more direct approach. For $M_4 \neq M'_4$ such that $\partial M_4 = M_3 = \partial M'_4$, we have

$$e^{iK_{M_4}}/e^{iK_{M'_4}} = e^{i[\alpha_1 \int_{X_4} \text{tr}(\tilde{R}_{(1)}^2) + \alpha_2 \int_{X_4} \text{tr}(\tilde{R}_{(2)}^2)]}, \quad (\text{C.3})$$

where X_4 is a closed manifold obtained by gluing M_4, M'_4 along their shared boundary, after reversing the orientation on M'_4 . Since we start with a spin manifold M_3 , we assume that M_4, M'_4 are also spin manifolds, and therefore so is X_4 . On the closed spin manifold X_4 , the Atiah-Singer index theorem implies

$$\int_{X_4} \text{tr}(\tilde{R}_{(1)}^2) = \int_{X_4} \text{tr}(\tilde{R}_{(2)}^2) \in 2\pi \times 192\pi\mathbb{Z}. \quad (\text{C.4})$$

In particular, one can choose M'_4 such that the integer on the right hand side is 1, in which case

$$e^{iK_{M_4}}/e^{iK_{M'_4}} = e^{2\pi i(\alpha_1 + \alpha_2)192\pi}. \quad (\text{C.5})$$

An M_4 -independent $e^{iK_{M_4}} = e^{iK}$ then requires $\alpha_1 + \alpha_2 \in \frac{1}{192\pi}\mathbb{Z}$.

D Calculation of gravitational pseudo Chern-Simons currents

Here we derive the contributions (2.98) to the bulk currents, which come from the gpCS term $-\beta_1 \int_{M_3} \tilde{\mathcal{R}} e^a De_a$ in the effective action. We write

$$\delta \int_{M_3} \tilde{\mathcal{R}} e^a De_a = \int_{M_3} (e^a De_a) \delta \tilde{\mathcal{R}} + \int_{M_3} \tilde{\mathcal{R}} \delta (e^a De_a). \quad (\text{D.1})$$

It's convenient to calculate the first contribution in terms of scalars using $e^a De_a = -oc|e|d^3x$. We need the formula $\delta \tilde{\mathcal{R}} = -\delta g_{\mu\nu} \tilde{\mathcal{R}}^{\mu\nu} + (\nabla_\mu \nabla_\nu - g_{\mu\nu} \nabla^2) \delta g_{\mu\nu}$ relating the curvature variation to the metric variation, and $\delta g_{\mu\nu} = 2e_{a(\nu} \delta e_{\mu)}^a$ relating the metric variation to the vielbein variation. We find

$$\int_{M_3} (e^a De_a) \delta \tilde{\mathcal{R}} = -2o \int_{M_3} |e| \left[\left(\tilde{\nabla}^\mu \tilde{\nabla}^\nu - g^{\mu\nu} \tilde{\nabla}^2 \right) c - \tilde{\mathcal{R}}^{\mu\nu} c \right] e_{a\nu} \delta e_\mu^a. \quad (\text{D.2})$$

The second contribution in (D.1) is simpler to calculate in terms of differential forms [156],

$$\begin{aligned}
\delta \int \tilde{\mathcal{R}} e_a D e^a & \\
&= \int_M \tilde{\mathcal{R}} (\delta e^a T_a + e^a d\delta e_a + e^a \delta \omega_{ab} e^b + e^a \omega_{ab} \delta e^b) \\
&= \int_M \left(\tilde{\mathcal{R}} 2\delta e_a T^a - \tilde{\mathcal{R}} \delta \omega_{ab} e^a e^b - \delta e_a e^a d\tilde{\mathcal{R}} \right) + \int_{\partial M} \delta e_a \tilde{\mathcal{R}} e^a,
\end{aligned} \tag{D.3}$$

which implies

$$\begin{aligned}
*\mathbf{J}^a &= -\beta_1 \left(2\tilde{\mathcal{R}} T^a - e^a d\tilde{\mathcal{R}} \right), \quad *\mathbf{J}^{ab} = -\beta_1 \left(-\tilde{\mathcal{R}} e^a e^b \right), \\
*\mathbf{j}^a &= -\beta_1 \tilde{\mathcal{R}} e^a, \quad *\mathbf{j}^{ab} = 0.
\end{aligned} \tag{D.4}$$

Here we kept track of boundary terms and calculated the contributions to boundary currents $\mathbf{j}^a = \mathbf{j}_\mu^a dx^\mu$, $\mathbf{j}^{ab} = \mathbf{j}_\mu^{ab} dx^\mu$, which are relevant for our discussion in section 2.5.4.2. Collecting all of the bulk contributions one finds (2.98).

In section 2.5.4.2 we wrote down (2.98) for a product geometry with respect to the coordinate z , and assumed torsion vanishes. Here we generalize to non-zero torsion. With non zero torsion, (2.100) generalizes to

$$\begin{aligned}
\langle \mathbf{J}^{\alpha z} \rangle_{\text{gpCS}} &= -\beta_1 \frac{1}{|e|} \varepsilon^{z\alpha\beta} \partial_\beta \tilde{\mathcal{R}}, \\
\langle \mathbf{J}^{z\alpha} \rangle_{\text{gpCS}} &= \beta_1 \left[\frac{1}{|e|} \varepsilon^{z\alpha\beta} \partial_\beta \tilde{\mathcal{R}} + \frac{1}{|e|} \varepsilon^{z\beta\gamma} C_{\beta\gamma}{}^\alpha \tilde{\mathcal{R}} \right].
\end{aligned} \tag{D.5}$$

For $z = t$, which describes a time independent situation, we find

$$\begin{aligned}
\langle J_E^i \rangle_{\text{gpCS}} &= \beta_1 \varepsilon^{ij} \partial_j \tilde{\mathcal{R}}, \\
\langle P_i \rangle_{\text{gpCS}} &= -\beta_1 \left[g_{ik} \varepsilon^{kj} \partial_j \tilde{\mathcal{R}} + 2o|e| \tilde{\mathcal{R}} C_{12i} \right],
\end{aligned} \tag{D.6}$$

which generalizes (2.101). Explicit expressions for the contorsion C_{12i} are given in appendix B.4. Equation (D.6) is compatible with the operator equation (2.48), and the density response (2.99).

In the case $z = y$, the inflow (2.103) generalizes to

$$\begin{aligned}
\langle t_{\text{cov } \alpha}^y \rangle_{\text{gpCS}} &= -|e| \langle \mathbf{J}_\alpha^y \rangle_{\text{gpCS}} \\
&= -\beta_1 \left[g_{\alpha\beta} \varepsilon^{\beta\gamma y} \partial_\gamma \tilde{\mathcal{R}} + 2o|e| C_{01\alpha} \tilde{\mathcal{R}} \right].
\end{aligned} \tag{D.7}$$

For the order parameter $\Delta = \Delta_0 e^{i\theta(t,x)} (1 + f(t,x), \pm i)$ that we consider in this case, we find using appendix B.4 that $C_{01t} = 0$, $C_{01x} = e_1^{i\frac{1}{2}} \partial_t g_{ij}$. The boundary current (2.104) is unchanged, but the

bulk+boundary conservation equation (2.105) is generalized to

$$\tilde{\nabla}_\alpha \langle j^\alpha_\beta \rangle_{\text{gpCS}} - C_{ab\beta} \langle j^{[ab]} \rangle_{\text{gpCS}} = \langle J^{y\beta} \rangle_{\text{gpCS}}, \quad (\text{D.8})$$

so that bulk+boundary conservation still holds for the current from gpCS, in the presence of torsion.

E Perturbative calculation of the relativistic effective action

Here we present a perturbative calculation of the effective action for the RC background fields e, ω induced by a Majorana spinor in 2+1 dimensions. A perturbative calculation requires three types of input: free propagators, interaction vertices, and a renormalization scheme to handle UV divergences. In our case the propagator and vertices are standard in the context of the coupling of relativistic fermions to gravity, but the renormalization scheme will not be standard in this context.

The standard renormalization schemes used in the literature are aimed at preserving Lorentz symmetry, obtaining properly quantized coefficients for CS terms, and obtaining finite results that do not depend on a regulator [156, 157]. This is usually done as follows. First, one introduces a Lorentz invariant regulator, such as a frequency and wave-vector cutoff Λ_{rel} , then one introduces Pauli-Villars regulators, and tunes their masses such that the limit $\Lambda_{\text{rel}} \rightarrow \infty$ produces finite results and properly quantized CS coefficients.

In contrast, we take the lattice model (2.15) as a microscopic description of the p -wave SC, and the relativistic continuum limit as an approximation of it. As we obtained naturally in sections 2.2.1 and 2.2.3, this means that there are four Majorana spinors, with different orientations and masses, and a wave-vector cutoff $\Lambda_{UV} \sim 1/a$, but no frequency cutoff, as dictated by the lattice model. Note that these multiple Majorana spinors are not Pauli-Villars regulators, simply because they are all fermions. None of them has the “wrong statistics”. The cutoff Λ_{UV} is a physical parameter of the model and we do not wish to take it to infinity. Thus wave-vector integrals cannot diverge. In contrast, since time is continuous, there is no physical frequency cutoff, and divergences in frequency integrals do appear. These divergences are unphysical, and can be viewed as a byproduct of the construction of the path integral by time discretization. These divergences need to be renormalized in the usual sense, and we do this by minimal subtraction.

To set up the perturbative calculation, we write the action S_{RC} in terms of the spinor densities $\Psi = |e|^{1/2} \chi$, and using the explicit form (B.3),

$$\begin{aligned} S_{\text{RC}} &= \frac{1}{2} \int d^3x \bar{\Psi} \left[\frac{1}{2} i e_a^\mu \gamma^a \overleftrightarrow{\partial}_\mu - \frac{1}{4} \omega_{abc} \varepsilon^{abc} - m \right] \Psi \\ &= \frac{1}{2} \int d^3x \bar{\Psi} \left[i e_a^\mu \gamma^a \partial_\mu + \frac{i}{2} (\partial_\mu e_a^\mu) \gamma^a - \frac{1}{4} \omega_{abc} \varepsilon^{abc} - m \right] \Psi. \end{aligned} \quad (\text{E.1})$$

Assuming for now that the vielbein has a positive orientation, we insert $e_a^\mu = \delta_a^\mu + h_a^\mu$ with small h , and

split the action into an inverse propagator G^{-1} and vertices V ,

$$\begin{aligned} S_{\text{RC}} &= \frac{1}{2} \int d^3x \Psi^\dagger \gamma^0 [G^{-1} + V] \Psi, \\ G^{-1} &= i\delta_a^\mu \gamma^a \partial_\mu - m, \quad V = V_1 + V_2, \\ V_1 &= i\gamma^a h_a^\mu \partial_\mu + \frac{i}{2} \gamma^a (\partial_\mu h_a^\mu), \quad V_2 = -\frac{1}{4} \omega_{abc} \varepsilon^{abc}. \end{aligned} \tag{E.2}$$

The vertex V_1 is first order in the perturbation h . The vertex V_2 is given explicitly by

$$V_2 = -\frac{1}{4} \omega_{ab\mu} e_c^\mu \varepsilon^{abc} = -\frac{1}{4} \omega_{ab\mu} \delta_c^\mu \varepsilon^{abc} - \frac{1}{4} \omega_{ab\mu} h_c^\mu \varepsilon^{abc}, \tag{E.3}$$

and therefore contains a term of order ω and a term quadratic in the perturbations, of order $h\omega$. Terms in vertices which are nonlinear in perturbations are sometimes called contact terms, and the above contribution to V_2 is the only contact term in our scheme. Note that there is no vertex related to the volume element $|e|$, because the fundamental fermionic degree of freedom is the spinor density Ψ , see appendix B.3. In expressions written in terms of h_a^μ we use $\eta_{\mu\nu}$ to raise and lower coordinate indices and δ_a^μ to map internal indices to coordinate indices, so in practice there is no difference between these indices in such expressions.

The perturbative expansion of the effective action is given by

$$\begin{aligned} 2W_{\text{RC}} &= -2i \log \text{Pf} (i\gamma^0 (G^{-1} + V)) \\ &= -i \text{Tr} (\log i\gamma^0 G^{-1}) \\ &\quad - i \text{Tr} (GV) + \frac{i}{2} \text{Tr} (GV)^2 + O(V^3), \end{aligned} \tag{E.4}$$

which, apart from the first term, is a sum over Feynman diagrams with a fermion loop and any number of vertices V . We will be interested in W_{RC} to second order in the perturbations h and ω and up to third order in derivatives. Terms of first order in h, ω correspond to properties of the unperturbed ground state, or vacuum, while terms of second order correspond to linear response coefficients. The first term is independent of h, ω and corresponds to the ground state energy of the unperturbed system. This information can also be obtained from the term linear in h , and we therefore ignore $\text{Tr} \log i\gamma^0 G^{-1}$ in the following. Expanding the vertices,

$$\begin{aligned} 2W_{\text{RC}} &= -i \text{Tr} (GV_1) - i \text{Tr} (GV_2) + \frac{i}{2} \text{Tr} (GV_1)^2 \\ &\quad + \frac{i}{2} \text{Tr} (GV_2)^2 + i \text{Tr} (GV_1 GV_2) + O(V^3). \end{aligned} \tag{E.5}$$

These functional traces can now be written as integrals over Fourier components and traces over spinor indices,

$$\begin{aligned}
\text{Tr}(GV_1) &= -h_a^\mu(p=0) \int_q q_\mu \text{tr}(\gamma^a G_q), \\
\text{Tr}(GV_2) &= \omega(p=0) \int_q \text{tr}(G_q), \\
\text{Tr}(GV_1)^2 &= \int_p h_a^\mu(p) h_b^\nu(-p) \int_q \left(q + \frac{1}{2}p\right)_\mu \left(q + \frac{1}{2}p\right)_\nu \text{tr}(\gamma^a G_q \gamma^b G_{p+q}), \\
\text{Tr}(GV_2)^2 &= \int_p \omega(p) \omega(-p) \int_q \text{tr}(G_q G_{p+q}), \\
\text{Tr}(GV_1 GV_2) &= - \int_p h_a^\mu(p) \omega(-p) \int_q \left(q + \frac{1}{2}p\right)_\mu \text{tr}(\gamma^a G_q G_{p+q}),
\end{aligned} \tag{E.6}$$

where $\omega = -\frac{1}{4}\omega_{ab\mu}e_c^\mu\varepsilon^{abc}$, and $\int_p = \int \frac{d^3p}{(2\pi)^3}$. Our conventions for the Fourier transform of a function f is $f(x) = \int_q e^{iq_\mu x^\mu} f(q)$. The Fourier transform of the Greens function is then $G_q = -\frac{1}{\not{q}+m} = -\frac{\not{q}-m}{q^2-m^2}$, where $\not{q} = q_a \gamma^a$. The spinor traces are evaluated using the usual identities for gamma matrices in 2+1 dimensions,

$$\begin{aligned}
\text{tr}(\gamma^a) &= 0, \quad \text{tr}(\gamma^a \gamma^b) = 2\eta^{ab}, \quad \text{tr}(\gamma^a \gamma^b \gamma^c) = \pm 2i\varepsilon^{abc}, \\
\text{tr}(\gamma^a \gamma^b \gamma^c \gamma^d) &= 2(\eta^{ab}\eta^{cd} - \eta^{ac}\eta^{bd} + \eta^{ad}\eta^{bc}).
\end{aligned} \tag{E.7}$$

The sign \pm distinguishes the two inequivalent representations of gamma matrices in 2+1 dimensions, and with our chosen representation, $\text{tr}(\gamma^a \gamma^b \gamma^c) = 2i\varepsilon^{abc}$. Using these identities yields for the single vertex diagrams

$$\begin{aligned}
\text{Tr}(GV_1) &= 2\eta^{ab} h_a^\mu(p=0) \int_q \frac{q_\mu q_b}{q^2 - m^2}, \\
\text{Tr}(GV_2) &= 2m\omega(p=0) \int_q \frac{1}{q^2 - m^2}.
\end{aligned} \tag{E.8}$$

The expressions for the diagrams with two vertices are more complicated, so let us start by analyzing the single vertex diagrams. This will suffice to demonstrate our renormalization scheme and compare it to direct calculations within the lattice model and to renormalizations which are more natural in the context of relativistic QFT.

E.1 Single vertex diagrams

From (E.5) and (E.8) it follows that

$$W_{\text{RC}} = \Lambda_\mu^a \int d^3x h_a^\mu + s \int d^3x \omega + O(V^2), \tag{E.9}$$

where

$$\Lambda_{\mu}^a = -i\eta^{ab} \int \frac{d^3q}{(2\pi)^3} \frac{q_{\mu}q_b}{q^2 - m^2}, \quad s = -i \int \frac{d^3q}{(2\pi)^3} \frac{m}{q^2 - m^2}, \quad (\text{E.10})$$

can now be recognized as the energy-momentum tensor and spin density of the unperturbed ground state,

$$\begin{aligned} \langle J_{\mu}^a \rangle &= -\Lambda_{\mu}^a, \\ \langle J^{ab\mu} \rangle &= -\frac{1}{4} \frac{1}{2} \langle \bar{\chi}\chi \rangle \delta_c^{\mu} \varepsilon^{abc} = -\frac{1}{4} s \delta_c^{\mu} \varepsilon^{abc}. \end{aligned} \quad (\text{E.11})$$

Performing a Wick rotation $q_0 \mapsto iq_0$,

$$\Lambda_{\mu}^a = \delta^{ab} \int \frac{d^3q}{(2\pi)^3} \frac{q_{\mu}q_b}{|q|^2 + m^2}, \quad s = - \int \frac{d^3q}{(2\pi)^3} \frac{m}{|q|^2 + m^2}, \quad (\text{E.12})$$

where $|\cdot|$ is the euclidian norm. We start by calculating s in our lattice motivated renormalization scheme. In this scheme the integral reads

$$s = - \int_{|q| < \Lambda_{UV}} \frac{d^2\mathbf{q}}{(2\pi)^2} \int_{-\infty}^{\infty} \frac{dq_0}{2\pi} \frac{m}{q_0^2 + |\mathbf{q}|^2 + m^2}, \quad (\text{E.13})$$

where Λ_{UV} is a physical cutoff related to the lattice spacing by $\Lambda_{UV} \sim a^{-1}$. The q_0 integral converges, and does not require renormalization. It yields the result within the lattice motivated scheme,

$$s = -\frac{1}{2} \int_{|q| < \Lambda_{UV}} \frac{d^2\mathbf{q}}{(2\pi)^2} \frac{m}{\sqrt{|\mathbf{q}|^2 + m^2}}, \quad (\text{E.14})$$

and adding the operator ordering correction gives the ground state charge density

$$\rho = \langle J^t \rangle = -\frac{1}{2} \int_{|q| < \Lambda_{UV}} \frac{d^2\mathbf{q}}{(2\pi)^2} \left(1 - \frac{m}{\sqrt{|\mathbf{q}|^2 + m^2}} \right). \quad (\text{E.15})$$

After summing over low energy Majorana spinors and restoring units, this coincides with the relativistic limit of the exact ground state charge density of the lattice model [15],

$$\rho = -\frac{1}{2} \int_{BZ} \frac{d^2\mathbf{q}}{(2\pi)^2} \left(1 - \frac{h_{\mathbf{q}}}{\sqrt{|\Delta_{\mathbf{q}}|^2 + h_{\mathbf{q}}^2}} \right), \quad (\text{E.16})$$

where $h_{\mathbf{q}}, \Delta_{\mathbf{q}}$ were defined in section 2.2.1.

For comparison we calculate the s integral in a standard renormalization scheme of relativistic QFT. In this approach the integral does not converge. We introduce a frequency and wave-vector cutoff Λ_{rel} ,

and restrict the integration to $|q| < \Lambda_{\text{rel}}$. This yields

$$s = - \int_{|q| < \Lambda_{\text{rel}}} \frac{d^3 q}{(2\pi)^3} \frac{m}{|q|^2 + m^2} = -\frac{\Lambda_{\text{rel}} m}{2\pi^2} + \frac{m^2 \text{sgn} m}{4\pi} + O\left(\frac{m}{\Lambda_{\text{rel}}}\right). \quad (\text{E.17})$$

A simple way to proceed is to perform minimal subtraction, which means we remove the diverging piece, and take $\Lambda_{\text{rel}}/m \rightarrow \infty$. This gives the fully relativistic result

$$s = \frac{m^2 \text{sgn} m}{4\pi}. \quad (\text{E.18})$$

Comparing with (2.67) we find $\zeta_H = s = \frac{m^2 \text{sgn} m}{4\pi}$ for a positive orientation which is essentially the torsional Hall viscosity of [156]⁴². The relativistic result can also be obtained by expanding the lattice result (E.14) in Λ_{UV} and keeping the $O(1)$ piece. This is a general feature, the $O(1)$ piece of any coefficient in the effective action is always relativistic.

Let us now turn to the calculation of the ground state energy-momentum tensor Λ_μ^a . With a relativistic regulator Λ_μ^a is $O(3)$ invariant and must therefore be proportional to the identity,

$$\Lambda_\mu^a = \delta^{ab} \int_{|q| < \Lambda_{\text{rel}}} \frac{d^3 q}{(2\pi)^3} \frac{q_\mu q_b}{|q|^2 + m^2} = \delta_\mu^a \frac{\Lambda}{2\kappa_N}, \quad (\text{E.19})$$

with the cosmological constant

$$\frac{\Lambda}{2\kappa_N} = \frac{1}{3} \int_{|q| < \Lambda_{\text{rel}}} \frac{d^3 q}{(2\pi)^3} \frac{|q|^2}{|q|^2 + m^2} = \frac{1}{3} \left[\frac{\Lambda_{\text{rel}}^3}{6\pi^2} - \frac{\Lambda_{\text{rel}} m^2}{2\pi^2} + \frac{|m|^3}{4\pi} + O\left(\frac{m}{\Lambda_{\text{rel}}}\right) \right]. \quad (\text{E.20})$$

Keeping the $O(1)$ piece we find the relativistic expression

$$\Lambda_\mu^a = \delta_\mu^a \frac{\Lambda}{2\kappa_N} = \delta_\mu^a \frac{|m|^3}{6\pi}, \quad (\text{E.21})$$

which again, is essentially the result of [156]. With the lattice motivated renormalization scheme,

$$\Lambda_\mu^a = \delta^{ab} \int_{|q| < \Lambda_{UV}} \frac{d^2 \mathbf{q}}{(2\pi)^2} \int_{-\infty}^{\infty} \frac{dq_0}{2\pi} \frac{q_\mu q_b}{q_0^2 + |\mathbf{q}|^2 + m^2}. \quad (\text{E.22})$$

Here the q_0 integral for Λ_t^0 does not converge, and needs to be regularized. We do this by introducing a frequency cutoff Λ_0 ,

$$\Lambda_\mu^a = \delta^{ab} \int_{|q| < \Lambda_{UV}} \frac{d^2 \mathbf{q}}{(2\pi)^2} \int_{-\Lambda_0}^{\Lambda_0} \frac{dq_0}{2\pi} \frac{q_\mu q_b}{q_0^2 + |\mathbf{q}|^2 + m^2}. \quad (\text{E.23})$$

Unlike Λ_{UV} which is a physical parameter of the model, Λ_0 is a fictitious cutoff which we take to infinity

⁴²It is not exactly the same result because we did not use the same relativistic renormalization scheme.

at the end of the calculation. The q_0 divergence can be interpreted as an artifact of time discretization [130]. At this point the domain of integration is not a ball in Euclidian Fourier space but a cylinder, so it is not invariant under $O(3)$, only under $O(2)$ ⁴³ and the reflection $q \mapsto -q$. This implies that the tensor Λ_μ^a takes the form

$$\begin{aligned}\Lambda_t^0 &= \int_{|\mathbf{q}| < \Lambda_{UV}} \frac{d^2 \mathbf{q}}{(2\pi)^2} \int_{-\Lambda_0}^{\Lambda_0} \frac{dq_0}{2\pi} \frac{q_0^2}{q_0^2 + |\mathbf{q}|^2 + m^2}, \\ \Lambda_j^A &= \frac{1}{2} \delta_j^A \int_{|\mathbf{q}| < \Lambda_{UV}} \frac{d^2 \mathbf{q}}{(2\pi)^2} \int_{-\Lambda_0}^{\Lambda_0} \frac{dq_0}{2\pi} \frac{|\mathbf{q}|^2}{q_0^2 + |\mathbf{q}|^2 + m^2},\end{aligned}\tag{E.24}$$

with all other components vanishing. The q_0 integral for the energy density Λ_t^0 gives

$$\Lambda_t^0 = \frac{1}{2} \int_{|\mathbf{q}| < \Lambda_{UV}} \frac{d^2 \mathbf{q}}{(2\pi)^2} \left[\frac{2\Lambda_0}{\pi} - \sqrt{|\mathbf{q}|^2 + m^2} + O\left(\frac{m}{\Lambda_0}\right) \right].\tag{E.25}$$

Keeping the $O(1)$ piece we find, within the lattice motivated scheme,

$$\Lambda_t^0 = -\frac{1}{2} \int_{|\mathbf{q}| < \Lambda_{UV}} \frac{d^2 \mathbf{q}}{(2\pi)^2} \sqrt{|\mathbf{q}|^2 + m^2},\tag{E.26}$$

which is the familiar expression for the ground state energy of a single Majorana fermion, which is half the energy of a filled Dirac sea. The q_0 integral for Λ_j^A converges and gives the pressure

$$\Lambda_j^A = \frac{1}{2} \delta_j^A \frac{1}{2} \int_{|\mathbf{q}| < \Lambda_{UV}} \frac{d^2 \mathbf{q}}{(2\pi)^2} \frac{|\mathbf{q}|^2}{\sqrt{|\mathbf{q}|^2 + m^2}}.\tag{E.27}$$

We see that the ground state energy density and pressure are no longer equal. In other words the ground state energy-momentum tensor is not Lorentz invariant, due to the lattice renormalization scheme. It may be surprising that the expression (E.26) for the energy density is part of an energy momentum tensor which is not Lorentz invariant. This has been discussed in the literature in the context of the cosmological constant problem [312–314].

Let us now compare the above with the lattice model. For the energy density we need to add the operator ordering correction,

$$\varepsilon = \langle t_{\text{cov } t}^t \rangle = \frac{1}{2} \int_{|\mathbf{q}| < \Lambda_{UV}} \frac{d^2 \mathbf{q}}{(2\pi)^2} \left(m - \sqrt{|\mathbf{q}|^2 + m^2} \right).\tag{E.28}$$

Restoring units and summing over Dirac points, we recognize the above as the relativistic approximation

⁴³More accurately, the domain of integration for each lattice fermion is not the disk $\{|\mathbf{q}| < \Lambda_{UV}\}$ but the square $[-\Lambda_{UV}/2, \Lambda_{UV}/2]^2$ with $\Lambda_{UV} = \pi/a$, which is a quarter of the Brillouin zone BZ , see section 2.2.3. The symmetry group of this domain is not $O(2)$ but the point group symmetry of the lattice $D_4 \subset O(2)$. This subtlety has no effect on the following.

of the ground state energy density of the lattice model [27],

$$\varepsilon = \frac{1}{2} \int_{BZ} \frac{d^2 \mathbf{q}}{(2\pi)^2} (h_{\mathbf{q}} - E_{\mathbf{q}}). \quad (\text{E.29})$$

The above calculations of simple ground state properties serve as consistency checks. We have seen explicitly that these quantities are UV sensitive. With the lattice motivated renormalization scheme the effective action produces physical quantities that approximate those of the lattice model, which are distinct from those obtained with a relativistic scheme. In the following we will focus on UV insensitive terms. In doing so we will also ignore operator ordering corrections, because these always contain $\delta^2(0) \sim \int_{|\mathbf{q}| < \Lambda_{UV}} \frac{d^2 \mathbf{q}}{(2\pi)^2} \sim \Lambda_{UV}^2$ and are therefore UV sensitive.

E.2 Two vertex diagrams

Let us now turn to the calculation of the more interesting second order terms, which correspond to linear responses. After performing the traces over gamma matrices one finds

$$\begin{aligned} \text{Tr}(GV_1)^2 = & -2im\varepsilon^{abc} \int_p h_a^\mu(p) h_b^\nu(-p) p_c \int_q \frac{(q + \frac{1}{2}p)_\mu (q + \frac{1}{2}p)_\nu}{(q^2 - m^2)((p+q)^2 - m^2)} \\ & + 2m^2 \eta^{ab} \int_p h_a^\mu(p) h_b^\nu(-p) \int_q \frac{(q + \frac{1}{2}p)_\mu (q + \frac{1}{2}p)_\nu}{(q^2 - m^2)((p+q)^2 - m^2)} \\ & + 2(\eta^{ac}\eta^{bd} - \eta^{ab}\eta^{cd} + \eta^{ad}\eta^{cb}) \int_p h_a^\mu(p) h_b^\nu(-p) \int_q \frac{(q + \frac{1}{2}p)_\mu (q + \frac{1}{2}p)_\nu q_c (p+q)_d}{(q^2 - m^2)((p+q)^2 - m^2)}, \end{aligned} \quad (\text{E.30})$$

$$\text{Tr}(GV_2)^2 = \int_p \omega(p) \omega(-p) \int_q \frac{2\eta^{ab} q_a (p+q)_b + 2m^2}{(q^2 - m^2)((p+q)^2 - m^2)}, \quad (\text{E.31})$$

$$\begin{aligned} \text{Tr}(GV_1 GV_2) = & -2i\varepsilon^{abc} \int_p h_a^\mu(p) \omega(-p) p_c \int_q \frac{(q + \frac{1}{2}p)_\mu q_b}{(q^2 - m^2)((p+q)^2 - m^2)} \\ & + 2m\eta^{ab} \int_p h_a^\mu(p) \omega(-p) \int_q \frac{(q + \frac{1}{2}p)_\mu (2q+p)_b}{(q^2 - m^2)((p+q)^2 - m^2)}. \end{aligned} \quad (\text{E.32})$$

One is then left with the calculation of the integrals over the loop momenta q in the above equations. The first step in doing so is Wick rotating to euclidian signature by changing $q_0 \mapsto iq_0$, $p_0 \mapsto ip_0$ in the q integrals.

At this point one can use Feynman parameters to simplify the form of the integrands, but since we are only interested in the effective action to low orders in derivatives of the background fields, we find it simpler to expand the integrands in powers of p/m .

We start with the first integral in (E.30), which contains the gCS term. Expanding the integrand in p/m we find

$$\begin{aligned} \frac{(q + \frac{1}{2}p)_\mu (q + \frac{1}{2}p)_\nu}{(q^2 + m^2)((p + q)^2 + m^2)} &= \frac{q_\mu q_\nu}{(m^2 + q^2)^2} + \left[\frac{p_{(\mu} q_{\nu)}}{(m^2 + q^2)^2} - 2 \frac{q_\mu q_\nu p \cdot q}{(m^2 + q^2)^3} \right] \\ &+ \left[\frac{p_\mu p_\nu}{4(m^2 + q^2)^2} - \frac{p^2 q_\mu q_\nu}{(m^2 + q^2)^3} - \frac{2p_{(\mu} q_{\nu)} p \cdot q}{(m^2 + q^2)^3} + \frac{4q_\mu q_\nu (p \cdot q)^2}{(m^2 + q^2)^4} \right] + O(p^3) \end{aligned} \quad (\text{E.33})$$

where terms are grouped according to their order in p/m . The q integral over the $O(1)$ terms diverges, and therefore produces a UV sensitive term in the effective action. With a relativistic renormalization we find

$$2W_{\text{RC}} = \frac{m^2 \text{sgn}(m)}{4\pi} \int d^3x h_a^\mu \eta_{\mu\nu} \varepsilon^{abc} \partial_b h_c^\nu + \dots \quad (\text{E.34})$$

Comparing with (2.67) and using $e_a D e^a = \varepsilon^{abc} h_{a\nu} \partial_b h_c^\nu d^3x + \dots$ we find again the torsional Hall viscosity $\zeta_H = \frac{m^2 \text{sgn}(m)}{4\pi}$, for positive orientation. With the lattice renormalization the $\eta_{\mu\nu}$ in the above is replaced by a non Lorentz invariant tensor, but in Sec.2 we are only interested in UV insensitive responses, so we will not discuss it here further (see Appendix H.1).

The q integral over the $O(p/m)$ terms vanishes because it is odd under the reflection $q \mapsto -q$.

The $O(p^2/m^2)$ contributions are most interesting for us. The q integral over these converges, and therefore produces UV insensitive terms in the effective action. Instead of calculating the integral with the finite physical Λ_{UV} , we can calculate it with $\Lambda_{UV}/m = \infty$ at the expense of producing small $O(m/\Lambda_{UV})$ corrections. Then the calculation reduces to a standard calculation within relativistic QFT which has appeared a few times in the literature with slightly different conventions [257–260], and which is done below for completeness. See also [261] for a recent heat kernel calculation and review of the literature, and [315] for similar computations in 4+1 dimensions. With $\Lambda_{UV}/m = \infty$ the integral is Lorentz invariant and this implies the standard reductions to radial functions such as $q_\mu q_\nu \mapsto \frac{1}{3} \eta_{\mu\nu} q^2$. The $O(p^2/m^2)$ contributions in (E.33) then reduce to

$$\begin{aligned} &\frac{1}{4} \frac{p_\mu p_\nu}{(m^2 + q^2)^2} - \frac{1}{3} \frac{p^2 \eta_{\mu\nu} q^2}{(m^2 + q^2)^3} - \frac{2}{3} \frac{p_\mu p_\nu q^2}{(m^2 + q^2)^3} \\ &+ \frac{4}{15} \frac{p^2 \eta_{\mu\nu} + 2p_\mu p_\nu}{(m^2 + q^2)^4} q^4, \end{aligned} \quad (\text{E.35})$$

and performing the q integral yields

$$\frac{1}{96\pi |m|} (p_\mu p_\nu - p^2 \eta_{\mu\nu}). \quad (\text{E.36})$$

This corresponds to the following term in the effective action

$$2W_{\text{RC}} = \frac{\text{sgn}(m)}{2} \frac{1}{96\pi} 2 \int d^3x h_a^\mu \varepsilon^{abc} \partial_c (\partial_\mu \partial_\nu - \partial^2 \eta_{\mu\nu}) h_b^\nu + \dots \quad (\text{E.37})$$

To identify this term it is easiest to fix a Lorentz gauge where $h_{[\mu\nu]} = 0$. In terms of the p -wave SC this corresponds to $U(1)$ gauge fixing the phase θ of the order parameter to 0, along with an additional boost which is only a symmetry in the relativistic limit. Then h corresponds also to the first order metric perturbation, $g_{\mu\nu} = \eta_{\mu\nu} - 2h_{(\mu\nu)} = \eta_{\mu\nu} - 2h_{\mu\nu}$, and the above corresponds to the expansion of the gCS term

$$2W_{\text{RC}} = \frac{\text{sgn}(m)}{2} \frac{1}{96\pi} \int Q_3(\tilde{\Gamma}) + \dots \quad (\text{E.38})$$

to second order in h . In performing such expansions we found the Mathematica package xAct very useful [316, 317]. Equation (E.38) corresponds to $\kappa_H = \frac{1}{48\pi} \frac{\text{sgn}(m)}{2}$. We note that within the perturbative calculation there is no difference between $\int Q_3(\tilde{\Gamma})$ and $\int Q_3(\tilde{\omega})$, see (2.70).

The above result is valid for a vielbein $e_a^\mu = \delta_a^\mu + h_a^\mu$ which has a positive orientation. A vielbein with a negative orientation can be written as $e_a^\mu = L_a^b (\delta_b^\mu + h_b^\mu)$ where L is a Lorentz transformation with $\det L = -1$. We can deal with such vielbeins by absorbing L into the gamma matrices, $\gamma^a \mapsto L_a^b \gamma^b$. The only effect that this change has on the traces (E.7) is changing $\text{tr}(\gamma^a \gamma^b \gamma^c) = 2i\varepsilon^{abc}$ to $\text{tr}(\gamma^a \gamma^b \gamma^c) = -2i\varepsilon^{abc}$. The metric is independent of the orientation and so is $\tilde{\Gamma}$, so the result valid for both orientations is

$$2W_{\text{RC}} = \frac{\text{sgn}(m) o}{2} \frac{1}{96\pi} \int Q_3(\tilde{\Gamma}) + \dots \quad (\text{E.39})$$

where $o = \text{sgn}(\det e)$ is the orientation. The second and third lines in (E.30) correspond, with a relativistic regulator, to $O(h^2)$ contributions to the cosmological constant and E-H term which are UV sensitive.

One can compute the other traces in the same manner. The only additional UV insensitive contribution comes from the second integral in (E.32). It is given by

$$2W_{\text{RC}} = \frac{\text{sgn}(m)}{2} \frac{1}{96\pi} \int d^3x 4\omega (\partial_\mu \partial_\nu - \partial^2 \eta_{\mu\nu}) 2h^{\mu\nu} + \dots \quad (\text{E.40})$$

This corresponds to the expansion of the gpCS term to second order in the vertices,

$$2W_{\text{RC}} = \frac{\text{sgn}(m)}{2} \frac{1}{96\pi} \int d^3x |e| \tilde{\mathcal{R}}_C + \dots \quad (\text{E.41})$$

where we have used (2.69), the expansion of the curvature $\tilde{\mathcal{R}} = -2(\partial_a \partial_b - \partial^2 \eta_{ab}) h^{ab} + O(h^2)$, the definition $c = \varepsilon^{abc}(\omega_{abc} - \tilde{\omega}_{abc})$, and the expansion $\tilde{\omega}_{abc} \varepsilon^{abc} = -\varepsilon^{abc} \partial_a h_{bc} + O(h^2)$ of the LC spin connection. Note that in the Lorentz gauge $h_{[ab]} = 0$, $\tilde{\omega}_{abc} \varepsilon^{abc}$ vanishes to first order. This completes the calculation of the UV insensitive terms in the effective action which we have studied in Sec.2.

F Non-relativistic geometric quantities and their perturbative expansion

We write $E_A^i = \delta_A^i + H_A^i$ for the inverse vielbein, and expand the relevant geometric quantities in H . For the inverse metric $G^{ij} = E_A^i \delta^{AB} E_B^j$ and volume element $\sqrt{G} = |E| = |\det(E_A^i)|$ we find

$$\begin{aligned} G^{ij} &= \delta^{ij} + 2H^{(ij)} + H_A^i H^{Aj} \\ &= \delta^{ij} + \delta G^{ij}, \\ \sqrt{G} &= 1 - H_A^A + \frac{1}{2} H_A^A H_B^B + \frac{1}{2} H_A^B H_B^A + O(H^3), \\ \log \sqrt{G} &= -H_A^A + \frac{1}{2} H_A^B H_B^A + O(H^3), \end{aligned} \tag{F.1}$$

where, in expanded expressions, all index manipulations are trivial, and in particular, there is no difference between coordinate indices i, j and $SO(2)_L$ indices A, B . Note that the strain used in Sec.3 is given by $u_{ij} = (G_{ij} - \delta_{ij})/2 = -H_{(ij)} + O(H^2)$. We use the notation $\varepsilon^{\mu\nu\rho}$ for the totally anti-symmetric (pseudo) tensor, normalized such that $\varepsilon^{xyt} = 1/\sqrt{G}$, as well as $\varepsilon^{ij} = \varepsilon^{ijt}$. The non-relativistic spin connection used in Sec.3 is the $SO(2)_L$ connection

$$\begin{aligned} \omega_t &= \frac{1}{2} \varepsilon^{AB} E_{Ai} \partial_t E_B^i \\ &= -\frac{1}{2} \partial_t (\varepsilon^{AB} H_{AB}) - \frac{1}{2} \varepsilon^{AB} H_{iA} \partial_t H_B^i + O(H^3), \\ \omega_j &= \frac{1}{2} \left(\varepsilon^{AB} E_{Ai} \partial_j E_B^i - \frac{1}{E} \varepsilon^{kl} \partial_k G_{lj} \right) \\ &= -\frac{1}{2} \partial_j (\varepsilon^{AB} H_{AB}) - \partial_{\perp}^j H_{(lj)} - \frac{1}{2} \varepsilon^{AB} H_{iA} \partial_j H_B^i + O(H^3), \end{aligned} \tag{F.2}$$

where $\partial_{\perp}^l = \varepsilon^{lk} \partial_k$, which is obtained naturally within Newton-Cartan geometry [164, 44]. This connection is torsion-full, but has a vanishing “reduced torsion” [41]. In Sec.3, a term $B/2m$ was implicitly added to ω_t , but here we will add it explicitly when writing expressions for S_{eff} and S_{ind} . Such a term appears in the presence of an additional background field E_0^i which couples to momentum density P_i [41, 164], and can be identified with $G^{ij} A_j/m$ in a Galilean invariant system, where $P_i = m G_{ij} J^j$. The Ricci

scalar is given by

$$\begin{aligned}
R &= 2\varepsilon^{ij} \partial_i \omega_j \\
&= 2\partial_\perp^i \partial_\perp^j H_{ij} + O(H^2) \\
&= -2(\partial^i \partial^j - \partial^2 \delta^{ij}) H_{ij} + O(H^2).
\end{aligned} \tag{F.3}$$

G Odd viscosity at non-zero wave-vector: generalities

G.1 Definition and T symmetry

We define the viscosity tensor as the linear response of stress to strain rate

$$T^{ij}(t, \mathbf{x}) = \int dt d^2 \mathbf{x}' \eta^{ij,kl}(t, \mathbf{x}, t', \mathbf{x}') \partial_{t'} H_{kl}(t', \mathbf{x}'), \tag{G.1}$$

where

$$\eta^{[ij],kl} = 0 = \eta^{ij,[kl]}. \tag{G.2}$$

In a translationally invariant system we can pass to Fourier components $T^{ij}(\omega, \mathbf{q}) = i\omega \eta^{ij,kl}(\omega, \mathbf{q}) H_{kl}(\omega, \mathbf{q})$. By definition, $\eta^{ij,kl}(t, \mathbf{x}, t', \mathbf{x}')$ is real, and therefore

$$\eta^{ij,kl}(\omega, \mathbf{q}) = \eta^{ij,kl}(-\omega, -\mathbf{q})^*. \tag{G.3}$$

Under time reversal T ,

$$\eta^{ij,kl}(\omega, \mathbf{q}) \mapsto \eta_T^{ij,kl}(\omega, \mathbf{q}) = \eta^{kl,ij}(\omega, -\mathbf{q}). \tag{G.4}$$

The even and odd viscosities are then defined by $\eta_{e,o} = (\eta \pm \eta_T)/2$, and satisfy $(\eta_{e,o})_T = \pm \eta_{e,o}$. More explicitly,

$$\begin{aligned}
\eta_e^{ij,kl}(\omega, \mathbf{q}) &= +\eta_e^{kl,ij}(\omega, -\mathbf{q}), \\
\eta_o^{ij,kl}(\omega, \mathbf{q}) &= -\eta_o^{kl,ij}(\omega, -\mathbf{q}).
\end{aligned} \tag{G.5}$$

We will see below that in isotropic (or $SO(2)$ invariant) systems η is even in \mathbf{q} , so that

$$\eta_e^{ij,kl}(\omega, \mathbf{q}) = +\eta_e^{kl,ij}(\omega, \mathbf{q}), \tag{G.6}$$

$$\eta_o^{ij,kl}(\omega, \mathbf{q}) = -\eta_o^{kl,ij}(\omega, \mathbf{q}), \tag{G.7}$$

which is identical to the definition of $\eta_{e,o}$ at $\mathbf{q} = 0$ [173–175, 160, 176].

G.2 $SO(2)$ and P symmetries

Complex tensors satisfying (G.2) and (G.7), in 2 spatial dimensions, form a vector space $V \cong \mathbb{C}^3$ which can be spanned by [174]

$$\sigma^{ab} = 2\sigma^{[a} \otimes \sigma^{b]}, \quad a, b = 0, x, z, \quad (\text{G.8})$$

where σ^x, σ^z are the symmetric Pauli matrices, and σ^0 is the identity matrix. Thus every odd viscosity tensor can be written as

$$\eta_o(\omega, \mathbf{q}) = \eta_{xz}(\omega, \mathbf{q}) \sigma^{xz} + \eta_{x0}(\omega, \mathbf{q}) \sigma^{x0} + \eta_{z0}(\omega, \mathbf{q}) \sigma^{z0}, \quad (\text{G.9})$$

with complex coefficients $\eta_{ab}(\omega, \mathbf{q})$. Under a rotation $R = e^{i\alpha(i\sigma^y)} \in SO(2)$ the metric perturbation and stress tensor transform as

$$\begin{aligned} H_{ij}(\omega, \mathbf{q}) &\mapsto R_i^k R_j^l H_{kl}(\omega, R^{-1} \cdot \mathbf{q}), \\ T^{ij}(\omega, \mathbf{q}) &\mapsto R_k^i R_l^j T^{kl}(\omega, R^{-1} \cdot \mathbf{q}), \end{aligned} \quad (\text{G.10})$$

where $(R \cdot \mathbf{q})^i = R_j^i q^j$. The same transformation rules apply for $R \in O(2)$, which defines the parity transformation P , in flat space. It follows that

$$\eta^{ij,kl}(\omega, \mathbf{q}) \mapsto R_{i'}^i R_{j'}^j R_{k'}^k R_{l'}^l \eta^{i'j',k'l'}(\omega, R^{-1} \cdot \mathbf{q}) \quad (\text{G.11})$$

under $O(2)$, which is compatible with (G.2), and the decomposition $\eta = \eta_o + \eta_e$. In particular, equation (G.11) shows that the viscosity tensor is P -even, or more accurately, a tensor under P rather than a pseudo-tensor. In an $SO(2)$ -invariant system, the viscosity tensor will also be $SO(2)$ -invariant

$$\eta^{ij,kl}(\omega, \mathbf{q}) = R_{i'}^i R_{j'}^j R_{k'}^k R_{l'}^l \eta^{i'j',k'l'}(\omega, R^{-1} \cdot \mathbf{q}), \quad R \in SO(2). \quad (\text{G.12})$$

Note that this holds even when $SO(2)$ symmetry is *spontaneously* broken, as in ℓ -wave SFs. At $\mathbf{q} = \mathbf{0}$, there is a unique tensor satisfying (G.12), namely

$$(\sigma^{xz})^{ij,kl} = -\frac{1}{2} (\varepsilon^{ik} \delta^{jl} + \varepsilon^{jk} \delta^{il} + \varepsilon^{il} \delta^{jk} + \varepsilon^{jl} \delta^{ik}), \quad (\text{G.13})$$

leaving a single odd viscosity coefficient $\eta_{xz}(\omega) = \eta_o^{(1)}(\omega)$ [173–175, 160, 176].

A non-zero \mathbf{q} , however, along with the tensors δ^{ij} and ε^{ij} , can be used to construct additional $SO(2)$ -invariant odd viscosity tensors, beyond σ^{xz} . From the data $\mathbf{q}, \delta^{ij}, \varepsilon^{ij}$, three linearly independent,

symmetric, rank-2 tensors can be constructed, which we take to be

$$\begin{aligned}(\tau^0)^{ij} &= q^2 \delta^{ij}, \\ (\tau^x)^{ij} &= -2q_\perp^i q^j / q^2, \\ (\tau^z)^{ij} &= 2q^i q^j / q^2 - \delta^{ij},\end{aligned}\tag{G.14}$$

where $q_\perp^i = \varepsilon^{ij} q_j$. The notation above is due to the relation

$$\begin{aligned}\begin{pmatrix} \tau^x \\ \tau^z \end{pmatrix} &= \begin{pmatrix} \cos 2\theta & -\sin 2\theta \\ \sin 2\theta & \cos 2\theta \end{pmatrix} \begin{pmatrix} \sigma^x \\ \sigma^z \end{pmatrix} \\ &= \frac{1}{q^2} \begin{pmatrix} q_x^2 - q_y^2 & -2q_x q_y \\ 2q_x q_y & q_x^2 - q_y^2 \end{pmatrix} \begin{pmatrix} \sigma^x \\ \sigma^z \end{pmatrix},\end{aligned}\tag{G.15}$$

where $\theta = \arg(\mathbf{q})$, so that τ^x, τ^z are a rotated version of σ^x, σ^z . Moreover, all three τ s are $SO(2)$ -invariant, $\tau^{ij}(\mathbf{q}) = R_{i'}^i R_{j'}^j \tau^{i'j'}(R^{-1} \cdot \mathbf{q})$, and can therefore be used to construct three $SO(2)$ -invariant odd viscosity tensors

$$\tau^{ab} = 2\tau^{[a} \otimes \tau^{b]}, \quad a, b = 0, x, z,\tag{G.16}$$

which form a basis for V . Any odd viscosity tensor (at $\mathbf{q} \neq \mathbf{0}$) can then be written as

$$\eta_o(\omega, \mathbf{q}) = \eta_o^{(1)}(\omega, \mathbf{q}) \tau^{xz} + \eta_o^{(2)}(\omega, \mathbf{q}) \tau^{0x} + \eta_o^{(3)}(\omega, \mathbf{q}) \tau^{0z}.\tag{G.17}$$

Furthermore, for an $SO(2)$ -invariant η_o , the coefficients $\eta_o^{(1)}, \eta_o^{(2)}, \eta_o^{(3)}$ depend on \mathbf{q} through its norm, owing to the $SO(2)$ -invariance of τ^{ab} . We therefore arrive at the general form of an $SO(2)$ -invariant odd viscosity tensor,

$$\eta_o(\omega, \mathbf{q}) = \eta_o^{(1)}(\omega, q^2) \tau^{xz} + \eta_o^{(2)}(\omega, q^2) \tau^{0x} + \eta_o^{(3)}(\omega, q^2) \tau^{0z}.\tag{G.18}$$

In particular, we see that η_o is even in \mathbf{q} (and the same applies also to the even viscosity η_e). To determine the small ω, \mathbf{q} behavior of the coefficients we change to the \mathbf{q} -independent basis of σ s,

$$\begin{aligned}\eta_o(\omega, \mathbf{q}) &= \eta_o^{(1)}(\omega, q^2) \sigma^{xz} \\ &\quad + [\eta_o^{(2)}(\omega, q^2) (q_x^2 - q_y^2) + \eta_o^{(3)}(\omega, q^2) (2q_x q_y)] \sigma^{0x} \\ &\quad + [\eta_o^{(2)}(\omega, q^2) (-2q_x q_y) + \eta_o^{(3)}(\omega, q^2) (q_x^2 - q_y^2)] \sigma^{0z}.\end{aligned}\tag{G.19}$$

In gapped systems (such as QH states) η_o will be regular around $\omega = 0 = q$, and so will the coefficients $\eta_o^{(1)}, \eta_o^{(2)}, \eta_o^{(3)}$. In gapless systems (such as ℓ -wave SFs) there will be a singularity at $\omega = 0 = q$, but the limit $q \rightarrow 0$ at $\omega \neq 0$ will be regular. In both cases, the limit $q \rightarrow 0$ at $\omega \neq 0$ of (G.19) reduces to the known result $\eta_o(\omega, \mathbf{0}) = \eta_o^{(1)}(\omega, 0) \sigma^{xz}$ [173–175, 160, 176].

G.3 PT symmetry

The combination PT of parity and time-reversal is a symmetry in any system in which T is broken (perhaps spontaneously) due to some kind of angular momentum, as in QH states, ℓ -wave SFs, and active chiral fluids [183]. Here we consider the implications of PT symmetry on (G.19).

From the definition (G.14) it is clear that τ^0 and τ^z are P -even, while τ^x is P -odd. Therefore, τ^{xz}, τ^{0x} are P -odd while τ^{0z} is P -even (and all three are T -even). Since η_o is T -odd and P -even, and using (G.18), it follows that $\eta_o^{(1)}$ and $\eta_o^{(2)}$ are P, T -odd, while $\eta_o^{(3)}$ is T -odd but P -even. In particular, $\eta_o^{(3)}$ is PT -odd, and must vanish in PT -symmetric systems. The odd viscosity tensor in $SO(2)$ and PT symmetric systems is therefore given by

$$\begin{aligned} \eta_o(\omega, \mathbf{q}) = & \eta_o^{(1)}(\omega, q^2) \sigma^{xz} \\ & + \eta_o^{(2)}(\omega, q^2) [(q_x^2 - q_y^2) \sigma^{0x} - 2q_x q_y \sigma^{0z}]. \end{aligned} \quad (\text{G.20})$$

This form is confirmed by previous results for QH states [34], and by the results presented in Sec.3 for ℓ -wave SFs. The same form is obtained at $\mathbf{q} = \mathbf{0}$, but in the presence of vector, or pseudo-vector, anisotropy \mathbf{b} , in which case we find

$$\begin{aligned} \eta_o(\omega) = & \eta_o^{(1)}(\omega) \sigma^{xz} \\ & + \eta_o^{(2)}(\omega) [(b_x^2 - b_y^2) \sigma^{0x} - 2b_x b_y \sigma^{0z}], \end{aligned} \quad (\text{G.21})$$

which explains the tensor structure found in [263, 264].

G.4 Frequency dependence and reality conditions

In closed and clean systems, like the ℓ -wave SFs studied in Sec.3, the viscosity can be obtained from an induced action

$$\begin{aligned} S_{\text{ind}} \supset & \frac{1}{2} \int dt dt' d^2 \mathbf{x} d^2 \mathbf{x}' H_{ij}(t, \mathbf{x}) \eta^{ij,kl}(t - t', \mathbf{x} - \mathbf{x}') \partial_{t'} H_{kl}(t', \mathbf{x}') \\ = & \frac{1}{2} \int \frac{d\omega}{2\pi} \frac{d^2 \mathbf{q}}{(2\pi)^2} H_{ij}(-\omega, -\mathbf{q}) i\omega \eta^{ij,kl}(\omega, \mathbf{q}) H_{kl}(\omega, \mathbf{q}). \end{aligned} \quad (\text{G.22})$$

As a result, η satisfies the additional property,

$$\eta^{ij,kl}(\omega, \mathbf{q}) = -\eta^{kl,ij}(-\omega, -\mathbf{q}), \quad (\text{G.23})$$

which, along with (G.7)-(G.6) and the fact that η is even in \mathbf{q} , implies that η_o (η_e) is even (odd) in ω ,

$$\begin{aligned} \eta_e^{ij,kl}(\omega, \mathbf{q}) &= -\eta_e^{ij,kl}(-\omega, \mathbf{q}), \\ \eta_o^{ij,kl}(\omega, \mathbf{q}) &= +\eta_o^{ij,kl}(-\omega, \mathbf{q}). \end{aligned} \quad (\text{G.24})$$

This result, along with (G.3) and the fact that η is even in \mathbf{q} , implies that η_o (η_e) is real (imaginary),

$$\begin{aligned}\eta_e^{ij,kl}(\omega, \mathbf{q}) &\in i\mathbb{R}, \\ \eta_o^{ij,kl}(\omega, \mathbf{q}) &\in \mathbb{R}.\end{aligned}\tag{G.25}$$

These general properties are satisfied by the odd viscosity tensor computed in Sec.3. These are also compatible with the examples worked out in [175], as well with viscosity-conductivity relations that hold in Galilean invariant systems (in conjugation with known properties of the conductivity) [248, 175, 163].

We note that some care is required when interpreting (G.24)-(G.25) around singularities of η . For example, the first equation in (G.24) *naively* implies that $\eta_e(0, \mathbf{q}) = 0$, which in particular implies that the bulk and shear viscosities $\eta_e(0, \mathbf{0}) = \zeta \sigma^0 \otimes \sigma^0 + \eta^s (\sigma^x \otimes \sigma^z + \sigma^z \otimes \sigma^x)$ vanish in the closed, clean, case. This however, is not quite correct, due to a possible singularity of η_e at $\omega = 0$, as well as the usual infinitesimal imaginary part of ω required to obtain the retarded response. For example, for free fermions, reference [175] finds $\eta^s(\omega, \mathbf{0}) \sim \frac{i}{\omega + i\epsilon} = \pi\delta(\omega) + i\text{PV}\frac{1}{\omega}$ (where PV is the principle value), which has an infinite real part at $\omega = 0$, in analogy with the Drude behavior of the conductivity.

G.5 Odd viscosity from Gaussian integration: a technical result

We now restrict attention to ℓ -wave SFs. The effective Lagrangian, perturbatively expanded to second order, and in the absence of the $U(1)$ background, takes the form

$$\mathcal{L}_{\text{eff}} = \frac{1}{2}\theta\mathcal{G}^{-1}\theta + \mathcal{V}\theta + \mathcal{C},\tag{G.26}$$

where the Green's function \mathcal{G} is independent of H , the vertex \mathcal{V} is linear in H , and the contact term \mathcal{C} is quadratic in H . Performing Gaussian integration over θ yields the induced Lagrangian

$$\mathcal{L}_{\text{ind}} = -\frac{1}{2}\mathcal{V}\mathcal{G}\mathcal{V} + \mathcal{C},\tag{G.27}$$

and comparing with (G.22) one can read off η_o . In Appendix H we write explicit expressions for a Galilean invariant \mathcal{L}_{eff} , which we then expand to obtain explicit expressions for $\mathcal{G}^{-1}, \mathcal{V}, \mathcal{C}$. Appendix I then describes the resulting \mathcal{L}_{ind} . Here we take a complementary approach and obtain the general form of η_o from (G.27), using the formalism developed above, based only on $SO(2)$ and PT symmetries.

The motivation for the analysis in this section is the following. The power counting described in Sec.3.2 is designed such that the $O(p^n)$ Lagrangian $\mathcal{L}_n \subset \mathcal{L}_{\text{eff}}$ produces $O(p^n)$ contributions to \mathcal{L}_{ind} . Therefore, naively, one expects the $O(q^2)$ odd viscosity to depend on $\mathcal{L}_0, \mathcal{L}_2$, and \mathcal{L}_3 (since $\mathcal{L}_1 = 0$). Using the notation $\eta_o = \eta_{\mathcal{V}} + \eta_{\mathcal{C}}$ for the parts of η_o due to $-\mathcal{V}\mathcal{G}\mathcal{V}/2$ and \mathcal{C} , respectively, the result of this section is that $\eta_{\mathcal{V}}$, to $O(q^2)$, is actually independent of \mathcal{L}_3 .

We now describe the details. For $\eta_{\mathcal{C}}$, we cannot do better than the general discussion thus far - it is given by (G.19), with $\eta_o^{(3)} = 0$, and both $\eta_o^{(1)}, \eta_o^{(2)}$ are real and regular at $\omega = 0 = q$, since \mathcal{L}_{eff} , and \mathcal{C} in particular, are obtained by integrating out gapped degrees of freedom (the Higgs modes and the

fermion ψ). For $\eta_{\mathcal{V}}$, however, we can do better. We first write more explicitly

$$\begin{aligned}\theta \mathcal{G}^{-1} \theta &= \frac{1}{2} \theta(-\omega, -\mathbf{q}) \mathcal{G}^{-1}(\omega, \mathbf{q}) \theta(\omega, \mathbf{q}), \\ \mathcal{V} \theta &= \theta(-\omega, -\mathbf{q}) V^{ij}(\omega, \mathbf{q}) H_{ij}(\omega, \mathbf{q}).\end{aligned}\tag{G.28}$$

Based on $SO(2)$ and PT symmetries, the objects \mathcal{G}^{-1}, V^{ij} take the forms

$$\begin{aligned}\mathcal{G}^{-1}(\omega, \mathbf{q}) &= D(\omega^2, q^2), \\ V^{ij}(\omega, \mathbf{q}) &= i\omega a(\omega^2, q^2) (\rho^0)^{ij} + i\omega b(\omega^2, q^2) (\rho^z)^{ij} + s_{\theta} c(\omega^2, q^2) (\rho^x)^{ij},\end{aligned}\tag{G.29}$$

where

$$\begin{aligned}(\rho^0)^{ij} &= \delta^{ij}, \\ (\rho^x)^{ij} &= q_{\perp}^{(i} q^{j)}, \\ (\rho^z)^{ij} &= q^i q^j,\end{aligned}\tag{G.30}$$

are, in this context, more convenient than the τ s (G.14), and a, b, c, D are general functions of their arguments which are P, T -even, real, and regular at $\omega = 0 = q$, as follows from the same properties of \mathcal{L}_{eff} . In particular, we will use the following expansions

$$\begin{aligned}a(0, q^2) &= a_0 + a_1 q^2 + O(q^4), \\ b(0, q^2) &= b_0 + O(q^2), \\ c(0, q^2) &= c_0 + c_1 q^2 + O(q^4), \\ D(0, q^2) &= D_1 q^2 + D_2 q^4 + O(q^6),\end{aligned}\tag{G.31}$$

where $D_0 = 0$ because θ enters \mathcal{L}_{eff} only through its derivatives. The odd viscosity $\eta_{\mathcal{V}}$ is then given by

$$\begin{aligned}\eta_{\mathcal{V}}(\omega, \mathbf{q}) &= -\frac{1}{2i\omega} \frac{V(-\omega, -\mathbf{q}) \otimes V(\omega, \mathbf{q}) - V(\omega, \mathbf{q}) \otimes V(-\omega, -\mathbf{q})}{D(\omega, \mathbf{q})} \\ &= \frac{2s_{\theta} c(\omega^2, q^2)}{D(\omega^2, q^2)} [a(\omega^2, q^2) \rho^{0x} + b(\omega^2, q^2) \rho^{zx}],\end{aligned}\tag{G.32}$$

which is of the form (G.19), with $\eta_{\text{o}}^{(3)} = 0$ and

$$\begin{aligned}\eta_{\mathcal{V}}^{(1)}(\omega, q^2) &= -\frac{s_{\theta} c(\omega^2, q^2)}{2D(\omega^2, q^2)} b(\omega^2, q^2) q^4, \\ \eta_{\mathcal{V}}^{(2)}(\omega, q^2) &= \frac{s_{\theta} c(\omega^2, q^2)}{D(\omega^2, q^2)} [a(\omega^2, q^2) + b(\omega^2, q^2) q^2].\end{aligned}\tag{G.33}$$

Setting $\omega = 0$ and expanding in q , we find

$$\begin{aligned}\eta_{\mathcal{V}}^{(1)}(0, q^2) &= -\frac{s_\theta c_0 b_0}{2D_1} q^2 + O(q^4), \\ \eta_{\mathcal{V}}^{(2)}(0, q^2) &= \frac{s_\theta}{D_1} \left[a_0 c_0 q^{-2} + \left(a_0 c_1 + a_1 c_0 + b_0 c_0 - a_0 c_0 \frac{D_2}{D_1} \right) \right] + O(q^2).\end{aligned}\tag{G.34}$$

Having identified the coefficients $a_0, a_1, b_0, c_0, c_1, D_1, D_2$ that determine $\eta_{\mathcal{V}}$ to $O(q^2)$, we now determine the order in the derivative expansion of \mathcal{L}_{eff} in which these enter. Explicitly, the above coefficients are defined by

$$\begin{aligned}\mathcal{L}_{\text{eff}} \supset & \frac{1}{2} \theta(-\omega, -\mathbf{q}) (D_1 q^2 + D_2 q^4) \theta(\omega, \mathbf{q}) \\ & + \theta(-\omega, -\mathbf{q}) \left[i\omega (a_0 + a_1 q^2) \delta^{ij} + i\omega b_0 q^i q^j + s_\theta (c_0 + c_1 q^2) q^i q_\perp^j \right] H_{ij}(\omega, \mathbf{q}).\end{aligned}\tag{G.35}$$

We see that c_1 enters \mathcal{L}_{eff} at $O(p^3)$, while all other coefficients enter at a lower order, and come from $\mathcal{L}_0, \mathcal{L}_2$. In particular, $\eta_{\mathcal{V}}^{(1)}$ in (G.34) is independent of \mathcal{L}_3 . Even though c_1 is the coefficient of an $O(p^3)$ term, it is actually due to \mathcal{L}_2 . Using (F.2) we identify $c_0 \theta q^2 q^i q_\perp^j H_{ij} = -s_\theta c_1 \partial^i \theta \partial^2 \omega_i$, which must be a part of

$$\frac{c_1}{2} (\partial_i \theta - A_i - s_\theta \omega_i) \partial^2 (\partial_i \theta - A_i - s_\theta \omega_i).\tag{G.36}$$

This is an $O(p^2)$ term, and in fact comes from $\mathcal{L}_2^{(2)} \subset \mathcal{L}_2$, see (H.7). Thus, both $\eta_{\mathcal{V}}^{(1)}, \eta_{\mathcal{V}}^{(2)}$ in (G.34) are completely independent of \mathcal{L}_3 .

H Effective action and its perturbative expansion

H.1 Zeroth order

It is useful to write the zeroth order scalar X as

$$X = \left(\partial_t \theta - \mathcal{A}_t - \frac{s_\theta}{2m} B \right) - \frac{1}{2m} G^{ij} (\partial_i \theta - \mathcal{A}_i) (\partial_j \theta - \mathcal{A}_j),\tag{H.1}$$

where

$$\mathcal{A}_\mu = A_\mu + s_\theta \omega_\mu.\tag{H.2}$$

We will also use $\mathcal{B} = B + \frac{s_\theta}{2} R$, $\mathcal{E}_i = E_i + s_\theta E_{\omega,i}$ for the magnetic and electric fields obtained from \mathcal{A}_μ , where $E_{\omega,i} = \partial_t \omega_i - \partial_i \omega_t$. Expanding $\mathcal{L}_0 = P(X)$ to second order in the fields, one finds (up to total

derivatives)

$$\begin{aligned}
\sqrt{G}\mathcal{L}_0 &= \frac{1}{2} \frac{n_0}{m} \theta \left[\partial^2 - c_s^{-2} \partial_t^2 \right] \theta \\
&\quad + \left[-\frac{n_0}{m} \left(\partial_i \mathcal{A}^i - c_s^{-2} \partial_t \left(\mathcal{A}_t + \frac{s_\theta}{2m} B \right) \right) - n_0 \partial_t \sqrt{G} \right] \theta \\
&\quad + \left[-n_0 \sqrt{G} \mathcal{A}_t - \frac{1}{2} \frac{n_0}{m} \left(\mathcal{A}^2 - c_s^{-2} \left(\mathcal{A}_t + \frac{s_\theta}{2m} B \right)^2 \right) + P_0 \sqrt{G} \right] \\
&= \frac{1}{2} \theta \mathcal{G}^{-1} \theta + \mathcal{V} \theta + \mathcal{C},
\end{aligned} \tag{H.3}$$

where $\partial^2 = \partial^i \partial_i$, $\mathcal{A}^2 = \mathcal{A}_i \mathcal{A}^i$, and we defined the inverse Green's function \mathcal{G}^{-1} , vertex \mathcal{V} , and contact terms \mathcal{C} , respectively. These are used in section I below to obtain S_{ind} .

In (H.3), the geometric objects \sqrt{G} and ω_μ should be interpreted as expanded to the required order according to (F.1)-(F.2). In particular, the term $-n_0 \sqrt{G} \mathcal{A}_t$ includes $-s_\theta n_0 \sqrt{G} \omega_t$, which produces the leading contribution to $\eta_o^{(1)}$. To see this, we expand

$$\begin{aligned}
\sqrt{G} \omega_t &= -\frac{1}{2} \partial_t (\varepsilon^{AB} H_{AB}) + \frac{1}{2} \partial_t (\varepsilon^{AB} H_{AB}) H_i^i - \frac{1}{2} \varepsilon^{AB} H_{iA} \partial_t H_B^i + O(H^3) \\
&= -\frac{1}{2} \partial_t (\varepsilon^{AB} H_{AB}) - \frac{1}{2} \varepsilon^{AB} H_{Ai} \partial_t H_B^i + O(H^3),
\end{aligned} \tag{H.4}$$

which is identical to the expansion (F.1) of ω_t , apart from $H_{iA} \leftrightarrow H_{Ai}$. Ignoring total derivatives, this reduces to

$$\begin{aligned}
\sqrt{G} \mathcal{L}_0 &\supset -s_\theta n_0 \sqrt{G} \omega_t \\
&= -\frac{1}{2} s_\theta n_0 \left[\partial_t (\varepsilon^{AB} H_{AB}) H_i^i - \varepsilon^{AB} \delta^{ij} H_{(Ai)} \partial_t H_{(Bj)} \right] + O(H^3) \\
&= \frac{1}{2} s_\theta n_0 \varepsilon^{AB} H_{Ai} \partial_t H_B^i + O(H^3).
\end{aligned} \tag{H.5}$$

Comparing with (G.13) and (G.22), the second term in the second line corresponds to $\eta_o^{(1)} = -s_\theta n_0/2$. The first term in the second line depends on the anti-symmetric part of H , and shows that the full expression (H.5) actually corresponds to a *torsional* Hall (or odd) viscosity [155, 156] $\zeta_H = -s_\theta n_0$, which can be read off from the third line. The appearance of the torsional Hall viscosity at the level of S_{eff} (but not at the level of S_{ind} , see section I) can be understood from the mapping of [1] of the p -wave SF to a Majorana spinor in Riemann-Cartan space-time.

H.2 Second order

The full expression for \mathcal{L}_2 is given by $\mathcal{L}_2 = \sum_{i=1}^6 \mathcal{L}_2^{(i)}$, where [199]

$$\begin{aligned}
\mathcal{L}_2^{(1)} &= F_1(X) R, \\
\mathcal{L}_2^{(2)} &= F_2(X) (mK_i^i - \nabla^2 \theta)^2, \\
\mathcal{L}_2^{(3)} &= F_3(X) \left\{ -m^2 (G^{ij} \partial_t K_{ij} - K^{ij} K_{ij}) - m \nabla_i E^i + \frac{1}{4} F^{ij} F_{ij} \right. \\
&\quad \left. + 2m \left[\partial_i K_j^j - \nabla^j \left(K_{ji} + \frac{1}{2m} F_{ji} \right) \right] \nabla^i \theta + R_{ij} \nabla_i \theta \nabla_j \theta \right\}, \\
\mathcal{L}_2^{(4)} &= F_4(X) G^{ij} \partial_i X \partial_j X, \\
\mathcal{L}_2^{(5)} &= F_5(X) \left[\left(\partial_t - \frac{1}{m} \nabla^i \theta \partial_i \right) X \right]^2, \\
\mathcal{L}_2^{(6)} &= F_6(X) (mK_i^i - \nabla^2 \theta) \left[\left(\partial_t - \frac{1}{m} \nabla^i \theta \partial_i \right) X \right].
\end{aligned} \tag{H.6}$$

The terms $\mathcal{L}_2^{(5)}$ and $\mathcal{L}_2^{(6)}$ were not written explicitly in [199] because, on shell (on the equation of motion for θ), they are proportional to $\mathcal{L}_2^{(4)}$ up to $O(p^4)$ corrections, and can therefore be eliminated by a redefinition of F_4 . However, for the purpose of comparing the general S_{eff} with the microscopic expression (J.19), it is convenient to work off shell and keep all terms explicit.

Specializing to 2+1 dimensions and expanding to second order in fields, one finds

$$\begin{aligned}
\sqrt{G} \mathcal{L}_2^{(1)} &= F_1'(\mu) R \left(\partial_t \theta - \mathcal{A}_t - \frac{s_\theta}{2m} B \right), \\
\sqrt{G} \mathcal{L}_2^{(2)} &= F_2(\mu) \left[-m^2 H_i^i \partial_t^2 H_j^j + 2m \partial_t H_k^k \partial^j (\partial_j \theta - \mathcal{A}_j) - (\partial_i \theta - \mathcal{A}_i) \partial^i \partial^j (\partial_i \theta - \mathcal{A}_i) \right], \\
\sqrt{G} \mathcal{L}_2^{(3)} &= F_3(\mu) \left(m^2 H^{(ij)} \partial_t^2 H_{(ij)} + \frac{1}{2} B^2 - 2m \varepsilon^{ij} \omega_i \partial_t (\partial_j \theta - \mathcal{A}_j) - B \mathcal{B} \right) \\
&\quad + F_3'(\mu) \left(\partial_t \theta - \mathcal{A}_t - \frac{s_\theta}{2m} B \right) (m^2 \partial_t^2 H_i^i - m \partial_i E^i), \\
\sqrt{G} \mathcal{L}_2^{(4)} &= -F_4(\mu) \left(\partial_t \theta - \mathcal{A}_t - \frac{s_\theta}{2m} B \right) \partial^2 \left(\partial_t \theta - \mathcal{A}_t - \frac{s_\theta}{2m} B \right), \\
\sqrt{G} \mathcal{L}_2^{(5)} &= -F_5(\mu) \left(\partial_t \theta - \mathcal{A}_t - \frac{s_\theta}{2m} B \right) \partial_t^2 \left(\partial_t \theta - \mathcal{A}_t - \frac{s_\theta}{2m} B \right), \\
\sqrt{G} \mathcal{L}_2^{(6)} &= -F_6(\mu) \left[m \partial_t H_i^i + \partial^j (\partial_j \theta - \mathcal{A}_j) \right] \partial_t \left(\partial_t \theta - \mathcal{A}_t - \frac{s_\theta}{2m} B \right),
\end{aligned} \tag{H.7}$$

from which one can easily extract the second order corrections to $\mathcal{G}^{-1}, \mathcal{V}, \mathcal{C}$, of (H.3). Note that $\mathcal{L}_2^{(3)}$ includes a term $\propto \varepsilon^{ij} \omega_i \partial_t \mathcal{A}_j = \varepsilon^{ij} \omega_i \partial_t (A_j + s_\theta \omega_j)$. Comparing with (H.8) below, it is clear that distinguishing $\mathcal{L}_2^{(3)}$ from \mathcal{L}_{gCS} is non-trivial. This is in fact the same problem of extracting the central charge from the Hall viscosity addressed in Sec.3.4, but at the level of S_{eff} (where θ is viewed as a background field) rather than S_{ind} (where θ has been integrated out). Accordingly, the central charge can be computed by applying Eq.(3.17) to the response functions obtained from S_{eff} . Additionally, relying on LGS, one can extract F_3 as the coefficient of $H^{(ij)} \partial_t^2 H_{(ij)}$. Both approaches produce the same central charge

(3.11) in the perturbative computation of Sec.3.3 and Appendix J.5.

H.3 Gravitational Chern-Simons term

The gCS Lagrangian is given explicitly by

$$\begin{aligned}\mathcal{L}_{\text{gCS}} &= -\frac{c}{48\pi} \left[\left(\omega_t + \frac{B}{2m} \right) R - \varepsilon^{ij} \omega_i \partial_t \omega_j \right] \\ &= -\frac{c}{48\pi} \left[\omega d\omega + \frac{1}{2m} B R \right].\end{aligned}\tag{H.8}$$

Its expansion to second order in fields, using (F.1)-(F.2), is

$$\sqrt{G} \mathcal{L}_{\text{gCS}} = -\frac{c}{48\pi} \left[\varepsilon^{AB} H_{(Ai)} \partial_\perp^i \partial_\perp^j \partial_t H_{(Bj)} - \frac{1}{m} A_i \partial_\perp^i \partial_\perp^j \partial_\perp^k H_{(jk)} \right].\tag{H.9}$$

As opposed to $\sqrt{G}\omega_t$, the gCS term \mathcal{L}_{gCS} is (locally) $SO(2)_L$ gauge invariant, and accordingly depends only on the metric, or, within the perturbative expansion, on the symmetric part $H_{(ij)}$. From this expansion one can read off the gCS contributions to the odd viscosity η_o , and to the odd, mixed, static susceptibility $\chi_{TJ,o}$, described in Sec.3.4.

H.4 Additional terms at third order

To obtain reliable results at $O(p^3)$ we, in principle, need the full Lagrangian \mathcal{L}_3 , which includes, but is not equal to, \mathcal{L}_{gCS} . Nevertheless, we argue that $\mathcal{L}_3 - \mathcal{L}_{\text{gCS}}$ does not contribute to the quantity of interest in this section - η_o to $O(q^2)$. We already demonstrated in Appendix G.5 that the vertex part of the odd viscosity η_V is independent of \mathcal{L}_3 , and it remains to show that the contact term part η_C is independent of $\mathcal{L}_3 - \mathcal{L}_{\text{gCS}}$. We do not have a general proof, but we address this issue in two ways:

1. Within the microscopic model (3.8), the perturbative computation of Appendix J.5 provides an explicit expression for η_C , which is completely saturated by the effective action presented thus far. Thus η_C is independent of $\mathcal{L}_3 - \mathcal{L}_{\text{gCS}}$ in the particular realization (3.8).
2. The term \mathcal{L}_3 is P, T -odd, and therefore vanishes in an s -wave SF. On the other hand, it suffices to consider the gs -wave SF where $s_\theta = 0$ (but $\ell \neq 0$), since for $s_\theta \neq 0$ the spin connection included in $\nabla_\mu \theta$ will only produce $O(p^4)$ corrections. By contracting Galilean vectors, we were able to construct four P, T -odd terms in $\mathcal{L}_3 - \mathcal{L}_{\text{gCS}}$ for the gs -wave SF,

$$\mathcal{L}_3 - \mathcal{L}_{\text{gCS}} \supset \ell \left[C_1(X) \tilde{E}_i E_\omega^i + C_2(X) \varepsilon^{ij} \tilde{E}_i E_{\omega,j} + C_3(X) \partial_i X E_\omega^j + C_4(X) \varepsilon^{ij} \partial_i X E_{\omega,j} \right].\tag{H.10}$$

where \tilde{E}_i is the electric field of the improved $U(1)$ connection $\tilde{A}_t = A_t + \frac{1}{2m} \nabla^i \theta \nabla_i \theta$, $\tilde{A}_i = \partial_i \theta - s_\theta \omega_i$ [163]. Perturbatively expanding these, we do not find any $O(q^2)$ contributions to η_C (or to η_V , in accordance with Appendix G.5).

I Induced action

The arguments presented in Sec.3 suffice to establish the quantization of $\tilde{\eta}_o$ and $\tilde{\chi}_{TJ,o}$ directly from S_{eff} - an explicit expression for S_{ind} is not required. Nevertheless, it is instructive to compute certain contributions in S_{ind} to demonstrate these results explicitly, and also to reproduce simpler properties of ℓ -wave SFs. Here we will compute the contribution of $\mathcal{L}_0 + \mathcal{L}_2^{(1)} \subset \mathcal{L}_{\text{eff}}$ to the induced Lagrangian \mathcal{L}_{ind} , and, along the way, demonstrate explicitly the relation between $\text{vars} = 0$ QH states and CSFs alluded to in Sec.3.5.

The starting point is the induced action due to $\mathcal{L}_0 = P(X)$, obtained from (H.3). It is given by

$$\begin{aligned} \mathcal{L}_{\text{ind}} &= -\frac{1}{2}\mathcal{V}\mathcal{G}\mathcal{V} + \mathcal{C} \\ &= P_0\sqrt{G} - n_0\mathcal{A}_t \\ &\quad + \frac{1}{2}\frac{n_0}{m}\frac{\mathcal{B}^2 - c_s^{-2}\mathcal{E}^2 + \frac{s_\theta c_s^{-2}}{m}\mathcal{E}^i\partial_i B - \frac{s_\theta^2 c_s^{-2}}{4m^2}(\partial B)^2}{\partial^2 - c_s^{-2}\partial_t^2} \\ &\quad - n_0\frac{m\left(\partial_t\sqrt{G}\right)^2/2 + \left(\mathcal{E}^i - \frac{s_\theta}{2m}\partial_i B\right)\partial_i\sqrt{G}}{\partial^2 - c_s^{-2}\partial_t^2}. \end{aligned} \tag{I.1}$$

This expression contains, rather compactly, the entire linear response of the ℓ -wave SF to $O(p)$ in the derivative expansion, as well as certain $O(p^2)$ contributions [163], and should be interpreted as expanded to second order using (F.1)-(F.2). In using (F.2), one can set $H_{[AB]} = 0$, since S_{ind} is $SO(2)_L$ invariant and the anti-symmetric part $H_{[AB]}$ corresponds to the $SO(2)_L$ phase of the vielbein E_A^i . Technically, $H_{[AB]}$ always appears in the combination $\partial_\mu(\theta + s_\theta\epsilon^{AB}H_{AB}/2) \subset \nabla_\mu\theta$, so that integrating out θ eliminates $H_{[AB]}$.

Note that, diagrammatically, equation (I.1) corresponds to linear response at tree-level. Higher orders in θ will generate diagrams with θ running in loops, which can be shown to produce $O(p^3)$ corrections above the leading order to any observable [199], and are therefore irrelevant for the purpose of q^2 corrections to η_o .

The $O(p^0)$ part of (I.1) is obtained by setting $s_\theta = 0$, as in an s -wave SF,

$$\begin{aligned} \mathcal{L}_{\text{ind},0} &= P_0\sqrt{G} - n_0\mathcal{A}_t + \frac{1}{2}\frac{n_0}{m}\frac{B^2 - c_s^{-2}E^2}{\partial^2 - c_s^{-2}\partial_t^2} \\ &\quad - n_0\frac{m\left(\partial_t\sqrt{G}\right)^2/2 + E^i\partial_i\sqrt{G}}{\partial^2 - c_s^{-2}\partial_t^2} \end{aligned} \tag{I.2}$$

The first line contains the ground state pressure and density P_0, n_0 , as well as the London diamagnetic function $\rho_e = \frac{n_0}{m}\frac{1}{q^2 - c_s^{-2}\omega^2}$ and the ideal Drude longitudinal conductivity $\sigma_e = -\frac{n_0}{m}\frac{i\omega c_s^{-2}}{q^2 - c_s^{-2}\omega^2}$ of the SF

[163]. The second line contains the mixed response and mixed static susceptibility

$$\begin{aligned}\kappa_e^{ij,k} &= -n_0 \delta^{ij} \frac{iq^k}{q^2 - c_s^{-2} \omega^2}, \\ \chi_{TJ,e}^{ij,t} &= n_0 \delta^{ij} \frac{q^2}{q^2 - c_s^{-2} \omega^2},\end{aligned}\tag{I.3}$$

defined in Sec.3.4, as well as the inverse compressibility $K^{-1} = -n_0 m \frac{\omega^2}{q^2 - c_s^{-2} \omega^2}$ (which agrees with the thermodynamic expression $K^{-1} = n_0^2 \frac{\partial \mu}{\partial n_0} = n_0 m c_s^2$ at $q = 0$). In particular, the ℓ -wave SF is indeed a superfluid - the even viscosity η_e vanishes to zeroth order in derivatives (see [175] for a subtlety in separating K^{-1} from η_e).

The $O(p)$ part of the (I.1) is P, T -odd and vanishes when $s_\theta = 0$. It is given by

$$\begin{aligned}\mathcal{L}_{\text{ind},1} &= -s_\theta n_0 \omega_t \\ &+ \frac{1}{2} \frac{s_\theta n_0}{m^2 c_s^2} \frac{E^i \partial_i B}{\partial^2 - c_s^{-2} \partial_t^2} \\ &- s_\theta n_0 \frac{(E_\omega^i - \frac{1}{2m} \partial_i B) \partial_i \sqrt{G}}{\partial^2 - c_s^{-2} \partial_t^2}.\end{aligned}\tag{I.4}$$

The first and third lines produce the following odd viscosity [163],

$$\begin{aligned}\eta_o^{(1)} &= -\frac{1}{2} s_\theta n_0, \\ \eta_o^{(2)} &= \frac{1}{2} s_\theta n_0 \frac{1}{q^2 - c_s^{-2} \omega^2},\end{aligned}\tag{I.5}$$

and setting $\omega = 0$ one obtains the leading terms in equation (3.13). By using the identity (up to a total derivative)

$$E^i \partial_i B = \frac{1}{2} \varepsilon^{\mu\nu\rho} A_\mu \partial_\nu \partial^2 A_\rho,\tag{I.6}$$

the second line of (I.4) can be written as a non-local CS term

$$\mathcal{L}_{\text{ind}} \supset \frac{1}{2} \sigma_o(\omega, q) \varepsilon^{\mu\nu\rho} A_\mu i p_\nu A_\rho\tag{I.7}$$

with the odd (or Hall) conductivity $\sigma_o(\omega, q) = \sigma_o^0 q^2 / (q^2 - c_s^{-2} \omega^2)$, $\sigma_o^0 = s_\theta n_0 / 2m^2 c_s^2$ [192–195, 153, 196, 197, 163], with $\sigma_o(0, q) = \sigma_o^0$ unquantized, and $\sigma_o(\omega, 0) = 0$, in accordance with the boundary $U(1)_N$ -neutrality [1].

To demonstrate explicitly that c cannot be extracted from the odd viscosity alone, it suffices to add the $O(p^2)$ term $\mathcal{L}_2^{(1)} = F_1(X) R \subset \mathcal{L}_2$. The situation is particularly simple for the special case

$F_1(X) = -s_\theta^2 P'(X)/4m$. Then

$$\begin{aligned} P\left(X - \frac{s_\theta^2}{4m}R\right) &= P(X) - \frac{s_\theta^2}{4m}P'(X)R + O(p^4) \\ &= P(X) + F_1(X)R + O(p^4), \end{aligned} \quad (\text{I.8})$$

which shows that $F_1(X)R$ can be absorbed into $P(X)$ by a modification of X . The scalar $X - \frac{s_\theta^2}{4m}R$ is useful because, unlike X , it depends on A_μ and ω_μ *only* through the combination $\mathcal{A}_\mu = A_\mu + s_\theta\omega_\mu$. This is evident in (H.1), where B rather than $\mathcal{B} = B + \frac{s}{2}R$ appears. It is then clear that, to $O(p^3)$, adding $\mathcal{L}_2^{(1)} = F_1(X)R = -\frac{s_\theta^2}{4m}P'(X)R$ to $\mathcal{L}_0 = P(X)$ amounts to changing B to \mathcal{B} in the induced Lagrangian (I.1),

$$\begin{aligned} \mathcal{L}_{\text{ind}} &= P_0\sqrt{G} - n_0\mathcal{A}_t \\ &+ \frac{1}{2}\frac{n_0}{m}\frac{\mathcal{B}^2 - c_s^{-2}\mathcal{E}^2 + \frac{s_\theta c_s^{-2}}{m}\mathcal{E}^i\partial_i\mathcal{B} - \frac{s_\theta^2 c_s^{-2}}{4m^2}(\partial\mathcal{B})^2}{\partial^2 - c_s^{-2}\partial_t^2} \\ &- n_0\frac{m\left(\partial_t\sqrt{G}\right)^2/2 + \left(\mathcal{E}^i - \frac{s_\theta}{2m}\partial_i\mathcal{B}\right)\partial_i\sqrt{G}}{\partial^2 - c_s^{-2}\partial_t^2}. \end{aligned} \quad (\text{I.9})$$

The only contribution to η_o , beyond (I.5), comes from the term proportional to $\mathcal{E}^i\partial_i\mathcal{B}$. By using the identity (I.6) for \mathcal{A}_μ , this term can be written as the sum of non-local CS, WZ1, and WZ2 terms, which generalizes (I.7) to

$$\mathcal{L}_{\text{ind}} \supset \frac{1}{2}\sigma_o(\omega, q)\varepsilon^{\mu\nu\rho}(A_\mu + s_\theta\omega_\mu)ip_\nu(A_\rho + s_\theta\omega_\rho). \quad (\text{I.10})$$

Most importantly, this includes a non-local version of WZ2, which is indistinguishable from \mathcal{L}_{gCS} at $\omega = 0$, where $\sigma_o(0, q) = \sigma_o^0$ is a constant. Noting that $F_1' = -s_\theta^2 P''/4m = -(s_\theta/2)\sigma_o^0$, and comparing to (H.8), it follows that c and F_1' will enter the $\omega = 0$ odd viscosity only through the combination $c + 48\pi s_\theta F_1'$. In more detail, the odd viscosity tensor due to $\mathcal{L}_0 + \mathcal{L}_2^{(1)} + \mathcal{L}_{\text{gCS}}$, is given by

$$\begin{aligned} \eta_H^{(1)}(\omega, q^2) &= -\frac{1}{2}s_\theta n_0 - \left(\frac{c}{24} \frac{1}{4\pi} + \frac{s_\theta}{2} F_1' \frac{q^2}{q^2 - c_s^{-2}\omega^2}\right) q^2 + O(q^4), \\ \eta_H^{(2)}(\omega, q^2) &= \frac{1}{2}s_\theta n_0 \frac{1}{q^2 - c_s^{-2}\omega^2} + \left(\frac{c}{24} \frac{1}{4\pi} + \frac{s_\theta}{2} F_1' \frac{q^2}{q^2 - c_s^{-2}\omega^2}\right) + O(q^2), \end{aligned} \quad (\text{I.11})$$

which, at $\omega = 0$, is a special case of equation (12) of the main text.

Equation (I.11) remains valid away from the special point $F_1 = -s_\theta^2 P'/4m$, even though (I.10) does not. Examining the perturbatively expanded \mathcal{L}_0 (H.3) and $\mathcal{L}_2^{(1)}$ (H.7), we see that a general F_1 amounts to replacing B in (I.1) with $B + \alpha \frac{s_\theta}{2}R$, where $\alpha = -\frac{4mF_1'}{s_\theta^2 P''} \neq 1$ generically (as well as in the microscopic

model (J.24)-(3.11)). The general induced Lagrangian due to $\mathcal{L}_0 + \mathcal{L}_2^{(1)}$, valid to $O(p^3)$, is then given by

$$\begin{aligned} \mathcal{L}_{\text{ind}} = & P_0 \sqrt{G} - n_0 \mathcal{A}_t \\ & + \frac{1}{2} \frac{n_0}{m} \frac{\mathcal{B}^2 - c_s^{-2} \mathcal{E}^2 + \frac{s_\theta c_s^{-2}}{m} \mathcal{E}^i \partial_i (B + \alpha \frac{s_\theta}{2} R) - \frac{s_\theta^2 c_s^{-2}}{4m^2} (\partial B)^2}{\partial^2 - c_s^{-2} \partial_t^2} \\ & - n_0 \frac{m \left(\partial_t \sqrt{G} \right)^2 / 2 + \left[\mathcal{E}^i - \frac{s_\theta}{2m} \partial_i (B + \alpha \frac{s_\theta}{2} R) \right] \partial_i \sqrt{G}}{\partial^2 - c_s^{-2} \partial_t^2}, \end{aligned} \quad (\text{I.12})$$

and, along with the \mathcal{L}_{gCS} , produces the odd viscosity (I.11). This expression does not depend on A_μ, ω_μ only through \mathcal{A}_μ , but the terms contributing to (I.11) still vanish $s_\theta = 0$, which is why the *improved* odd viscosity due to (I.12) vanishes. In addition to $\mathcal{L}_2^{(1)}$, the second order terms $\mathcal{L}_2^{(2)}, \mathcal{L}_2^{(3)}$ (H.6) also produce q^2 corrections to the odd viscosity, but not to the improved odd viscosity.

Though equation (I.10) describes only a part of \mathcal{L}_{ind} , and is non-generic, it does reveal the analogy between ℓ -wave SFs and $\text{vars} = 0$ QH states, described in Sec.3.5, in a very simple setting. Indeed, comparing (I.10) with Eq.(3.7), we see that ℓ -wave SFs are analogous to $\text{vars} = 0$ QH states, with $\bar{s} = s_\theta = \ell/2$, but with a non-local, non-quantized, Hall conductivity, in place of the filling factor $\nu/2\pi$. Additionally, both QH states and ℓ -wave SFs have the same gCS term (H.8), with c the boundary chiral central charge.

J Detailed analysis of the microscopic model Eq.(3.8)

J.1 Symmetry

The microscopic action S_m of Eq.(3.8) is invariant under $U(1)_N$ gauge transformations,

$$\psi \mapsto e^{-i\alpha} \psi, \quad \Delta^j \mapsto e^{-2i\alpha} \Delta^j, \quad A_\mu \mapsto A_\mu + \partial_\mu \alpha, \quad (\text{J.1})$$

which implies the current conservation $\partial_\mu (\sqrt{G} J^\mu) = 0$, where $\sqrt{G} J^\mu = -\delta S / \delta A_\mu$. It is also clear that S_m is invariant under *time-independent* spatial diffeomorphisms, generated by $\delta x^i = \xi^i(\mathbf{x})$, if ψ transforms as a function, A_μ as a 1-form, Δ^j as a vector, and G_{ij} as a rank-2 tensor. As described in section 3.1, due to its Galilean symmetry in flat space, S_m is also invariant under time-dependent spatial diffeomorphisms $\delta x^i = \xi^i(\mathbf{x}, t)$, provided one modifies the transformation rule of A_i to Eq.(3.1).

J.2 Effective action and fermionic Green's function

Starting with the microscopic action (3.8), the effective action for the order parameter Δ in the A, G background is obtained by integrating out the (generically) gapped fermion ψ ,

$$e^{iS_{\text{eff},m}[\Delta; A, G]} = \int \mathcal{D}(G^{1/4} \psi) \mathcal{D}(G^{1/4} \psi^\dagger) e^{iS_m[\psi; \Delta, A, G]}, \quad (\text{J.2})$$

where $G^{1/4} = (\det G_{ij})^{1/4}$ is the square root of the volume element \sqrt{G} . The form of the measure is fixed by the fact that the fundamental fermionic degree of freedom is the fermion-density $\tilde{\psi} = G^{1/4}\psi$, which satisfies the usual canonical commutation relation $\{\tilde{\psi}^\dagger(\mathbf{x}), \tilde{\psi}(\mathbf{y})\} = \delta^{(2)}(\mathbf{x} - \mathbf{y})$ as an operator [242, 243, 34, 1]. This is to be contrasted with $\{\psi^\dagger(\mathbf{x}), \psi(\mathbf{y})\} = \delta^{(2)}(\mathbf{x} - \mathbf{y})/\sqrt{G(\mathbf{x})}$ which ties the fermion to the background metric. In terms of $\tilde{\psi}$ the action (3.8) takes the form

$$S_m = \int d^2x dt \left[\tilde{\psi}^\dagger \frac{i}{2} \overleftrightarrow{\nabla}_t \tilde{\psi} - \frac{1}{2m} G^{ij} \nabla_i \tilde{\psi}^\dagger \nabla_j \tilde{\psi} + \left(\frac{1}{2} \Delta^i \tilde{\psi}^\dagger \nabla_i \tilde{\psi} + h.c. \right) - \mathcal{U} \right], \quad (\text{J.3})$$

where $\nabla_\mu = \partial_\mu + iA_\mu - \frac{1}{4}\partial_\mu \log G$ is the covariant derivative for densities, and $\mathcal{U} = \frac{1}{2\lambda} \sqrt{G} G_{ij} \Delta^{i*} \Delta^j$. Passing to the BdG form of the fermionic part of the action, in terms of the Nambu spinor-density $\tilde{\Psi}^\dagger = (\tilde{\psi}^\dagger, \tilde{\psi})$ (which is a Majorana spinor-density [1]), one finds

$$\begin{aligned} S_m &= \int d^2x dt \left\{ \frac{1}{2} \tilde{\Psi}^\dagger \gamma^0 \left[i\gamma^0 \partial_t - A_t + \frac{1}{2m} \nabla_i G^{ij} \nabla_j + \frac{i}{2} \gamma^{\tilde{A}} (e_A^i \partial_i + \partial_i e_A^i) \right] \tilde{\Psi} - \mathcal{U} \right\} \\ &= \int d^2x dt \left\{ \frac{1}{2} \tilde{\Psi}^\dagger \gamma^0 \mathcal{G}^{-1} \tilde{\Psi} - \mathcal{U} \right\}, \end{aligned}$$

where derivatives act on all fields to the right; $\tilde{A} = 1, 2$ is an index for $U(1)_N$, viewed as a copy of $SO(2)$; the gamma matrices are $\gamma^0 = \sigma^z$, $\gamma^1 = -i\sigma^x$, $\gamma^2 = i\sigma^y$, satisfying $\{\gamma^\mu, \gamma^\nu\} = 2\eta^{\mu\nu}$ with $\eta^{\mu\nu} = \text{diag}[1, -1, -1]$, and $\text{tr}(\gamma^0 \gamma^1 \gamma^2) = 2i$; and

$$e_A^i = \begin{pmatrix} \text{Re} \Delta^x & \text{Re} \Delta^y \\ \text{Im} \Delta^x & \text{Im} \Delta^y \end{pmatrix} \quad (\text{J.4})$$

is the *emergent* vielbein [28, 1], to be distinguished from the background vielbein E_A^i (with an $SO(2)_L$ index $A = 1, 2$) that was introduced in Sec. 3.1 and that will be used momentarily. We also defined the inverse Green's function \mathcal{G}^{-1} . The effective action (J.2) is then given by the logarithm of the Pfaffian

$$\begin{aligned} S_{\text{eff,m}} &= -i \log \text{Pf}(i\gamma^0 \mathcal{G}^{-1}) - \int d^2x dt \mathcal{U} \\ &= -\frac{i}{2} \log \text{Det}(i\gamma^0 \mathcal{G}^{-1}) - \int d^2x dt \mathcal{U}. \end{aligned} \quad (\text{J.5})$$

J.3 Fermionic ground state topology

For a given Δ^j , the fermion ψ is gapped, unless the chemical potential μ or chirality $\ell = \text{sgn}(\text{Im}(\Delta^{x*} \Delta^y))$ are tuned to 0, and forms a fermionic topological phase characterized by the bulk Chern number. Assuming $A_\mu = 0$ and space-time independent Δ^i, G^{ij} , it is given by [27]

$$C = \frac{1}{24\pi^2} \text{tr} \int d^3q \varepsilon^{\alpha\beta\gamma} (\mathcal{G} \partial_\alpha \mathcal{G}^{-1}) (\mathcal{G} \partial_\beta \mathcal{G}^{-1}) (\mathcal{G} \partial_\gamma \mathcal{G}^{-1}) \in \mathbb{Z}, \quad (\text{J.6})$$

and determines the boundary chiral central charge $c = C/2$ [15, 104, 27, 107]. Here the fermionic Green's function \mathcal{G} is Fourier transformed to Euclidian 3-momentum $q = (iq_0, \mathbf{q})$ (see (J.16)). For the particular model (3.8) one finds

$$c = -(\ell/4) (\text{sgn}(\mu) + \text{sgn}(m)) \in \{0, \pm 1/2\}, \quad (\text{J.7})$$

see [15, 27, 1] for similar expressions. Note that the central charge is well defined for both $m > 0$ and $m < 0$, even though the single particle dispersion is not bounded from below in the latter, and many physical quantities naively diverge (we will see below that certain physical quantities diverge also with $m > 0$). A negative mass can occur as an effective mass in lattice models, in which case the lattice spacing provides a natural cutoff (which must be smooth in momentum space for (J.6) to hold). In any case, a negative mass makes it possible to obtain both fundamental central charges $c = \pm 1/2$, for fixed ℓ , within the model (3.8). All possible $c \in (1/2)\mathbb{Z}$ can then be obtained by stacking layers of the model (3.8) with the same ℓ but different m, μ . Thus the model (3.8) suffices to generate a representative for all topological phases of the p -wave CSF. For concreteness, below we will work only with $m > 0$, in which case c is given by Eq.(3.9).

J.4 Symmetry breaking and bosonic ground state in the presence of a background metric

For time independent fields A, G, Δ the effective action reduces to

$$S_{\text{eff},m}[\Delta; G] = - \int d^2x dt \varepsilon_0[\Delta; G], \quad (\text{J.8})$$

where ε_0 is the ground-state energy-density as a function of the fields. In flat space $G_{ij} = \delta_{ij}$, with $A_t = -\mu$ and $A_i = 0$, and assuming Δ is constant, it is given by [27, 1]

$$\varepsilon_0 = \frac{1}{2} \int \frac{d^2\mathbf{q}}{(2\pi)^2} \left(\xi_{\mathbf{q}} - \sqrt{\xi_{\mathbf{q}}^2 + g^{ij} q_i q_j} \right) + \frac{1}{2\lambda} \delta_{ij} g^{ij}, \quad (\text{J.9})$$

where

$$\xi_{\mathbf{q}} = |\mathbf{q}|^2 / 2m - \mu \quad (\text{J.10})$$

is the single particle dispersion, and $g^{ij} = \Delta^{(i} \Delta^{j)*} = \delta^{\bar{A}\bar{B}} e_{\bar{A}}^i e_{\bar{B}}^j$ is the *emergent metric* - a dynamical metric to be distinguished from the background metric G^{ij} . The ground state configuration of g^{ij} is determined by minimizing ε_0 , while the overall phase θ of the order parameter and the chirality ℓ , of which g^{ij} is independent, are left undetermined. Thus g^{ij} corresponds to a massive Higgs field, while θ is a Goldstone field. The energy-density (J.9) is UV divergent, and requires regularization. We do this in the simplest manner, by introducing a momentum cutoff $q^2 < \Lambda^2$. Since the divergence disappears for $g^{ij} = 0$ (assuming $m > 0$), this can be thought of as a small, but non-vanishing, range $1/\Lambda$ for the

interaction mediated by Δ . With a finite Λ , the energy-density is well defined and has a unique global minimum at $g^{ij} = \Delta_0^2 \delta^{ij}$, with Δ_0 determined by the self-consistent equation

$$\frac{1}{4} \int^\Lambda \frac{d^2 \mathbf{q}}{(2\pi)^2} \frac{|\mathbf{q}|^2}{\sqrt{\xi_{\mathbf{q}}^2 + \Delta_0^2 |\mathbf{q}|^2}} = \frac{1}{\lambda}. \quad (\text{J.11})$$

For $\mu > 0$ the non-interacting system has a Fermi surface, and a solution exists for all $\lambda > 0$, which is the statement of the BCS instability. For $\mu < 0$, the non-interacting system is gapped, and a solution exists if the interaction is large enough compared with the gap, $\lambda \Lambda^{-4} \gtrsim |\mu|$. Consider now the case of a general constant metric G_{ij} , and let us introduce a constant vielbein E such that $G_{ij} = E_i^A \delta_{AB} E_j^B$. The inverse transpose $E^{-T} = (E^{-1})^T$ is given in coordinates by E_A^i . We also introduce the internal order parameter $\Delta^A = E_i^A \Delta^i$. The action (J.3) then reduces to

$$S_m = \int d^2 x dt \left[\tilde{\psi}^\dagger i \partial_t \tilde{\psi} - \frac{\delta^{AB}}{2m} E_A^i \partial_i \tilde{\psi}^\dagger E_B^j \partial_j \tilde{\psi} + \left(\frac{1}{2} \Delta^A E_A^i \tilde{\psi}^\dagger \partial_i \tilde{\psi} + h.c \right) - \sqrt{G} \frac{1}{2\lambda} \delta_{AB} \Delta^A \Delta^B \right]. \quad (\text{J.12})$$

This is identical to the flat space case, with ∂_i replaced by $E_A^i \partial_i$. We also need to change the UV cutoff to $\delta^{AB} E_A^i q_i E_B^j q_j = G^{ij} q_i q_j < \Lambda^2$. This is natural since we interpret Λ^2 as a range of the interaction mediated by Δ , which should be defined in terms of the geodesic distance rather than the Euclidian distance. It follows that the flat space result (J.9) is modified to

$$\begin{aligned} \varepsilon_0 &= \frac{1}{2} \int_{|E^{-T} \mathbf{q}|^2 < \Lambda^2} \frac{d^2 \mathbf{q}}{(2\pi)^2} \left(\xi_{E^{-T} \mathbf{q}} - \sqrt{\xi_{E^{-T} \mathbf{q}}^2 + g^{AB} E_A^i E_B^j q_i q_j} \right) + \sqrt{G} \frac{1}{2\lambda} \delta_{AB} g^{AB} \\ &= \sqrt{G} \left[\frac{1}{2} \int_{q^2 < \Lambda^2} \frac{d^2 \mathbf{k}}{(2\pi)^2} \left(\xi_{\mathbf{k}} - \sqrt{\xi_{\mathbf{k}}^2 + g^{AB} k_A k_B} \right) + \frac{1}{2\lambda} \delta_{AB} g^{AB} \right], \end{aligned} \quad (\text{J.13})$$

where $\mathbf{k} = E^{-T} \mathbf{q}$, or $k_A = E_A^i q_i$, and $g^{AB} = \Delta^{(A} \Delta^{B)*} = \delta^{\bar{A}\bar{B}} e_{\bar{A}}^A e_{\bar{B}}^B$ is the *internal* emergent metric. This is identical to the $G_{ij} = \delta_{ij}$ result (J.9), apart from the volume element \sqrt{G} , and the fact that it is the internal metric g^{AB} that appears, rather than g^{ij} . It is then clear that minimizing (J.13) with respect to g^{AB} gives

$$g^{AB} = \Delta_0^2 \delta^{AB}, \text{ or } g^{ij} = \Delta_0^2 G^{ij}, \quad (\text{J.14})$$

with the same Δ_0 of (J.11), which is G independent. Thus, the emergent metric is proportional to the background metric in the ground state. This solution corresponds to emergent vielbeins $e_{\bar{A}}^A \in O(2)$, or order parameters $\Delta^A = \Delta_0 e^{2i\theta} (1, \pm i)$, which is the $p_x \pm ip_y$ configuration, and implies the SSB pattern

$$(\mathbb{Z}_{2,T} \ltimes U(1)_N) \times (\mathbb{Z}_{2,P} \ltimes SO(2)_L) \rightarrow \begin{cases} \mathbb{Z}_{2,PT} \ltimes U(1)_{L-\frac{\ell}{2}N} & \ell \in 2\mathbb{Z} + 1 \\ \mathbb{Z}_{2,PT} \ltimes U(1)_{L-\frac{\ell}{2}N} \times \mathbb{Z}_{2,(-1)^N} & \ell \in 2\mathbb{Z} \end{cases}, \quad (\text{J.15})$$

described less formally in Eq.(1.2). Note that fermion parity $\mathbb{Z}_{2,(-1)^N}$ is the \mathbb{Z}_2 subgroup of $U(1)_{L-\frac{\ell}{2}N}$ for odd ℓ . For Δ^j , we find the ground state configuration Eq.(3.10). As described in Sec.3.3, we will ignore the massive Higgs fluctuations, and obtain $S_{\text{eff}}[\theta; A, G]$ by plugging the ground state configuration (3.10) into the functional Pfaffian (J.5).

J.5 Perturbative expansion

We now write $E_A^i = \delta_A^i + H_A^i$ and $e_A^A = \Delta_0 \delta_A^A$ (which corresponds to $\Delta^A = \Delta_0(1, i)^A$) and expand (J.4) to second order in H, A . Due to $SO(2)_L$ gauge symmetry, the anti-symmetric part of H can be interpreted as the Goldstone field, $\theta = (s_\theta/2)\varepsilon_{AB}H^{AB}$. The $p_x - ip_y$ configuration $\Delta^A = \Delta_0(1, -i)^A$ can be incorporated by changing the sign of one of the gamma matrices $\gamma^{\tilde{A}}$. The expansion in H, A produces a splitting of the propagator into an unperturbed propagator and vertices, $\mathcal{G}^{-1} = \mathcal{G}_0^{-1} + \mathcal{V}$, where \mathcal{V} further splits as $\mathcal{V} = \mathcal{V}_1 + \mathcal{V}_2$, where \mathcal{V}_1 (\mathcal{V}_2) is first (second) order in the fields. The terms in \mathcal{V}_2 are often referred to as contact terms. Using (F.1) we find the explicit form of $\mathcal{G}_0^{-1}, \mathcal{V}_1, \mathcal{V}_2$ in Fourier components,

$$\begin{aligned}\mathcal{G}_0^{-1}(q) &= -\gamma^0 q_0 - \Delta_0 \gamma^j q_j - \xi_{\mathbf{q}}, \\ \mathcal{V}_1(q, p) &= -A_{t,p} - \Delta_0 \gamma^A (H_A^i)_p q_i \\ &\quad - \frac{1}{m} \left[q_i q_j - \frac{1}{4} (p_i p_j - \delta_{ij} p^2) \right] H_p^{ij} + \gamma^0 \frac{1}{m} A_p^j q_j, \\ \mathcal{V}_2(q, 0) &= -\frac{1}{2m} (H_A^i H^{Aj})_{p=0} q_i q_j - \frac{1}{8m} (\partial^j H_A^A \partial_j H_B^B)_{p=0} \\ &\quad - \gamma^0 \frac{2}{m} (A_i H^{(ij)})_{p=0} q_j - \frac{1}{2m} (A^j A_j)_{p=0}.\end{aligned}\tag{J.16}$$

Here $(\cdots)_p$ denotes the p Fourier component of the field (\cdots) , and we set $p = 0$ in \mathcal{V}_2 since only this component will be relevant. The unperturbed Greens's function is given explicitly by

$$\mathcal{G}_0(q) = -\frac{q_0 \gamma^0 + \Delta_0 q_i \gamma^i - \xi_{\mathbf{q}}}{q_0^2 - q_i q^i - \xi_{\mathbf{q}}^2}.\tag{J.17}$$

The perturbative expansion of S_{eff} is obtained from (J.5) by using $\log [\text{Det}(\cdot)] = \text{Tr} [\log(\cdot)]$, and expanding the logarithm in \mathcal{V} ,

$$\begin{aligned}S_{\text{eff,m}} &= -i \text{Tr} \{ \log [i \gamma^0 (\mathcal{G}_0^{-1} + \mathcal{V})] \} \\ &= -\frac{i}{2} \text{Tr} (\log i \gamma^0 \mathcal{G}_0^{-1}) - \frac{i}{2} \text{Tr} (\mathcal{G}_0 \mathcal{V}) + \frac{i}{4} \text{Tr} (\mathcal{G}_0 \mathcal{V})^2 + O(\mathcal{V}^3) \\ &= -\frac{i}{2} \text{Tr} (\mathcal{G}_0 \mathcal{V}_1) - \frac{i}{2} \text{Tr} (\mathcal{G}_0 \mathcal{V}_2) + \frac{i}{4} \text{Tr} (\mathcal{G}_0 \mathcal{V}_1 \mathcal{G}_0 \mathcal{V}_1) + \cdots,\end{aligned}\tag{J.18}$$

where in the last line we kept explicit only terms at first and second order in H, A (the term of zeroth order was described in the previous section). Writing the functional traces as integrals over Fourier

components and traces over spinor indices, we then find

$$S_{\text{eff},m} = -\frac{i}{2}\text{tr} \int_q \mathcal{V}_1(q, 0) \mathcal{G}_0(q) - \frac{i}{2}\text{tr} \int_q \mathcal{V}_2(q, 0) \mathcal{G}_0(q) \quad (\text{J.19})$$

$$+ \frac{i}{4}\text{tr} \int_{p,q} \mathcal{G}_0\left(q - \frac{1}{2}p\right) \mathcal{V}_1(q, -p) \mathcal{G}_0\left(q + \frac{1}{2}p\right) \mathcal{V}_1(q, p) + \dots,$$

where $\int_q = \int \frac{d^2 q d q_0}{(2\pi)^3}$. We are interested in S_{eff} to third order in derivatives, which amounts to expanding the above expression to $O(p^3)$, and evaluating the resulting traces and integrals. These computations were performed systematically using Mathematica, and can be found in the supplemental material of Ref.[2]. The result, focusing on terms relevant for $\eta_o, \tilde{\eta}_o$ to $O(q^2)$, is compatible with the general effective action of Sec.3.2, as confirmed by comparing (J.19) to the perturbatively expanded S_{eff} . This comparison provides explicit expressions for all of the coefficients that appear in S_{eff} , as we now describe. The ground state pressure $P(\mu)$ diverges logarithmically, and is given by

$$P = \frac{1}{2} \int^\Lambda \frac{d^2 q}{(2\pi)^2} \left[\frac{q^2}{2m} - \frac{\frac{1}{2}\Delta_0^2 q^2 + \frac{q^2}{2m} \left(\frac{q^2}{2m} - \mu\right)}{\sqrt{\Delta_0^2 q^2 + \left(\frac{q^2}{2m} - \mu\right)^2}} \right] \quad (\text{J.20})$$

$$= -\frac{m^3 \Delta_0^4}{4\pi} \left(1 - 2\frac{\mu}{m\Delta_0^2}\right) \log \Lambda + O(\Lambda^0).$$

Directly computing the ground state density n_0 and leading odd viscosity $\eta_o^{(1)}$ one finds

$$n_0 = \frac{1}{2} \int \frac{d^2 q}{(2\pi)^2} \left[1 - \frac{\left(\frac{q^2}{2m} - \mu\right)}{\sqrt{\Delta_0^2 q^2 + \left(\frac{q^2}{2m} - \mu\right)^2}} \right] \quad (\text{J.21})$$

$$= \frac{m^2 \Delta_0^2}{2\pi} \log \Lambda + O(\Lambda^0),$$

$$\eta_o^{(1)} = -\frac{\ell}{16} \int \frac{d^2 q}{(2\pi)^2} \frac{\Delta_0^2 q^2 \left(\frac{q^2}{2m} + \mu\right)}{\left[\left(\frac{q^2}{2m} - \mu\right)^2 + q^2 \Delta_0^2\right]^{3/2}} \quad (\text{J.22})$$

$$= -\frac{\ell m^2 \Delta_0^2}{8\pi} \log \Lambda + O(\Lambda^0),$$

so the relations $n_0 = P'(\mu)$, and $\eta_o^{(1)} = -(\ell/4)n_0$, described in Sec.3, are maintained to leading order in the cutoff. As explained in Appendix J.4, the cutoff Λ corresponds to a non-vanishing interaction range, which softens the contact interaction in the model (3.8). With a space-independent metric, a smooth cutoff can easily be implemented by replacing

$$\Delta^A E_A^j \tilde{\psi}_{-\mathbf{q}}^\dagger i q_j \tilde{\psi}_{\mathbf{q}}^\dagger \mapsto \Delta^A E_A^j \tilde{\psi}_{-\mathbf{q}}^\dagger \left(i q_j e^{-q_k q_l G^{kl}/\Lambda^2} \right) \tilde{\psi}_{\mathbf{q}}^\dagger, \quad (\text{J.23})$$

for example, in the Fourier transformed Eq.(J.12), and should lead to the *exact* relations $n_0 = P'(\mu)$, $\eta_0^{(1)} = -(\ell/4)n_0$. However, a computation of the q^2 correction to η_0 requires a space-dependent metric, where a non-vanishing interaction range involves the geodesic distance and complicates the vertex \mathcal{V} in (J.16) considerably. Moreover, all other coefficients in S_{eff} converge, and we can therefore work with the simple contact interaction, $\Lambda = \infty$. For the second derivative P'' , we find

$$\frac{P''}{m} = \frac{1}{2\pi} \begin{cases} 1 \\ \frac{1}{1+2\kappa} \end{cases}, \quad (\text{J.24})$$

where $\kappa = |\mu|/m\Delta_0^2 > 0$, and the cases refer to $\mu > 0$ and $\mu < 0$. This coefficient determines the odd (or Hall) conductivity $\sigma_o^0 = (\ell/2)P''/2m$ and has been computed previously in the literature [192–195, 153, 196, 197, 163, 198]. Note that P'' is continuous at $\mu = 0$, while P''' is not, in accordance with the third order phase transition found in an exact solution of the model (3.8) in the absence of background fields [318].

The coefficients P'', F'_1, F_2, F_3 were presented in Sec.3.3. The remaining coefficients F_4, F_5, F_6 , are irrelevant for the quantities discussed in Sec.3, and are presented here for completeness,

$$F_4 = \frac{1}{24\pi\mu} \begin{cases} \frac{\kappa-2}{2} \\ \frac{1}{1+2\kappa} \end{cases}, \quad F_5 = \frac{1}{24\pi\mu\Delta_0^2} \begin{cases} 1 \\ -\frac{1}{(1+2\kappa)^2} \end{cases}, \quad F_6 = -\frac{\kappa}{24\pi\mu} \begin{cases} \frac{1}{2} \\ \frac{1}{(1+2\kappa)^2} \end{cases}. \quad (\text{J.25})$$

As stated in Sec.3.3, there is a sense in which the relativistic limit $\kappa \rightarrow 0$, or $m \rightarrow \infty$, reproduces the effective action of a massive Majorana spinor in Riemann-Cartan space-time (Sec.2.5). Taking the relativistic limit of the dimensionful coefficients (J.25), one finds $F_6 = 0$, while $F_4 = -\Delta_0^2 F_5 \neq 0$ describe a relativistic term which is second order in torsion, and was not written explicitly in Sec.2.5.

K Further details regarding Eq.(4.2)

This appendix involves basic facts in CFT, which can be found in e.g [102, 103].

K.1 Definition of h_0 and ambiguities in its value

A chiral topological phase of matter has a finite-dimensional ground state subspace on the spatial torus. A basis $\{|a\rangle\}_{a=1}^N$ for the torus ground state subspace exists, such that each state $|a\rangle$ corresponds to a conformal family in the boundary CFT [278, 212, 213], constructed over a primary with right/left moving conformal weights $h_a^{(l)}, h_a^{(r)} \geq 0$. The corresponding chiral and total conformal weights are then given by $h_a = h_a^{(l)} - h_a^{(r)}$ and $h_a^+ = h_a^{(l)} + h_a^{(r)}$, respectively. The chiral and total central charges of the CFT are similarly defined in terms of the left/right moving central charges, $c = c^{(l)} - c^{(r)}$ and $c^+ = c^{(l)} + c^{(r)}$.

When the torus is cut to a cylinder with finite circumference L , the ground state degeneracy is lifted, generically leaving a unique ground state. The lowest energy eigenstates on the cylinder can also be

labeled as $\{|a\rangle\}_{a=1}^N$. Each $|a\rangle$ corresponds to a non-universal choice of state in the conformal family labeled by $h_a^{(l)}, h_a^{(r)}$, which need not be the primary, as demonstrated explicitly in Appendix L below.

If the boundary is described by an idealized CFT, all $|a\rangle$ s correspond to primaries, and the corresponding energies are given by $E_a = (4\pi v/L)(h_a^+ - c^+/24)$, relative to the ground state energy on the torus, where v is the velocity of the CFT and L is the circumference of the cylinder. These expressions receive exponentially small corrections of $O(Le^{-R/\xi})$ and $O(Re^{-L/\xi})$, where ξ is the bulk correlation length and R is the length of the cylinder [98]. The cylinder ground state then corresponds to the CFT ground state, the primary with minimal h_a^+ .

More generally, each state $|a\rangle$ corresponds to either a primary or a descendent, and has conformal weights $h_a^{(l)} + n_a^{(l)}, h_a^{(r)} + n_a^{(r)}$, where $n_a^{(l)}, n_a^{(r)} \in \mathbb{N}_0$. The corresponding energies E_a differ from the idealized $(4\pi v/L)(h_a^+ - c^+/24)$, and the choice of conformal family a_0 with minimal E_{a_0} is non-universal. In terms of $n_a = n_a^{(l)} - n_a^{(r)}$, we then define $h_0 := h_{a_0} + n_{a_0}$, the chiral conformal weight associated with the cylinder ground state $|a_0\rangle$. The value of h_0 therefore carries two ambiguities: a choice of conformal family $a_0 \in \{a\}$, and the choice of a state in the conformal family, $n_{a_0} \in \mathbb{N}_0$. As described in Sec.4.1.1, the only universal statement is $\theta_0 = e^{2\pi i h_0} \in \{\theta_a\}$, where $\theta_a = e^{2\pi i h_a}$ are the topological spins of bulk anyons.

The result of Ref.[212] for the momentum polarization is given terms of the low lying cylinder eigenstates $|a\rangle$,

$$\langle a|T_R|a\rangle = \exp\left[\alpha N_x + \frac{2\pi i}{N_x}\left(h_a - \frac{c}{24}\right) + o(N_x^{-1})\right], \quad (\text{K.1})$$

where the lattice spacing is set to 1, $N_x = L$. It follows that the thermal expectation value $\tilde{Z}/Z = \text{Tr}(T_R e^{-\beta H})/Z$ is equal to $\exp\left[\alpha N_x + \frac{2\pi i}{N_x}\left(h_0 - \frac{c}{24}\right) + o(N_x^{-1})\right]$, if the temperature β^{-1} is much lower than the boundary energy differences $\sim N_x^{-1}$, namely $\beta^{-1} = o(N_x^{-1})$, as described in Sec.4.1.

K.2 The value of h_0 in fermionic phases of matter

Fermionic topological phases are microscopically comprised of fermions (and possibly bosons), and have the fermion parity $(-1)^{N_f}$ as a global symmetry [319, 19, 320, 321]. It is therefore useful to probe such phases with a background \mathbb{Z}_2 gauge field corresponding to $(-1)^{N_f}$, or a spin structure. For our purposes, this amounts to considering both periodic and anti-periodic boundary conditions around non-contractible cycles in space-time.

In Sec.4 we were only interested in locally sign-free QMC representations of thermal partition functions, and sign-free geometric manipulations that can be performed to these. We therefore restricted attention to thermal boundary conditions in the imaginary time direction (see Sec.4.4.1), and to periodic boundary conditions around the spatial cylinder. These boundary conditions cannot generically be modified without introducing signs into the QMC weights.

Here we provide a fuller picture by considering the behavior of h_0 with both periodic and anti-periodic boundary conditions, in the closed x direction of the spatial cylinder. Since h_0 is a ground state

property, the time direction is open and does not play a role.

For a fermionic chiral topological phase, the boundary CFT is also fermionic. The primary conformal weights $\{h_a\}$ then depend on the choice of boundary conditions (in the x direction), and as a result, so will the set of topological spins $\{\theta_a\}$ in which $\theta_0 = e^{2\pi i h_0}$ is valued. In particular, the vacuum spin $\theta_I = 0$ will not be included in $\{\theta_a\}$ for periodic boundary conditions, while for anti-periodic boundary conditions, both the vacuum $\theta_I = 1$ and the spin $\theta_\psi = -1$ of the microscopic fermion will appear [102, 213]. Note that θ_ψ does not correspond to an emergent fermion, as in e.g the toric code [322], and therefore does not imply an additional ground state on the torus.

As an example, consider the series of Laughlin phases at filling $1/q$, with $q \in \mathbb{N}$, all of which have the chiral central charge $c = 1$. These correspond to $U(1)_q$ Chern-Simons theories. First, for $q \in 2\mathbb{N}$ the phase is bosonic, and we consider only periodic boundary conditions. The primary conformal weights are given by $h_a = a^2/2q$ [323, 55], with $a \in \mathbb{N}_0$. The topological spins $\theta_a = e^{2\pi i h_a}$ depend only on $a \bmod q$, and the q spins $\{\theta_a\}_{a=0}^{q-1}$ correspond to the q degenerate ground states that appear on the torus. In particular, the vacuum spin $\theta_I = 1$ is obtained for $a = 0$.

For $q \in 2\mathbb{N} - 1$ the phase is fermionic, and we consider both periodic and anti-periodic boundary conditions. For periodic boundary conditions the weights are given by $h_a = (a + 1/2)^2/2q$ [55]. As in the bosonic case, $\theta_a = e^{2\pi i h_a}$ depend only on $a \bmod q$, with $\{\theta_a\}_{a=0}^{q-1}$ corresponding to the q degenerate ground states on the torus. Unlike the bosonic case, the vacuum spin $\theta_I = 1$ is not included in $\{\theta_a\}_{a=0}^{q-1}$. For anti-periodic boundary conditions, the weights are given by $h_a = a^2/2q$ as in the bosonic case [323]. The set $\{\theta_a\}_{a=0}^{q-1}$ again corresponds to the q torus ground states, but now $\theta_\psi = \theta_{a=q} = -1$ is an additional topological spin that corresponds to the physical Fermion ψ [215].

The simplest fermionic Laughlin phase is given by $q = 1$, and corresponds to an integer quantum Hall state, or a Chern insulator [105, 106], which is studied in detail in Appendix L below. The Chern insulator has a unique ground state on the torus, and accordingly, there is a unique topological spin $\theta_\sigma = e^{2\pi i (1/8)}$ for periodic boundary conditions on the cylinder, and two topological spins $\theta_I = 1, \theta_\psi = -1$ for anti-periodic boundary conditions. Here ψ corresponds the physical fermions from which the Chern insulator is comprised. The object carrying the spin θ_σ is the complex analog of the celebrated Majorana zero mode supported on vortices in the bulk of a chiral p -wave superconductor [15, 104].

L Momentum polarization with non CFT boundaries

As reviewed in Sec.4.1, the existing analytic derivation of Eq.(4.2) relies on the CFT description of the physical boundaries of the cylinder, and of the line $y = 0$ where T_R is discontinuous [212]. In this appendix we perform an analytic and numerical study that shows that, at least for free fermions, the relevant CFT expressions and the resulting Eq.(4.2), hold even if the boundary is not described by an idealized CFT. We will however, find a number of subtleties which have not been demonstrated in the literature, as already described below Eq.(4.1) and in Appendix K.

L.1 CFT finite-size correction in non CFT boundaries

The main ingredient in the analytic derivation of Eq.(4.2) is the expression (4.1) for the finite size correction to the momentum density in CFT [212]. In this appendix we show that, at least in the non-interacting case, Equation (4.1) remains valid, with $\theta_0 = e^{2\pi i h_0} \in \{\theta_a\}$, even when the boundary cannot be described by a CFT.

We will consider a Chern insulator, such as the prototypical Haldane model [105]. When the boundary degrees of freedom can be described by a CFT, they correspond to the Weyl fermion CFT, where $c = \pm 1$ and the primary conformal weights are $h_\sigma = \pm 1/8$ ($h_I = 0, h_\psi = \pm 1/2$) for periodic (anti-periodic) boundary conditions, as described in Appendix K.2. The sign corresponds to the two possible chiralities. More generally, on a lattice with spacing 1, the boundary supports a complex fermion with an energy dispersion ε_k , where $k = k_x$ takes values in the Brillouin zone $\mathbb{R}/2\pi\mathbb{Z}$ for an infinite circumference $L = \infty$, or its discretization $(2\pi/L)\mathbb{Z}_L$ ($(2\pi/L)(\mathbb{Z}_L + 1/2)$), for $L < \infty$ and periodic (anti-periodic) boundary conditions. The only requirement on ε_k is that it be *chiral*, in the sense that it connects the two separated bulk energy bands. If the intersections k_l and k_u with the lower and upper bulk bands, respectively, satisfy $k_l < k_u$ ($k_l > k_u$), we say that the boundary is right (left) moving, or has a positive (negative) chirality, see Fig.12.

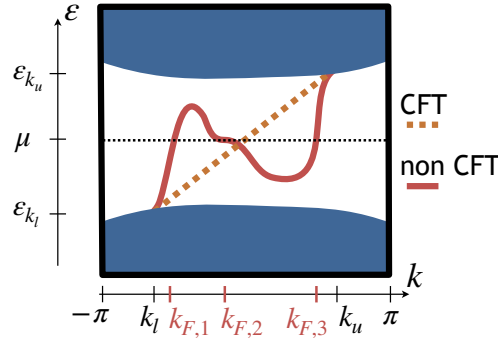


Figure 12: Schematic band structure, energy ε as a function of momentum $k = k_x$ in the periodic x direction, of a Chern insulator on the cylinder. The figure shows the bulk energy bands (blue) and the chiral boundary dispersion, with two dispersion branches, on a single boundary component (orange and red curves). The opposite chirality branches on the second boundary component are not drawn. The momenta k_l and k_u correspond to the intersections of the boundary dispersion with the lower and upper bulk bands, respectively. Since $k_u > k_l$, both dispersion branches have a positive chirality. The orange line indicates the idealized linear dispersion with a single Fermi momentum $k_F = 0$, which corresponds to the Weyl fermion CFT. The solid red curve corresponds to a more general chiral branch, with three Fermi momenta $k_{F,1}, k_{F,2}, k_{F,3}$, where the dispersion around $k_{F,2}$ takes a (non-generic) non-linear form. With periodic boundary conditions around the cylinder, both dispersion branches produce the same L^{-2} correction to the momentum density in Eq.(L.2), with a positive chirality $+$, up to a mod 1 ambiguity: $1/12 \mapsto 1/12 + n$, $n \in \mathbb{N}$.

More generally, the dispersion will contain several dispersion branches $\{\varepsilon_{j,k}\}_{j=1}^J$, but since the momentum density is additive in j we restrict attention to a single branch. Without loss of generality, we also fix the chemical potential $\mu = 0$, in which case the Fermi momentum k_F satisfies $\varepsilon_{k_F} = 0$. The

value of k_F plays an important role is the subsequent analysis.

The simplest dispersion that satisfies the above requirements is the linear one $\varepsilon_k = v(k - k_F)$. For $k_F = 0$ this corresponds to the Weyl fermion CFT. The presence of $k_F \neq 0$ corresponds to the addition of a chemical potential vk_F , which breaks the conformal symmetry. The generic form is $\varepsilon_k = v(k - k_F) + O(k - k_F)^2$. A non-generic dispersion can take the form $\varepsilon_k = v_3(k - k_F)^3 + O(k - k_F)^4$, and there may be several Fermi momenta if the dispersion is non monotonic, see Fig.12.

In all cases the many-body ground state momentum is given by summing the momenta of all filled single Fermion states $p(L) = \frac{1}{L} \sum_{\varepsilon_k < 0} k$, where the sum runs over $k \in (2\pi/L) \mathbb{Z}_L$ such that ε_k is negative and in the bulk energy gap. In order to obtain p as a continuous function of L , we treat the bulk energy gap as a smooth cutoff $p(L) = \frac{1}{L} \sum_{\varepsilon_k < 0} kC(\varepsilon_k)$, where the function $C(\varepsilon)$ goes to 1 (0) fast enough as ε goes to 0 (ε_{k_l} or ε_{k_u})⁴⁴. The cutoff C represents the smooth delocalization of boundary eigenstates as their energy nears the bulk energy bands.

To obtain the L dependence of $p(L)$, we will use the Euler-Maclaurin formula

$$\begin{aligned} \sum_{n=n_1}^{n_2} f(n) &= \int_{n_1}^{n_2} f(x) dx + \frac{f(n_2) + f(n_1)}{2} \\ &+ \frac{1}{6} \frac{f'(n_2) - f'(n_1)}{2!} - \frac{1}{30} \frac{f'''(n_2) - f'''(n_1)}{4!} + R, \end{aligned} \quad (\text{L.1})$$

where the remainder satisfies $|R| \leq \frac{2\zeta(5)}{(2\pi)^5} \int_{n_1}^{n_2} |f^{(5)}(x)| dx$. We begin by considering periodic boundary conditions, where we set $f(n) = (2\pi n/L^2) C(\varepsilon_{2\pi n/L})$. Assuming a single, vanishing, Fermi momentum $k_F = 0$, we set $(n_1, n_2) = (-\infty, 0)$ for positive chirality, and $(n_1, n_2) = (0, \infty)$ for negative chirality. Equation (L.1) then gives

$$p(L) = p(\infty) \pm \frac{2\pi}{L^2} \frac{1}{12} + O\left(\frac{1}{L^4}\right), \text{ as } L \rightarrow \infty, \quad (\text{L.2})$$

where $p(\infty) = \int_{\varepsilon_k < 0} kC(\varepsilon_k) dk/2\pi$ and $\pm = \text{sgn}(k_u - k_l)$ is the chirality. The $1/L^2$ correction in (L.2) comes from $f'(0) = 2\pi/L^2$ in (L.1). We see that the leading finite size correction $h_0 - c/24$ is unchanged from its CFT value $h_\sigma - c/24 = \pm 1/12$, even when a CFT description does not apply.

The case of a single non-zero Fermi momentum $k_F \neq 0$ is more interesting, as it demonstrates that the integer part of h_0 can change as a function of L and k_F . The direct derivation of the end result from the Euler-Maclaurin formula is surprisingly lengthy, so we omit it and present a more direct route to the end result. To be concrete, assume a positive chirality and $k_F > 0$. The Euler-Maclaurin formula leads to cutoff independent results, so we can restrict attention to cutoff functions $C(\varepsilon_k)$ which are identically 1 for $0 < k < k_F$. Since these can serve as cutoff functions for the case $k_F = 0$ as well, we can deduce

⁴⁴It suffices that $C'(\varepsilon)$ vanish at $\varepsilon = 0, \varepsilon_{k_l}, \varepsilon_{k_u}$.

the $k_F \neq 0$ momentum density $p(L, k_F)$ from the $k_F = 0$ momentum density $p(L)$,

$$\begin{aligned} p(L, k_F) &= \frac{1}{L} \sum_{k < k_F} k C(\varepsilon_k) \\ &= \frac{1}{L} \sum_{k < 0} k C(\varepsilon_k) + \frac{1}{L} \sum_{0 < k < k_F} k \\ &= p(L) + \frac{2\pi}{L^2} \sum_{l=1}^n l, \end{aligned} \tag{L.3}$$

where $n = \lfloor k_F L / 2\pi \rfloor$. Using Eq.(L.2), we then have

$$p(L, k_F) = p(\infty) + \frac{2\pi}{L^2} \left[\frac{1}{12} + \sum_{l=1}^n l \right] + O\left(\frac{1}{L^4}\right), \tag{L.4}$$

where $p(\infty)$ is the momentum density at $L = \infty$ and $k_F = 0$. We see that the value of $h_0 - c/24$ is only equal to the idealized CFT result $h_\sigma - c/24 = 1/12$ modulo 1, while the integer part jumps periodically as a function of k_F at fixed number of sites L , or as the number of sites L at fixed k_F . Treating k_F as fixed and valued in $(-\pi, \pi]$, the period in L is given by $q = |2\pi/k_F| \geq 2$, which need not be an integer. As described in Appendix K, the mod 1 ambiguity is attributed to h_0 rather than c , which corresponds to the topological spin $\theta_0 = \theta_\sigma = e^{2\pi i(1/8)}$.

The interpretation of Eq.(L.4) is straight forward. As the number of sites L increases, the single particle momenta $(2\pi/L) \mathbb{Z}_L$ become denser in the Brillouin zone $\mathbb{R}/2\pi\mathbb{Z}$. The n th jump in h_0 correspond to the motion of a single particle state with momentum $2\pi n/L$ through k_F and into the Fermi sea, adding a momentum density $2\pi n/L^2$ to the ground state.

Figure 13 presents the results of numerical computations of the momentum polarization Eq.(4.2) in a Chern insulator with $k_F \neq 0$. Details of the model and computations can be found in the supplemental material of Ref.[3]. In particular, Fig.13(a) verifies Eq.(L.4).

A subtle point, not mentioned above, is that when $k_F L / 2\pi \in \mathbb{Z}$, which happens only when $k_F / 2\pi = a/b$ is rational and $L \in b\mathbb{N}$, a single particle state with momentum exactly k_F exists, leading to an accidental degeneracy on the cylinder, between two many-body ground states with momentum densities given by Eq.(L.4) with n and $n+1$. The momentum polarization (4.2) then gives the average momentum density in the two ground-states, as visualized by the grey dotted line in Fig.13(a). For such system sizes the value $\theta_0 = -\theta_\sigma$ may be obtained rather than the generic $\theta_0 = \theta_\sigma$.

The same analysis can be performed for anti-periodic boundary conditions, where we sum over single particle momenta $k \in \frac{2\pi}{L} (\mathbb{Z}_L + \frac{1}{2})$. Equation (L.4) is then modified to

$$\begin{aligned} p(L, k_F) &= p(\infty) \\ &+ \frac{2\pi}{L^2} \left[-\frac{1}{24} + \sum_{l=1}^n \left(l - \frac{1}{2} \right) \right] + O\left(\frac{1}{L^4}\right), \end{aligned} \tag{L.5}$$

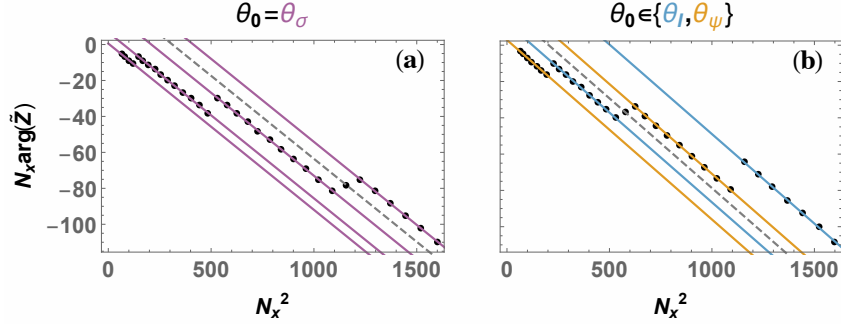


Figure 13: Numerical results for the momentum polarization Eq.(4.2), in a Chern insulator with $k_F \neq 0$. Black dots mark numerically obtained values of $N_x \arg \tilde{Z}$ as a function of N_x^2 . (a) Periodic boundary conditions. Purple lines indicate linear fits, with approximately the same slope and intercepts $2\pi(1/12 + \sum_{l=1}^n l)$ with the y axis, with $n = 0, 1, 2, 3$, in accordance with Eq.(L.4). This allows for the extraction of the topological spin $\theta_\sigma = e^{2\pi i(1/8)}$. To illustrate the possibility of accidental degeneracies, we choose $k_F = 3/34$, where a degeneracy occurs for $N_x = 34$, and the average value of $N_x \arg \tilde{Z}$ between the two ground states is obtained. A grey dotted line indicates the average of the two neighboring purple lines. (b) Anti-periodic boundary conditions. Colored lines indicate linear fits, with approximately the same slope, and intercepts $2\pi[-1/24 + \sum_{l=1}^n (l - 1/2)]$, with $n = 1, 2, 3, 4$, in accordance with Eq.(L.5). The value $n = 0$ is not obtained as it occurs only for small circumferences $N_x < 6$ where $N_x \arg \tilde{Z}$ is not computed. Orange lines correspond to the fermion spin $\theta_\psi = -1$, while blue lines correspond to the vacuum spin $\theta_I = 0$. To illustrate the possibility of accidental degeneracies, we choose $k_F = (5/2)/24$, where an accidental degeneracy occurs for $N_x = 24$.

where $n = \lfloor \frac{k_F L}{2\pi} - \frac{1}{2} \rfloor$. As a function of L , jumps in $h_0 - c/24$ occur with the same period $q = |2\pi/k_F| \geq 2$, but are shifted by $q/2$. Moreover, $h_0 - c/24$ now attains two values modulo 1, namely $h_I - c/24 = -1/24$ and $h_\psi - c/24 = 1/2 - 1/24$.

Equation (L.5) therefore demonstrates explicitly the statements made in Appendix K.1. For $k_F = 0$, the cylinder ground state of the Chern insulator corresponds to the idealized Weyl fermion CFT. A single value $h_0 = 0$ is attained, which is the conformal weight h_I of the CFT vacuum. A non-vanishing k_F corresponds to the addition of a chemical potential to the CFT, which changes the energies of the CFT states, favoring a CFT excited state over the CFT vacuum. The cylinder ground state of the Chern insulator may then correspond to any CFT state in the conformal family of either the vacuum I or fermion ψ , which need not be primary. From the bulk TFT perspective, we see that $\theta_0 = e^{2\pi i h_0}$ may be equal to either of the topological spins $\theta_I = 1, \theta_\psi = -1$ as a function of L .

As in the case of periodic boundary conditions, accidental degeneracies on the cylinder occur when $k_F L/2\pi \in \mathbb{Z} + 1/2$, changing the value of h_0 attained from the momentum polarization to its average over the degenerate states. For such system sizes, the value $\theta_0 = \pm \sqrt{\theta_I \theta_\psi}$ is obtained than the generic $\theta_0 \in \{\theta_I, \theta_\psi\}$.

Equation (L.5) is verified numerically in Fig.13(b), which demonstrates that the value of $\theta_0 = e^{2\pi i h_0}$, obtained from the momentum polarization (4.2), takes different values in the set $\{\theta_a\}$ of topological spins as a function of system size L , apart from accidental degeneracies.

L.2 No finite-size correction at finite temperature

The line $y = 0$ where T_R jumps can be interpreted as an additional boundary component at the 'entanglement temperature' β_*^{-1} . Reference [212] used the modular transformations of CFT partition functions to demonstrate that when $\beta_* \ll L/v$, this boundary component does not contribute to the $1/L$ correction to $\log \tilde{Z}$. Here, we note that the same result holds for free fermions with a general dispersion ε_k . The contribution of the additional boundary component to $\log \tilde{Z}$ is given by $\log \tilde{Z}_*(L) = L f_*(L)$, with the free energy density

$$f_*(L) = \frac{1}{L} \sum_k \log(1 + e^{iak} e^{-\beta_* \varepsilon_k}) C(\varepsilon_k). \quad (\text{L.6})$$

Using Eq.(L.1) one finds $f_*(L) = f_*(\infty) + O(L^{-4})$ for both periodic and anti-periodic boundary conditions, which implies $\log \tilde{Z}_* = L f_*(\infty) + O(L^{-3})$, with no $1/L$ contribution. The complex number $f_*(\infty) = \int \log(1 + e^{iak} e^{-\beta_* \varepsilon_k}) C(\varepsilon_k) dk / 2\pi$ contributes to the non-universal α in Eq.(4.2).

M Cutting the torus along an arbitrary vector

For $\mathbf{d} = (d_x, 0)$ we restrict to $N_x = n_x d_x$, $n \in \mathbb{N}$, viewing d_x as an enlarged lattice spacing, and treating n as a reduced number of sites along the circumference in place of N_x . The same logic applies to $\mathbf{d} = (0, d_y)$. For $\mathbf{d} = (d_x, d_y)$ with both $d_x, d_y \neq 0$, we restrict to system sizes $(N_x, N_y) = n\mathbf{d}$, such that the line $l = \text{span}_{\mathbb{R}} \mathbf{d}$ is a diagonal of the rectangle $nN_x \times nN_y$ and corresponds to a circle on the torus $(\mathbb{R}/N_x\mathbb{Z}) \times (\mathbb{R}/N_y\mathbb{Z})$. Cutting X along this line produces a cylinder C of circumference $L = n|\mathbf{d}|$. We then view $|\mathbf{d}|$ as a lattice spacing and n as the number of sites along the circumference. Note that the distance between the boundary components of the resulting cylinder is $R = nd_x d_y / |\mathbf{d}|$, and the thermodynamic limit is indeed obtained as $n \rightarrow \infty$. With these identifications the momentum polarization (4.2) remains unchanged, apart from a modification of the non-universal α to $\alpha|\mathbf{d}|^2$.

N Dealing with accidental degeneracies on the cylinder

As demonstrated in Appendix L, for certain system sizes N_x accidental degeneracies occur on the cylinder, and the function $\theta_0(N_x) = e^{2\pi i h_0(N_x)}$ obtained from Eq.(4.2) may take values outside the set $\{\theta_a\}$, namely $\theta_0 = \pm \sqrt{\theta_a \theta_b}$ for a two-fold degeneracy. In this appendix we complete the derivation of Result 1 and 1F by considering the possibility of such degeneracies.

First, even in the presence of degeneracies, θ_0 is valued in a finite set. Therefore, Eq.(4.5) still implies that $\epsilon' = n/m$ is rational, and that $\theta_0(N_x) e^{-2\pi i c/24} = e^{-2\pi i \epsilon' N_x^2}$ periodically covers a subset $S \ni 1$ of m th roots of unity, for all large enough N_x . We denote by $\mathcal{N} \subset \mathbb{N}$ the set of circumferences N_x for which a degeneracy appears and $\theta_0(N_x) \notin \{\theta_a\}$. If circumferences $N_x \in m\mathbb{N}$, where $e^{2\pi i \epsilon' N_x^2} = 1$, are not all contained in \mathcal{N} , then $1 = \theta_0(N_x) e^{-2\pi i c/24} \in \{\theta_a e^{-2\pi i c/24}\}$, as stated in Results 1 and 1F.

We are left with the complementary case, where degeneracies occur for all $N_x \in m\mathbb{N}$, i.e $m\mathbb{N} \subset \mathcal{N}$.

Note that this case is highly fine tuned, as it ties together the non-universal $\epsilon' = n/m$ and the set \mathcal{N} of N_x s where accidental degeneracies appear. In order to deal with this case, we make use of the Frobenius-Perron theorem to resolve the degenerate ground-state subspace, without introducing signs. The analysis applies only to the bosonic setting of Result 1, and is similar to that made in Sec.4.6. We now have a Hamiltonian H' on the cylinder, which has an exactly degenerate ground-state subspace for all $N_x \in m\mathbb{N}$, and has non-positive matrix elements in the on-site homogenous basis $|s\rangle$. The Frobenius-Perron theorem implies that an orthonormal basis $|i\rangle$ with non-negative entries may be chosen for the ground state subspace, $\langle s|i\rangle \geq 0$ for all s, i . It follows that the matrix elements of T_R in the basis $|i\rangle$ are non-negative, $M_{ij} := \langle i|T_R|j\rangle \geq 0$. Taking the N_x th matrix power of M we have $(M^{N_x})_{ij} \geq 0$. Equation (4.2) implies that the eigenvalues of M^{N_x} are of the form $e^{-\delta' N_x^2} e^{-2\pi i \epsilon' N_x^2 + o(1)} \theta_a e^{-2\pi i c/24}$, so we can write $(M^{N_x})_{ij} = e^{-\delta' N_x^2} e^{-2\pi i \epsilon' N_x^2 + o(1)} T_{ij}$, where T_{ij} has eigenvalues $\{\lambda\} \subset \{\theta_a e^{-2\pi i c/24}\}$. In particular, T_{ij} is unitary. Since $e^{2\pi i \epsilon' N_x^2} = 1$ for all $N_x \in m\mathbb{N}$, we see that T_{ij} also has non-negative entries, and is therefore a permutation matrix, containing 1 in its spectrum (see Sec.4.6). It follows that $1 \in \{\lambda\} \subset \{\theta_a e^{-2\pi i c/24}\}$, asserting Result 1.

We are currently unaware of an analog of the Frobenius-Perron theorem in the context of DQMC, that may be used to resolve the degenerate ground-state subspace without introducing signs. Instead, we will make a physical assumption under which Result 1F holds. Namely, we will assume that the fine tuned constraint $\epsilon' = n/m$ and $m\mathbb{N} \subset \mathcal{N}$ may be lifted by a sign-free perturbation. This includes (i) perturbations to the effective single-fermion Hamiltonian $h_{\phi(\tau)}$ that do not violate the algebraic condition $h_{\phi(\tau)} \in \mathcal{C}_h$, (ii) perturbations to the bosonic action S_ϕ that maintain its reality, and (iii) changes of the vector \mathbf{d} along which the torus is cut to a cylinder, as described in Appendix M, which will generically change the details of the boundary spectrum, including the non-universal number ϵ' and the set \mathcal{N} of N_x s where accidental degeneracies appear. A robustness of ϵ' and the set \mathcal{N} , both non-universal, under all three of the above deformations certainly goes beyond the low energy description of a chiral TFT in the bulk and a chiral CFT on the boundary. We also adopt this assumption in the fermionic spontaneously-chiral setting of Result 2F.

A stochastic variant of the above assumption may also be adopted to establish the bosonic spontaneously-chiral Result 2, but a stronger statement can in fact be made, by again making use of the Frobenius-Perron theorem to resolve the accidentally degenerate ground states. The Frobenius-Perron theorem does not immediately complete the derivation of Result 2, since the former is a ground state statement, while the latter made use of the finite temperature $\Delta E \ll \beta^{-1} \ll N_x^{-1}$, where ΔE is the exponentially small finite-size splitting between low lying symmetry breaking eigenstates. This difficulty does not arise in the 'classical symmetry breaking' scenario, where $\Delta E = 0$. In the generic case $\Delta E \neq 0$, we can make progress under the assumption that the \mathcal{T}, \mathcal{P} -even state $W[|+\rangle + |-\rangle]$ has lower energy than the \mathcal{T}, \mathcal{P} -odd state $W[|+\rangle - |-\rangle]$, rather than the opposite possibility. The derivation of Result 2 in Sec.4.3.1 can then be repeated at zero temperature. In particular, Eq.(4.9) and its analysis are unchanged.

O A 'non-local design principle' for chiral topological matter

As stated in Sec.4.4.3, the composition $\mathsf{T} = \mathcal{P}^{(0)}\mathcal{T}^{(1/2)}$ of the spin-less reflection with the spin-1/2 time-reversal, naturally provides a design-principle for a class of models for chiral topological matter. Here we describe such T -invariant models for chiral topological superconductors.

The simplest model is comprised of two copies, labeled by $\sigma = \uparrow, \downarrow$, of a spin-less $p+ip$ superconductor,

$$H = \sum_{\mathbf{x}, \mathbf{x}', \sigma, \sigma'} \left[\psi_{\sigma, \mathbf{x}}^\dagger h_{\mathbf{x}, \mathbf{x}', \sigma, \sigma'} \psi_{\sigma, \mathbf{x}'} + \psi_{\sigma, \mathbf{x}}^\dagger \Delta_{\mathbf{x}, \mathbf{x}', \sigma, \sigma'} \psi_{\sigma, \mathbf{x}'}^\dagger + h.c. \right]. \quad (\text{O.1})$$

Here

$$\Delta = \begin{pmatrix} \Delta_0 (d^x + i d^y) & 0 \\ 0 & \Delta_0 (d^x + i d^y) \end{pmatrix}, \quad (\text{O.2})$$

where $d_{\mathbf{x}\mathbf{x}'}^x$ ($d_{\mathbf{x}\mathbf{x}'}^y$) is the anti-symmetric x (y) difference operator,

$$\begin{aligned} d_{\mathbf{x}\mathbf{x}'}^x &= (\delta_{x, x'+1} - \delta_{x+1, x}) \delta_{y, y'} / 2, \\ d_{\mathbf{x}\mathbf{x}'}^y &= \delta_{x, x'} (\delta_{y, y'+1} - \delta_{y+1, y'}) / 2, \end{aligned} \quad (\text{O.3})$$

and $\Delta_0 \in \mathbb{R} - \{0\}$. Additionally,

$$h = \begin{pmatrix} t & 0 \\ 0 & t \end{pmatrix}, \quad (\text{O.4})$$

and the hopping t is real and reflection symmetric, e.g

$$t_{\mathbf{x}, \mathbf{x}'} = \frac{1}{2} t_0 (\delta_{x, x'+1} + \delta_{x+1, x'}) \delta_{y, y'} + (x \leftrightarrow y) - \mu, \quad (\text{O.5})$$

with $t_0 > 0$, $\mu \in \mathbb{R}$. It is well known that the chemical potential μ can be used to tune the model between gapped SPT phases with $c = 0, -1, 1$, for $|\mu| > 2t_0$, $-2t_0 < \mu < 0$, $0 < \mu < 2t_0$, respectively, see e.g [1]. Additionally, the Hamiltonian is invariant under the combination of the unitary spin-less reflection $\mathcal{P}^{(0)} : \psi_{\sigma, (x, y)} \mapsto \psi_{\sigma, (x, -y)}$ and the anti-unitary spin-full time-reversal $\mathcal{T}^{(1/2)} : \psi_{\uparrow, \mathbf{x}} \mapsto \psi_{\downarrow, \mathbf{x}}, \psi_{\downarrow, \mathbf{x}} \mapsto -\psi_{\uparrow, \mathbf{x}}$.

The model can be written in the BdG form

$$H = \sum_{\mathbf{x}, \mathbf{x}'} \Psi_{\mathbf{x}}^\dagger h_{\text{BdG}}^{\mathbf{x}, \mathbf{x}'} \Psi_{\mathbf{x}'}, \quad (\text{O.6})$$

where $\Psi_{\mathbf{x}}^T = (\psi_{\uparrow\mathbf{x}}, \psi_{\downarrow\mathbf{x}}, \psi_{\uparrow\mathbf{x}}^\dagger, \psi_{\downarrow\mathbf{x}}^\dagger)$ is the Nambu spinor (a Majorana spinor), and

$$h_{\text{BdG}} = \begin{pmatrix} h & \Delta \\ -\Delta^* & -h^* \end{pmatrix}. \quad (\text{O.7})$$

The “single-fermion” space on which h_{BdG} acts is $\mathcal{H}_{1\text{F}} = \mathcal{H}_X \otimes \mathcal{H}_{\text{spin}} \otimes \mathcal{H}_{\text{Nambu}} \cong \mathbb{C}^{|X|} \otimes \mathbb{C}^2 \otimes \mathbb{C}^2$. The spin-less reflection acts on $\mathcal{H}_{1\text{F}}$ as $\mathcal{P}^{(0)} = \mathcal{P}_X^{(0)} \otimes I_2 \otimes I_2$, where $\mathcal{P}_X^{(0)} = \delta_{x,x'} \delta_{y,-y'}$. The spin-full time-reversal acts by $\mathcal{T}^{(1/2)} = I_{|X|} \otimes iY \otimes I_2 \mathcal{K}$, where Y is the Pauli matrix and \mathcal{K} is the complex conjugation. The operator $\mathsf{T} = \mathcal{P}^{(0)} \mathcal{T}^{(1/2)}$ satisfies $\mathsf{T}^2 = -I$ and $[\mathsf{T}, h_{\text{BdG}}] = 0$, and is therefore a time-reversal design principle which applies to h_{BdG} , implying $\det(\partial_\tau + h_{\text{BdG}}) \geq 0$. Since h_{BdG} acts on the Majorana spinor Ψ , the relevant quantity is actually the Pfaffian $\text{Pf}(\partial_\tau + h_{\text{BdG}}) = \sqrt{\det(\partial_\tau + h_{\text{BdG}})} \geq 0$, where the principle branch of the square root is chosen.

The Hamiltonian h_{BdG} can be considerably generalized while maintaining $[\mathsf{T}, h_{\text{BdG}}] = 0$, by taking

$$h = \begin{pmatrix} t & r \\ -r^* & t^* \end{pmatrix}, \quad (\text{O.8})$$

$$\Delta = \begin{pmatrix} e^{i\alpha} (|\Delta_x| d^x + i |\Delta_y| d^y)^{|\ell|} & e^{i\tilde{\alpha}} \left(|\tilde{\Delta}_x| d^x + i |\tilde{\Delta}_y| d^y \right)^{|\tilde{\ell}|} \\ -e^{-i\tilde{\alpha}} \left(|\tilde{\Delta}_x| d^x + i |\tilde{\Delta}_y| d^y \right)^{|\tilde{\ell}|} & e^{-i\alpha} (|\Delta_x| d^x + i |\Delta_y| d^y)^{|\ell|} \end{pmatrix},$$

where $t_{\mathbf{x},\mathbf{x}'}, r_{\mathbf{x},\mathbf{x}'}$ are general matrices, and $\ell \in 2\mathbb{Z} + 1$ ($\tilde{\ell} \in 2\mathbb{Z}$) is the angular momentum channel of the triplet (singlet) pairing. This can be further generalized to a sum over all angular momentum channels $\sum_{\ell \in 2\mathbb{Z}+1} e^{i\alpha_\ell} (|\Delta_{\ell,x}| d^x + i |\Delta_{\ell,y}| d^y)^{|\ell|}$ and similarly for $\tilde{\ell}$. The model is Hermitian for $t = t^\dagger$, $r = -r^T$, but this is not required to avoid the sign problem.

In order to obtain an interacting model, the parameters $\phi = \{t, r, \alpha_\ell, \tilde{\alpha}_{\tilde{\ell}}, |\Delta_{\ell,x}|, |\Delta_{\ell,y}|, |\tilde{\Delta}_{\tilde{\ell},x}|, |\tilde{\Delta}_{\tilde{\ell},y}|\}$ can now be promoted to space-time dependent bosonic fields, with any action $S_\phi \in \mathbb{R}$. The model will be sign-free as long as h_{BdG} remains T -invariant for all configurations ϕ , which requires that only reflection-even configurations $\phi(\tau, x, y) = \phi(\tau, x, -y)$ are summed over. As discussed in Sec.4.4.3, this implies non-local interactions, which effectively fold the chiral system into a non-chiral system of half of space.

P Locality and homogeneity of known design principles

In this appendix we review all fermionic design principles known to us, clarify their common features, and describe the conditions under which they are *on-site homogeneous*, imply a *term-wise sign-free* DQMC representation, and allow a *locally sign-free DQMC* simulation, as defined in Sec.4.4.2. The design principles are stated as algebraic conditions satisfied by the effective single-fermion Hamiltonian $h_\phi = h_{\phi(\tau)}$ and the corresponding imaginary-time evolution $U_\phi = \text{TO} e^{-\int_0^\beta h_{\phi(\tau)} d\tau}$, or in terms of the operator $D_\phi = \partial_\tau + h_\phi$, see Sec.4.4.1.

Contraction semi-groups and Majorana time reversals The time-reversal design principle covered in Sec.4.4.3 is a special case of a broad class of design principles that were recently discovered and unified [208–210]. These are stated in terms of Majorana fermions, where ψ is real and $\bar{\psi} = \psi^T$, in which case h_ϕ is anti-symmetric and the determinants in (4.16) are replaced by their square roots. Reference [210] shows that if

$$\mathbf{J}_1 h_\phi - h_\phi^* \mathbf{J}_1 = 0, \quad (\text{P.1})$$

$$i (\mathbf{J}_2 h_\phi - h_\phi^* \mathbf{J}_2) \geq 0, \quad (\text{P.2})$$

where the matrices $\mathbf{J}_1, \mathbf{J}_2$ are real and orthogonal, and obey $\mathbf{J}_1^T = \pm \mathbf{J}_1$, $\mathbf{J}_2^T = -\mathbf{J}_2$, $\{\mathbf{J}_1, \mathbf{J}_2\} = 0$, then $\text{Det}(I + U_\phi) \geq 0$. The equality (P.1) corresponds to an anti-unitary symmetry $\mathbf{T}_1 = \mathbf{J}_1 \mathcal{K}$, $\mathbf{T}_1^2 = \pm I$, where \mathcal{K} is the complex conjugation. If the inequality (P.2) is replaced by an equality, it corresponds to an additional anti-unitary symmetry, $\mathbf{T}_2 = \mathbf{J}_2 \mathcal{K}$, $\mathbf{T}_2^2 = -I$. The case $\mathbf{T}_1^2 = -I$ then reduces to the standard time-reversal \mathbf{T} described in Sec.4.4.3, while $\mathbf{T}_1^2 = I$ corresponds to the 'Majorana class' of Ref.[208]. More generally, the inequality (P.2) states that the left hand side is a positive semi-definite matrix, and implies that h_ϕ is a generator of the contraction semi-group defined by the Hermitian metric $\eta_2 = i\mathbf{J}_2$, $\eta_2^2 = I$, $[\mathbf{T}_1, \eta_2] = 0$. Explicitly, Eq.(P.1)-(P.2) can be written as

$$[\mathbf{T}_1, h_\phi] = 0, \quad \eta_2 h_\phi + h_\phi^\dagger \eta_2 \geq 0, \quad (\text{P.3})$$

and imply

$$[\mathbf{T}_1, U_\phi] = 0, \quad \eta_2 - U_\phi^\dagger \eta_2 U_\phi \geq 0. \quad (\text{P.4})$$

In the language of Sec.4.4.2, for fixed \mathbf{T}_1, η_2 , the set \mathcal{C}_h contains all matrices h_ϕ satisfying (P.3). It is clear that this set is additive: $h_1 + h_2 \in \mathcal{C}_h$ for all $h_1, h_2 \in \mathcal{C}_h$. The set \mathcal{C}_U contains all matrices U_ϕ satisfying Eq.(P.4), and is multiplicative: $U_1 U_2 \in \mathcal{C}_U$ for all $U_1, U_2 \in \mathcal{C}_U$.

A sufficient condition on \mathbf{T}_1, η_2 that guarantees that the design principle they define is on-site homogenous is that they are of the form $\mathbf{T}_1 = I_{|X|} \otimes \mathbf{t}_1$, $\eta_2 = I_{|X|} \otimes e_2$, written in terms of the decomposition $\mathcal{H}_{1F} \cong \mathbb{C}^{|X|} \otimes \mathbb{C}^{\text{d}_F}$ of the single-fermion space. The permutation matrices $O^{(\sigma)}$ defined in Eq.(4.19) then commute with η_2 and \mathbf{T}_1 . Since $O^{(\sigma)}$ are also unitary, we have $O^{(\sigma)} \in \mathcal{C}_U$ for all $\sigma \in S_X$. All examples described in Refs.[208–210] are of the on-site homogenous form $\mathbf{T}_1 = I_{|X|} \otimes \mathbf{t}_1$, $\eta_2 = I_{|X|} \otimes e_2$.

As in our discussion of \mathbf{T} in Sec.4.4.3, the locality of $\mathbf{T}_1 = I_{|X|} \otimes \mathbf{t}_1$ means that it can be applied term-wise, by symmetrizing the local terms $h_{\phi;\mathbf{x}} \mapsto \frac{1}{2} (h_{\phi;\mathbf{x}} + \mathbf{T}_1 h_{\phi;\mathbf{x}} \mathbf{T}_1^{-1})$. A similar procedure for η_2 is only possible if the inequality in Eq.(P.3) holds as an equality (as in Ref.[208]). The contraction semi-group defined by η_2 then reduces to an orthogonal group, and one can enforce the term-wise relations $\eta_2 h_{\phi;\mathbf{x}} + h_{\phi;\mathbf{x}}^\dagger \eta_2 = 0$ by $h_{\phi;\mathbf{x}} \mapsto \frac{1}{2} (h_{\phi;\mathbf{x}} - \eta_2 h_{\phi;\mathbf{x}}^\dagger \eta_2)$.

Collecting the above, we see that if \mathbf{T}_1, η_2 can be brought to the form $\mathbf{T}_1 = I_{|X|} \otimes \mathbf{t}_1$, $\eta_2 = I_{|X|} \otimes e_2$ by the same single-fermion local unitary u , then a DQMC representation which is \mathbf{T}_1 -symmetric, and respects Eq.(P.3) terms-wise, leads to a locally-sign free DQMC simulation.

Split orthogonal group Another recently discovered design principle is defined in terms of the split orthogonal group $O(n, n)$ [205]: if $U_\phi \in O(n, n)$, then the sign of $\text{Det}(I + U_\phi)$ depends only on the connected component of $O(n, n)$ to which U_ϕ belongs. If the sign of e^{-S_ϕ} is manifestly compatible with the connected component of U_ϕ in $O(n, n)$, one has $p(\phi) = e^{-S_\phi} \text{Det}(I + U_\phi) \geq 0$. More explicitly, the statement $U_\phi \in O(n, n)$ implies that U_ϕ is a real matrix and $\eta - U_\phi^T \eta U_\phi = 0$, where $\eta = \text{diag}(I_n, -I_n)$. Restricting to the identity component $O_0(n, n)$, this amounts to the statements that h_ϕ is in the Lie algebra $\mathfrak{o}(n, n)$: it is real and satisfies $\eta h_\phi + h_\phi^T \eta = 0$.

In a basis independent formulation, the data that defines the design principle is an anti-unitary \tilde{T} , such that $\tilde{T}^2 = I$, and a Hermitian metric $\tilde{\eta}$ with canonical form η , such that $[\tilde{T}, \tilde{\eta}] = 0$. The set \mathcal{C}_h is then given by matrices h_ϕ satisfying

$$[\tilde{T}, h_\phi] = 0, \quad \tilde{\eta} h_\phi + h_\phi^\dagger \tilde{\eta} = 0, \quad (\text{P.5})$$

while \mathcal{C}_U is defined by

$$[\tilde{T}, U_\phi] = 0, \quad \tilde{\eta} - U_\phi^\dagger \tilde{\eta} U_\phi = 0. \quad (\text{P.6})$$

The analogy with (P.3)-(P.4) is now manifest, with the inequalities strengthened to equalities. Accordingly, the $O(n, n)$ design-principle is on-site homogeneous if $\tilde{T} = I_{|X|} \otimes \tilde{\mathbf{t}}$ and $\tilde{\eta} = I_{|X|} \otimes \tilde{\mathbf{e}}$. If these forms can be obtained by conjugation of $\tilde{T}, \tilde{\eta}$ with the same single-fermion local unitary u , then a DQMC representation which is sign-free due to $\tilde{T}, \tilde{\eta}$, leads to a locally-sign free DQMC simulation.

The above statements hold for U_ϕ in the identity component $O_0(n, n)$, which is always the case when $h_\phi \in \mathfrak{o}(n, n)$ and $U_\phi = \text{TO}e^{-\int_0^\beta h_{\phi(\tau)} d\tau}$. Time evolutions in the additional three connected components of $O(n, n)$ can be obtained by operator insertions generalizing $U_\phi = U_k \cdots U_2 U_1$ to $U_k \cdots O_2 U_2 O_1 U_1$, where $O \in O(n, n)/O_0(n, n)$ [205]. These can be incorporated into the framework of Sec.4.4, if each O_k is supported on a disk of radius w around a site \mathbf{x}_k , i.e $(O_k)_{\mathbf{x}, \mathbf{y}} = \delta_{\mathbf{x}, \mathbf{y}}$ if $|\mathbf{x} - \mathbf{x}_k| > w$ or $|\mathbf{y} - \mathbf{x}_k| > w$. With this generalization, all sign-free examples described in Ref.[205] amount to locally sign-free DQMC.

Solvable fermionic and bosonic actions Reference [207] described a design principle that nontrivially relates the fermionic action $S_{\psi, \phi} = \bar{\psi} D_\phi \psi$ and bosonic action S_ϕ . A fermionic action was termed 'solvable' if D_ϕ has the form

$$D_\phi = \begin{pmatrix} 0 & M_\phi \\ -M_\phi^\dagger & 0 \end{pmatrix}, \quad (\text{P.7})$$

which clearly implies $\text{Det}(D_\phi) = |\text{Det}(M_\phi)|^2 \geq 0$. Here the imaginary time circle $\mathbb{R}/\beta\mathbb{Z}$ is discretized to $\mathbb{Z}_\beta = \mathbb{Z}/\beta\mathbb{Z}$, and D_ϕ is treated as a matrix on $\mathbb{C}^\beta \times \mathcal{H}_{1F} = \mathbb{C}^\beta \times \mathbb{C}^{|X|} \times \mathbb{C}^{d_F}$, with indices $(\tau, \mathbf{x}, \alpha), (\tau', \mathbf{x}', \alpha')$ for time, space, and internal degrees of freedom. For example, the Hamiltonian form $D_\phi = \partial_\tau + h_{\phi(\tau)}$ is discretized to

$$[D_\phi]_{(\tau, \mathbf{x}, \alpha), (\tau', \mathbf{x}', \alpha')} = (\delta_{\tau, \tau'} - \delta_{\tau-1, \tau'}) \delta_{\mathbf{x}, \mathbf{x}'} \delta_{\alpha, \alpha'} + \delta_{\tau-1, \tau'} [h_{\phi(\tau)}]_{(\mathbf{x}, \alpha), (\mathbf{x}', \alpha')} . \quad (\text{P.8})$$

In a basis independent language, Eq.(P.7) corresponds to

$$\{\Gamma, D_\phi\} = 0, \quad D_\phi^\dagger = -D_\phi, \quad (\text{P.9})$$

where Γ is a 'chiral symmetry', $\Gamma^2 = I$, $\Gamma = \Gamma^\dagger$. Eq.(4.18) is then obtained in a basis where $\Gamma = \text{diag}(I, -I)$. Note however that Γ acts on D_ϕ rather than h_ϕ , and that the form (P.7) requires a non-canonical transformation away from the Hamiltonian form (P.8). We refer to Γ as on-site homogeneous if it is of the form $\Gamma = I_\beta \otimes I_{|X|} \otimes \gamma$, and to D_ϕ as local if $D_\phi = \sum_{\tau, \mathbf{x}} D_{\phi; \tau, \mathbf{x}}$ where each term $D_{\phi; \tau, \mathbf{x}}$ is supported on a disk of radius r around (τ, \mathbf{x}) , and depends on the values of ϕ at points within this disk. The action D_ϕ is 'term-wise solvable' if each $D_{\phi; \tau, \mathbf{x}}$ satisfies (P.9). Any local D_ϕ obeying (P.9) with $\Gamma = I_\beta \otimes I_{|X|} \otimes \gamma$ can be made term-wise solvable by replacing $D_{\phi; \tau, \mathbf{x}} \mapsto \frac{1}{2} (D_{\phi; \tau, \mathbf{x}} - \Gamma D_{\phi; \tau, \mathbf{x}} \Gamma)$ and then $D_{\phi; \tau, \mathbf{x}} \mapsto \frac{1}{2} (D_{\phi; \tau, \mathbf{x}} - D_{\phi; \tau, \mathbf{x}}^\dagger)$. The twisted fermionic boundary conditions in (4.21) are implemented by declaring that the index ' $(\tau = 0, \mathbf{x}, \alpha)$ ' that appears in Eq.(P.8) corresponds to $(\tau = \beta, x + \lambda\Theta(y), y, \alpha)$ with $\lambda \neq 0$. Equation (P.9) then holds for all λ if $\Gamma = I_\beta \otimes I_{|X|} \otimes \gamma$. Under these conditions, solvable fermionic actions can then be incorporated into the definition of locally sign-free DQMC given in Sec.4.4.

All examples given in Ref.[207] have an on-site Γ and local D_ϕ , and it follows from the above discussion that, under these conditions, solvable fermionic actions can then be incorporated into the definition of locally sign-free DQMC given in Sec.4.4.

A bosonic action S_ϕ for a complex valued field $\phi = |\phi| e^{i\theta}$ was termed 'solvable' in Ref.[207] if

$$S_\phi = S_{|\phi|} - \sum_{u, u'} \beta_{u, u'} |\phi_u| |\phi_{u'}| \cos(\varepsilon_u \theta_u + \varepsilon_{u'} \theta_{u'}), \quad (\text{P.10})$$

where $u = (\mathbf{x}, \tau)$, $u' = (\mathbf{x}', \tau')$, and $\varepsilon_u, \varepsilon_{u'} \in \{\pm 1\}$, and $\beta_{u, u'} \geq 0$. For such actions, it was shown that all correlators $\int D\phi e^{-S_\phi} \phi_{u_1} \cdots \phi_{u_k}$ are non-negative, and therefore ϕ can be added to the diagonal in (P.7) with a positive coupling constant $g > 0$, $D_\phi = \begin{pmatrix} g\phi & M \\ -M^\dagger & g\phi \end{pmatrix}$, without introducing signs, though D_ϕ is no longer solvable. Solvable bosonic actions are easily incorporated into the framework of Sec.4.4, as long as they are local in the sense of Eq.(4.18), and in particular, $\beta_{u, u'} = 0$ unless the points u and u' are close.

References

- [1] Omri Golan and Ady Stern. Probing topological superconductors with emergent gravity. *Phys. Rev. B*, 98:064503, Aug 2018.

- [2] Omri Golan, Carlos Hoyos, and Sergej Moroz. Boundary central charge from bulk odd viscosity: Chiral superfluids. *Phys. Rev. B*, 100:104512, Sep 2019.
- [3] Omri Golan, Adam Smith, and Zohar Ringel. Intrinsic sign problem in fermionic and bosonic chiral topological matter. *Phys. Rev. Research*, 2:043032, Oct 2020.
- [4] Felix Rose, Omri Golan, and Sergej Moroz. Hall viscosity and conductivity of two-dimensional chiral superconductors. *SciPost Phys.*, 9:6, July 2020.
- [5] Adam Smith, Omri Golan, and Zohar Ringel. Intrinsic sign problems in topological quantum field theories. *Phys. Rev. Research*, 2:033515, Sep 2020.
- [6] Klaus von Klitzing. The quantized hall effect. *Rev. Mod. Phys.*, 58:519–531, Jul 1986.
- [7] Klaus von Klitzing. Metrology in 2019. *Nature Physics*, 13(2):198–198, 2017.
- [8] JE Avron, R Seiler, and B Simon. Homotopy and quantization in condensed matter physics. *Physical review letters*, 51(1):51, 1983.
- [9] DJ Thouless, Mahito Kohmoto, MP Nightingale, and M Den Nijs. Quantized hall conductance in a two-dimensional periodic potential. *Physical Review Letters*, 49(6):405, 1982.
- [10] Luis Alvarez-Gaume and Edward Witten. Gravitational anomalies. *Nuclear Physics B*, 234(2):269–330, 1984.
- [11] Luis Alvarez-Gaume, S Della Pietra, and G Moore. Anomalies and odd dimensions. *Annals of Physics*, 163(2):288–317, 1985.
- [12] Reinhold A Bertlmann. *Anomalies in quantum field theory*, volume 91. Oxford University Press, 2000.
- [13] Curtis G Callan and Jeffrey A Harvey. Anomalies and fermion zero modes on strings and domain walls. *Nuclear Physics B*, 250(1):427–436, 1985.
- [14] Stephen G Naculich. Axionic strings: covariant anomalies and bosonization of chiral zero modes. *Nuclear Physics B*, 296(4):837–867, 1988.
- [15] Nicholas Read and Dmitry Green. Paired states of fermions in two dimensions with breaking of parity and time-reversal symmetries and the fractional quantum hall effect. *Physical Review B*, 61(15):10267, 2000.
- [16] Xiao-Gang Wen. Classifying gauge anomalies through symmetry-protected trivial orders and classifying gravitational anomalies through topological orders. *Physical Review D*, 88(4):045013, 2013.

- [17] Shinsei Ryu, Joel E Moore, and Andreas WW Ludwig. Electromagnetic and gravitational responses and anomalies in topological insulators and superconductors. *Physical Review B*, 85(4):045104, 2012.
- [18] Edward Witten. Fermion path integrals and topological phases. *Rev. Mod. Phys.*, 88:035001, Jul 2016.
- [19] Daniel S Freed and Michael J Hopkins. Reflection positivity and invertible topological phases. *arXiv preprint arXiv:1604.06527*, 2016.
- [20] Ken Shiozaki, Hassan Shapourian, Kiyonori Gomi, and Shinsei Ryu. Many-body topological invariants for fermionic short-range entangled topological phases protected by antiunitary symmetries. *Phys. Rev. B*, 98:035151, Jul 2018.
- [21] Shiing-Shen Chern and James Simons. Characteristic forms and geometric invariants. *Annals of Mathematics*, 99(1):48–69, 1974.
- [22] R Jackiw and S-Y Pi. Chern-simons modification of general relativity. *Physical Review D*, 68(10):104012, 2003.
- [23] Per Kraus and Finn Larsen. Holographic gravitational anomalies. *Journal of High Energy Physics*, 2006(01):022, 2006.
- [24] Edward Witten. Three-dimensional gravity revisited. *arXiv preprint arXiv:0706.3359*, 2007.
- [25] Michael Stone. Gravitational anomalies and thermal hall effect in topological insulators. *Physical Review B*, 85(18):184503, 2012.
- [26] Fiorenzo Bastianelli and Peter Van Nieuwenhuizen. *Path integrals and anomalies in curved space*. Cambridge University Press, 2006.
- [27] GE Volovik. *The universe in a helium droplet*. Oxford University Press New York, 2009.
- [28] GE Volovik. The gravitational topological chern-simons term in a film of superfluid $^3\text{He-A}$. *Pisma v ZhETF*, 51:111–114, 1990.
- [29] FDM Haldane. ” hall viscosity” and intrinsic metric of incompressible fractional hall fluids. *arXiv preprint arXiv:0906.1854*, 2009.
- [30] FDM Haldane. Geometrical description of the fractional quantum hall effect. *Physical review letters*, 107(11):116801, 2011.
- [31] Zhong Wang, Xiao-Liang Qi, and Shou-Cheng Zhang. Topological field theory and thermal responses of interacting topological superconductors. *Physical Review B*, 84(1):014527, 2011.

- [32] Tao Qin, Qian Niu, and Junren Shi. Energy magnetization and the thermal hall effect. *Physical review letters*, 107(23):236601, 2011.
- [33] Yizhi You, Gil Young Cho, and Eduardo Fradkin. Theory of nematic fractional quantum hall states. *Physical Review X*, 4(4):041050, 2014.
- [34] Alexander G Abanov and Andrey Gromov. Electromagnetic and gravitational responses of two-dimensional noninteracting electrons in a background magnetic field. *Physical Review B*, 90(1):014435, 2014.
- [35] Andrey Gromov and Alexander G Abanov. Density-curvature response and gravitational anomaly. *Physical review letters*, 113(26):266802, 2014.
- [36] Atsuo Shitade and Taro Kimura. Bulk angular momentum and hall viscosity in chiral superconductors. *Physical Review B*, 90(13):134510, 2014.
- [37] Atsuo Shitade. Heat transport as torsional responses and keldysh formalism in a curved spacetime. *Progress of Theoretical and Experimental Physics*, 2014(12), 2014.
- [38] YeJe Park and F. D. M. Haldane. Guiding-center hall viscosity and intrinsic dipole moment along edges of incompressible fractional quantum hall fluids. *Phys. Rev. B*, 90:045123, Jul 2014.
- [39] Andrey Gromov, Gil Young Cho, Yizhi You, Alexander G Abanov, and Eduardo Fradkin. Framing anomaly in the effective theory of the fractional quantum hall effect. *Physical review letters*, 114(1):016805, 2015.
- [40] Andrey Gromov and Alexander G Abanov. Thermal hall effect and geometry with torsion. *Physical review letters*, 114(1):016802, 2015.
- [41] Barry Bradlyn and N Read. Low-energy effective theory in the bulk for transport in a topological phase. *Physical Review B*, 91(12):125303, 2015.
- [42] Barry Bradlyn and N Read. Topological central charge from berry curvature: Gravitational anomalies in trial wave functions for topological phases. *Physical Review B*, 91(16):165306, 2015.
- [43] Semyon Klevtsov and Paul Wiegmann. Geometric adiabatic transport in quantum hall states. *Physical review letters*, 115(8):086801, 2015.
- [44] Andrey Gromov, Kristan Jensen, and Alexander G Abanov. Boundary effective action for quantum hall states. *Physical review letters*, 116(12):126802, 2016.
- [45] Andrey Gromov and Dam Thanh Son. Bimetric theory of fractional quantum hall states. *Physical Review X*, 7(4):041032, 2017.
- [46] Andrey Gromov, Scott D Geraedts, and Barry Bradlyn. Investigating anisotropic quantum hall states with bimetric geometry. *Physical review letters*, 119(14):146602, 2017.

- [47] Semyon Klevtsov. Laughlin states on higher genus riemann surfaces. *arXiv preprint arXiv:1712.09980*, 2017.
- [48] Semyon Klevtsov. Lowest landau level on a cone and zeta determinants. *Journal of Physics A: Mathematical and Theoretical*, 50(23):234003, 2017.
- [49] Semyon Klevtsov, Xiaonan Ma, George Marinescu, and Paul Wiegmann. Quantum hall effect and quillen metric. *Communications in Mathematical Physics*, 349(3):819–855, 2017.
- [50] Ryota Nakai, Shinsei Ryu, and Kentaro Nomura. Laughlin’s argument for the quantized thermal hall effect. *Physical Review B*, 95(16):165405, 2017.
- [51] P Wiegmann. Inner nonlinear waves and inelastic light scattering of fractional quantum hall states as evidence of the gravitational anomaly. *Physical review letters*, 120(8):086601, 2018.
- [52] Andrea Cappelli and Lorenzo Maffi. Bulk-boundary correspondence in the quantum hall effect. *Journal of Physics A: Mathematical and Theoretical*, 51(36):365401, Jul 2018.
- [53] Nathan Schine, Michelle Chalupnik, Tankut Can, Andrey Gromov, and Jonathan Simon. Measuring electromagnetic and gravitational responses of photonic landau levels. *arXiv preprint arXiv:1802.04418*, 2018.
- [54] Anton Kapustin and Lev Spodyneiko. Thermal hall conductance and a relative topological invariant of gapped two-dimensional systems. *arXiv preprint arXiv:1905.06488*, 2019.
- [55] Liangdong Hu, Zhao Liu, DN Sheng, FDM Haldane, and W Zhu. Microscopic diagnosis of universal geometric responses in fractional quantum hall liquids. *arXiv preprint arXiv:2002.05565*, 2020.
- [56] Chien-Hung Lin and Michael Levin. Generalizations and limitations of string-net models. *Phys. Rev. B*, 89:195130, May 2014.
- [57] Andrew C Potter and Ashvin Vishwanath. Protection of topological order by symmetry and many-body localization. *arXiv preprint arXiv:1506.00592*, 2015.
- [58] Nathanan Tantivasadakarn and Ashvin Vishwanath. Full commuting projector hamiltonians of interacting symmetry-protected topological phases of fermions. *Phys. Rev. B*, 98:165104, Oct 2018.
- [59] Jun Ho Son and Jason Alicea. Commuting-projector hamiltonians for chiral topological phases built from parafermions. *Phys. Rev. B*, 97:245144, Jun 2018.
- [60] T. B. Wahl, H.-H. Tu, N. Schuch, and J. I. Cirac. Projected entangled-pair states can describe chiral topological states. *Phys. Rev. Lett.*, 111:236805, Dec 2013.
- [61] Thorsten B. Wahl, Stefan T. Haßler, Hong-Hao Tu, J. Ignacio Cirac, and Norbert Schuch. Symmetries and boundary theories for chiral projected entangled pair states. *Phys. Rev. B*, 90:115133, Sep 2014.

- [62] J. Dubail and N. Read. Tensor network trial states for chiral topological phases in two dimensions and a no-go theorem in any dimension. *Phys. Rev. B*, 92:205307, Nov 2015.
- [63] Ji-Yao Chen, Laurens Vanderstraeten, Sylvain Capponi, and Didier Poilblanc. Non-abelian chiral spin liquid in a quantum antiferromagnet revealed by an ipeps study. *Phys. Rev. B*, 98:184409, Nov 2018.
- [64] D. M. Ceperley. Path integrals in the theory of condensed helium. *Rev. Mod. Phys.*, 67:279–355, Apr 1995.
- [65] F.F. Assaad and H.G. Evertz. World-line and determinantal quantum monte carlo methods for spins, phonons and electrons. *Lecture Notes in Physics*, pages 277–356, 2008.
- [66] Fakher F. Assaad and Igor F. Herbut. Pinning the order: The nature of quantum criticality in the hubbard model on honeycomb lattice. *Phys. Rev. X*, 3:031010, Aug 2013.
- [67] Shailesh Chandrasekharan and Anyi Li. Quantum critical behavior in three dimensional lattice gross-neveu models. *Phys. Rev. D*, 88:021701, Jul 2013.
- [68] Ribhu K Kaul, Roger G Melko, and Anders W Sandvik. Bridging lattice-scale physics and continuum field theory with quantum monte carlo simulations. *Annu. Rev. Condens. Matter Phys.*, 4(1):179–215, 2013.
- [69] Snir Gazit, Fakher F. Assaad, Subir Sachdev, Ashvin Vishwanath, and Chong Wang. Confinement transition of \mathbb{Z}_2 gauge theories coupled to massless fermions: Emergent quantum chromodynamics and $so(5)$ symmetry. *Proceedings of the National Academy of Sciences*, 115(30):E6987–E6995, 2018.
- [70] Erez Berg, Samuel Lederer, Yoni Schattner, and Simon Trebst. Monte carlo studies of quantum critical metals. *Annual Review of Condensed Matter Physics*, 10(1):63–84, 2019.
- [71] Zi-Xiang Li and Hong Yao. Sign-problem-free fermionic quantum monte carlo: Developments and applications. *Annual Review of Condensed Matter Physics*, 10(1):337–356, 2019.
- [72] Matthias Troyer and Uwe-Jens Wiese. Computational complexity and fundamental limitations to fermionic quantum monte carlo simulations. *Phys. Rev. Lett.*, 94:170201, May 2005.
- [73] Milad Marvian, Daniel A. Lidar, and Itay Hen. On the computational complexity of curing non-stoquastic hamiltonians. *Nature Communications*, 10(1):1571, 2019.
- [74] Joel Klassen, Milad Marvian, Stephen Piddock, Marios Ioannou, Itay Hen, and Barbara Terhal. Hardness and ease of curing the sign problem for two-local qubit hamiltonians. *arXiv preprint arXiv:1906.08800*, 2019.

- [75] M. B. Hastings. How quantum are non-negative wavefunctions? *Journal of Mathematical Physics*, 57(1):015210, 2016.
- [76] Zohar Ringel and Dmitry L Kovrizhin. Quantized gravitational responses, the sign problem, and quantum complexity. *Science advances*, 3(9):e1701758, 2017.
- [77] Raimundo R. dos Santos. Introduction to quantum monte carlo simulations for fermionic systems. *Brazilian Journal of Physics*, 33(1):36–54, Mar 2003.
- [78] C. N. Varney, C.-R. Lee, Z. J. Bai, S. Chiesa, M. Jarrell, and R. T. Scalettar. Quantum monte carlo study of the two-dimensional fermion hubbard model. *Phys. Rev. B*, 80:075116, Aug 2009.
- [79] J. P. F. LeBlanc, Andrey E. Antipov, Federico Becca, Ireneusz W. Bulik, Garnet Kin-Lic Chan, Chia-Min Chung, Youjin Deng, Michel Ferrero, Thomas M. Henderson, Carlos A. Jiménez-Hoyos, E. Kozik, Xuan-Wen Liu, Andrew J. Millis, N. V. Prokof'ev, Mingpu Qin, Gustavo E. Scuseria, Hao Shi, B. V. Svistunov, Luca F. Tocchio, I. S. Tupitsyn, Steven R. White, Shiwei Zhang, Bo-Xiao Zheng, Zhenyue Zhu, and Emanuel Gull. Solutions of the two-dimensional hubbard model: Benchmarks and results from a wide range of numerical algorithms. *Phys. Rev. X*, 5:041041, Dec 2015.
- [80] A. Kantian, M. Dolfi, M. Troyer, and T. Giamarchi. Understanding repulsively mediated superconductivity of correlated electrons via massively parallel density matrix renormalization group. *Phys. Rev. B*, 100:075138, Aug 2019.
- [81] S. Hands, I. Montvay, S. Morrison, M. Oevers, L. Scorzato, and J. Skullerud. Numerical study of dense adjoint matter in two color qcd. *The European Physical Journal C*, 17(2):285–302, Oct 2000.
- [82] C. R. Allton, S. Ejiri, S. J. Hands, O. Kaczmarek, F. Karsch, E. Laermann, Ch. Schmidt, and L. Scorzato. Qcd thermal phase transition in the presence of a small chemical potential. *Phys. Rev. D*, 66:074507, Oct 2002.
- [83] V. A. Goy, V. Bornyakov, D. Boyda, A. Molochkov, A. Nakamura, A. Nikolaev, and V. Zakharov. Sign problem in finite density lattice QCD. *Progress of Theoretical and Experimental Physics*, 2017(3), 03 2017.
- [84] Mitali Banerjee, Moty Heiblum, Vladimir Umansky, Dima E Feldman, Yuval Oreg, and Ady Stern. Observation of half-integer thermal hall conductance. *Nature*, page 1, 2018.
- [85] Chong Wang, Ashvin Vishwanath, and Bertrand I. Halperin. Topological order from disorder and the quantized hall thermal metal: Possible applications to the $\nu = 5/2$ state. *Phys. Rev. B*, 98:045112, Jul 2018.

- [86] David F. Mross, Yuval Oreg, Ady Stern, Gilad Margalit, and Moty Heiblum. Theory of disorder-induced half-integer thermal hall conductance. *Phys. Rev. Lett.*, 121:026801, Jul 2018.
- [87] Steven H. Simon. Interpretation of thermal conductance of the $\nu = 5/2$ edge. *Phys. Rev. B*, 97:121406, Mar 2018.
- [88] Ken K. W. Ma and D. E. Feldman. Partial equilibration of integer and fractional edge channels in the thermal quantum hall effect. *Phys. Rev. B*, 99:085309, Feb 2019.
- [89] Juven Wang, Xiao-Gang Wen, and Edward Witten. Symmetric gapped interfaces of spt and set states: Systematic constructions. *Phys. Rev. X*, 8:031048, Aug 2018.
- [90] Bei Zeng, Xie Chen, Duan-Lu Zhou, and Xiao-Gang Wen. *Quantum information meets quantum matter*. Springer, 2019.
- [91] Xie Chen, Zheng-Cheng Gu, Zheng-Xin Liu, and Xiao-Gang Wen. Symmetry protected topological orders and the group cohomology of their symmetry group. *arXiv preprint arXiv:1106.4772*, 2011.
- [92] Anton Kapustin, Ryan Thorngren, Alex Turzillo, and Zitao Wang. Fermionic symmetry protected topological phases and cobordisms. *Journal of High Energy Physics*, 2015(12):1–21, Dec 2015.
- [93] Anton Kapustin and Ryan Thorngren. Fermionic spt phases in higher dimensions and bosonization. *Journal of High Energy Physics*, 2017(10), Oct 2017.
- [94] Xiao-Liang Qi and Shou-Cheng Zhang. Topological insulators and superconductors. *Reviews of Modern Physics*, 83(4):1057, 2011.
- [95] X. G. WEN. Topological orders in rigid states. *International Journal of Modern Physics B*, 04(02):239–271, 1990.
- [96] Xie Chen, Zheng-Cheng Gu, and Xiao-Gang Wen. Local unitary transformation, long-range quantum entanglement, wave function renormalization, and topological order. *Phys. Rev. B*, 82:155138, Oct 2010.
- [97] Chetan Nayak, Steven H Simon, Ady Stern, Michael Freedman, and Sankar Das Sarma. Non-abelian anyons and topological quantum computation. *Reviews of Modern Physics*, 80(3):1083, 2008.
- [98] L. Cincio and G. Vidal. Characterizing topological order by studying the ground states on an infinite cylinder. *Phys. Rev. Lett.*, 110:067208, Feb 2013.
- [99] Lucile Savary and Leon Balents. Quantum spin liquids: a review. *Reports on Progress in Physics*, 80(1):016502, Nov 2016.
- [100] Michael Levin and Ady Stern. Fractional topological insulators. *Phys. Rev. Lett.*, 103:196803, Nov 2009.

- [101] Ady Stern. Fractional topological insulators: A pedagogical review. *Annual Review of Condensed Matter Physics*, 7(1):349–368, 2016.
- [102] Paul Ginsparg. Applied conformal field theory. *arXiv preprint hep-th/9108028*, 1988.
- [103] P. Di Francesco, P. Mathieu, and D. Sénéchal. *Conformal Field Theory*. Graduate texts in contemporary physics. Island Press, 1996.
- [104] Alexei Kitaev. Anyons in an exactly solved model and beyond. *Annals of Physics*, 321(1):2–111, 2006.
- [105] F. D. M. Haldane. Model for a quantum hall effect without landau levels: Condensed-matter realization of the "parity anomaly". *Phys. Rev. Lett.*, 61:2015–2018, Oct 1988.
- [106] Xiao-Liang Qi, Taylor L Hughes, and Shou-Cheng Zhang. Topological field theory of time-reversal invariant insulators. *Physical Review B*, 78(19):195424, 2008.
- [107] Shinsei Ryu, Andreas P Schnyder, Akira Furusaki, and Andreas WW Ludwig. Topological insulators and superconductors: tenfold way and dimensional hierarchy. *New Journal of Physics*, 12(6):065010, 2010.
- [108] Hidenori Takagi, Tomohiro Takayama, George Jackeli, Giniyat Khaliullin, and Stephen E Nagler. Concept and realization of kitaev quantum spin liquids. *Nature Reviews Physics*, 1(4):264–280, 2019.
- [109] Edward Witten. Quantum field theory and the jones polynomial. *Communications in Mathematical Physics*, 121(3):351–399, Sep 1989.
- [110] CL Kane and Matthew PA Fisher. Quantized thermal transport in the fractional quantum hall effect. *Physical Review B*, 55(23):15832, 1997.
- [111] Andrea Cappelli, Marina Huerta, and Guillermo R Zemba. Thermal transport in chiral conformal theories and hierarchical quantum hall states. *Nuclear Physics B*, 636(3):568–582, 2002.
- [112] Sébastien Jezouin, FD Parmentier, A Anthore, U Gennser, A Cavanna, Y Jin, and F Pierre. Quantum limit of heat flow across a single electronic channel. *Science*, 342(6158):601–604, 2013.
- [113] Mitali Banerjee, Moty Heiblum, Amir Rosenblatt, Yuval Oreg, Dima E Feldman, Ady Stern, and Vladimir Umansky. Observed quantization of anyonic heat flow. *Nature*, 545(7652):75, 2017.
- [114] Y. Kasahara, T. Ohnishi, Y. Mizukami, O. Tanaka, Sixiao Ma, K. Sugii, N. Kurita, H. Tanaka, J. Nasu, Y. Motome, T. Shibauchi, and Y. Matsuda. Majorana quantization and half-integer thermal quantum hall effect in a kitaev spin liquid. *Nature*, 559(7713):227–231, 2018.
- [115] Roberto Ferreira Pérez. Conserved current for the cotton tensor, black hole entropy and equivariant pontryagin forms. *Classical and Quantum Gravity*, 27(13):135015, 2010.

- [116] JE Avron, Ruedi Seiler, and Petr G Zograf. Viscosity of quantum hall fluids. *Physical review letters*, 75(4):697, 1995.
- [117] Andrey Gromov and Barry Bradlyn. Geometric theory of anisotropic quantum hall states. *arXiv preprint arXiv:1703.01304*, 2017.
- [118] JM Luttinger. Theory of thermal transport coefficients. *Physical Review*, 135(6A):A1505, 1964.
- [119] NR Cooper, BI Halperin, and IM Ruzin. Thermoelectric response of an interacting two-dimensional electron gas in a quantizing magnetic field. *Physical Review B*, 55(4):2344, 1997.
- [120] Ryota Nakai, Shinsei Ryu, and Kentaro Nomura. Finite-temperature effective boundary theory of the quantized thermal hall effect. *New Journal of Physics*, 18(2):023038, 2016.
- [121] Giandomenico Palumbo and Jiannis K Pachos. Holographic correspondence in topological superconductors. *Annals of Physics*, 372:175–181, 2016.
- [122] T Can, YH Chiu, M Laskin, and P Wiegmann. Emergent conformal symmetry and geometric transport properties of quantum hall states on singular surfaces. *Physical review letters*, 117(26):266803, 2016.
- [123] Andrey Gromov. Geometric defects in quantum hall states. *Physical Review B*, 94(8):085116, 2016.
- [124] Nathan Schine, Albert Ryou, Andrey Gromov, Ariel Sommer, and Jonathan Simon. Synthetic landau levels for photons. *Nature*, 534(7609):671, 2016.
- [125] Dieter Vollhardt and Peter Wölfle. *The superfluid phases of helium 3*. Courier Corporation, 2013.
- [126] Catherine Kallin and John Berlinsky. Chiral superconductors. *Reports on Progress in Physics*, 79(5):054502, apr 2016.
- [127] Masatoshi Sato and Yoichi Ando. Topological superconductors: a review. *Reports on Progress in Physics*, 80(7):076501, May 2017.
- [128] Gregory Moore and Nicholas Read. Nonabelions in the fractional quantum hall effect. *Nuclear Physics B*, 360(2-3):362–396, 1991.
- [129] A Yu Kitaev. Fault-tolerant quantum computation by anyons. *Annals of Physics*, 303(1):2–30, 2003.
- [130] Rev Shankar. Renormalization-group approach to interacting fermions. *Reviews of Modern Physics*, 66(1):129, 1994.

- [131] L. V. Levitin, R. G. Bennett, A. Casey, B. Cowan, J. Saunders, D. Drung, Th. Schurig, and J. M. Parpia. Phase diagram of the topological superfluid ^3He confined in a nanoscale slab geometry. *Science*, 340(6134):841–844, 2013.
- [132] P. M. Walmsley and A. I. Golov. Chirality of superfluid ^3He -a. *Phys. Rev. Lett.*, 109:215301, Nov 2012.
- [133] H. Ikegami, Y. Tsutsumi, and K. Kono. Chiral symmetry breaking in superfluid ^3He -a. *Science*, 341(6141):59–62, 2013.
- [134] N. Zhelev, T. S. Abhilash, E. N. Smith, R. G. Bennett, X. Rojas, L. Levitin, J. Saunders, and J. M. Parpia. The a-b transition in superfluid helium-3 under confinement in a thin slab geometry. *Nature Communications*, 8:15963, Jul 2017.
- [135] Chuanwei Zhang, Sumanta Tewari, Roman M. Lutchyn, and S. Das Sarma. $p_x + ip_y$ superfluid from s -wave interactions of fermionic cold atoms. *Phys. Rev. Lett.*, 101:160401, Oct 2008.
- [136] Masatoshi Sato, Yoshiro Takahashi, and Satoshi Fujimoto. Non-abelian topological order in s -wave superfluids of ultracold fermionic atoms. *Phys. Rev. Lett.*, 103:020401, Jul 2009.
- [137] Guocai Liu, Ningning Hao, Shi-Liang Zhu, and W. M. Liu. Topological superfluid transition induced by a periodically driven optical lattice. *Phys. Rev. A*, 86:013639, Jul 2012.
- [138] Ningning Hao, Guocai Liu, Ning Wu, Jiangping Hu, and Yupeng Wang. Chiral f -wave topological superfluid in triangular optical lattices. *Phys. Rev. A*, 87:053609, May 2013.
- [139] Shao-Liang Zhang, Li-Jun Lang, and Qi Zhou. Chiral d -wave superfluid in periodically driven lattices. *Phys. Rev. Lett.*, 115:225301, Nov 2015.
- [140] Abdelâali Boudjemâa. Unconventional superfluids of fermionic polar molecules in a bilayer system. *Physics Letters A*, 381(20):1745 – 1748, 2017.
- [141] Ningning Hao, Huaiming Guo, and Ping Zhang. Topological orbital superfluid with chiral d -wave order in a rotating optical lattice. *New Journal of Physics*, 19(8):083020, aug 2017.
- [142] PN Brusov and VN Popov. Superfluidity and bose excitations in He-3 films. *Zh. Eksp. Teor. Fiz.*, 80:1564–1576, 1981.
- [143] G. E. Volovik and M. A. Zubkov. Higgs bosons in particle physics and in condensed matter. *Journal of Low Temperature Physics*, 175(1-2):486–497, Oct 2013.
- [144] J. A. Sauls. On the nambu fermion-boson relations for superfluid ^3He . *Physical Review B*, 95(9), 2017.
- [145] Wei-Han Hsiao. Universal collective modes in two-dimensional chiral superfluids. *Phys. Rev. B*, 100:094510, Sep 2019.

- [146] Lin Jiao, Sean Howard, Sheng Ran, Zhenyu Wang, Jorge Olivares Rodriguez, Manfred Sigrist, Ziqiang Wang, Nicholas P. Butch, and Vidya Madhavan. Chiral superconductivity in heavy-fermion metal $U\text{Te}_2$. *Nature*, 579(7800):523–527, 2020.
- [147] Dam Thanh Son. Is the composite fermion a dirac particle? *Phys. Rev. X*, 5:031027, Sep 2015.
- [148] Dam Thanh Son. The dirac composite fermion of the fractional quantum hall effect. *Annual Review of Condensed Matter Physics*, 9(1):397–411, Mar 2018.
- [149] D. E. Feldman. Comment on “interpretation of thermal conductance of the $\nu = 5/2$ edge”. *Phys. Rev. B*, 98:167401, Oct 2018.
- [150] Jin-Peng Xu, Mei-Xiao Wang, Zhi Long Liu, Jian-Feng Ge, Xiaojun Yang, Canhua Liu, Zhu An Xu, Dandan Guan, Chun Lei Gao, Dong Qian, Ying Liu, Qiang-Hua Wang, Fu-Chun Zhang, Qi-Kun Xue, and Jin-Feng Jia. Experimental detection of a majorana mode in the core of a magnetic vortex inside a topological insulator-superconductor $\text{Bi}_2\text{Te}_3/\text{NbSe}_2$ heterostructure. *Phys. Rev. Lett.*, 114:017001, Jan 2015.
- [151] Gerbold C. Ménard, Sébastien Guissart, Christophe Brun, Raphaël T. Leriche, Mircea Trif, François Debontridder, Dominique Demaille, Dimitri Roditchev, Pascal Simon, and Tristan Cren. Two-dimensional topological superconductivity in $\text{Pb}/\text{Co}/\text{Si}(111)$. *Nature Communications*, 8(1), Dec 2017.
- [152] GE Volovik and VM Yakovenko. Fractional charge, spin and statistics of solitons in superfluid ^3He film. *Journal of Physics: Condensed Matter*, 1(31):5263, 1989.
- [153] Michael Stone and Rahul Roy. Edge modes, edge currents, and gauge invariance in $p_x + ip_y$ superfluids and superconductors. *Physical Review B*, 69(18):184511, 2004.
- [154] Tomás Ortín. *Gravity and strings*. Cambridge University Press, 2004.
- [155] Taylor L Hughes, Robert G Leigh, and Eduardo Fradkin. Torsional response and dissipationless viscosity in topological insulators. *Physical review letters*, 107(7):075502, 2011.
- [156] Taylor L Hughes, Robert G Leigh, and Onkar Parrikar. Torsional anomalies, hall viscosity, and bulk-boundary correspondence in topological states. *Physical Review D*, 88(2):025040, 2013.
- [157] Onkar Parrikar, Taylor L Hughes, and Robert G Leigh. Torsion, parity-odd response, and anomalies in topological states. *Physical Review D*, 90(10):105004, 2014.
- [158] Michael Geracie, Siavash Golkar, and Matthew M Roberts. Hall viscosity, spin density, and torsion. *arXiv preprint arXiv:1410.2574*, 2014.
- [159] Philip Kim. *Graphene and Relativistic Quantum Physics*, pages 1–23. Springer International Publishing, Cham, 2017.

- [160] Carlos Hoyos. Hall viscosity, topological states and effective theories. *International Journal of Modern Physics B*, 28(15):1430007, 2014.
- [161] N. Read. Non-abelian adiabatic statistics and hall viscosity in quantum hall states and $p_x + ip_y$ paired superfluids. *Physical Review B*, 79(4), 2009.
- [162] N Read and EH Rezayi. Hall viscosity, orbital spin, and geometry: paired superfluids and quantum hall systems. *Physical Review B*, 84(8):085316, 2011.
- [163] Carlos Hoyos, Sergej Moroz, and Dam Thanh Son. Effective theory of chiral two-dimensional superfluids. *Physical Review B*, 89(17):174507, 2014.
- [164] Sergej Moroz and Carlos Hoyos. Effective theory of two-dimensional chiral superfluids: gauge duality and newton-cartan formulation. *Physical Review B*, 91(6):064508, 2015.
- [165] J. Nissinen and G. E. Volovik. Thermal nieh-yan anomaly in weyl superfluids. *Phys. Rev. Research*, 2:033269, Aug 2020.
- [166] Jaakko Nissinen. Emergent spacetime and gravitational nieh-yan anomaly in chiral $p + ip$ weyl superfluids and superconductors. *Phys. Rev. Lett.*, 124:117002, Mar 2020.
- [167] Ze-Min Huang, Bo Han, and Michael Stone. Nieh-yan anomaly: Torsional landau levels, central charge, and anomalous thermal hall effect. *Phys. Rev. B*, 101:125201, Mar 2020.
- [168] Ze-Min Huang, Bo Han, and Michael Stone. Hamiltonian approach to the torsional anomalies and its dimensional ladder. *Phys. Rev. B*, 101:165201, Apr 2020.
- [169] Sara Laurila and Jaakko Nissinen. Torsional landau levels and geometric anomalies in condensed matter weyl systems. *arXiv preprint arXiv:2007.10682*, 2020.
- [170] Ze-Min Huang and Bo Han. Torsional anomalies and bulk-dislocation correspondence in weyl systems. *arXiv preprint arXiv:2003.04853*, 2020.
- [171] Ashk Farjami, Matthew D. Horner, Chris N. Self, Zlatko Papić, and Jiannis K. Pachos. Geometric description of the kitaev honeycomb lattice model. *Phys. Rev. B*, 101:245116, Jun 2020.
- [172] Matthew D. Horner, Ashk Farjami, and Jiannis K. Pachos. Equivalence between vortices, twists, and chiral gauge fields in the kitaev honeycomb lattice model. *Phys. Rev. B*, 102:125152, Sep 2020.
- [173] J. E. Avron, R. Seiler, and P. G. Zograf. Viscosity of quantum hall fluids. *Phys. Rev. Lett.*, 75:697–700, Jul 1995.
- [174] J. E. Avron. Odd viscosity. *Journal of Statistical Physics*, 92(3):543–557, Aug 1998.

- [175] Barry Bradlyn, Moshe Goldstein, and N. Read. Kubo formulas for viscosity: Hall viscosity, ward identities, and the relation with conductivity. *Phys. Rev. B*, 86:245309, Dec 2012.
- [176] Matthew F. Lapa and Taylor L. Hughes. Swimming at low reynolds number in fluids with odd, or hall, viscosity. *Phys. Rev. E*, 89:043019, Apr 2014.
- [177] Andrew Lucas and Piotr Surówka. Phenomenology of nonrelativistic parity-violating hydrodynamics in 2+1 dimensions. *Phys. Rev. E*, 90:063005, Dec 2014.
- [178] Mohammad Sherafati, Alessandro Principi, and Giovanni Vignale. Hall viscosity and electromagnetic response of electrons in graphene. *Phys. Rev. B*, 94:125427, Sep 2016.
- [179] Luca V. Delacrétaz and Andrey Gromov. Transport signatures of the hall viscosity. *Phys. Rev. Lett.*, 119:226602, Nov 2017.
- [180] Thomas Scaffidi, Nabhanila Nandi, Burkhard Schmidt, Andrew P. Mackenzie, and Joel E. Moore. Hydrodynamic electron flow and hall viscosity. *Phys. Rev. Lett.*, 118:226601, Jun 2017.
- [181] Thomas I. Tügel and Taylor L. Hughes. Hall viscosity and the acoustic faraday effect. *Phys. Rev. B*, 96:174524, Nov 2017.
- [182] Sriram Ganeshan and Alexander G. Abanov. Odd viscosity in two-dimensional incompressible fluids. *Phys. Rev. Fluids*, 2:094101, Sep 2017.
- [183] Debarghya Banerjee, Anton Souslov, Alexander G Abanov, and Vincenzo Vitelli. Odd viscosity in chiral active fluids. *Nature Communications*, 8(1):1573, 2017.
- [184] Alexander Bogatskiy and Paul Wiegmann. Edge wave and boundary vorticity layer of vortex matter. *arXiv preprint arXiv:1812.00763*, 2018.
- [185] Tobias Holder, Raquel Queiroz, and Ady Stern. Unified description of the classical hall viscosity. *arXiv preprint arXiv:1903.05541*, 2019.
- [186] Anton Souslov, Kinjal Dasbiswas, Michel Fruchart, Suriyanarayanan Vaikuntanathan, and Vincenzo Vitelli. Topological waves in fluids with odd viscosity. *Phys. Rev. Lett.*, 122:128001, Mar 2019.
- [187] Vishal Soni, Ephraim Bililign, Sofia Magkiriadou, Stefano Sacanna, Denis Bartolo, Michael J Shelley, and William Irvine. The free surface of a colloidal chiral fluid: waves and instabilities from odd stress and hall viscosity. *arXiv preprint arXiv:1812.09990*, 2018.
- [188] A. I. Berdyugin, S. G. Xu, F. M. D. Pellegrino, R. Krishna Kumar, A. Principi, I. Torre, M. Ben Shalom, T. Taniguchi, K. Watanabe, I. V. Grigorieva, M. Polini, A. K. Geim, and D. A. Bandurin. Measuring hall viscosity of graphene’s electron fluid. *Science*, 2019.

- [189] Maarten FL Golterman, Karl Jansen, and David B Kaplan. Chern-simons currents and chiral fermions on the lattice. *Physics Letters B*, 301(2-3):219–223, 1993.
- [190] Scientific background on the nobel prize in physics 2016, 2016.
- [191] B Mera. Topological response of gapped fermions to a $u(1)$ gauge field. *arXiv preprint arXiv:1705.04394*, 2017.
- [192] GE Volovik. Quantized hall effect in superfluid helium-3 film. *Physics Letters A*, 128(5):277–279, 1988.
- [193] J Goryo and K Ishikawa. Abelian chern-simons term in superfluid $^3\text{He-A}$. *Physics Letters A*, 246(6):549–559, 1998.
- [194] J Goryo and K Ishikawa. Observation of induced chern-simons term in p- and t-violating superconductors. *Physics Letters A*, 260(3):294–299, 1999.
- [195] Akira Furusaki, Masashige Matsumoto, and Manfred Sigrist. Spontaneous hall effect in a chiral p-wave superconductor. *Physical Review B*, 64(5):054514, 2001.
- [196] Rahul Roy and Catherine Kallin. Collective modes and electromagnetic response of a chiral superconductor. *Physical Review B*, 77(17):174513, 2008.
- [197] Roman M Lutchyn, Pavel Nagornykh, and Victor M Yakovenko. Gauge-invariant electromagnetic response of a chiral $p_x + ip_y$ superconductor. *Physical Review B*, 77(14):144516, 2008.
- [198] Daniel Ariad, Eytan Grosfeld, and Babak Seradjeh. Effective theory of vortices in two-dimensional spinless chiral p-wave superfluids. *Physical Review B*, 92(3):035136, 2015.
- [199] DT Son and M Wingate. General coordinate invariance and conformal invariance in nonrelativistic physics: Unitary fermi gas. *Annals of Physics*, 321(1):197–224, 2006.
- [200] Nicholas Metropolis and S. Ulam. The monte carlo method. *Journal of the American Statistical Association*, 44(247):335–341, 1949. PMID: 18139350.
- [201] F Barahona. On the computational complexity of ising spin glass models. *Journal of Physics A: Mathematical and General*, 15(10):3241–3253, oct 1982.
- [202] Sergey Bravyi, David P. Divincenzo, Roberto Oliveira, and Barbara M. Terhal. The complexity of stoquastic local hamiltonian problems. *Quantum Info. Comput.*, 8(5):361–385, May 2008.
- [203] Dominik Hangleiter, Ingo Roth, Daniel Nagaj, and Jens Eisert. Easing the monte carlo sign problem. *arXiv preprint arXiv:1906.02309*, 2019.
- [204] Shailesh Chandrasekharan and Uwe-Jens Wiese. Meron-cluster solution of fermion sign problems. *Phys. Rev. Lett.*, 83:3116–3119, Oct 1999.

- [205] Lei Wang, Ye-Hua Liu, Mauro Iazzi, Matthias Troyer, and Gergely Harcos. Split orthogonal group: A guiding principle for sign-problem-free fermionic simulations. *Phys. Rev. Lett.*, 115:250601, Dec 2015.
- [206] R. Blankenbecler, D. J. Scalapino, and R. L. Sugar. Monte carlo calculations of coupled boson-fermion systems. i. *Phys. Rev. D*, 24:2278–2286, Oct 1981.
- [207] Shailesh Chandrasekharan. Fermion bag approach to fermion sign problems. *The European Physical Journal A*, 49(7):90, 2013.
- [208] Zi-Xiang Li, Yi-Fan Jiang, and Hong Yao. Majorana-time-reversal symmetries: A fundamental principle for sign-problem-free quantum monte carlo simulations. *Phys. Rev. Lett.*, 117:267002, Dec 2016.
- [209] Z. C. Wei, Congjun Wu, Yi Li, Shiwei Zhang, and T. Xiang. Majorana positivity and the fermion sign problem of quantum monte carlo simulations. *Phys. Rev. Lett.*, 116:250601, Jun 2016.
- [210] Zhong-Chao Wei. Semigroup approach to the sign problem in quantum monte carlo simulations. *arXiv preprint arXiv:1712.09412*, 2017.
- [211] Michael A. Levin and Xiao-Gang Wen. String-net condensation: A physical mechanism for topological phases. *Phys. Rev. B*, 71:045110, Jan 2005.
- [212] Hong-Hao Tu, Yi Zhang, and Xiao-Liang Qi. Momentum polarization: An entanglement measure of topological spin and chiral central charge. *Phys. Rev. B*, 88:195412, Nov 2013.
- [213] Michael P. Zaletel, Roger S. K. Mong, and Frank Pollmann. Topological characterization of fractional quantum hall ground states from microscopic hamiltonians. *Phys. Rev. Lett.*, 110:236801, Jun 2013.
- [214] Thomas I. Tügel and Taylor L. Hughes. Hall viscosity and momentum transport in lattice and continuum models of the integer quantum hall effect in strong magnetic fields. *Phys. Rev. B*, 92:165127, Oct 2015.
- [215] Parsa Hassan Bonderson. *Non-Abelian anyons and interferometry*. PhD thesis, California Institute of Technology, 2007.
- [216] Tian Lan, Liang Kong, and Xiao-Gang Wen. Theory of (2+1)-dimensional fermionic topological orders and fermionic/bosonic topological orders with symmetries. *Phys. Rev. B*, 94:155113, Oct 2016.
- [217] Po-Shen Hsin, Ying-Hsuan Lin, Natalie M. Paquette, and Juven Wang. An effective field theory for fractional quantum hall systems near $\nu = 5/2$. *arXiv preprint arXiv:2005.10826*, 2020.

- [218] J. Fröhlich and F. Gabbiani. Braid statistics in local quantum theory. *Reviews in Mathematical Physics*, 02(03):251–353, 1990.
- [219] Michael H. Freedman, Michael Larsen, and Zhenghan Wang. A modular functor which is universal for quantum computation. *Communications in Mathematical Physics*, 227(3):605–622, 2002.
- [220] Frank Arute, Kunal Arya, Ryan Babbush, Dave Bacon, Joseph C. Bardin, Rami Barends, Rupak Biswas, Sergio Boixo, Fernando G. S. L. Brandao, David A. Buell, Brian Burkett, Yu Chen, Zijun Chen, Ben Chiaro, Roberto Collins, William Courtney, Andrew Dunsworth, Edward Farhi, Brooks Foxen, Austin Fowler, Craig Gidney, Marissa Giustina, Rob Graff, Keith Guerin, Steve Habegger, Matthew P. Harrigan, Michael J. Hartmann, Alan Ho, Markus Hoffmann, Trent Huang, Travis S. Humble, Sergei V. Isakov, Evan Jeffrey, Zhang Jiang, Dvir Kafri, Kostyantyn Kechedzhi, Julian Kelly, Paul V. Klimov, Sergey Knysh, Alexander Korotkov, Fedor Kostritsa, David Landhuis, Mike Lindmark, Erik Lucero, Dmitry Lyakh, Salvatore Mandrà, Jarrod R. McClean, Matthew McEwen, Anthony Megrant, Xiao Mi, Kristel Michielsen, Masoud Mohseni, Josh Mutus, Ofer Naaman, Matthew Neeley, Charles Neill, Murphy Yuezhen Niu, Eric Ostby, Andre Petukhov, John C. Platt, Chris Quintana, Eleanor G. Rieffel, Pedram Roushan, Nicholas C. Rubin, Daniel Sank, Kevin J. Satzinger, Vadim Smelyanskiy, Kevin J. Sung, Matthew D. Trevithick, Amit Vainsencher, Benjamin Villalonga, Theodore White, Z. Jamie Yao, Ping Yeh, Adam Zalcman, Hartmut Neven, and John M. Martinis. Quantum supremacy using a programmable superconducting processor. *Nature*, 574(7779):505–510, 2019.
- [221] Rajarshi Bhattacharyya, Mitali Banerjee, Moty Heiblum, Diana Mahalu, and Vladimir Umansky. Melting of interference in the fractional quantum hall effect: Appearance of neutral modes. *Phys. Rev. Lett.*, 122:246801, Jun 2019.
- [222] J. Nakamura, S. Liang, G. C. Gardner, and M. J. Manfra. Direct observation of anyonic braiding statistics. *Nature Physics*, 16(9):931–936, 2020.
- [223] Bernd Rosenow, Ivan P. Levkivskyi, and Bertrand I. Halperin. Current correlations from a mesoscopic anyon collider. *Phys. Rev. Lett.*, 116:156802, Apr 2016.
- [224] H. Bartolomei, M. Kumar, R. Bisognin, A. Marguerite, J.-M. Berroir, E. Bocquillon, B. Plaçais, A. Cavanna, Q. Dong, U. Gennser, Y. Jin, and G. Fève. Fractional statistics in anyon collisions. *Science*, 368(6487):173–177, 2020.
- [225] G. E. Volovik. An analog of the quantum hall effect in a superfluid ^3He film. *Soviet Physics - JETP (English Translation)*, 67(9):1804–1811, 1988.
- [226] B Andrei Bernevig and Taylor L Hughes. *Topological insulators and topological superconductors*. Princeton University Press, 2013.
- [227] Alexei Kitaev. Periodic table for topological insulators and superconductors. *arXiv preprint arXiv:0901.2686*, 2009.

- [228] Doru Sticlet. *Edge states in Chern Insulators and Majorana fermions in topological superconductors*. PhD thesis, Paris 11, 2012.
- [229] Sean M Carroll. *Spacetime and geometry. An introduction to general relativity*, volume 1. Cambridge University Press, 2004.
- [230] Michael Forger and Hartmann Römer. Currents and the energy-momentum tensor in classical field theory: a fresh look at an old problem. *Annals of Physics*, 309(2):306–389, 2004.
- [231] Yasuhiro Tada, Wenxing Nie, and Masaki Oshikawa. Orbital angular momentum and spectral flow in two-dimensional chiral superfluids. *Physical review letters*, 114(19):195301, 2015.
- [232] Grigorii Efimovich Volovik. Orbital momentum of chiral superfluids and the spectral asymmetry of edge states. *JETP letters*, 100(11):742–745, 2015.
- [233] Atsuo Shitade and Yuki Nagai. Orbital angular momentum in a nonchiral topological superconductor. *Physical Review B*, 92(2):024502, 2015.
- [234] Mikio Nakahara. *Geometry, topology and physics*. CRC Press, 2003.
- [235] Aydin Cem Keser and Victor Galitski. Analogue stochastic gravity in strongly-interacting bose-einstein condensates. *arXiv preprint arXiv:1612.08980*, 2016.
- [236] Michel Leclerc. Canonical and gravitational stress-energy tensors. *International Journal of Modern Physics D*, 15(07):959–989, 2006.
- [237] Jorge Zanelli. Chern–simons forms in gravitation theories. *Classical and Quantum Gravity*, 29(13):133001, 2012.
- [238] A Quelle, C Morais Smith, Thomas Kvorning, and Thors Hans Hansson. Edge majoranas on locally flat surfaces: The cone and the möbius band. *Physical Review B*, 94(12):125137, 2016.
- [239] Yaacov E Kraus, Assa Auerbach, HA Fertig, and Steven H Simon. Majorana fermions of a two-dimensional $p_x + i p_y$ superconductor. *Physical Review B*, 79(13):134515, 2009.
- [240] Sergej Moroz, Carlos Hoyos, and Leo Radzihovsky. Chiral $p \pm i p$ superfluid on a sphere. *Physical Review B*, 93(2):024521, 2016.
- [241] Juan Manes, Raymond Stora, and Bruno Zumino. Algebraic study of chiral anomalies. *Communications in Mathematical Physics*, 102(1):157–174, 1985.
- [242] Stephen W Hawking. Zeta function regularization of path integrals in curved spacetime. *Communications in Mathematical Physics*, 55(2):133–148, 1977.
- [243] Kazuo Fujikawa. Comment on chiral and conformal anomalies. *Physical Review Letters*, 44(26):1733, 1980.

- [244] Maissam Barkeshli, Suk Bum Chung, and Xiao-Liang Qi. Dissipationless phonon hall viscosity. *Physical Review B*, 85(24):245107, 2012.
- [245] D Schmeltzer. Propagation of phonons in topological superconductors induced by strain fields instantons. *International Journal of Modern Physics B*, 28(10):1450059, 2014.
- [246] D Schmeltzer and Avadh Saxena. Detecting majorana fermions in topological superconductors using stress. *Annals of Physics*, 385:546–562, 2017.
- [247] N Read. Non-abelian adiabatic statistics and hall viscosity in quantum hall states and $p_x + i p_y$ paired superfluids. *Physical Review B*, 79(4):045308, 2009.
- [248] Carlos Hoyos and Dam Thanh Son. Hall viscosity and electromagnetic response. *Physical review letters*, 108(6):066805, 2012.
- [249] Oleg Andreev. On nonrelativistic diffeomorphism invariance. *Physical Review D*, 89(6), 2014.
- [250] Michael Geracie, Dam Thanh Son, Chaolun Wu, and Shao-Feng Wu. Spacetime symmetries of the quantum hall effect. *Physical Review D*, 91(4):045030, 2015.
- [251] Oleg Andreev. More on nonrelativistic diffeomorphism invariance. *Physical Review D*, 91(2), 2015.
- [252] Michael Geracie. Transport in superfluid mixtures. *Physical Review B*, 95(13), 2017.
- [253] Frank Ferrari and Semyon Klevtsov. Fqhe on curved backgrounds, free fields and large n . *Journal of High Energy Physics*, 2014(12):86, 2014.
- [254] T Can, M Laskin, and P Wiegmann. Fractional quantum hall effect in a curved space: gravitational anomaly and electromagnetic response. *Physical review letters*, 113(4):046803, 2014.
- [255] Tankut Can, Michael Laskin, and Paul B Wiegmann. Geometry of quantum hall states: Gravitational anomaly and transport coefficients. *Annals of Physics*, 362:752–794, 2015.
- [256] Semyon Klevtsov, Xiaonan Ma, George Marinescu, and Paul Wiegmann. Quantum hall effect and quillen metric. *Communications in Mathematical Physics*, 349(3):819–855, Nov 2016.
- [257] MA Goni and MA Valle. Massless fermions and $(2+1)$ -dimensional gravitational effective action. *Physical Review D*, 34(2):648, 1986.
- [258] Jochum J Van der Bij, Robert D Pisarski, and Sumathi Rao. Topological mass term for gravity induced by matter. *Physics Letters B*, 179(1):87–91, 1986.
- [259] I Vuorio. Parity violation and the effective gravitational action in three dimensions. *Physics Letters B*, 175(2):176–178, 1986.
- [260] I Vuorio. Erratum: Parity violation and the effective gravitational action in three dimensions. *Physics Letters B*, 181(3,4):416, 1986.

- [261] Maxim Kurkov and Dmitri Vassilevich. Gravitational parity anomaly with and without boundaries. *Journal of High Energy Physics*, 2018(3):72, Mar 2018.
- [262] Judith Hoeller and Nicholas Read. Second-order geometric responses and central charge. *Bulletin of the American Physical Society*, 2018.
- [263] Francisco Peña Benitez, Kush Saha, and Piotr Surówka. Berry curvature and hall viscosities in an anisotropic dirac semimetal. *Phys. Rev. B*, 99:045141, Jan 2019.
- [264] Bendeguz Offertaler and Barry Bradlyn. Viscoelastic response of quantum hall fluids in a tilted field. *Phys. Rev. B*, 99:035427, Jan 2019.
- [265] Susanne Viefers. Quantum hall physics in rotating bose–einstein condensates. *Journal of Physics: Condensed Matter*, 20(12):123202, feb 2008.
- [266] Heidar Moradi and Xiao-Gang Wen. Universal wave-function overlap and universal topological data from generic gapped ground states. *Phys. Rev. Lett.*, 115:036802, Jul 2015.
- [267] Alexander Altland and Ben D Simons. *Condensed matter field theory*. Cambridge University Press, 2010.
- [268] Jing Yu, Xing-Hai Zhang, and Su-Peng Kou. Majorana edge states for F_2 topological orders of the wen plaquette and toric code models. *Phys. Rev. B*, 87:184402, May 2013.
- [269] Seth Lloyd. Universal quantum simulators. *Science*, 273(5278):1073–1078, 1996.
- [270] Jia-Wei Mei and Xiao-Gang Wen. Modular matrices from universal wave-function overlaps in gutzwiller-projected parton wave functions. *Phys. Rev. B*, 91:125123, Mar 2015.
- [271] Félix Rose, Omri Golan, and Sergej Moroz. Hall viscosity and conductivity of two-dimensional chiral superconductors. *arXiv preprint arXiv:2004.02590*, 2020.
- [272] Subir Sachdev. *Quantum Phase Transitions*. Cambridge University Press, 2 edition, 2011.
- [273] S. M. A. Rombouts, K. Heyde, and N. Jachowicz. Quantum monte carlo method for fermions, free of discretization errors. *Phys. Rev. Lett.*, 82:4155–4159, May 1999.
- [274] Congjun Wu and Shou-Cheng Zhang. Sufficient condition for absence of the sign problem in the fermionic quantum monte carlo algorithm. *Phys. Rev. B*, 71:155115, Apr 2005.
- [275] Johannes S Hofmann, Fakher F Assaad, Raquel Queiroz, and Eslam Khalaf. A search for correlation-induced adiabatic paths between distinct topological insulators. *arXiv preprint arXiv:1912.07614*, 2019.
- [276] Joji Nasu, Junki Yoshitake, and Yukitoshi Motome. Thermal transport in the kitaev model. *Phys. Rev. Lett.*, 119:127204, Sep 2017.

- [277] Zheng-Cheng Gu, Zhenghan Wang, and Xiao-Gang Wen. Classification of two-dimensional fermionic and bosonic topological orders. *Phys. Rev. B*, 91:125149, Mar 2015.
- [278] Yi Zhang, Tarun Grover, Ari Turner, Masaki Oshikawa, and Ashvin Vishwanath. Quasiparticle statistics and braiding from ground-state entanglement. *Phys. Rev. B*, 85:235151, Jun 2012.
- [279] Heidar Moradi and Xiao-Gang Wen. Universal topological data for gapped quantum liquids in three dimensions and fusion algebra for non-abelian string excitations. *Phys. Rev. B*, 91:075114, Feb 2015.
- [280] Huan He, Heidar Moradi, and Xiao-Gang Wen. Modular matrices as topological order parameter by a gauge-symmetry-preserved tensor renormalization approach. *Phys. Rev. B*, 90:205114, Nov 2014.
- [281] Jia-Wei Mei, Ji-Yao Chen, Huan He, and Xiao-Gang Wen. Gapped spin liquid with F_2 topological order for the kagome heisenberg model. *Phys. Rev. B*, 95:235107, Jun 2017.
- [282] Qi Zhang, Zi-Qi Wang, and Guang-Ming Zhang. Non-hermitian effects of the intrinsic signs in topologically ordered wavefunctions. *arXiv preprint arXiv:2005.03841*, 2020.
- [283] Tianxing Ma, Zhongbing Huang, Feiming Hu, and Hai-Qing Lin. Pairing in graphene: A quantum monte carlo study. *Phys. Rev. B*, 84:121410, Sep 2011.
- [284] Annica M Black-Schaffer and Carsten Honerkamp. Chiral d-wave superconductivity in doped graphene. *Journal of Physics: Condensed Matter*, 26(42):423201, sep 2014.
- [285] Giacomo Torlai, Juan Carrasquilla, Matthew T. Fishman, Roger G. Melko, and Matthew P. A. Fisher. Wavefunction positivization via automatic differentiation. *arXiv preprint arXiv:1906.04654*, 2019.
- [286] Andrei Alexandru, Paulo F. Bedaque, Henry Lamm, and Scott Lawrence. Finite-density monte carlo calculations on sign-optimized manifolds. *Phys. Rev. D*, 97:094510, May 2018.
- [287] Andrei Alexandru, Gokce Basar, Paulo F. Bedaque, and Neill C. Warrington. Complex paths around the sign problem. *arXiv preprint arXiv:2007.05436*, 2020.
- [288] H. J. M. van Bemmelen, D. F. B. ten Haaf, W. van Saarloos, J. M. J. van Leeuwen, and G. An. Fixed-node quantum monte carlo method for lattice fermions. *Phys. Rev. Lett.*, 72:2442–2445, Apr 1994.
- [289] Shiwei Zhang, J. Carlson, and J. E. Gubernatis. Constrained path monte carlo method for fermion ground states. *Phys. Rev. B*, 55:7464–7477, Mar 1997.
- [290] Peter Broecker, Juan Carrasquilla, Roger G. Melko, and Simon Trebst. Machine learning quantum phases of matter beyond the fermion sign problem. *Scientific Reports*, 7(1):8823, 2017.

- [291] Riccardo Rossi. Determinant diagrammatic monte carlo algorithm in the thermodynamic limit. *Phys. Rev. Lett.*, 119:045701, Jul 2017.
- [292] R. Bondesan and Z. Ringel. Classical topological paramagnetism. *Phys. Rev. B*, 95:174418, May 2017.
- [293] Scott D. Geraedts and Olexei I. Motrunich. Monte carlo study of a $u(1) \times u(1)$ system with π -statistical interaction. *Phys. Rev. B*, 85:045114, Jan 2012.
- [294] Scott D. Geraedts and Olexei I. Motrunich. Phases and phase transitions in a $u(1) \times u(1)$ system with $\theta = 2\pi/3$ mutual statistics. *Phys. Rev. B*, 86:045106, Jul 2012.
- [295] Snir Gazit and Ashvin Vishwanath. Bosonic topological phase in a paired superfluid. *Phys. Rev. B*, 93:115146, Mar 2016.
- [296] Tyler D. Ellison, Kohtaro Kato, Zi-Wen Liu, and Timothy H. Hsieh. Symmetry-protected sign problem and magic in quantum phases of matter, 2020.
- [297] SM Girvin, AH MacDonald, and PM Platzman. Magneto-roton theory of collective excitations in the fractional quantum hall effect. *Physical Review B*, 33(4):2481, 1986.
- [298] Steven H. Simon and Bertrand I. Halperin. Finite-wave-vector electromagnetic response of fractional quantized hall states. *Phys. Rev. B*, 48:17368–17387, Dec 1993.
- [299] Siavash Golkar, Dung Xuan Nguyen, Matthew M. Roberts, and Dam Thanh Son. Higher-spin theory of the magnetorotons. *Phys. Rev. Lett.*, 117:216403, Nov 2016.
- [300] Dung Xuan Nguyen, Andrey Gromov, and Dam Thanh Son. Fractional quantum hall systems near nematicity: Bimetric theory, composite fermions, and dirac brackets. *Phys. Rev. B*, 97:195103, May 2018.
- [301] Dung Xuan Nguyen, Siavash Golkar, Matthew M. Roberts, and Dam Thanh Son. Particle-hole symmetry and composite fermions in fractional quantum hall states. *Phys. Rev. B*, 97:195314, May 2018.
- [302] Sevag Gharibian, Yichen Huang, Zeph Landau, and Seung Woo Shin. Quantum hamiltonian complexity. *Foundations and Trends® in Theoretical Computer Science*, 10(3):159–282, 2015.
- [303] Tameem Albash and Daniel A. Lidar. Adiabatic quantum computation. *Rev. Mod. Phys.*, 90:015002, Jan 2018.
- [304] Karel Van Acoleyen, Michaël Mariën, and Frank Verstraete. Entanglement rates and area laws. *Phys. Rev. Lett.*, 111:170501, Oct 2013.
- [305] Shailesh Chandrasekharan. Anomaly cancellation in 2+ 1 dimensions in the presence of a domain wall mass. *Physical Review D*, 49(4):1980, 1994.

- [306] CD Fosco and A Lopez. Dirac fermions and domain wall defects in $2+1$ dimensions. *Nuclear Physics B*, 538(3):685–700, 1999.
- [307] Kristan Jensen, R Loganayagam, and Amos Yarom. Thermodynamics, gravitational anomalies and cones. *Journal of High Energy Physics*, 2013(2):88, 2013.
- [308] C Wetterich. Spinors in euclidean field theory, complex structures and discrete symmetries. *Nuclear Physics B*, 852(1):174–234, 2011.
- [309] Edward Witten. Fermion path integrals and topological phases. *arXiv preprint arXiv:1508.04715*, 2015.
- [310] Thomas Friedrich. *Dirac operators in Riemannian geometry*, volume 25. American Mathematical Soc., 2000.
- [311] S Deser, L Griguolo, and D Seminara. Definition of chern-simons terms in thermal qed 3 revisited. *Communications in mathematical physics*, 197(2):443–450, 1998.
- [312] Giovanni Ossola and Alberto Sirlin. Considerations concerning the contributionsof fundamental particles to the vacuum energy density. *The European Physical Journal C-Particles and Fields*, 31(2):165–175, 2003.
- [313] Jurjen F Koksma and Tomislav Prokopec. The cosmological constant and lorentz invariance of the vacuum state. *arXiv preprint arXiv:1105.6296*, 2011.
- [314] Matt Visser. Lorentz invariance and the zero-point stress-energy tensor. *arXiv preprint arXiv:1610.07264*, 2016.
- [315] Federico Bonetti, Thomas W Grimm, and Stefan Hohenegger. One-loop chern-simons terms in five dimensions. *Journal of High Energy Physics*, 2013(7):43, 2013.
- [316] David Brizuela, José M Martín-García, and Guillermo A Mena Marugán. xpert: computer algebra for metric perturbation theory. *General Relativity and Gravitation*, 41(10):2415, 2009.
- [317] José M. Martín-García. xact: Efficient tensor computer algebra for the wolfram language.
- [318] Stefan M. A. Rombouts, Jorge Dukelsky, and Gerardo Ortiz. Quantum phase diagram of the integrable $p_x + ip_y$ fermionic superfluid. *Phys. Rev. B*, 82:224510, Dec 2010.
- [319] Anton Kapustin, Ryan Thorngren, Alex Turzillo, and Zitao Wang. Fermionic symmetry protected topological phases and cobordisms. *Journal of High Energy Physics*, 2015(12):1–21, 2015.
- [320] Tian Lan, Liang Kong, and Xiao-Gang Wen. Classification of $(2+1)$ -dimensional topological order and symmetry-protected topological order for bosonic and fermionic systems with on-site symmetries. *Phys. Rev. B*, 95:235140, Jun 2017.

- [321] David Aasen, Ethan Lake, and Kevin Walker. Fermion condensation and super pivotal categories. *Journal of Mathematical Physics*, 60(12):121901, 2019.
- [322] A.Yu. Kitaev. Fault-tolerant quantum computation by anyons. *Annals of Physics*, 303(1):2 – 30, 2003.
- [323] M. Fremling, T. H. Hansson, and J. Suorsa. Hall viscosity of hierarchical quantum hall states. *Phys. Rev. B*, 89:125303, Mar 2014.